Respiratory Virus Coinfection and Superinfection Exclusion

Anna Sims

Submitted in fulfilment of the requirements for the

Degree of Doctor of Philosophy

College of Medical, Veterinary and Life Sciences

University of Glasgow

January 2024

This thesis is dedicated to:

Anne Twomey (née Brennan)

26th November 1936 – 20th August 2023

Granny, I wish you were here and I hope you are proud.

Abstract

Influenza A virus (IAV) and severe acute respiratory syndrome coronavirus 2 (SARS-CoV-2) are responsible for two of the deadliest pandemics in modern history, and the emergence of pandemic respiratory viruses remains constant threat to human life. The emergence of novel pandemic viruses is driven by genetic exchange between existing viruses during coinfection of cells. Coinfection of cells can be controlled by superinfection exclusion (SIE), a mechanism by which a previously infected cell becomes resistant to secondary viral infection after a period of time. SIE is known to be induced following IAV infection but its mechanism is unknown, while SIE has not yet been observed for any coronavirus, including SARS-CoV-2. In this thesis, I use isogenic reporter viruses to study SIE, defining the kinetics of onset for IAV and presenting the first evidence for SIE for SARS-CoV-2. I demonstrate that in both cases SIE onset does not occur immediately, but that infected cells shift from a permissive to exclusionary state within 6 hours of primary infection. I used this system to investigate the mechanism for IAV SIE, showing that it is unlikely to be driven by direct competition between the viruses, or by the cellular interferon response. I then modelled the foci of infection observed within infected hosts *in vitro* using plaque assays. For both viruses, I also show how SIE at the level of individual cells affects the ability of virus populations to coinfect cells during localised viral spread. I found that viruses within one plaque could coinfect freely, as all new infections were of cells that had not yet established SIE. In contrast, viruses spreading towards each other from separate plaques could only establish minimal regions of overlap before SIE blocked further coinfection. For IAV, these interactions were then also observed in the lungs of infected mice. The results suggests that the kinetics of SIE onset separate a spreading infection into discrete regions, within which interactions between virus populations can occur freely, and between which they are blocked. These findings are likely to apply other viruses that induce SIE. Finally, I investigated the potential for coinfection between IAV and SARS-CoV-2. I found no evidence of SIE, but instead found evidence of viral interference mediated by type-1 interferon. Understanding the mechanisms and dynamics of SIE could help us understand coinfection and the generation of novel pandemic viruses, and potentially aid in predicting when new pandemics will arise.

Graphical Abstract

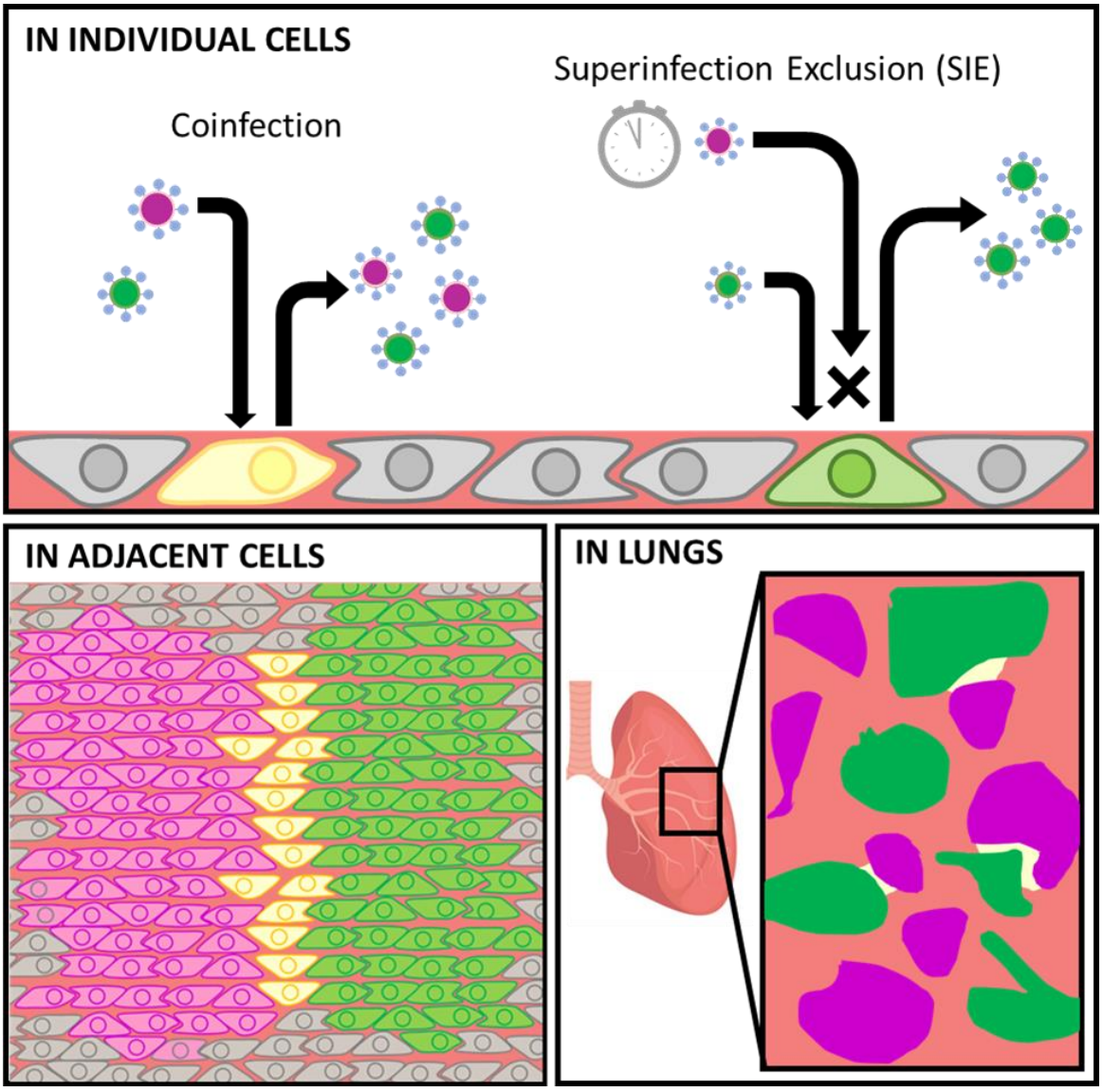

Contents

List of Figures

Chapter 1: Introduction

Chapter 2: Materials and Methods

Chapter 3: Defining the kinetics of SIE by induced by IAV

Chapter 4: Exploring the impact of SIE on the patterning of IAV infections during localised viral spread

List of Tables

Chapter 1: Introduction

Chapter 2: Materials and Methods

Publications

Publications obtained from work included in this thesis:

- Sims A, Tornaletti LB, Jasim S, Pirillo C, Devlin R, Hirst JC, et al. Superinfection exclusion creates spatially distinct influenza virus populations. PLoS Biol. 2023;21: 1–19. doi:10.1371/journal.pbio.3001941

  Primer article:

  - Lowen AC, Ferreri LM. Exclusion of latecomers yields a patchwork of viral subpopulations within hosts. PLoS Biol. 2023;21: e3001994. doi:10.1371/journal.pbio.3001994

  Nature News and Views Article:

  - Farjo M, Brooke CB. When influenza viruses don't play well with others. Nature News and Views. 2023;616: 668–669. doi:10.1038/d41586-023-00983-5

  Times Article:

  - Puttnick H. Flu symptoms caused by a "battle of bugs" in your throat. The Times. 10 Feb 2023. Available: https://www.thetimes.co.uk/article/flu-symptoms-caused-by-a-battle-of-bugs-in-your-throat-w97h2lrvs

- Pirillo C, Al Khalidi S, Sims A, Devlin R, Zhao H, Pinto R, et al. Cotransfer of antigen and contextual information harmonizes peripheral and lymph node conventional dendritic cell activation. Sci Immunol. 2023;8. doi:10.1126/sciimmunol.adg8249

Publications obtained from work not included in this thesis:

- Lytras S, Wickenhagen A, Sugrue E, Stewart DG, Swingler S, Sims A, et al. Resurrection of 2'-5'-oligoadenylate synthetase 1 (OAS1) from the ancestor of modern horseshoe bats blocks SARS-CoV-2 replication. PLoS Biol. 2023;21: e3002398. Available: doi:10.1371/journal.pbio.3002398

Acknowledgements

First and foremost, I would like to thank my supervisor, Ed Hutchinson. Your enthusiasm for open, collaborative, and interesting science is inspiring and I have learnt a lot from you. Thank you for your many wonderful ideas, and for giving me the freedom to follow my (often less wonderful) ideas. You have spent four (and a bit) years of your life guiding me to develop into an independent scientist, I hope you consider it time well spent.

I would like to thank the members of the Hutchinson Lab, past and present: Sarah Cole, Lea Meyer, Seema Jasim, Huailong Zhao, Jack Hirst, Vaidehi Patel and especially my fellow PhD students: Daniel Weir, Jake MacLeod and Cal Bentley-Abbot. Chatting and laughing with you all has been the light of many of the harder days in this process - despite it being so annoying for everyone else in our open plan office. Thank you all for your kind words, support, and excellent ideas. To Daniel and Cal, the current PhD students of the Hutchinson lab, you're some of the cleverest people I've ever had the pleasure to meet and, when I leave the lab, I leave it in your capable hands.

I want to thank my excellent collaborators at the Beatson Institute, Ed Roberts and Chiara Pirillo. This project would be nowhere near as cool as it is without your contributions.

Many people have supplied invaluable troubleshooting advice, without which I'm not sure I'd have a single figure in this thesis. Colin Loney, you are a wonderful person and an even better microscopist, if that is possible. Rute Maria Pinto, Emma Davies, and Matt Turnball, you were always there when I needed lab advice, thank you so much. Thank you to Sarah Cole and Agnieszka Szemiel for helping train me for CL3 work.

I have unfortunately experienced some direct sexism during my time at the CVR. I would like to thank Fiona Graham and Donna Macpherson for doing as much as they could to support me within a system not designed to protect women.

On a more personal note, I would like to thank the many wonderful friends I have made during my time in Glasgow. I've had so many laughs over these four (and a bit) years, thanks to you all. To my day ones, Alex, Spyros, Innes and Kasim, it was a privilege to go through every step of this experience with you. Faye, Eilidh and Stephen, thank you so much for being such fantastic friends to me. To Lois, all I can say is thank you for everything, although I know it doesn't cover it. To Kieran, thank you for making this last year one of the best of my life.

Thank you to my family: Mum, Dad, Ciara and Jonny. Thank you for supporting me even though I upped and decided to move 400 miles away to Glasgow. To Flynn, Ivy, Tilly and Fitz – thank you. To my absolute legend and total wreck of a car, The Chev. It's truly astonishing that you lasted all four years. Thanks, old gal.

The last thank you goes to my biggest supporter, my Granny. You always said that education is freedom and, of course, you were completely right. I never for a moment doubted your love or support for me during this PhD – I wish you could have seen me finish it. I hope that you are proud of me and that at some point I will see you again.

Author Declaration

I declare that, except where explicit reference is made to the contribution of others, that this thesis is the result of my own work and has not been submitted for any other degree at the University of Glasgow or any other institution.

Anna Sims

January 2024

Abbreviations

(Q)LAIV	(Quadrivalent) live attenuated influenza vaccine
AAT	ACE2 TMPRSS2 overexpressing A549 cells
ACE2	Angiotensin converting enzyme 2
AIV	Avian influenza virus
AZ	AstraZeneca
BNEPs	Bottleneck enforcing proteins
BSA	Bovine serum albumin
BVDV	Bovine Viral Diarrhoea Virus
CHIKV	Chikungunya virus
CI	Confidence intervals
CME	Clathrin mediated endocytosis
COVID-19	Pandemic disease caused by SARS-CoV-2
CoVs	Coronaviruses
DENV	Dengue virus
DIPs	Defective interfering particles
DMEM	Dulbecco's Modified Eagle Medium
DMSO	Dimethylsulfoxide
DMVs	Double membrane vesicles
DTT	Dithiothreitol
DVG	Defective viral genome
eGFP	Enhanced green fluorescent protein
EM	Electron microscopy
ER	Endoplasmic Reticulum
ERGIC	ER-Golgi intermediate compartment
FBS	Foetal Bovine Serum
FDA	Federal Drug Administration
FFU	Focus forming units
FIPS	Fully infectious particles
gD	Glycoprotein D
GFU	Green forming units
HA	Haemagglutinin
HCV	Hepatitis C Virus
HDAC6	Histone deacetylase 6
HIV-1	Human Immunodeficiency Virus – 1
Hpi	Hours post infection
HPV	Human papilloma virus
HSV-1	Herpes Simplex Virus -1
IAV	Influenza A Virus
IBV	Influenza B virus
IFN	Interferon
IFNAR	interferon receptor
ISG	Interferon stimulated gene
JAK	Janus kinase
JUNV	Junin Virus
KO	Knock out
LLOQ	Lower limit of quantification
M1	Matrix 1
MDCK	Mardin-Darby canine kidney cells
MEM	Minimum Essential Media
MOI	Multiplicity of infection
mRNA	Messenger RNA

NA	Neuraminidase
NDV	Newcastle disease virus
NEP	Nuclear export protein - also known as NS2
NLS	Nuclear localisation signals
NP	Nucleoprotein
NPI	Non-pharmaceutical intervention
NS1	Non-structural protein 1
PA	Polymerase acidic protein
PB1 or PB2	Polymerase basic proteins 1 or 2
PBST	Phosphate buffered saline (PBS) with 0.1% Tween-20
PCR	Polymerase chain reaction
PFU	Plaque forming units
PIV3	Parainfluenza virus 3
PR8	A lab adapted influenza A virus, A/Puerto Rico/8/34
RBP	Receptor binding pocket
RdRp	RNA-dependent RNA-polymerase
RFU	Red forming units
RSV	Respiratory syncytial virus
RT	Room temperature
Rux	Ruxolitinib
RVFV	Rift Valley Fever Virus
S	SARS-CoV-2 spike protein
SA	Sialic acid
SARS-CoV-2	Severe Acute Respiratory Syndrome corona virus 2
SD	Standard deviation
SDM	Social distancing measures
SDS	Sodium dodecyl sulfate
SFV	Semliki Forest Virus
SIE	Superinfection exclusion
SIPs	Semi-infectious particles
ssRNA	Single stranded RNA
SST	Total sum of squares
SV	Sindbis Virus
TCV	Turnip Crinkle virus
TMPRSS2	Transmembrane serine protease 2
TPCK	N-tosyl-L-phenylalanine chloromethyl ketone
UK	United Kingdom
URT	Upper respiratory tract
VACV	Vaccinia Virus
VGM	Viral growth media
VOCs	Variants of concern
vRNPs	Viral ribonucleoprotein
VSV	Vesticular Stomatitis Virus
VVIs	Virus-virus interactions
WHO	World Health Organisation
WNV	West Nile Virus
WSN	A lab adapted influenza A virus, A/WSN/1933
WT	Wild type

Chapter 1: Introduction

1.1 Respiratory Viruses

1.1.1 Importance

Diseases of the respiratory system are a major risk to human life, with the Office of National Statistics (ONS) reporting an average of 74,080 deaths per year in the England and Wales from these diseases in the period 2015 - 2019 [1]. Many of these deaths can be attributed to influenza, the disease caused by influenza viruses. Influenza viruses typically infect the upper respiratory tract, causing a dry cough, sore throat, fever, headache, muscle pain and fatigue. The disease typically lasts two weeks, and most people recover without medical intervention. However, in severe cases, influenza viruses can infect the lower respiratory tract causing more serious illness, often accompanied by pneumonia from secondary bacterial infection. Influenza can infect people from all age groups but those at increased risk include children under five years of age and elderly people, in addition to pregnant or immunocompromised individuals and those with chronic lung conditions [2].

In late 2019 a novel coronavirus emerged in Wuhan, China and rapidly spread, causing a pandemic to be declared in 2020 by the World Health Organisation (WHO) [3]. This virus was called Severe Acute Respiratory Syndrome Coronavirus 2 (SARS-CoV-2), and caused the disease known as Coronavirus Disease 2019 (COVID-19) [4]. According the ONS, COVID-19 was the leading cause of death in England and Wales in 2020 and was responsible for 69,101 deaths in total in that year [1]. SARS-CoV-2 is a respiratory virus that primarily infects the upper and lower respiratory tract. The symptoms of COVID-19 typically include fever, chills and sore throat, but may also be accompanied by headache, cough, muscle aches, fatigue and loss or change of sense of taste or smell. The disease typically lasts up to two weeks, but some experience ongoing symptoms, which has been classified as “long COVID.” In some people, SARS-CoV-2 can cause destruction of the lung tissue leading to difficulty breathing, chest pain and loss of consciousness. As with influenza, severe SARS-CoV-2 infection can lead to pneumonia and potentially death. High risk individuals include those with pre-

existing health conditions including HIV, diabetes, cancer, obesity and dementia, in addition to immunosuppressed individuals [4].

Respiratory viruses are a massive risk to human life and reducing their burden is of dire importance. This thesis will focus on two of the most important respiratory viruses in terms of human mortality, influenza A viruses (IAV) and SARS-CoV-2 and examine what happens when these viruses interact during coinfections.

1.1.2 Control Strategies

Our current strategies to control influenza and COVID-19 fall into three main categories: non-pharmaceutical intervention (NPI), antiviral drugs, and vaccination. It may be obvious to state, but is nevertheless important to note, that no one control strategy should be used in isolation. Lessons from previous pandemics and modelling studies have shown that using multiple strategies leads to the most robust reduction in transmission [5,6]. Therefore ongoing research into redundant control strategies, and critically engagement with the public, is key to effective control.

I wish to briefly acknowledge that the access to certain control strategies is not uniform across the world, which has left some people at increased burden of respiratory virus disease. This has occurred, and is occurring, due to often complicated (although sometimes extremely simple) reasons. This injustice must be addressed before we can have effective control of influenza and COVID-19.

1.1.2.1 Non-pharmaceutical interventions (NPIs)

Respiratory viruses, including IAV and SARS-CoV-2, spread between humans via respiratory secretions [7]. This can either occur via direct physical contact between infected individual and susceptible individual, indirect contact (usually via contaminated surfaces or objects) or contact with respiratory droplets or aerosols in the air. Non-pharmaceutical interventions aim to reduce the likelihood that a susceptible individual will encounter contaminated respiratory secretions, thereby reducing infection and disease incidence.

Social-distancing measures (SDMs) aim to reduce viral disease by blocking contact between infected and non-infected individuals, thereby limiting transmission by all the modes previously mentioned. One of the most drastic SDMs is full lockdown, whereby people are advised to stay in their houses, schools and business are closed, and only essential services still run. During the COVID-19 pandemic, many governments world-wide used this strategy to prevent the rapid spread of SARS-CoV-2, a strategy that was largely successful [8,9]. Lockdown however is hugely disruptive to society, and in the long term can have detrimental effects on individuals' mental and physical health due to lack of social connection and support [10]. Therefore, it is not a long term solution for control of respiratory viruses and is typically only deployed in the most drastic and dire of circumstances. Other SDMs, for example where the population is encouraged to avoid crowds and keep a safe (typically 2 metre) distance from others, are less disruptive but may still be used effectively. This distance ensures that direct and droplet and aerosol transmission is minimised. The distance that droplets and aerosolised viruses can travel effectively has been reviewed by Wang *et al.* 2021 [11]. SDMs such as these were used during the 1918-19 "Spanish" influenza pandemic in the United States and are estimated to have saved thousands of lives [12].

Other NPI methods include personal hygiene strategies such as frequent hand-washing, which reduces transmission by blocking indirect contact with contaminated hands. Other strategies, such as covering the mouth and nose during coughing or sneezing and the use of face-masks, block transmission via droplets and aerosols, and also block indirect transmission by preventing the deposition of virus onto surfaces. These strategies are less disruptive for the public, but due to their individual nature, they are hard to enforce and their effectiveness in isolation hard to estimate in a pandemic setting [13]. When used in combination with other control strategies however, and will substantial public cooperation, they can be extremely powerful tools to control respiratory viral disease.

Interestingly, the strategies deployed during the COVID-19 pandemic drastically reduced the incidence of influenza. This was especially evident in the winter 2020-21 season and may have led

to the potential eradication of the influenza B virus (IBV) Yamagata lineage, which was last detected in March 2020 [14].

NPIs of all types are important disease control strategies and are often deployed at the beginning of pandemics, before pharmaceutical interventions are available to the public.

1.1.2.2 Antiviral drugs

Antivirals are important for reducing symptoms and saving lives. In keeping with the scope of this thesis I will focus on case studies were antiviral drugs have been used to block transmission of IAV and SARS-CoV-2, and the challenges involved in using them for this purpose.

Antiviral drugs can be used to prevent transmission either by reducing the amount of live virus shed from the infected patient (treatment), or by preventing infection of an uninfected individual who is a direct contact of a case (prophylaxis). Meta-analysis of studies of using oseltamivir and zanamivir, two drugs used to treat influenza [15], as prophylactic agents for contacts sharing a household with an infected person concluded that they were 67-89% effective [16]. Indeed, the Federal Drug Administration (FDA) has approved these drugs for prophylactic use in the latest season (2023-24) [17]. The data for whether these drugs reduce transmission in a household when used to treat the infected person is less conclusive, and any reduction in transmission appears to be modest (reviewed by Hayden *et al.* 2022) [18]. One of the main problems with use of antiviral drugs in households is the timely identification and administering of the drugs to susceptible people, which seems to be key to success. As peak shedding of influenza viruses typically precedes symptoms [19,20], this requires large scale surveillance of the population or patients to very quickly make themselves known to healthcare providers. It also requires costly stockpiles of drugs. Therefore, although effective, antiviral prophylaxis may not be the most effective strategy to control influenza.

Another challenge to using antiviral drugs to control viral disease is the risk of transmitting drug-resistant variants. The concern here is that use of antiviral drug provides a strong selection bias for variants that are resistant, leading to these viruses dominating the viral population, rendering the drug useless over time. This process has been repeatedly demonstrated for influenza viruses

(reviewed by Hussain *et al*. 2017 [21]). An interesting case study is molnupiravir, a drug used to treat COVID-19 by increasing the error rate of the SARS-CoV-2 polymerase, thereby introducing mutations into the genome [22]. Molnupiravir action increases the incidence of specifically G-to-A and C-to-T mutations, which researchers observed in increased frequency in circulating SARS-CoV-2 genomes around the time that the drug came into widespread use. This implies that viruses can escape lethality from the drug and be transmitted onwards. Although most mutations introduced by the use of molnupiravir are likely to be detrimental to the virus, it is possible that some may be beneficial and confer a selective advantage, leading to the generation of, for example, immune escape variants.

A key challenge to the development of any antiviral drug is the intertwining of virus replication with normal cellular function. Due to this, it is challenging to find targets that block virus functions without blocking essential cellular processes. Ongoing research is required to identify potential druggable targets.

Altogether, although antiviral drugs are important to enable us to treat patients and save lives, they have limited potential to control the incidence of influenza and COVID-19 in the population, due to the risk of drug resistance and practicalities of their use.

1.1.2.3 Vaccination

Vaccination is the preferred intervention to both reduce disease severity in infected patients, and to prevent transmission between individuals.

Vaccination was a particularly powerful strategy to control the COVID-19 pandemic. As SARS-CoV-2 was a virus novel to the human population it required the rapid development of a new vaccine, a feat that took monumental scientific effort. The result was that a number of highly effective and safe vaccines were designed and produced at speed. The design of each vaccine and a timeline of their development is reviewed in Chakraborty *et al*. 2023 [23]. The individual vaccines vary in their reported effectiveness, but it was clear during the pandemic that swift vaccination of a high percentage of the population led to rapid reduction in COVID-19 incidence [24]. Overall then, the

"greatest collaborative effort of the 21st Century" (as Chakraborty *et al*. 2023 would have it) was a resounding success. Some ongoing questions around SARS-CoV-2 vaccination remain: do we produce booster vaccines including newer variants that may escape the immune system? Do we provide these booster vaccines for everyone or just the most vulnerable? How do we equitably distribute vaccine doses across the world? These challenges will require monitoring, a protracted research effort and thoughtful policy making.

Influenza, by contrast, has much longer history of developed vaccines but there are several challenges associated with making an effective vaccine, as reviewed by Gouma *et al.* 2020 [25]. Firstly, due to their high mutation rate, influenza viruses quickly generate immune escape mutants and therefore the current formulations of the influenza vaccine must be updated every year. There is an ongoing effort to create a "universal" influenza vaccine which could direct the immune system to target conserved regions of influenza proteins (in particular the haemagglutinin (HA) stalk region), and therefore should protect against multiple circulating strains [26]. These vaccines are challenging to develop, but several are currently in clinical trials [27]. Secondly, vaccine effectiveness is a particular challenge for influenza, with the effectiveness varying wildly between seasons and subtypes [28]. There are many reasons for this, but one issue is that vaccine strains have traditionally been grown in embryonated chicken eggs and some (notably live attenuated influenza vaccines) are still prepared this way. This can cause the vaccine strains of the viruses to gain egg-specific adaptations which make it immunologically distinct from the circulating strains, leading to poor vaccine efficacy, a particular challenge for H3N2 strains of IAV [29]. The final challenge for effective control of influenza via vaccination is vaccine uptake. The vaccination programme in the UK focuses on three groups: primary school aged children, people over the age of 65 and those with underlying risk factors (including pregnant people and healthcare workers) [30]. The primary aim of this programme, as stated by Public Health England (PHE) (29), is not necessarily to prevent the transmission of influenza viruses in the population, but to protect those at most risk of dying of the disease. Therefore, it is unlikely that based on current vaccination programmes we will be able to

sufficiently control influenza virus transmission in the way we did for SARS-CoV-2 in the wider population.

Overall, ongoing research, vaccination policy and public education effort is required to effectively deploy vaccination and other strategies to control influenza and COVID-19.

1.1.3 Circulation and Emergence

Having examined the diseases caused by these viruses, and the methods we can deploy to control the incidence of disease, we must now examine how these viruses emerge and are maintained in the human population.

The incidence of human disease caused by respiratory viruses peaks during the winter months in temperate climates, as shown by human hospitalisation and mortality data [31,32]. There have been many reasons postulated in the literature for this seasonal incidence ranging from environmental factors, to human behavioural and immunological changes [33]. As influenza viruses circulate, they accumulate mutations leading to gradual changes in the surface glycoproteins, HA and neuraminidase (NA). This is known as “antigenic drift” and is the main reason for the need for yearly updates to the influenza vaccine to include the newest circulating strains. In the initial stages of the COVID-19 pandemic, there was much debate about whether the novel coronavirus SARS-CoV-2 would settle into a seasonal pattern along the lines of other respiratory viruses [34–36]. We have so far experienced four winter seasons since the virus emerged, and the data suggest that the virus is falling into a seasonal patterns in temperate climates [35].

For influenza viruses and for coronaviruses such as SARS-CoV-2, there is potential for a greater risk to human life than seasonal epidemics, through the emergence of pandemic viruses. Pandemic viruses emerge from strains circulating in animal reservoirs that then jump species into humans (in a process known as zoonosis) [37]. This process led to the emergence of SARS-CoV-2 in 2020, and also led to the deadliest influenza pandemic ever recorded which killed an estimated 50 million people following its emergence in 1918 [38]. These viruses are so deadly because they have acquired novel glycoprotein molecules which has never been seen before by human immune

systems, and therefore emerge into a naïve population. The sudden acquisition of whole proteins or sections of proteins is known as “antigenic shift” and is mostly driven by genetic exchange between different strains of the virus. For influenza viruses, genetic exchange occurs via reassortment, where viruses can swap whole genome segments during genome packaging. For SARS-CoV-2 genetic exchange occurs via recombination, where viruses can swap sections of the genome during replication. The emergence of new pandemic viruses is a near certainty and therefore intense surveillance programs are in place to monitor which respiratory virus strains are circulating in the same regions, and therefore might undergo genetic exchange. For this to occur, two strains of virus must simultaneously infect the same host, in a process known as coinfection.

1.2 Coinfection

Coinfection is the infection of host simultaneously with multiple different pathogens [39). It most commonly occurs through superinfection, which can be defined as the acquisition of an infection following an earlier infection.

Typically, although not always, coinfections involving multiple varieties of microorganism are described as mixed infections. ‘Coinfection’ is usually used to describe infections by multiple different types of one pathogen, for example between viruses from different families (e.g. IAV and SARS-CoV-2), or by multiple different strains of one virus (e.g. H1N1 and H3N2 strains of IAV) [40].

Coinfection can occur at multiple scales: at the whole host, at the level of organs or systems or at the level of individual cells.

1.2.1 Coinfection in the respiratory tract

1.2.1.1 Prevalence

It has previously been a common assumption that diseases in patients are caused by a single aetiological agent, perhaps due to diagnostic laboratories often testing samples for a single pathogen. However, technological advances such as multiplex polymerase chain reaction (PCR) assays and sequencing have allowed us to assess the prevalence of coinfection in natural infections the respiratory tract. Data for the prevalence of natural coinfection in single cells is still lacking due to technical difficulties obtaining cells from infected patients. Instead, we usually estimate the

prevalence of coinfected cells from recombinant and reassortant viral progeny and from experimental animal infections. We will consider experimental systems for studying the prevalence of cellular coinfection in this thesis, for IAV in chapter 3.2, and for SARS-CoV-2 in chapter 6.2.

Coinfection between respiratory viruses in the respiratory tract is relatively common, with multiple distinct viruses being detected in between 10-30% of infections [41–48]. By contrast, coinfection of patients with different strains of the same respiratory virus seems relatively rare. For IAV, one study conducted in New Zealand screened over a thousand samples that were positive for the pandemic H1N1 2009 virus (H1N1pdm) and identified 13 samples that were also positive for seasonal H1N1 influenza (coinfection rate = 1.1%) [49]. A similar coinfection rate was found using multiplex PCR between H3N2 and H1N1 seasonal viruses (1 out of 93 IAV positive samples, coinfection rate = 1.1%) [50]. Most evidence for coinfection between strains of IAV comes from small outbreak case studies [51–53], the biggest of which found six patients coinfected with H1N1pdm and seasonal H3N2 out of 40 patients with laboratory confirmed IAV infection (coinfection rate = 15%) [54]. IAV and influenza B virus (IBV) coinfections also appears to be rare, with one study finding that out of 199 H1N1pdm positive samples, none were IBV positive [55].

For SARS-CoV-2, the incidence of coinfection by multiple divergent lineages also seems relatively rare. This is likely partly due to the rapid replacement of different lineages within geographical areas during the COVID-19 pandemic [56]. One study found 53 samples out of 21,387 that were coinfected with viruses from distinct lineages, the most common being Omicron lineages BA.1 and BA.2 (coinfection rate = 0.26%) (56). Another large-scale study (~30,000 samples tested) identified even lower rates of coinfection of around 0.06% (57). This study found one patient coinfected with viruses from the delta and omicron lineages, which was confirmed in a smaller outbreak study with two patients (58).

Therefore, multiplex PCR and sequencing studies have revealed that respiratory virus coinfection in patients is common, but coinfection between different strains of the same virus may be relatively rare.

1.2.1.2 Risk factors

Multiple studies highlight that young children are the most likely age group to be coinfected with multiple respiratory viruses (44, 48, 59). One large-scale study reported that coinfection rates in children under five is as high as 35%, compared to 5.8% in adults [47]. Studies also show that hospitalised patients are at increased risk of respiratory virus coinfection [44,45], with one study finding that coinfection rates are three times higher in hospitalised patients than in outpatients (12 to 4% respectively) [42]. Similarly, coinfection with multiple strains of SARS-CoV-2 is associated with exposure in a hospital environment [61]. This perhaps highlights the likelihood of patients acquiring secondary nosocomial infections following hospitalisation. For example, during the COVID-19 pandemic, of patients admitted to hospital approximately 19% were found to be coinfected with SARS-CoV-2 and another pathogen (viral, bacterial or pathogen in origin). However, when subsequently swabbed in hospital, it was found that 24% of the patients were coinfected [62].

1.2.1.3 Clinical consequences

The impact of respiratory viral coinfection on clinical outcome is a complicated topic. Different outcomes have been reported with different combinations of viruses [41,45].

One of the clearest links is the association of poor clinical outcomes with patients coinfected with influenza viruses and SARS-CoV-2. A meta-analysis of 118 studies found that coinfected patients hospitalised for SARS-CoV-2 infection were more likely to die than patients with SARS-CoV-2 single infection. They also found an increase in the need for mechanical ventilation and an increase in hospital stay in coinfected patients [62]. An analysis of nearly 7000 patients similarly concluded that SARS-CoV-2 coinfection with influenza is associated with increased likelihood of ventilation, and coinfection with influenza and adenoviruses increases the likelihood of mortality [63]. Similarly, coinfection of SARS-CoV-2 with rhinovirus was found to be detrimental, where patients was more likely to be transferred to intensive care than patients infected with rhinovirus alone [64]. Conversely, coinfection between SARS-CoV-2 and respiratory syncytial virus (RSV) was found to have similar clinical outcomes to singly infected patients (in mechanical ventilation and mortality) [63].

Therefore, although it is hard to generalise the clinical impact of coinfection between different respiratory viruses, coinfection between the viruses this thesis focuses on, IAV and SARS-CoV-2 is associated with poor patient outcomes.

1.3 Virus-virus interactions (VVIs) and sociovirology

The coinfection of hosts and individual cells allows viruses to interact with each other. In this section we will discuss the virus-virus interactions (VVIs) that happen (1) within the host and (2) within individual cells. VVIs can have sweeping effects on viral population diversity, pathogenesis, transmission and even the emergence of pandemic viruses. Although we are focussing on IAV and SARS-CoV-2, the interactions discussed in this section are not just applicable to respiratory virus infection and can be generalised for most, if not all, viral coinfections.

Similar to our understanding of interactions between animal species [65], generally the outcome of VVIs can be conceptualised into 3 groups: competition, cooperation, or tolerance. These outcomes are determined by the impact of one virus on the fitness (ability to replicate and transmit) of the other. Competition occurs when at least one virus has reduced fitness during coinfection, cooperation occurs when both viruses have an increased fitness during coinfection, and tolerance occurs when coinfection does not affect the fitness of either virus. An interesting case comes with parasitism, where one virus requires coinfection with another virus to replicate, as occurs between virophages and giant viruses [66]. The outcomes of coinfection are determined by complex networks of VVIs, some of which we will cover in this section.

Diaz-Muñoz *et al.* 2017 proposed applying social evolution theory to VVIs, to create a framework termed sociovirology [67]. Sociovirology considers how cooperative, altruistic and competitive traits may have evolved between viruses. Here it is important to note that social traits are observed at the population level but evolution is driven by natural selection which acts on individual viral genomes. Therefore, social traits will only evolve if they provide a selection advantage to the individual genomes performing them, and not solely if they benefit the population as a whole. However, as replicating genetically identical relatives is genetically equivalent to replicating the

individual, cooperation between progeny viruses is likely to offer a selective advantage to the individual genomes through kin selection. Kin selection is well-accepted to occur between related animals [68], bacteria [69] and parasites [70], and has also been expanded to viruses [71,72]. Alternatively, in a situation where coinfection commonly occurs between genetically dissimilar viruses, a sociovirological perspective would predict that competitive traits will be more favourable and are likely to fix at the population level. As this framework seeks to generalise a broad spectrum of VVIs, there are many examples and specific caveats, but it nevertheless offers intriguing framework to conceptualise VVIs.

Sociovirology is an expanding and somewhat controversial area of study as viruses have often been considered too simple to perform complex social behaviour [73]. However, the discovery of the bacteriophage arbitrium system demonstrates that viruses are capable of forms of sociality [74]. Social behaviour between bacteria, algae and other single celled organisms is generally well accepted [75], and sociovirology puts viruses within the same framework that has been applied to higher order systems in ecology.

1.3.1 VVIs within hosts

When viruses infect the same hosts but not the same cells, VVIs occur without direct interactions between viral proteins, and therefore are conducted in a paracrine fashion. This means that interaction at the host level is most often mediated through interferon (IFN) and other cytokine signalling (reviewed by Kumar *et al.* 2018 [40] and Du *et al*. 2022 [39]). I will briefly review examples of host level VVIs in this section.

1.3.1.1 Viral enhancement

In some cases, coinfection at the host level results in an enhancement of viral replication [76–78]. The simplest example of this is where one virus infection results in immunodeficiency, resulting in enhancement of other virus infection, as occurs with Human Immunodeficiency Virus (HIV) enhancing infection by respiratory viruses such as IAV [79–81]. Secondary viral infection of hosts can also be a trigger for the reactivation of latent infections, likely through upregulation of the immune response [76,82].

1.3.1.2 Viral interference

Viral interference occurs when coinfection results in the repression of another virus, again mediated predominantly by interferon, as reviewed by Dianzani, 1975 [83]. The main idea is that infection by the first virus triggers a strong immune response that blocks the replication of the other virus at the whole host level. This has been demonstrated for a myriad of coinfecting respiratory viral combinations (reviewed by Piret and Boivin. 2022 [84]) including recently between IAV and SARS-CoV-2 by Dee *et al*. 2023 [85]. This can create populations of hosts with temporary resistance to viral infection, which can be observed in waves of case numbers at a population level [86].

In the literature viral interference is often confused with the distinct phenomenon of superinfection exclusion (SIE), which is covered in section 1.4 and which will be the main topic of this thesis. A discussion of the differences between the two phenomena will occur in section 1.4.1.

1.3.2 VVIs within cells

Next, we will discuss some types of VVIs inside cells. This is not an exhaustive list as interactions inside cells are very specific according to the combination of coinfecting viruses and the replication cycle of those viruses. I have focused this section on interactions that can occur between viruses from the same viral family, as these are the most relevant for shaping viral diversity, and most relevant to this thesis.

Although not covered in detail in here, it is important to note that there are VVIs occurring within cells between unrelated viruses. Most often this is mediated via what is termed by sociovirology as “public goods” [67,73]. Public goods are factors that are produced by one virus which can benefit another virus. A clear example is an IFN antagonist, which blocks the innate cellular immune response, allowing the producer virus to replicate, but also benefits a secondary coinfecting virus [87,88]. Another example is pseudotyping, where a virus particle contains envelope proteins of a different virus. Recently, it was shown that coinfection between IAV and RSV can produce hybrid particles containing IAV genomes with glycoproteins from both viruses [89]. It was shown that these hybrid particles could evade IAV neutralising antibodies and infect cells that lacked IAV receptors,

demonstrating that IAV can use RSV glycoproteins as a public good to expand its cellular tropism. These types of VVIs are important, specific and generally underappreciated.

For this thesis I wanted to focus on the relatively well-characterised VVIs that occur between related viruses. I will review this below, with a specific focus on IAV and SARS-CoV-2.

1.3.2.2 Genetic exchange

As briefly covered in section 1.1.3, genetic exchange is the main driver behind the emergence of pandemic strains of IAV and, arguably, SARS-CoV-2 [90,91]. Genetic exchange between viruses requires the coinfection of individual cells. Genetic exchange is mediated by reassortment for IAV and recombination for SARS-CoV-2. Here we will cover the mechanisms and regulation of reassortment and recombination.

Reassortment occurs via the packaging of genome segments from different parental viruses into nascent viral particles. This is possible for any virus with a segmented genome, including IAV (the genome structure of IAV is reviewed in section 3.1). During the replication of coinfecting IAVs within a cell, the genome segments from both viruses come together and gather at the cell membrane prior to budding. In theory, whether each segment originated from each parental virus is determined randomly to create viruses of any combination, however in practice some segments tend to be coinherited together, likely mediated by RNA-RNA interactions between the segments [92]. Studies have suggested that the RNA-RNA interactions occur between the packaging signals on the segments, as swapping of packaging signals allowed the production of recombinant viruses not observed in nature [93,94]. By extension, if the genome segments of coinfecting viruses have incompatible packaging signals such that it cannot form the key RNA-RNA interactions, they are unable to successfully reassort, a phenomenon known as segment mismatch [95].

Recombination, in contrast to reassortment, occurs during replication of the viral genome rather than during packaging. For SARS-CoV-2 this typically this occurs via a template switch mechanism, whereby the viral polymerase dissociates from one viral genome, and attaches to another before continuing to replicate – which results in the swapping of whole sections of the viral genomes [96].

This process requires genomes from different viruses to not just to be in the same cell, but most likely located in the same double membrane vesicles (DMVs) which is the subcellular site of SARS-CoV-2 genome replication [97]. The precise triggers which cause the polymerase to template switch are currently unknown, but it is likely controlled by genetic similarity between the virus genomes, or RNA secondary structure, or a combination of the two [97].

1.3.2.3 Multiplicity reactivation

Brooke *et al*. 2013 revealed that most IAV virus particles do not encode all the essential proteins to productively infect a cell [98]. Particles that do not effectively encode the complete influenza genome are termed semi-infectious particles (SIPs), and they constitute around 90% of the viral particle population. In SIPs one or more of the viral proteins are not produced in a functional form during infection This could be due to a variety of reasons, for example the dysfunctional segment may carry deleterious mutations, be degraded before it reaches the nucleus for replication, or be missing entirely. To induce a productive infection, SIPs must be complemented with another virus particle carrying a functional genome segment [99,100]. This is known as multiplicity reactivation and can only occur during coinfection of a cell with multiple SIPs or through the coinfection of a SIP with a wild type (WT) viral particle (also known as a fully infectious particle (FIP)). Although IAVs provide the clearest example of this phenomenon, it could theoretically occur between coinfecting viruses of any viral family, if they are carrying a lethal mutation [101].

1.3.2.4 Defective interference

Defective interference is mediated by defective interfering particles (DIPs) which carry defective viral genomes (DVGs). DVGs are naturally generated during the replication of many viruses, including IAV and SARS-CoV-2 [102,103]. DVGs come in a variety of forms (as reviewed by Vignuzzi and López. 2019 [104]). The most common form have a single large internal deletion which removes the coding information for one or multiple genes, while retaining the ability of the genome to be replicated and packaged into new virions. As DIPs lack at least one gene, they usually need to coinfect cells with a particle that provides the missing gene, usually a wild-type particle (WT), in order to replicate [105,106]. However, because DVGs are usually shorter than the WT genome, they

are replicated faster and therefore compete for viral polymerase complexes and for space inside nascent virus particles. It has also been suggested that DIPs trigger stronger interferon responses than WT particles, therefore interfering with the ability of WT particles to infect and replicate [107]. Over time this leads to the virus population becoming overwhelmed with DIPs and therefore the number of WT particles reduce. However, as DVGs cannot replicate without coinfection with WT particles, this leads to a reduction in DIPs, and the subsequent recovery of the WT population. This leads to a classical cyclical pattern in the proportion of DIPs and WT particles in the population [108].

As IAV SIPs and DIPs both carry at least one non-functional gene and rely on coinfection for replication, parallels can be drawn between the two types of particle. A distinction between them can be made on several grounds, summarised in table 1.1 below, the simplest of which is that the non-functional segment in SIPs does not compete with the WT virus, whereas DVGs in DIPs do. However, the non-functioning gene in a SIP may on some level interfere with the production of WT particles. For example, because that gene is missing, it could alter the stoichiometry of the viral proteins inside the cell, leading to less efficient replication, a theory known as gene dosing [109]. As another example, the non-functioning protein may fold incorrectly, triggering a strong innate immune response. Similarly, there have been descriptions of DVGs that vary in their ability to induce innate immune responses, suggesting the presence of “strong” and “weak” DIPs [110]. This leads to the question: how interfering does a SIP need to be in order to count as a DIP? In reality, it is likely that there is a spectrum in IAV particle diversity: from WT particle, to truly non-interfering SIP, to DIP.

Table 1.1: Differences between influenza virus DIPs and SIPs

DIPs	**SIPs**
DVG interferes with the production of WT particles	Non-functional gene does not interfere with production of WT particles
Production is favoured in high multiplicity of infection (MOI) passaging conditions [102]	Production occurs in low MOI passaging conditions [98]
DVGs are mostly generated from the polymerase gene segments [111]	Non-functional genes originate in equal proportion across all genome segments [112]
Proportion displays cyclical pattern throughout the course of infection [108]	Proportion remains stable throughout the course of infection (Seema Jasim, unpublished data).

1.4 Superinfection Exclusion (SIE)

In simple terms, SIE (also known as homologous interference, superinfection interference or superinfection inhibition) is the phenomenon whereby a secondary infecting virus is blocked from infecting a cell which has been previously infected with a genetically similar virus. In this way, SIE is a mechanistic barrier to coinfection at the single cell level.

There are three important requirements for the establishment of SIE: an individual cell, that has been infected previously, with a virus related to the one that is being excluded. This distinguishes SIE from viral interference which is defined as the suppression of replication of one virus in the presence of another virus (as previously discussed section 1.2.3.2). The difference between SIE and viral interference will be discussed in the next section.

1.4.1 SIE versus Viral interference

Table 1.2: The differences between the phenomena of SIE and viral interference

Superinfection Exclusion	**Viral Interference**
Exclusion requires both viruses to be present in the same cell	Exclusion can occur if the two viruses are present in the cell monolayer, whole organ, or whole organism.
Measured by a reduction in the number of coinfected cells	Usually measured by a reduction in viral replication (eg viral titre)
Mediated by a variety of intracellular mechanisms	Mediated by paracrine immune signalling (such as interferon)
Acts between closely related viruses	Can act between distantly related viruses

Both SIE and viral interference phenomena reduce the likelihood the viruses will coinfect cells, but they work at different scales. SIE is an effect observed in individual cells and requires the viruses to be present in the same cell. It is not a systemic effect. There is, to my knowledge, only one example in the literature where the exclusion state was transferable from cell to cell. In this study, Vero cells persistently infected with Junin virus (JUNV) could transfer the SIE phenotype to naïve Vero cells. However, this was only possible if the membranes were touching, showing that it did not involve long-range signalling [113]. Observations of SIE in the literature mostly focus on measuring the expression of the proteins or RNA of the superinfecting virus in previously infected cells [114–116]. Viral interference, on the other hand, is primarily a systemic effect and therefore the interacting

viruses can be in completely different part of the body. For instance, early studies found mice inoculated with yellow fever virus (YFV) were protected from death induced by IAV despite the different tissue affinities of these viruses [117] Most viral interference interactions are measured by a reduction in viral titres of each virus (comprehensively reviewed by Kumar *et al.* 2018 [40]). It should be noted that often SIE is also accompanied by a reduction in viral titre, and therefore the phenomena can only be distinguished by detecting viral replication in individual cells.

As would be expected for what is primarily a systemic effect, viral interference is assumed to be mediated by a secreted factor. In mammalian systems then, it is most often attributed to the action of interferon, as discussed in section 1.3.1.2 [118,119]. The theory is that one virus triggers an innate immune response, and therefore the release of interferon, which then restricts the replication of the other virus [83]. A specific example of this can be seen in a recent study by Dee *et al.* 2023 [85], in which they reported that IAV and RSV induced increased the innate immune response in bronchial epithelial cultures, which then greatly restricted SARS-CoV-2 replication. Blocking the interferon response using a drug called BX795 restored SARS-CoV-2 replication. Similarly, IAV restricts RSV both *in vivo* and *in vitro*, a phenomenon associated with expression of interferon-induced IFIT proteins [120]. This phenomenon is not limited to respiratory viruses: Rubella virus (RUBV) interferes with the ability of vesticular stomatitis virus (VSV) and Newcastle Disease Virus (NDV) to infect cells, however this restriction was reduced in cells that are defective in the interferon response [121]. In contrast to viral interference, there is increasing evidence that SIE is not mediated by interferon. For example, exclusion at the single cell level can be achieved even in Vero cells which lack expression of the interferon receptor, as was shown with influenza viruses [122] and rat borna viruses [123]. Similarly, SIE induced by Chikungunya virus (CHIKV) is maintained even when blocking the interferon receptor using antibodies [124]. For vaccinia virus (VACV), a block to infection found at the fusion of viral endosomal membrane was shown to be independent of interferon-inducible transmembrane proteins, indicating that these proteins are not involved in SIE [125]. In this thesis, I show that a drug that blocks the interferon response does not impact SIE initiated by influenza responses, and nor does knockout of key interferon mediator IRF3 (section 5.4 of this thesis).

Therefore, evidence from a wide variety of different viruses suggests that SIE is not mediated by interferon, in contrast to viral interference. Instead, mechanisms for SIE vary greatly between different viruses. The mechanisms for SIE for mammalian viruses will be reviewed in section 1.4.3.

The final difference we observe between SIE and viral interference is that SIE acts between closely related viruses. As interferon is produced by cells in response to the infection of most viruses, and can effectively restrict the replication of most viruses, it can act between heterologous viruses. SIE, by contrast, is driven by mechanisms distinct to each virus and the exclusion effect is specialised to homologous or closely related viruses. SIE has primarily been observed when the superinfecting and primary infecting viruses are isogenic, as is the case for our investigation of SIE by IAV and SARS-CoV-2 in this thesis [126,127]. There is evidence that the exclusion effect is strongest when the viruses are closely related to each other [113,127]. This raises the question, how closely related do the viruses have to be to be subject to SIE? There is evidence that the distinction might be at the level of viral family: as VACV could exclude a related orthopoxvirus, but not a flavivirus or a rhabdovirus [125]. A similar study using WNV showed that the exclusion effect was reduced when superinfecting with increasingly distantly-related flaviviruses and was abolished when superinfecting with a non-flavivirus [126]. Whereas, the related retroviruses Simian Immunodeficiency Virus (SIV) and HIV-1 were shown to effectively exclude each other [128], as were the H1N1 and H3N2 subtypes of IAV [122]. However, this seems to not always be the case, as cells that had established SIE following herpes simplex virus 1 (HSV-1) infection were resistant to infection by HSV-1, but not to infection by related virus HSV-2 [129]. There has been some suggestion in the literature that exclusion is maintained when the mechanism targets a common feature of the coinfecting virus replication cycles. For example, cells infected with parainfluenza virus 3 (PIV3) become refractory to PIV3 infection due to cleavage of sialic acid (SA) by the viral haemagglutinin-neuraminidase (HN) protein, but this does inhibit infection by HSV-1 because this virus does not use SA for entry [130]. This intuitively makes sense, but the extent to which it applies to all SIE mechanisms is unknown. There is one example in the literature of interferon-independent SIE in which a virus, in this case CHIKV, blocks the infection of a cell by unrelated viruses (in this case

IAV) [124]. This mechanism is currently unknown but does indicate that SIE induced by some viruses may act on unrelated viruses, perhaps by blocking viral use of a host factor common to the replication cycle of the coinfecting viruses.

Thus, I propose that distinction be made between the phenomena of SIE and viral interference. This is because they act at different scales, using different mechanisms and work to restrict different types of viruses. I believe this will help avoid confusion in the literature, and aid understanding of both phenomena.

1.4.2 Timing of SIE

SIE is a temporal effect, as the block to secondary infection does not typically occur immediately after primary infection of a cell. Often this leads to a situation where initially the cells are permissive to secondary infection, and as time between infection events is increased, the cells become less permissive to infection.

The kinetics of SIE induction between different viruses varies wildly. Alphaviruses such as SFV initiate SIE extremely quickly following primary infection, in some cases within as little as 15 minutes [131,132]. It seems most mammalian viruses institute SIE within 4 – 8 hours of primary infection [116,122,131,133]. I found that for IAV, the rate of SIE onset can be increased by changing increasing amount of primary infecting virus (shown in section 5.3 of this thesis). I hypothesise that this could be because increasing MOI can increase the rate of virus replication [116,134], which could speed up the onset of SIE. The link between the length of the virus lifecycle and the timing of the onset of SIE is not known. The idea that a faster virus replication cycle results in a faster onset of SIE is intuitive for SIE mechanisms that require expression of certain virus proteins. However, for viruses where the mechanism of SIE is unknown, the possible link between replication rate and rate of onset of SIE is more obscure.

How long does the exclusion state in the cells last? For viruses that cause cytopathic effect in the cells they infect, such as IAV, we presume that the exclusion effect is maintained until the cell dies [116]. For viruses that establish persistent infection, it seems that exclusion is associated with the

continued expression of viral proteins, which has been shown up to 21 days in persistent bornavirus infection [113,115,123,135]. In one study with cells persistently infected with bovine viral diarrhoea virus (BVDV) the researchers noticed that infected cells lost their exclusion phenotype by 3 days post superinfection. As the progeny of the persisting virus could establish exclusion in fresh cells, the researchers concluded that persistent infection changed the cells such that they eventually became permissive to superinfection, showing that SIE is not a final established state for this virus [132].

1.4.3 Mechanisms of SIE for Mammalian Viruses

I have decided to focus this review on the mechanisms of SIE between mammalian viruses. This is because, although SIE is also established by plant, avian and bacterial virus infection [136–138], I hypothesise that the mechanisms will be less relevant to the focus of this thesis, namely IAV and SARS-CoV-2.

Mammalian viruses from diverse viral families have been observed establishing SIE. Superinfecting viruses can be blocked at various stages of their lifecycle, but broadly the stages affected by SIE cluster into three groups: blocks at adsorption, at the point of entry and uncoating, and at viral replication and translation of viral proteins. These groups are summarised in table 1.3 and fig. 1.1 below and explained in the following sections.

Some viruses appear in the table more than once, where multiple mechanisms have been proposed in the literature at different stages of the virus lifecycle. The reasons for multiple SIE mechanisms could be threefold. Firstly, by instituting multiple redundant blocks, superinfection could be more tightly controlled. A cascade of blocking effects could also ensure SIE is effective at different times following primary infection, as is the case for Semliki Forest Virus (SFV) [131]. Secondly, the same virus could achieve SIE through different mechanisms in different cell types due to the availability of cellular factors [113,139]. Finally, different SIE mechanisms may occur if a virus is in a different replicative mode. For example, a mechanism of SIE is active when JUNV has established a persistent infection in a cell, but that specific mechanism is absent if the virus enters an active infection cycle [113,140].

Virus where SIE is observed	Stage of the virus lifecycle	Mechanism	References
Human Immunodeficiency Virus 1 (HIV-1)	Adsorption	Internalisation and reduced replacement of receptor	[128,141,142]
Foamy Virus (FV)	Adsorption	Mechanism unknown (possibly block access to receptor)	[141,143]
Measles Virus (MV)	Adsorption	Redistribution of receptor	[115,144]
Human Papilloma Virus (HPV)	Adsorption	Mechanism unknown (possibly downregulation of receptor)	[145]
Influenza A Virus (IAV)	Adsorption	Destruction of receptor	[146]
Parainfluenza virus 3 (PIV3)	Adsorption	Destruction of receptor	[130]
Newcastle disease virus (NDV)	Adsorption	Destruction of receptor	[147]
Bovine Viral Diarrhoea Virus (BVDV)	Adsorption	Mechanism unknown (possibly interaction of viral protein and receptor)	[132]
Semliki Forest Virus (SFV)	Adsorption	Block access to receptor	[131]
Vaccinia Virus (VACV)	Adsorption	Physical repellent of superinfecting virus	[148]
Vesticular Stomatitis Virus (VSV)	Entry	Reduced endocytosis	[127,149]
Vaccinia Virus (VACV)	Entry	Block at cell surface and endosome fusion	[125,133,150]
Semliki Forest Virus (SFV)	Entry/uncoating	Block at endosome fusion and uncoating of nucleocapsid	[131]
Herpes Simplex Virus – 1 (HSV-1)	Entry	Block endosome fusion via downregulation of cellular fusion molecule	[129,151]
Pseudorabies virus (PRV)	Entry	Mechanism unknown	[152]
HSV-1	Post-entry	Mechanism unknown	[152]
Chikingunya virus (CHIKV)	Replication	Mechanism unknown	[124]
Borna Disease Virus (BDV)	Replication	Mechanism unknown (requires expression of viral proteins)	[123]
IAV	Replication and translation	Mechanism unknown (possibly competition for cellular replication components)	[116,122]
Hepatitis C Virus (HCV)	Replication and Translation	Mechanism unknown (possibly competition for cellular replication components)	[114,153]
West Nile Virus (WNV)	Replication and translation	Competition for cellular replication components synthesis	[126]
Rubella Virus (RUBV)	Replication and translation	Mechanism unknown (possibly cleavage of antigenomes)	[135]

Sindbis Virus (SV)	Replication	Mechanism unknown (possibly block synthesis of RNA)	[154,155]
Junin Virus (JUNV)	Budding	Distruption to release of virus particles	[139]

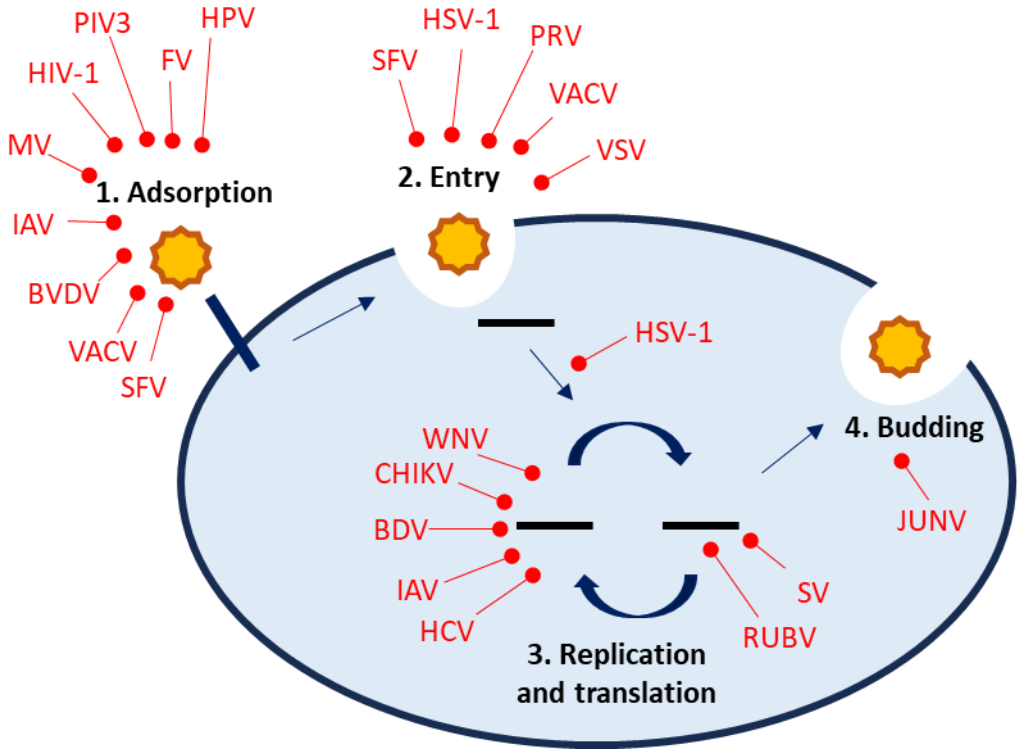

Figure 1.1: Stages of the mammalian virus lifecycle where SIE blocks secondary infection.

Semliki Forest virus (SFV), Vaccinia virus (VACV), Bovine Viral Diahorreal virus (BVDV), Influenza A virus (IAV), Measles virus (MV), Human Immunodeficiency virus -1 (HIV-1), Parainfluenza virus 3 (PIV3), Foamy virus (FV), Human papilloma virus (HPV), Herpes Simplex virus -1 (HSV-1), Pseudorabies rabies (PRV), Vasticular Stomatitis virus (VSV), West Nile virus (WNV), Chikingunya virus (CHIKV), Borna Diseases virus (BDV), Hepatitius C virus (HCV), Rubella virus (RUBV). Sindbis virus (SV), Junin virus (JUNV)

Adsorption

As the first step of the virus lifecycle, blocking adsorption to a previously infected cell is the first opportunity for the induction of SIE. Adsorption, which refers to the attachment of viruses to the surface of the target cell, is mediated by attachment factor proteins on virus particles binding to receptor molecules on the surface of the cell. Therefore, it follows that the availability of receptors acts as a potential bottleneck to regulate superinfection. Reducing the access of a superinfecting virus to receptors can occur in four main ways.

Firstly, the primary infecting virus can mediate the removal of the receptors from the cell surface. There is significant evidence that several retroviruses actively downregulate the surface expression of their receptors to prevent superinfection [141]. For example, HIV-1 Nef protein binds directly to the viral receptor CD4, which induces endocytosis of the receptor and its degradation within the lysosome [128]. Simultaneously, another viral protein, Vpu, blocks the transport of newly synthesised CD4 receptor complexes to the cell surface, instead retaining them in the Golgi complex [142]. Together, these mechanisms work to remove available receptor molecules from the cell surface.

Secondly, viruses can block physical access of the secondary virus to the viral receptor. For Foamy Virus (FV) [143], and Semliki Forest virus (SFM) [131], SIE is mediated by the expression of viral attachment proteins on the cell surface. For both, the overexpression of these proteins correlated with how resistant the cells are to superinfection, but for FV this was specifically shown to require the full-length attachment protein Env being located at the plasma membrane. This suggests a mechanism whereby the viral attachment proteins block the viral receptors, therefore blocking secondary viral infection. Another way to block physical access of the superinfecting viruses to the receptors is through redistribution of the receptors. It has been shown that persistent measles virus infection results in the receptor, CD46, becoming relocated into islands irregularly dotted along the plasma membrane, which blocked superinfection. Uninfected cells, by contrast, display an even distribution of receptors and were susceptible to infection [115]. Therefore, blocking physical access to receptors allows control of superinfection potential.

Thirdly, the primary infecting viruses can destroy the receptor on the cell surface thereby blocking superinfection. Some viruses, such as IAV and paramyxoviruses, like parainfluenza virus 3 (PIV3) and Newcastle disease virus (NDV), encode proteins with neuraminidase (NA) activity, which cleave the sialic acid (SA) residues present on many cell surface glycoproteins, which act as the attachment factor for entry of these viruses [156]. The primary purpose of encoding protein with NA activity is to detach nascent viruses from the cell surface, but it has been shown that overexpressing the NA proteins of these viruses render cells refractory to secondary infection by the same virus [105,130,147]. Researchers also found these cells were resistant to infection with other viruses which use SA for attachment, whereas they were not resistant to superinfection with HSV-1 which attaches using a different receptor [130,147]. For SIE induced by influenza virus, the role of NA is controversial. One study found that neuraminidase inhibitors blocked the establishment of SIE for influenza viruses [146], showing that SIE is mediated directly by NA activity, however another study found no effect on SIE with NA inhibitors [122].

Finally, a very interesting mechanism has been proposed for vaccinia virus (VACV). It has been established through electron microscopy (EM) that nascent VACV virions can bud from infected cells from the tip of protrusions called microvilli [157]. It has been proposed that this mechanism may also be used to repel superinfecting genomes; physically pushing them away from previously infected cells [148]. The authors of this study propose that cells expressing A33 and A36 viral proteins early in infection results in the formation of actin tails that push the viruses towards the neighbouring cells, which explains the relatively rapid spread of VACV infectious foci compared to other related viruses. This is the first, and to our knowledge, the only description of physical repulsion of superinfecting viruses and offers an interesting alternative to more well-established mechanisms.

Overall, adsorption as an important point in a superinfecting virus lifecycle where infection can be restricted.

Entry and Uncoating

Following adsorption, the superinfecting viruses must enter the cytoplasm and then disassemble their protein coat to release the viral genomes (known as uncoating) ready for transcription and replication. For non-enveloped viruses, this occurs by forming pore in cellular membranes either at the surface or inside the cell. For enveloped viruses, fusion between the virus envelope and cellular membranes must occur. This commonly occurs via direct fusion at the plasma membrane, or by endocytosis into membrane-bound vesicles called endosomes, which then fuse with the viral membrane. Entry through these mechanisms and subsequent uncoating of secondary infecting viruses can be blocked following primary infection of a cell to restrict superinfection. In this section I will explore examples of how this can occur.

Some viruses enter cells exclusively through one entry mechanism, and therefore this can be restricted to induce SIE. For example, VSV enters cells through clathrin-mediated endocytosis (CME) [158], and this process is restricted following primary infection to block secondary infection [149]. By measuring cell markers on the surface of the cells, the researchers showed the SIE onset results in a reduction in the overall rate of endocytosis characterised by the retaining of the markers on the cell surface. Upon further investigation using electron microscopy (EM), the group found that there was a reduction in the number of clathrin-coated vesicles in the cells which were resistant to superinfection compared to uninfected cells. The group noted that of the vesicles that were present, many lacked the distinctive clathrin coat in the vesicles. The group did not suggest a direct mechanism for this, but another study also found that SIE of VSV restricts secondary viral infection at the entry step, and that this requires the expression of the functional viral transmembrane glycoprotein G [127]. Glycoprotein G, therefore, may act directly or indirectly to destabilise the formation of endocytic vesicles, reducing the rate of endocytosis and causing SIE onset, although direct evidence of this is lacking.

Some enveloped viruses enter cells both through both endocytosis and direct fusion at the plasma membrane, and therefore entry must be inhibited in multiple compartments to establish SIE [133]. This can be achieved by inhibiting the fusion step itself, as both entry mechanisms require fusion of

the envelope of secondary infecting viruses with the cellular membranes. An example of this is VACV, where SIE onset causes a reduction in the ability of the viral cores to enter the cytoplasm, as observed by EM [125]. SIE occurs due to the expression of A56 and K2 viral proteins from the primary infecting virus which then locate to the plasma membrane. These then form a heterodimer on the cell surface which binds to the fusion machinery on the virus particle and prevents later fusion of the virus with membranes, both within the endosome and at the cell surface [150]. An A56/K2 independent VACV SIE mechanism has also been discovered as mutant viruses that with defective A56 and K2 were still able to prevent membrane fusion of secondary infecting viruses, at an earlier stage than is inhibited by A56/K2 [125]. Therefore, it is possible that two mechanisms work together to establish an exclusion state in the cells which results in a complete block of release of viral cores into the cytoplasm.

Another strategy to prevent fusion of secondary infecting viruses is via the downregulation of cellular factors that aid in fusion, as is the case of HSV-1. Glycoprotein D (gD) is the receptor binding protein of HSV-1 and usually binds molecules including nectin-1 inside endosomes to trigger fusion of viral and cellular membranes [159]. Cells overexpressing gD was shown to block fusion of the virus without affecting the number of viruses adsorbed on the surface of cells [129]. It has therefore been suggested that the upregulated gD binds to cellular fusion factors and redistributes or downregulates them, blocking fusion [151]. Therefore, fusion can be suppressed by changing cellular or viral factors on either the endosomal or cellular surface.

Some viruses can block both the fusion and uncoating steps involved in entry to maintain a repressive state in the cells. SFV has been shown to block fusion, and therefore the release of nucleocapsids into the cytoplasm, by reducing the acidification of early endosomes [131]. Endosomal acidification is a key step for triggering fusion of many viruses, as it causes conformational changes in fusion proteins allowing them to mediate fusion [160]. Following fusion, SFV nucleocapsid cores rapidly uncoat once they are in the cytoplasm [161]. However, in cells infected previously with SFV, the capsids from secondary infecting viruses were remarkably stable in the cytoplasm, compared to the stability in uninfected cells [131]. The researchers noted that the

stability of secondary incoming capsids mirrored the stability of newly synthesised viral capsids produced during replication of the primary virus. No mechanism has been identified for this, but it is likely that the same mechanism that stabilises nascent capsids is acting on incoming capsids.

Therefore, entry of the virus particles into cells and uncoating of viral capsids are key points where regulation of superinfection can be maintained.

Replication

For many viruses, SIE has been described as a block at translation of viral gene products or the replication of the viral genome [114,122,126,135,153,154]. These viruses come from diverse viral families, replicate in different cellular compartments, and use different cellular and viral factors for replication however they all display a block at the same part of the viral lifecycle. Unlike during the adsorption and entry and uncoating steps, the secondary and primary infecting genomes are likely to be present in the same cellular compartment, and therefore mechanisms blocking replication is likely to affect the replication of both the primary and secondary genomes. Additionally, the genomes of the two viruses as they are likely to be genetically and structurally identical to one another. If replication is maintained from the primary infecting genomes while SIE is active, it is not currently clear how the mechanisms differentiation between primary and secondary viral genomes.

For positive-sense RNA viruses, where proteins can be translated directly from the genome, blocks to replication (and not translation) can be confirmed by transfecting minigenomes into cells and measuring viral protein expression. For WNV, for example, it was found that the block was specifically on RNA viral synthesis, as transfected RNA produced equal luciferase signal in cells that had established SIE compared to uninfected controls. By contrast, when cells were transfected with a luciferase template that required production of RNA prior to translation, the luciferase signal dropped 100 -1000-fold 24-72 hrs following infection [126]. Similarly in Rubella viruses, proteins from an RNA construct that can be translated but not replicated were found in cells that had established SIE, showing that protein translation was occurring as normal, while replication was repressed [135].

One study found that for HCV the SIE was controlled at the level of translation of secondary viral proteins. The group found a 2-fold reduction in a luciferase signal from reporter proteins produced from replication-deficient sub-genomic RNAs in cells that had established SIE, compared to cells that had not established SIE. This was shown to be a specific block to IRES-dependent translation, the translation mechanism used by HCV viral RNA, which did not affect cap-dependent translation, the mechanism most used by cellular mRNA [114,162]. This is disputed by another paper which found no effect of SIE on primary HCV translation, in a similar experimental system [153]. The reason for this discrepancy is unclear, but potentially as the reduction in signal following establishment of SIE is relatively modest (2-fold), it may be difficult to detect by other methods.

For many viruses, it was shown that SIE blocks secondary viral replication and translation, but no mechanism has yet been demonstrated. In all cases, various combinations of viral proteins are required for establishment of an SIE state in the cell, but it is not clear how these proteins establish SIE [124,126,135,153,154]. This is the case for IAV, where it was shown that an SIE-like state is established when the cell was transfected with the components to form actively influenza polymerase complexes (FluPol) capable of transcription or replication of RNA [122]. This complex is made of the polybasic protein 1 (PB1), polybasic protein 2 (PB2), polyacidic protein (PA), with the nucleoprotein (NP) required to encapsulate the template RNA for replication. The authors demonstrated that SIE was abolished when the PA component was removed, or when the template was missing the untranslated region sequences required for recognition by the polymerase, demonstrating the importance of active FluPol complexes in the absence of any other viral proteins.

Commonly it is suggested that primary infecting viruses block secondary virus replication and translation by saturating host factors that would also be required for the replication of a superinfecting virus [114,122,126]. This would imply that SIE is established because the primary and secondary virus compete for access to the host factors. Thus, if the ratio of secondary infecting to primary infecting viruses increases, we would expect secondary infecting viruses to be able to overcome the block instituted by the primary infecting virus. In section 5.3 of this thesis I found

that, for IAV, increasing amount of secondary infecting virus does not alter the SIE onset kinetics and therefore competition is not the primary mechanism driving SIE of IAVs [116].

Overall, the replication of superinfecting viruses is frequently blocked to maintain SIE. However, the mechanisms by which this occurs has not yet been fully elucidated.

Blocks at other stages of the life cycle

Blocks to viral egress seems to be rare as a strategy for SIE establishment, however the lack of reported mechanisms that focus on this area of the virus lifecycle could be explained by lack of investigation into the effect of SIE on this stage of the virus lifecycle. There is only one example in the literature where the budding of virus is implicated in maintenance of SIE [139]. The paper found that cells persistently infected with JUNV had a reduced level of viral adsorption and protein synthesis, but also that the primary and superinfecting viruses remain very closely cell associated compared to naïve cells. This was linked to the increased synthesis of TSG101, a protein involved in "pinching off" of several viruses, in the persistently infected cells [163]. Rather than aiding budding in the persistently infected cells, the authors propose that the altered stoichiometry of TSG101 may instead lead to inefficient budding, and/or the downregulation of cell receptors involved in budding. As with mechanisms restricting replication, it is hard to envision that a block to egress would not impact both the primary and secondary viruses. If differentiation is made, how this occurs is not currently known.

1.4.4 Applying sociovirology to SIE

As reviewed in section 1.3, sociovirology is framework that seeks to understand how traits of cooperation, competition and altruism evolved among viruses. We can apply this theory to SIE to understand how these mechanisms may have evolved. It is worth clearly stating that no evolutionary trait evolved for a specific purpose and cooperating or competing viruses do not "intend" to interact in a particular way. Rather, the mechanism of interaction gives selective advantage to a genotype which allows it to be retained over generations. In this section then, we are evaluating the potential selective advantages of SIE which may explain why it is a conserved mechanism across many diverse viral families.

First, we must consider the hypothesis that SIE did not evolve because preventing secondary infection provides any benefit to the virus but is a side effect of viral infection of a cell. We cannot rule out this possibility, indeed some compelling theories for how this might happen have been proposed. For example, for non-lytic viruses, it is advantageous to the virus population to prevent nascent progeny viruses from attaching to and re-entering the cell they were just produced from. Therefore, viruses may induce SIE mechanisms, not to prevent secondary infection, but to prevent their own progeny particles from being sequestered by an already-infected host cell. Another proposal has been made by Perdoncini Carvalho et al. 2022 [164], who argue that intracellular SIE mechanisms may have evolved to prevent replication from progeny genomes, thereby controlling the catastrophic error rate that would accumulate with multiple rounds of replication from error-filled progeny genomes.

Next, we must consider that it is not always clear whether SIE is driven by the virus or the host cell. In some cases where the mechanism of SIE is mediated by the expression of specific viral proteins, SIE is clearly virally driven. However, in many instances, the mechanism is unknown and we must consider that a host factor could be responsible. It is not obvious how SIE would provide a selective advantage for a host cell, given that cell is already infected and presumably making viral progeny. It is possible that SIE is caused by antiviral restriction mechanisms that are slow to become active, thereby not restricting primary infection but effective against a secondary virus. However, studies typically suggest that cellular immune mechanisms, especially interferon-dependent mechanisms, are not involved in the specific restriction of secondary viral infection [122–125]. In latent infections, where viral progeny is not being produced, superinfection can reactivate the latent virus which leads to cell death, as has been shown with HIV-1 [165]. However, the extent to which SIE is maintained in latent infections is not clear. Overall, although it is possible that SIE is cellular driven phenomenon, it has yet to be elucidated how cells would evolve such a mechanism.

If we assume that SIE is a virus driven mechanism specifically evolved to prevent secondary infection, what are the evolutionary benefits of this to individual virus genomes? SIE is a competitive trait. Early-stage restriction mechanisms that act at the point of adsorption, entry or replication

block the ability of a second virus to replicate its progeny. This ensures that viral replication resources are retained for the primary infecting virus. Late-stage restriction mechanisms are also competitive in nature, although they do not protect the primary infecting virus from competition inside the coinfected cell. Simulations using bacteriophage suggest that a population that initiates SIE should quickly outcompete a population that permits superinfection [166]. However, sociovirology principles guide that cooperative traits between genetically identical or related viruses are likely to be beneficial and fix in the population through kin selection, and SIE appears to be most functional between genetically similar individuals. What benefit does SIE provide to individual genomes which could explain this discrepancy?

For some viruses, SIE may offer a selective advantage by controlling how quickly new viruses are produced. Coinfection between IAVs has been shown to increase the rate of viral replication cycles which can lead to and increased viral burst size and faster immune activation in the host [134,167]. Faster replication cycles may also lead to premature cell death. It has been suggested that HIV-1 inhibits surface expression of its receptor CD4, and therefore superinfection, to prevent cell death and expand the period of effective virus production [168].

Another advantage of SIE might emerge for viruses that block the adsorption of superinfecting viruses as this frees up viruses to preferentially infect uninfected cells. This may be a way to inflate the number of cells the virus can infect when the quantity of virus particles is limiting, such as directly after transmission [169]. A striking example of this is VACV, where superinfecting viruses are physically pushed away from previously infected cells, leading to a greater size of the focus of infection than can be explained by single-cell replication kinetics [148]. Therefore, SIE mechanisms that prevent adsorption of secondary viruses could benefits the virus population, by allowing viruses to reach as many cells as possible.

Early-stage restriction mechanisms prevent the primary and secondary viruses from engaging in within-cell VVIs, some of which are reviewed in in section 1.3.2. Restricting VVIs could be beneficial when those VVIs are detrimental to virus replication at the individual and population level, as in the

case of defective interference. In defective interference, defective viral genomes (DVGs) compete with the full-length viral genome and parasitise the viral population. By blocking coinfection via SIE, the primary infecting virus may prevent coinfection between fully-intact viral genomes and DVGs, preventing parasitisation. Furthermore, DVG generation is more likely during when there are a high number of virus genomes in the cells [104]. Therefore, SIE may have evolved as a strategy to prevent DVG propagation by tightly controlling the number of genomes that enter and replicate in the cell.

Restricting VVIs via SIE is not so beneficial when those interactions are essential to maintaining viral replication, as in the case of IAV and multiplicity reactivation. As reviewed in section 1.3.2.3, SIPs make up the majority of the IAV population and require coinfection to induce productive infections in a process known as multiplicity reactivation [98,170]. Where coinfection is blocked by SIE, most viral genomes cannot propagate and overall the virus population risks collapse as it relies on the small proportion of WT particles for infection propagation [99,170]. However, there may be two ways for a virus to reduce this risk. Firstly, the time delay for onset of SIE allows the entry and replication of several viral genomes which may permit coinfection of SIPs. Secondly, if the onset of SIE requires replicating viral polymerases or specific viral proteins, as has been implied by some of the mechanisms reviewed above, SIE would mean that several of the viral gene products are being produced, and therefore the cell is less likely to be infected by a SIP and complementation may not be required.

More generally, coinfection has been shown to increase population diversity, not only though genetic exchange but also by assisting propagation of rare mutants [171,172]. Similarly, simulations using bacteriophage suggest that a population that initiates SIE has a reduced ability to acquire beneficial mutations than the population that tolerates superinfection [166]. Maintaining a diverse viral population, via high mutation rates and genetic exchange, is important for generating viruses with selective advantages such as immune escape mutants, but also it must be noted that this process would generate many deleterious mutants. The idea is that natural selection has optimised the high mutation rate of RNA viruses to balance the generation of mutants with a selective advantage and disadvantage. There is evidence that this is an ongoing process, as fidelity of viral

polymerase can adjust if selection pressure changes [173]. Perhaps the presence of SIE mechanisms, which reduce viral diversity by preventing genetic exchange, is accounted for by higher mutation rates. One could imagine a virus setting up a trade-off between diversity and SIE, if SIE offers a selective advantage to viruses that enact it.

To summarise, SIE as a virus-driven trait may have offered a selective advantage to viruses leading to its repeated evolution and conservation across many diverse viral families. As SIE is a temporal effect, some superinfection can still take place within a defined window of time in a cycle of infection, which may allow viruses to benefit from cooperative VVIs. However, through SIE, viruses can control the number of viral genomes that have access to the cell, preventing competition and controlling the rate of virus replication and the production of DVGs. Other fitness benefits of SIE to the viruses are likely specific to the individual mechanisms employed by different viruses, and therefore investigations into the specific mechanisms are still required to fully understand why SIE may have evolved.

1.4.5 Practical applications of SIE

This review of the mechanisms for SIE has focused on mammalian viruses, but it is important to note that the phenomenon has also been observed in many viruses of plants, bacteria and invertebrate hosts [174]. It is in these host organisms where SIE has been explored to solve practical problems.

Firstly, in plant sciences, SIE has been implicated in the phenomena of viral cross protection, a form of inoculation where previous infection of a plant with a mild viral strain protects the virus from subsequent infection with a more virulent strain [175,176]. Cross-protection has been used to protect a wide range of vital food crops such as beans, barley and cassava, and has been touted as a safer alternative to the use of pesticides or the politically charged genetic modification of plants to make them resistant to disease [177]. Although initially this phenomenon resembles viral interference acting at a whole organism level, there is evidence that the phenomenon is mediated by SIE happening at the level of individual plant cells, possibly through cleavage of incoming viral genomes by the plant intracellular RNA silencing mechanism [178]. The extent to which SIE

contributes to this effect remains to be fully elucidated, but it is well accepted that it is important for the phenomenon of cross protection.

SIE has also been implicated in protecting insect vectors from secondary infection with arboviruses that are more deadly to humans in order to prevent transmission [179]. For example, it has been shown that Sindbis virus causes post-transcriptional silencing of Dengue Virus (DENV) in mosquito cells and reduces transmission from mosquitos [180,181]. In a similar way, overexpression of Rift Valley Fever Virus (RVFV) N protein using a Semliki Forest Virus (SFV) expression system blocks subsequent RVFV infection and lowers infected titre release in mosquito cells [182]. There are also several viruses that only infect insects which block infection of human viruses such as chikungunya virus (CHIKV) [179]. Such finding leads to an interesting approach to potentially controlling the spread of deadly arboviruses [183,184].

Therefore, control of SIE has already been involved in solving world problems such as global food security and vector disease control. It is reasonable to hope that a growing understanding of SIE will allow us to manipulate a wider range of pathogenic viruses, including those affecting humans.

1.5 Thesis Aims

There are several knowledge gaps in our understanding of SIE. Coinfection of individual cells by viruses can sometimes be prevented by SIE. SIE is observed for many virus families and is achieved through many different, often poorly characterised, mechanisms. Respiratory viruses co-circulate in the winter in temperate climates and infect the same area of the body. Coinfection of hosts seems to occur relatively frequently, but the dynamics of the interactions that occur between viruses within hosts are poorly understood. It is unknown how frequently cellular coinfection occurs, and which viruses within a population are likely to coinfect cells. However, understanding these processes is important as cellular coinfection allows viruses to undergo genetic exchange, the main mechanism driving emergence of pandemic respiratory viruses.

In this thesis I will address some of these knowledge gaps for IAV and SARS-CoV-2, two respiratory viruses of high clinical importance. I will do this by investigating the kinetics of SIE onset by these

viruses and show how this controls the potential for coinfection between viruses within their hosts. This work is broken down into four aims, each of which are explored in a results chapter:

Aim 1: to characterise an isogenic IAV fluorescent reporter virus system for studying coinfection and to define the kinetics of SIE by IAV.

Aim 2: to explore how SIE at the level of individual cells affects IAV coinfection during localised viral spread, and to model these interactions both *in vitro* and *in vivo.*

Aim 3: to investigate potential mechanisms for SIE between IAVs.

Aim 4: to characterise an isogenic SARS-CoV-2 fluorescent reporter virus system for studying coinfection, to present the first evidence for SIE initiated by any coronavirus, and to explore the dynamics of coinfection between IAV and SARS-CoV-2.

By expanding our understanding of SIE by IAV and SARS-CoV-2, I will attempt to shed light on the interactions between viruses within hosts which can lead to the generation of novel pandemic respiratory viruses. By better understanding these processes, we can improve our knowledge of how these viruses emerge, and potentially develop new strategies to predict and prevent their emergence.

Chapter 2: Material and Methods

Unless otherwise stated, materials were supplied by ThermoFisher Scientific

2.1 Materials

2.1.1 Cells

Table 2.1: List of cell lines

Cell Line	Overexpressing/knock out (KO)	Origin	Source
Madin-Darby Canine Kidney (MDCK)		Dog kidney carcinoma	Prof. P Digard (Roslin Institute, University of Edinburgh)
Human embryonic kidney (HEK) 293T		Human embryonic kidney	Prof. S Wilson (MRC-University of Glasgow Centre for Virus Research)
A459 ACE2 TMPRSS2 (AAT)	Overexpressing ACE2 and TMPRSS2	Human lung adenocarcinoma	Prof. S Wilson (MRC-University of Glasgow Centre for Virus Research)
A549 IRF3 KO	Knockout of IRF3	Human lung adenocarcinoma	Dr C. Bamford (Queens University Belfast)

2.1.2 Antibodies

Table 2.2 List of primary antibodies

Target	Supplier	Catalogue Number	Species	Working dilution
IAV nucleoprotein (NP)	Prof. P Digard (Roslin Institute, University of Edinburgh)	N/A	Rabbit polyclonal	1:500
Mx1	Santa Cruz Biotecnology	H-285	Rabbit polyclonal	1:300
Alpha Tubulin	Sigma-Aldrich	T6199	Mouse monoclonal	1:1000
IRF3	Invitrogen	MA5-32348	Mouse monoclonal	1:500

Table 2.3 List of secondary antibodies

Target	Conjugate	Supplier	Catalogue Number	Species	Working dilution
Anti-rabbit IgG	800CW	Licor	926-32211	Goat	1:10,000
Anti-rabbit IgG	680RD	Licor	926-68071	Goat	1:10,000

Anti-mouse IgG	800CW	Licor	926-32210	Goat	1:10,000
Anti-rabbit IgG	Alexa Fluor 488 (green)	ThermoFisher Scientific	A11034	Goat	1:5000
Anti-rabbit IgG	Alexa Fluor 555 (red)	ThermoFisher Scientific	A31572	Goat	1:5000

2.1.3 Drugs

Table 2.4: List of drugs

Name	Supplier	Catalogue Number	Dilution used	Diluent
Ruxolitinib	Fisher Scientific	AC469381000	0.32 µM	Dimethylsulfoxide (DMSO) to 5mM then Mili-Q water to 0.32 µM
Human interferon (IFN) alpha-14	Biotechne R&D Systems	11145-1	1000 U	Mili-Q water

2.1.4 Buffers and Solutions

Table 2.5: Composition of buffers and solutions

Name	Recipe	Notes
PLP buffer	0.075 M lysine, 0.37 M sodium phosphate (pH 7.2), 2% formaldehyde (v/v), and 0.01 M $NaIO_4$	
Laemmli Buffer	Sodium dodecyl sulfate (SDS) sample dye with 5 µl/ml BaseMuncher benzonase and 100× protease/phosphatase inhibitor (ThermoFisher Scientific)	
SDS sample dye (100mL)	20% glycerol (v/v) with 2% SDS (w/v) with 24 mM Tris pH 6.8 with 0.1 M Dithiothreitol (DTT), 50x dye mix in Milli-Q water	Store in aliquots at -20 °C, do not reuse aliquots
50x dye mix	0.2% bromophenol blue (v/v) with 0.2% cyanol (v/v) in Milli-Q water	
Acid wash	10 mM HCl and 150 mM NaCl in Milli-Q water,	pH 3
Western blotting wash buffer	Phosphate buffered saline (PBS) with 0.1% Tween-20 (PBST) (w/v)	
Western blotting blocking buffer	5% skimmed milk powder (milfresh) in PBST (w/v)	Make fresh each time
Immunofluorescence (IF) permeabilisation buffer	0.1% Triton X-100 in PBS (w/v)	
IF blocking buffer	2% Foetal Bovine Serum (FBS) in PBS (v/v)	

2.2 Cell culture and virus stocks

2.2.1 Maintaining cells

Cells were maintained in complete media (Dulbecco's Modified Eagle Medium (DMEM, Gibco) supplemented with 10% Foetal Bovine Serum (FBS, Gibco)) in cell culture flasks (Corning). All cells were maintained at 37 °C and 5% CO_2 in a humidified incubator. For maintenance, when cells were confluent, they were washed with phosphate buffered saline (PBS, Gibco), followed by an incubation with TrypLE express trypsin (Gibco) at 37 °C until cells were detached from the surface of the flask. These cells were then re-suspended in appropriate medium before they were placed in flasks (passaging) or plated for experimentation. Cells were discarded once they reached passage number 40, or if the morphology of the cells had significantly changed.

2.2.2 Virus rescue

All handling of IAV PR8 and variant viruses (ColorFlu and BrightFlu) were performed at containment level (CL) 2. All handling of SARS-CoV-2 viruses were performed at CL3.

The wild-type (WT) PR8 was generated in HEK293T cells using the pDUAL reverse genetics system, a gift of Prof. R. Fouchier (Erasmus MC Rotterdam); as previously described [185]. The same protocol was used to rescue modified influenza A viruses. ColorFlu viruses (ColorFlu-eGFP and ColorFlu-mCherry) were rescued in HEK293T cells from a pHH21 plasmid encoding a modified NS segment with encoded fluorophores, supplied by Prof. Y. Kaowaoka (University of Wisconsin-Madison, University of Tokyo), and WT PR8 pDUAL plasmids for the remaining seven segments, with site-directed mutagenesis used to introduce the compensatory mutations (HA T380A and PB2 E712D) previously described in the original ColorFlu system [186]. Brightflu viruses were rescued using a plasmid encoding a modified NS segment with encoded fluorophores designed by Dr E. Roberts (synthesised by GeneArt, Invitrogen), alongside the PR8 pDUAL plasmids used to rescue ColorFlu.

SARS-CoV-2 reporter viruses were rescued by Dr. A. Wickenhagen (University of Glasgow- Centre for Virus Research, CVR) as previously described [187].

2.2.3 Preparation of virus stocks

Cells (MDCK for IAV, AAT for SARS-CoV-2) were seeded into T75 tissue culture flasks (Corning) to obtain 70% confluency on the day of infection. The flasks were inoculated with virus diluted to an MOI of 0.001 into 5 ml of the appropriate viral growth media (VGM; table 2.6) for 1 h. Following this, 10 ml of VGM was added and the flasks incubated for 2-3 days at 37 °C and 5% CO_2 in a humidified incubator. For fluorescent viruses, the fluorescence of the cells was monitored during this time using an EVOS fluorescent microscope (M5000, Invitrogen). When 90% of the cells were fluorescing or 90% cytopathic effect had been achieved, the media was collected and centrifuged at 1500 rpm for 3 minutes at 4 °C. Supernatant was then aliquoted and stored at -80 °C.

Table 2.6: Composition of viral growth media

Virus	**VGM recipe**
IAV	DMEM, 0.14% (w/v) bovine serum albumin (BSA; Gibco) and 1 µg/µl N-tosyl-L-phenylalanine chloromethyl ketone (TPCK)-treated trypsin
SARS-CoV-2	DMEM, 2% FBS

2.2.3 Titration of virus stocks

To calculate viral plaque titres, 10-fold serial dilutions of virus were prepared into appropriate VGM and 400 µl added to confluent cell monolayers in 6 well plates. The plates were then incubated at 37°C for 1 h, with gentle rocking every 30 minutes.

For IAV, the inoculum was then removed and replaced with an agarose overlay (table 2.7), which was allowed to set for 20 minutes at room temperature (RT) before transfer to a 37°C, 5% CO_2, humidified incubator.

For SARS-CoV-2, a liquid Avicel overlay (table 2.7) was added to the wells without removing the inoculum, the plates were then gently swirled before placing in a 37°C, 5% CO_2, humidified incubator. The plates were incubated for 2-3 days, taking care not to move the Avicel overlay plates as this would disturb the liquid overlay and disrupt the plaque phenotype. Following this, the SARS-CoV-2 plates were fixed for 1 h in 8% v/v formaldehyde in PBS prior to removal from CL3 suite, in accordance with the safety guidelines.

For both SARS-CoV-2 and IAV plates, the wells were then washed with PBS prior to addition of 1 ml of Coomassie blue stain (table 2.7) for at least 20 minutes. The stain was rinsed off the wells using water and number of plaques containing the highest number of countable (ie non-overlapping) plaques were counted and used to calculate the plaque titre using the following formula:

$$\text{Plaque Titre } \left(\frac{\text{PFU}}{\text{mL}}\right) = \frac{\text{Plaque count (PFU)}}{\text{Volume of innoculum (mL)}} \times \text{well dilution}$$

.

Table 2.7 Overlay and solutions used for viral titration

Solution Name	Recipe	Note
Agarose overlay for IAV titration	Equal volume of 2% (w/v) agarose (final 1% w/v) melted into phosphate buffered saline (PBS; Gibco), and of IAV-VGM, with TPCK trypsin at 1 µg/µl final concentration	TPCK trypsin should be added after mixing other components to avoid denaturing in hot agarose
Avicel overlay for SARS-CoV-2 titration	Equal volume 1.2% (w/v) Avicel (Sigma) in PBS (final 0.6% (w/v) and Minimum Essential Media (MEM).	
Coomassie Blue stain	2 g Coomassie Brilliant Blue dissolved in 250 ml water, with 75 ml acetic acid and 500 ml ethanol. Top up to 1 L with water	

For some experimental applications, the infectious titre of the fluorescently-tagged viruses was measured in focus forming units (FFU). While PFU counts viruses that are able to induce multicycle infection to form a plaque, FFU by contrast counts viruses that are able to induce a cell to become fluorescent during single cycle infection, and therefore also includes semi-infectious particles (SIPs) (reviewed in section 1.3.2.3). To obtain the FFU/mL titre, the virus stock was serially diluted 2-fold into VGM and used to infect a known number of appropriate cells for 1 h before replacing with complete media. After 16 h the cells were harvested into a single cell suspension using TrypLE express (Gibco) and the percentage of positive cells was then assessed using flow cytometry (discussed in detail in 2.4.4). First, for each sample, the number of viruses that caused that number

of positive cells was calculated. To do this, I assumed that viruses were applied to cells evenly, and that all the cells were susceptible to infection, and therefore the number of infected cells could be modelled by the Poisson distribution. The Poisson distribution formula as it relates to this thesis is given below:

$$P(X = k) = \frac{m^k e^{-m}}{k!}$$

Where P(X=k) is the proportion of positive cells at a multiplicity of infection (MOI) *m* (FFU/cell), infected by *k* viruses.

When there are no positive cells P(X=0), there are no viruses in the well (*k* = 0) and therefore:

$$P(X = 0) = \frac{m^0 e^{-m}}{0!}$$

Which can be simplified to:

$$P(X = 0) = e^{-m}$$

For the proportion of infected cells then, where k > 0

$$P(X > 0) = 1 - e^{-m}$$

When the proportion of positive cells (P) was measured and P(0<X>1), the formula can be rearranged to calculate the MOI in FFU/cell *m:*

$$m = -\ln(1 - P)$$

Thus, to calculate the virus titre (FFU/mL):

$$\text{Fluorescent Virus Titre}\left(\frac{\text{FFU}}{\text{mL}}\right) = \frac{m\ (\text{FFU/cell})}{\text{Volume of innoculum (mL)}} \times \text{cell number} \times \text{well dilution}$$

2.3 *In vivo* experiments

All of the work described in this section (mouse infections, sample preparation and imaging) was performed by Dr E. Roberts and Dr C. Pirillo at the Beatson Institute, Glasgow. All animal work was

carried out in line with the EU Directive 2010/63/eu and Animal (Scientific Procedures) Act 1986, under a project licence P72BA642F, and was approved by the University of Glasgow Animal Welfare and Ethics Review Board. Animals were housed in a barriered facility proactive in environmental enrichment.

2.3.1 Mouse Infections

To obtain images of red and green foci in the lungs of mice infected with ColorFlu, C57BL/6 mice (Charles River) were infected intranasally with a total of 1000 PFU of ColorFlu viruses (an equal mixture of mCherry and eGFP variants). To obtain images of Brightflu in mouse lungs, the infections were performed as described [188]. In brief, male C57BL/6 mice, more than 6 weeks old, were intranasally infected with 100 PFU of BrightFlu.

2.3.2 Imaging of mouse lungs

To obtain thick section confocal images of infections in mice, at the indicated number of days post infection animals were sacrificed and their lungs inflated with 2% low melt agarose. Lungs were fixed in PLP buffer overnight, 300 µm sections of lung were cut using a vibratome, and imaging was performed using an LSM 880 confocal microscope (Zeiss) using a 20x objective at 0.6x digital zoom with 5 µm z steps. Images were stitched and a maximum intensity projections were made using Imaris software (version 9.7.0, Bitplane).

To obtain lightsheet micrographs of infected mouse lungs, the specimens were fixed with PLP and cleared in ethyl cinnamate (Sigma-Aldrich) for 4 days before excess moisture was removed, and the lungs were mounted on a Zeiss mounting stub using Pattex Ultra Gel Super Glue. The mounted specimens were then immersed in ethyl cinnamate and imaged with a Zeiss Z.1 light sheet microscope and images were processed using Imaris software.

2.4 *In vitro* experiments

2.4.1 Immunofluorescence and Imaging

2.4.1.1 Confocal images of infected cells

Confocal images of Colorflu infected cells were obtained by infecting confluent MDCK cells on coverslips, with an MOI of 0.5 PFU/cell for each of the ColorFlu viruses, for 8 hours before fixation

in 4% (v/v) formaldehyde diluted in PBS (Sigma-Aldrich). To obtain images of SARS-CoV-2 infected cells, confluent AAT cells were infected with a 1:3 dilution of the viral stock in SARS-CoV-2 VGM for 24 h before fixation in 8% (v/v) formaldehyde in PBS. Following fixation, the cells were rinsed in PBS and the nucleus stained with 4',6-diamidino-2-phenylindole (DAPI). Coverslips were then mounted and imaged with the Zeiss Laser Scanning 710 confocal microscope. Images were processed using Zeiss Zen 2011 software.

2.4.1.2 SIPs Assay

To obtain images for analysis of semi-infectious particles (SIPs), IAV virus was diluted in IAV-VGM between the ranges of 10^{-1} and 10^{-6}. Virus was then used to infect confluent monolayers of MDCK cells in 6-well plates. After a 1 h incubation, the inoculum was removed, and an agarose overlay was added. 24 h later, the overlay was removed, and cells were fixed in 4% formaldehyde (Sigma-Aldrich) in PBS and permeabilized in 0.1% Triton X-100 (Sigma-Aldrich) in PBS. After blocking with 2% FBS in PBS, cells were incubated with rabbit α-NP antibody (table 2.2) and then washed in PBS before staining with an appropriate secondary antibody and DAPI in 2% FBS (table 2.3). A Celigo Imaging Cytometer (Nexcelom) was used to image the plates and quantify the number of singly infected foci and plaques for each well.

2.4.1.3 Plaque interaction assay

To obtain images of ColorFlu viruses spreading from a coinfected focus of infection, MDCK cell monolayers were infected with mCherry and eGFP tagged viruses, both at an MOI of 5 PFU/cell. At 1 hpi. the infected cells were dispersed with TrypLE express at 37°C for 15 minutes and diluted in VGM to create a single-cell suspension that was applied to uninfected MDCK cell monolayers. The cells were left to settle for 4 h, after which an agarose overlay was added and infections were left to proceed, as in a standard plaque assay.

To obtain images of interactions between initially separate foci of infection, cell monolayers (MDCK for ColorFlu, AAT for SARS-CoV-2) were infected with a diluted mixture of mCherry and eGFP or ZsGreen tagged viruses after which an overlay was applied and infections were left to proceed as in a standard plaque assay. ColorFlu infected plates were imaged through the agarose every 24 h in a

Celigo imaging cytometer (Nexcelom). Images were processed in FIJII ImageJ [189] using custom macros which can be accessed from a public GitHub repository: https://github.com/annasimsbiol/colorflu. SARS-CoV-2 infected plates were incubated for 72 h before fixation for in 8% (v/v) formaldehyde for 1 h. Following this, the plates were rinsed in PBS and imaged using the Celigo imaging cytometer (Nexcelom).

2.4.2 Viral Growth Kinetics

For ColorFlu single cycle growth kinetics, viruses were applied to confluent MDCK monolayers at an MOI of 2.5 PFU/cell and the cells were incubated with the inoculum for 1 h at 37°C and 5% CO_2 in a humidified incubator to allow the viruses to enter cells. Following this, the inoculum was removed, and the cells bathed in acid wash (table 2.5) for 1 minute, after which fresh VGM was added. Media were sampled at the time points indicated, clarified by low-speed centrifugation and stored at -80°C before titration by plaque assay.

Multicycle kinetics were determined as above, except that the cells were infected at an MOI of 0.001 PFU/cell and the acid wash step was omitted.

2.4.3 Western blotting

Cells were plated to 100% confluency in 12 well plates. 2 h prior to infection with ColorFlu mCherry (MOI 2 PFU/cell), wells were treated with 1000 pg IFN-alpha 14. After 1 h adsorption of virus onto cells, the inoculum was removed and replaced with VGM containing 0.32 µM ruxolitinib or equivalent volume of DMSO.

At 24 h the cells were washed with PBS before whole cell lysates were harvested into Laemmli buffer (table 2.5). Harvested lysates were either used immediately or snap frozen and stored at -20°C. Samples were boiled for 5 minutes at 95°C prior to loading. Wells were loaded with 15-20 µl of whole cell lysates. PageRuler prestained protein ladder was used as a reference marker for molecular mass. Proteins were resolved by SDS-PAGE on 4-12% Bis-Tris gel (BioRad) using running buffer (BioRad). Gels were run at 100 volts until the dye front reached the bottom of the gel. Separated proteins were electrotransferred using the Trans-Blot Turbo Transfer System (BioRad) onto nitrocellulose membranes for western blotting. Membranes were blocked for 1 h in blocking

buffer (table 2.5). Primary and secondary antibody incubations were performed in blocking buffer at the desired antibody dilution (Table 2.2 and 2.3). Membranes were washed three times in PBST for 5 min following each antibody incubation. Prior to scanning, membranes were washed two times in PBS and once in distilled water. Membranes were imaged on an Odyssey Infrared Imager (Licor) and analysed with Odyssey Image Studio Lite software (Licor).

2.4.4 Flow cytometry

2.4.4.1 Infection and sample generation

Cells were inoculated for 1 h with reporter viruses, diluted in VGM at the MOI indicated. After this the inoculum was removed and replaced with complete media. After the time intervals indicated, cells were inoculated for 1 h with a second reporter virus, at the MOI indicated. After 1 h this inoculum was removed and replaced with complete media, and the cells were incubated for a further 16 h at 37°C.

The proportions of cells expressing the different fluorophores were assessed using a Guava easyCyte HT System cytometer (Luminex). Briefly, infected and mock-infected cell monolayers were dissociated TrypLE express for 15 minutes and dispersed into a single-cell suspension before fixation in 4% formaldehyde (v/v) in PBS. Each sample was prepared and assayed as technical triplicates.

2.4.4.2 Gating strategy

Flow cytometry data were analysed in FlowJo software v10.6. The gating strategy is shown in figure 2.1. In brief, the cells were gated from debris using a gate across forward scatter and side scatter. Next, single cells were identified and separated from clumps of cells using a forward scatter length and forward scatter area gate.

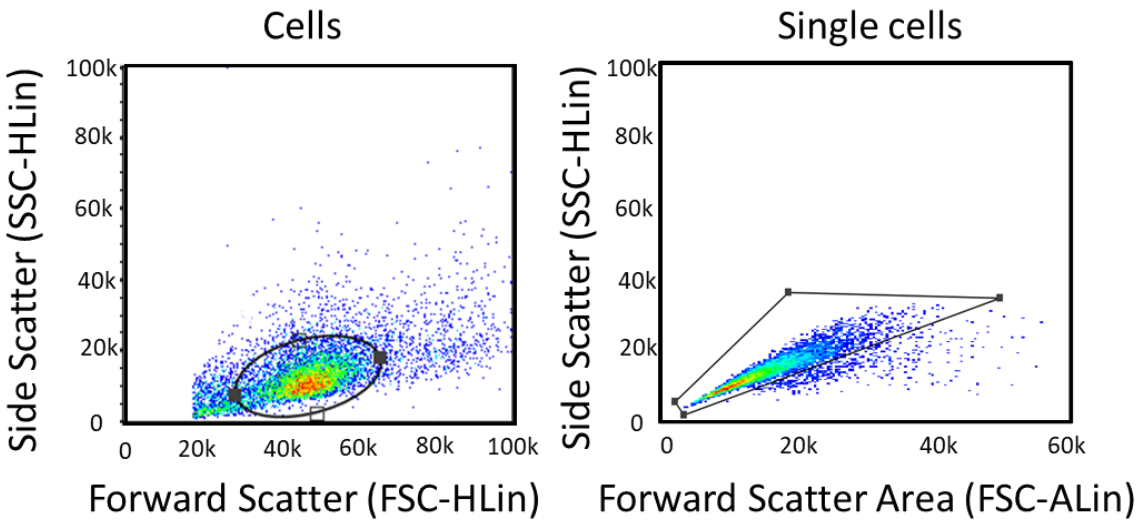

Fig 2.1: Gating strategy for identifying individual cells.

Gating to identify cells for analysis. Debris were removed from the analysis via an oval gate by forward and side scatter on linear scales. Clumps of cells were removed from the analysis using a polygonal gate by side scatter and side scatter area. Combining both steps leaves just single cells in the analysis.

The thresholds for assessing positive detection of the red and green fluorophores were set using the mock-infected cells as a negative control. I note that these experiments were difficult to control due, I believe, to the variable expression of the fluorophore so equal expression of the fluorophore during simultaneous infection (no SIE should have occurred) was used to determine data quality.

2.5 Analysis methods

2.5.1 Statistical analysis and data visualisation

Statistical analysis was carried out using Graphpad Prism (version 9.1.0). Statistical tests are described where applicable in the relevant method sections and figure legends within results chapters. Data were visualised using Graphpad Prism (version 9.1.0) or FIJI ImageJ [189].

2.5.2 Modelling of Infections

To model the interactions between two different viruses during simultaneous infection, I hypothesised that one of two scenarios could govern these interactions.

(1) The viruses tagged with the different fluorophores infect the cells independently of each other (i.e. no SIE occurs). Therefore, the probability that a cell is red is given by the probability that it has been infected by the red virus and has also not been infected by the green virus:

$$P_R = (1 - e^{(-MOI_R)}) \times (e^{(-MOI_G)})$$

where P_R is the proportion of cells that express only the red fluorophore, MOI_R is the input MOI of the red tagged virus and MOI_G is input MOI of the green tagged virus.

(2) Alternatively, I envisioned a mutually exclusive model where the presence of a virus with one fluorophore completely inhibits the ability of the other virus to infect the cell. Therefore, the probability that a cell is red can be calculated from the overall MOI and the proportion of the infecting viruses that carry the fluorophore of interest:

$$P_R = \left(\frac{MOI_R}{MOI_T}\right)(1 - e^{-MOI_T})$$

where P_R is the proportion of cells that express only the red fluorophore, MOI_T is the maximum input MOI of both viruses in the experiment, and MOI_R is the input MOI of the red tagged virus

To model interactions between viruses during the onset of SIE, I wanted to calculate the proportion of viruses that are able to cause a cell to be red or green independently of each other. To do this, I had to include the proportion of coinfected cells as a red and green cell separately. Therefore, the amount of viruses per cell (MOI) of “red forming units” (RFU; viruses that cause expression of the red fluorophore) is:

$$MOI_{RFU} = -\ln(1 - (P_R + P_{GR}))$$

where MOI_{RFU} is the concentration of red viruses per cell, P_R is the proportion of cells that express only the red fluorophore, and P_{GR} is the proportion of cells that express both red and green fluorophores (are coinfected). GFU/cell was calculated similarly.

The decrease in RFU with increasing intervals between primary (green) and secondary (red) infection was then modelled in three ways:

(1) A model where the RFU decreased linearly:

(2) A model where the RFU decreased exponentially

(3) A model where during the initial interval there would be no SIE (lag phase), after which point SIE would increase exponentially (exponential decay phase.

The following constraint was applied: The value of RFU could not fall below 0.

In the initial model fitting in section 3.4, no constraint was applied to the length of the lag phase.

In section 5.3 where less samples were taken of times between infection events, the length of the lag phase was constrained to 2 h to fit with the previous findings from section 3.4.

The models were fitted by the least squares method using GraphPad Prism (version 9.4.1; GraphPad). For model (1), the coefficient of variation r^2 was used to assess goodness of fit and represents a measure of the proportion of the variation in the RFU that is predictable from the time between infection events. A r^2 value = 1 was considered as threshold for reasonable fitness. For models (2) and (3) Total sum of squares (SST) was considered as a measure of goodness of fit and represents the squared difference between the measured data and their mean as given by the model. SST < 1 was considered as a threshold for reasonable fitness.

Chapter 3: Defining the kinetics of SIE induced by IAV

3.1 Introduction

3.1.1 IAV taxonomy

Influenza viruses, which are part of the *Orthomyxoviridae* family, are categorised into four known genera: A, B, C and D. A and B are the most important in the context of human disease as they cause worldwide seasonal epidemics of acute respiratory disease [191–193]. IAV, the subject of this chapter, is the most diverse genus and can infect a wide range of hosts including many bird and mammal species [194]. IAV is divided into subtypes based on the variation of the haemagglutinin (HA) and neuraminidase (NA) proteins on the surface of the virion [195].

3.1.2 IAV particle structure and genome

IAV is an enveloped virus whose virions are often depicted as spherical in shape and typically around 120nm in diameter (fig. 3.1). Several common laboratory strains of IAV almost exclusively produce particles of this shape, however clinical isolates of IAV can form filamentous virions which can be more than 10µm in length [196].

The IAV genome is composed of 8 segments of negative-sense single-stranded RNA (ssRNA), which are packaged in a cylindrical “7+1” form inside the virion [197]. Most of these segments encodes a single canonical protein, however, through alternative splicing and other mechanisms, some segments encode additional mature proteins from a single transcriptional start site [198–200]. IAV proteins are also often multifunctional, for example non-structural protein 1 (NS1) has roles in preventing the interferon response, enhancing translation of viral mRNA and preventing translation of host mRNA [201–203]. The mature IAV virions contains 10 virus-encoded proteins along with some host-derived components which are incorporated into the particles during their production [204,205].

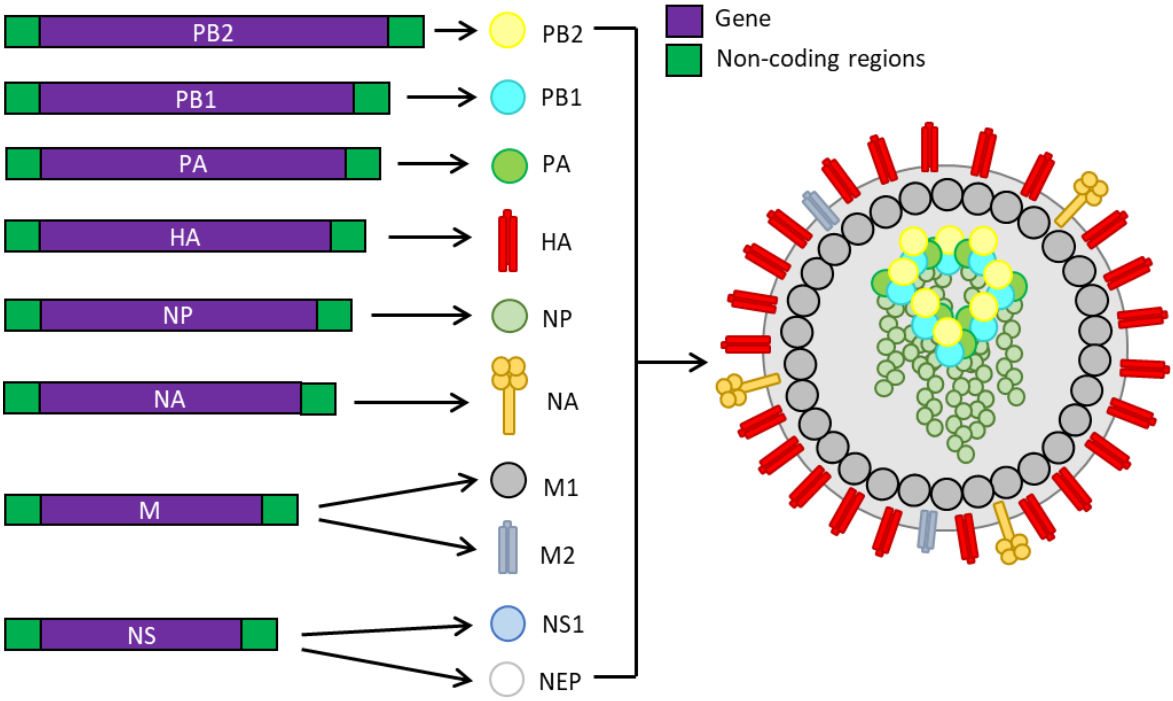

Figure 3.1a: Composition of influenza genome and virion

The 8 IAV RNA genome segments each contains a gene (in purple), polymerase basic proteins 1 and 2 (PB1 and PB2), polymerase acidic protein (PA), HA, nucleoprotein (NP), NA, M and NS. The gene is flanked by a 3' and 5' non-coding regions (in green). Each RNA segment is then expressed (indicated by the arrow) into mature protein. These are then assembled to produce the virus particles as represented on the right. Inside the virions, each RNA molecule is coated with NP monomers and is associated with the PB1, PB2 and PA proteins which together form the viral RNA-dependant RNA-polymerase (RdRp) complex. Together this forms the viral ribonucleoprotein complexes (vRNPs) which become packaged in a protein layer formed from M1 monomers. The vRNPs are arranged in a cylindrical conformation within the virion. The protein layer (known as the virus core) is coated in a lipid bilayer, from which protrudes the haemagglutinin (HA), neuraminidase (NA) and the M2 ion channel.

3.1.3 IAV replication cycle

The IAV replication cycle is a complicated process and there are still many things we do not understand. It is impossible to succinctly summarise all our knowledge in any detail, but here I have attempted to outline the key stages involved. A more in depth, but brief and easy to read outline of the replication cycle is available from Samji, 2009 [206]. A more complex and more up-to-date explanation of our knowledge has been summarised by Hutchinson and Yamauchi, 2018 [192].

In brief, IAV HA protein attaches to sialic acid residues which are found on many glycoproteins and glycolipids on the surface of human airway epithelial cells. This initial interaction determines cell tropism as mutation to the receptor binding pocket (RBP) of HA changes which types of sialic acid and therefore the cells it can bind [207,208]. Avian and human influenza viruses typically prefer binding to sialic acids with different linkages, and therefore this is considered as a major barrier for the cross-species transmission of influenza viruses [209]. The binding of HA to sialic acid tethers IAV to the cell, preventing it from being removed from the surface by the shearing force of mucus flow [210,211]. The binding of HA to a single sialylated receptor is often low affinity, but viruses can to bind to more than one receptor, leading to clustering of receptors on the surface of the cell and a high avidity interaction, and triggering endocytosis into the cell [212,213].

The endocytosis of the virus into host cells predominantly occurs by clathrin-mediated endocytosis (CME), although there is some evidence for clathrin-independent mechanisms [214,215]. CME is a specific mechanism of receptor-mediated endocytosis and results in the uptake of viruses in Ras-related protein 5 (Rab5)-positive early endosomes. Following endocytosis, the resultant vesicle is trafficked through the cell along microtubules [216]. During this process the endosome matures and becomes acidified through the action of proton pumps in the endosomal membrane [212]. The low pH and enrichment of potassium ions causes conformational changes to occur in HA, which expose the fusion peptide and allowing it to mediate the fusion of the viral envelope with the membrane of the late endosome [213] and the M2 proton channel to open causing an influx of more protons into the virion; ‘softening’ the M1 protein core surrounding the viral ribonucleoproteins (vRNPs) [217,218]. This, along with the action of histone deacetylase 6 (HDAC6) and the aggresome processing pathway, causes the breaking open of the viral core and the release of the vRNPs into the cytoplasm [219,220].

The vRNPs are then carried into the nucleus by transport machinery which recognises the nuclear localisation signals (NLSs) on each segment. Influenza is highly unusual as an RNA virus as genome replication occurs in the nucleus. In order to replicate the genome the viral RNA-dependant RNA-polymerase (RdRp) assembles and then synthesises a cRNA anti-genome, a full-length copy of the

viral segment but in positive-sense ssRNA, from which RdRp can make full-length negative-sense genome [207,221]. The virus then uses a cap-snatching mechanism mediated by PB2 to steal 5' caps from host mRNA and place them on the nascent viral mRNA, which acts as a primer for transcription of the viral mRNA. The cap also allows the recruitment the host cap-binding complex and subvert host translation to produce viral proteins [208].

The progeny vRNPs are assembled and exported to the ER where they attach to the lumen of Rab11-positive membranes, which bud into endosomes [222]. Export of the vRNPs into the cytoplasm is mediated by M1 and nuclear export protein (NEP) [223–225]. As the endosomes move along microtubules they fuse together to gather the nascent genome segments [226]. Virions are assembled at the plasma membrane on the apical side of polarised cells. Nascent virions bud out from the host cell, taking with them a section of the plasma membrane which contains HA, NA and M1 proteins embedded into it. The NA then acts as a sialidase to cleave the sialic acid residues from the cell surface allowing the new virus particles to be released [227,228].

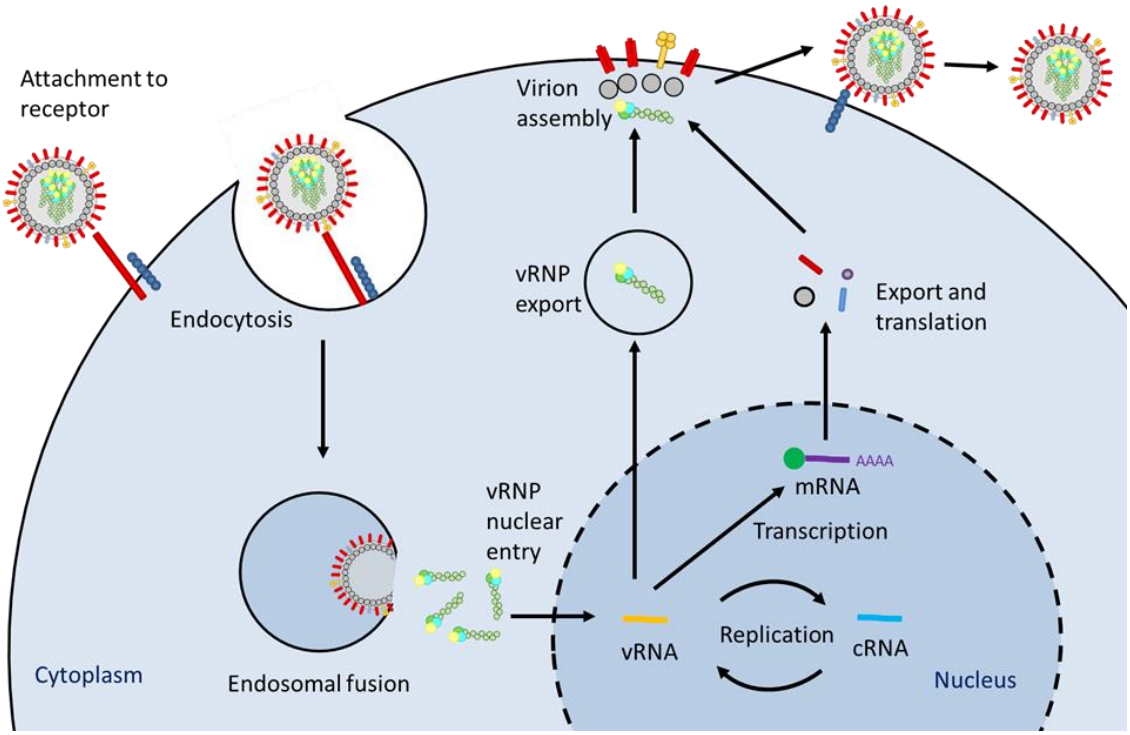

Figure 3.1b: Influenza virus replication cycle

First, the virion attaches to a susceptible cell via attachment of HA to sialic acid residues. The virion is then endocytosed facilitated by binding to a cellular receptor. Following endocytosis, the viral membrane fuses with the endosomal membrane mediated by HA, releasing the vRNPs into the cytoplasm. The vRNPs are then imported into the nucleus. The vRNA is transcribed into mRNA by the viral polymerase and trans-acting cellular polymerases such as RNA Pol II. The mRNA is then exported to the cytoplasm and translated to new viral proteins. New viral genomes are produced from cRNA templates. New vRNA molecules are encapsulated into nascent vRNPs and exported to the cell surface. New virions are assembled and pinches off. Finally, NA cleaves sialic acid attached to HA and the virion buds off.

3.1.4 Coinfection of cells with IAV

There is limited direct evidence of coinfection in individual cells during natural infections of IAV. Instead, estimations for the prevalence of coinfected cells are made from the production of reassortant viruses, the outcome of coinfection between different virus strains. Generation of reassortant viruses, and therefore coinfection, has been demonstrated to occur frequently in wild bird reservoirs [229–232]. Additionally, reassortment has been repeatedly demonstrated in experimental settings, both *in vivo* and *in vitro,* over a single round of replication [91,233–237]. Amplification of a virus that required coinfection for replication was observed experimentally, in the nasal passages of guinea pigs, indicating that coinfection occurred during multiple rounds of infection [234].

Coinfection of cells seems to be a particularly important for the IAV lifecycle as it has been shown to increase the rate of the virus production and increases the output of an infected cell – and therefore coinfection has been hypothesised to aid the virus in outcompeting the host immune system and increasing the chance of successful transmission between hosts [112,134]. Therefore, studies suggest that for IAVs, coinfection occurs often during natural and experimental infections and has consequences for viral evolution.

How these observed frequent coinfections occur in the face of SIE, a mechanism which restricts coinfection to a specific time interval between primary and secondary infection, is not well understood. Given the importance of coinfection for viral population propagation and diversity, understanding the capacity of influenza viruses to coinfect and the barriers that could prevent coinfection, including SIE, is crucially important to understand the evolution and replication of

influenza viruses. The evidence for the timings of onset of SIE during IAV infection will be reviewed in the next section.

3.1.5 Kinetics of SIE induced by IAV

SIE is a mechanism that represents a barrier to coinfection at the level of individual cells. Prior to the current work, the knowledge of IAV induced SIE was derived from studies of single cycle infections and came from measuring the number of coinfected cells at an "end-point", typically 6 h post primary infection [122,146]. These *in vitro* studies of SIE measured coinfection via the expression of coinfecting viral proteins and showed that robust reassortment occurs in this time frame. However, the detection of the coinfecting viruses necessitated that they be antigenically distinct, therefore this approach cannot be used to study closely genetically related viruses. Another study, Dou *et al*. 2017, took an approach that overcame this difficulty. In this study, the authors utilised single point mutations in each genome segment (called WSN^{ISO}, in comparison to WSN) to distinguish between primary and secondary infecting genomes which were then detected using single molecule RNA probes [238]. Using these isogenic viruses the researchers observed a decrease in WSN^{ISO} gene segment detection when the virus was used to superinfect cells that had been previously infected with WSN. This study observed decreasing ability for the secondary infecting genome viruses to enter the nucleus following 45 minutes of primary infection, but made no analysis of the kinetics of SIE onset. Therefore, we wanted to focus our attention on addressing the kinetics of SIE onset from simultaneous infection (0 h between primary and secondary infection) to "end-point" (6 h) and beyond.

The mechanisms for IAV SIE will be addressed in more detail in Chapter 5, but in brief there are two main hypotheses in the published literature. Huang *et al*. 2008 proposed that viral neuraminidase (NA) cleaves SA residues from the surface of the previously infected cells, preventing coinfection [146]. Sun and Brooke, 2018 on the other hand, found no role for viral NA, instead finding that an SIE-like state in the cell can be established by replicating influenza polymerase complexes regardless of the template being replicated [122]. This is bolstered by the findings of Dou *et al*. 2017 which found that WSN^{ISO} gene segments were blocked at the stage of nuclear import, while viral entry was

unimpaired [238]. At present the actual mechanism for SIE of IAV is not yet clear, and I hypothesise that mechanistic insight could be obtained by defining the kinetics of SIE onset.

3.1.6 Methods to detect cells coinfected by IAV

We wanted to focus this work on the interactions between genetically closely related viruses so that we can model interactions between progeny viruses, and because evidence shows that the exclusion effect of SIE is strongest when the viruses are closely related to each other (as reviewed in section 1.4.1). Investigating coinfection between closely related viruses has previously been challenging due to difficulty in telling the coinfecting viruses apart, due to requirement for distinct epitopes for detection by antibodies [122,146]. Approaches using RNA probes has been used to investigate coinfection of related viruses but is technically challenging and is difficult to perform bulk cell population analysis [238]. Therefore, I used fluorescent reporter IAVs, which allows me to easily distinguish between singly infected and coinfected cells in microscopy and flow cytometry assays, and as an approach has been used previously for investigations of SIE in other viruses [114,115]. Furthermore, reporter viruses allowed flexibility to apply the findings *in vitro* to *in vivo* systems such as whole organs, which can be experimentally challenging to label with nucleic acid probes or antibodies [186,239].

3.1.7 Chapter Aims

In this chapter, I determined that an established reporter virus system, ColorFlu, is suitable to measure coinfection between isogenic IAVs. Using these, I then assessed the potential for coinfection of cells during simultaneous infection. Following this, I defined the kinetics of SIE onset following IAV infection. I then demonstrate that the kinetics of SIE fit a plateau-exponential model which gives insight into possible mechanisms of SIE by IAV.

3.2 Reporter Viruses for Studying Coinfection and SIE

3.2.1 ColorFlu is a suitable system for studying coinfection and SIE

We wanted to focus this investigation of SIE on closely related viruses, firstly because genetic relatedness is a factor for SIE and secondly in order to model interactions between progeny viruses. Therefore, we selected “ColorFlu”, a previously established reporter IAV virus system based on

laboratory-adapted PR8 (H1N1) viruses [186]. These consist of isogenic variant viruses, for which 7 segments of the virus are of PR8 origin, with PB2 and HA segments carrying compensatory mutations that mitigate the fitness cost of encoding the fluorophore, as described in the original publication. In a change from the original method, I rescued the virus using the pDUAL PR8 rescue system by de Wit [185] – see section 2.2.2 for details. The segment 8 (NS segment) includes an inserted fluorophore gene (in this study, either eGFP or mCherry) (fig. 3.2). The NS1 protein of the PR8 is expressed as a fusion protein to the fluorophore. When ColorFlu viruses were used to infect MDCK cells in plaque assay conditions, I saw clear round fluorescent plaques at 3 dpi, indicating that the viruses initiate multicycle infection with maintained expression of the fluorophore (fig. 3.2). To determine whether I could identify individual singly and coinfected cells, MDCK cells were infected with a mixture of the two viruses on coverslips and imaged using confocal microscopy. At 8hpi, I observed cells where either eGFP or mCherry is expressed (shown in this thesis as green and magenta respectively). In the merged image, I observed cells where both fluorophores were expressed (shown as white) and cells that were uninfected (where only the blue nuclear DAPI stain can be seen) (fig. 3.3). Therefore, I determined that we can use ColorFlu viruses to distinguish between singly infected, coinfected and uninfected cells.

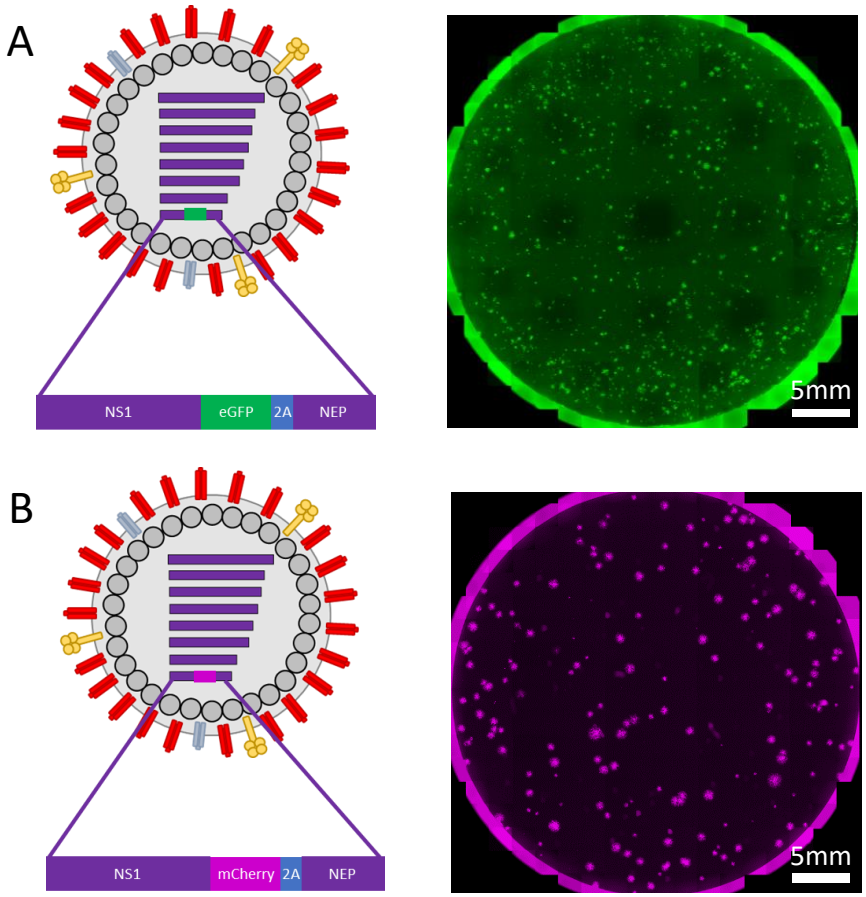

Figure 3.2: Schematic of ColorFlu viruses

Schematic of (A) eGFP and (B) mCherry ColorFlu variants as designed by Fukuyama and colleagues and image of virus plaques. Segment 8 encodes NS1 and NEP are viral proteins in addition to either eGFP and mCherry. 2A represents a foot-and-mouth virus protease 2A autoproteolytic site. Monolayers of MDCK cells were infected with 10-fold serial dilutions of ColorFlu viruses and incubated under plaque assay conditions. At 3 dpi the wells were imaged in the Celigo fluorescent microscope. Scale bar = 5mm.

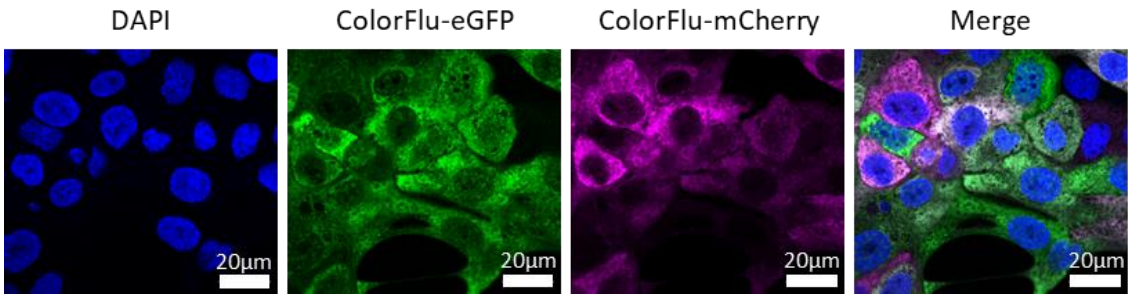

Figure 3.3: ColorFlu viruses as reporter viruses to measure coinfection.

Confocal images of ColorFlu infected cells. MDCK cells were infected with 0.5 MOI each of ColorFlu eGFP and mCherry on glass coverslips, with nuclei stained using DAPI. Images were taken 8 hpi using 63x objective lens. Scale bar = 20µm.

We wanted the pair of viruses to replicate at a similar rate so that during multicycle infection, one virus could not rapidly outcompete the other, as this could alter the dynamics of coinfection. To investigate this, I measured the single cycle (fig. 3.4A) and multicycle (fig. 3.4B) growth kinetics of the two chosen viruses. I determined that the viruses grew at a similar rate to each other – indeed there was no significant difference between the titre of the viruses at any timepoint (Mann–Whitney U test, $p > 0.05$). Therefore, I concluded that the viruses are well matched in their replication cycle, and therefore were suitable for my investigation.

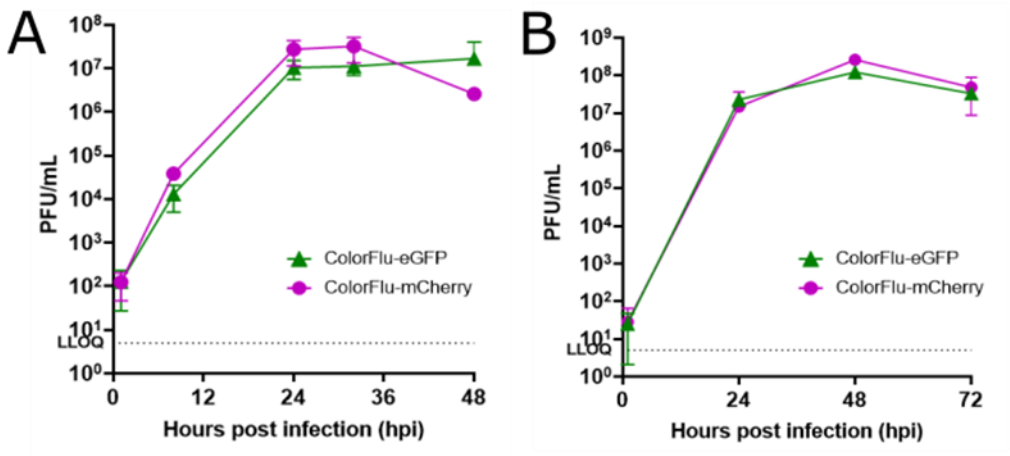

Figure 3.4: ColorFlu viruses tagged with mCherry and eGFP have similar growth kinetics.

(A) Single cycle and (B) multicycle growth kinetics of ColorFlu viruses were assessed by infecting MDCK cell monolayers at an MOI of 2.5 and 0.001 PFU/cell respectively and harvesting the supernatant at the time points indicated. Virus titre was assessed using plaque assay on MDCK cells. The mean and SD are shown (n = 3). For all time points in A and B, the titres of ColorFlu-mCherry and ColorFlu-eGFP were not significantly different (Mann–Whitney U test, $p > 0.05$). LLOQ = Lower limit of quantification.

Next, we wanted to assess whether expression of the fluorophore is a good measure of whether the cell is infected or not. As the NS1-fluorophore fusion protein has been artificially introduced into the virus, it is conceivable that it may unstable and therefore only be expressed in only a subset of infected cells. I assessed this by performing plaque assays with ColorFlu viruses, removing the overlay at 24 hpi and co-staining by indirect immunofluorescence (IF) using a viral nucleoprotein (NP) antibody (fig. 3.5A). The plaques that were fluorophore- or NP-positive were counted using the gating tool in the on the Celigo microscope software. As most infected foci express both the

fluorophore and NP, we can assume fluorophore expression is a reasonable measure for infection status of the cell (fig. 3.5B).

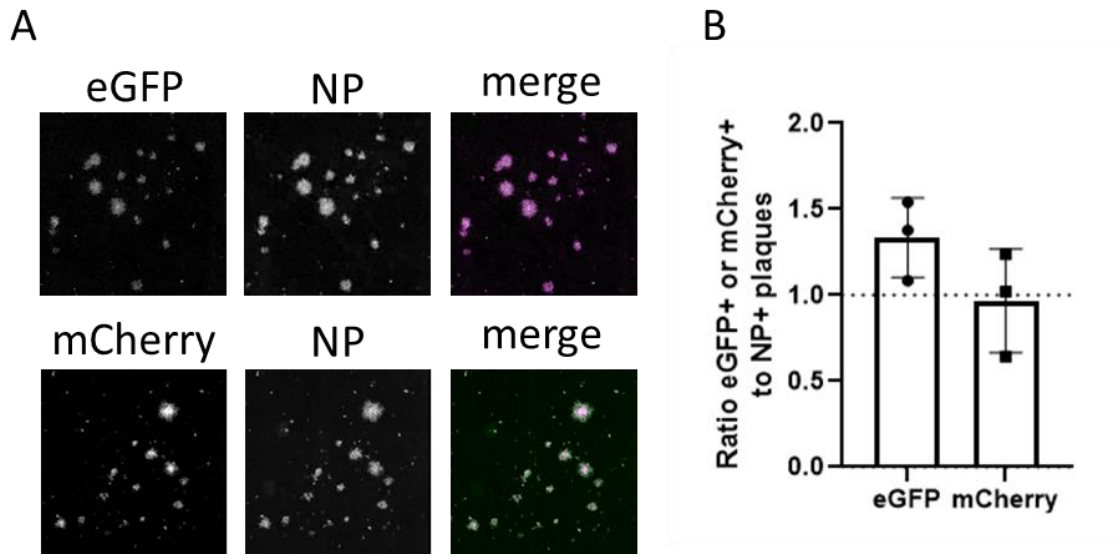

Figure 3.5: Expression of ColorFlu NS1-fluorophore proteins are a reasonable assumption for the infection state of the cell.

Monolayers of MDCK cells were infected with 10-fold serial dilutions of ColorFlu viruses and incubated under plaque assay conditions. At 24 hpi the agarose was removed, and the cells immunostained with a IAV NP antibody and visualised using a secondary antibody in the opposite red or green colour encoded by the virus. (A) Images of plaques taken using Celigo fluorescence microscope (B) Plaques over 2500µm^2 counted. Data shown as ratio of fluorophore positive plaques (eGFP$^+$ or mCherry$^+$) to NP positive plaques (NP$^+$), each data point represents each well with a different virus dilution from one experiment, and SD. Line at 1 denotes equal proportion between fluorophore and NP positive plaques.

Unexpectedly, for ColorFlu-eGFP, I found more eGFP-positive plaques than NP-positive plaques (average ratio = 1.32). We reasoned that this may be due to an increase of SIPs in the population which when infecting a cell induce the expression of eGFP but not NP. To investigate this, I used an assay to quantify SIPs employed by Brooke *et al*. 2013 [98]. In brief, in this assay cells were infected at a low MOI under plaque assay conditions, such that each focus of infection is initiated by one particle. At 24 hpi, the overlay was removed, and cells were stained using an IAV NP antibody. The number of foci in each well were counted that form either a plaque (which is defined in this assay as 3 or more adjacent NP+ cells) which denotes infection by a fully infectious particle (FIP), or an abortive infection (defined as 1 or 2 adjacent infected cells) which would occur if cells are infected

by a SIP (gating strategy shown in fig. 3.6A). I found that the eGFP encoding viruses did not have a significant increase in the proportion of virions that are SIPs compared to either mCherry expressing ColorFlu or to WT PR8 virus (Kruskal-Wallis test $p>0.05$) (fig. 3.6B). Therefore, the finding that there are more GFP+ plaques than NP+ plaques cannot be explained by an enrichment of SIPs. Therefore, I believe that this observation is due to increased detection of eGFP compared to mCherry or immunostained NP. The reason for this is not clear but could be due to increased stability of the NS1-eGFP fusion protein, or increased detection due to autofluorescence of the cells in the green channel. Overall, as eGFP or mCherry is expressed in all NP positive plaques, we can use the fluorophore expression as a reasonable marker of viral infection.

Overall, I found that the ColorFlu viruses used in this study were suitable for investigating coinfection between related viruses. This was because firstly, the viruses express the fluorophore proteins stably during multicycle infection, secondly, that we can distinguish between singly, coinfected and uninfected cells by measuring the expression of the fluorophore, and finally that the viruses replicate with similar kinetics.

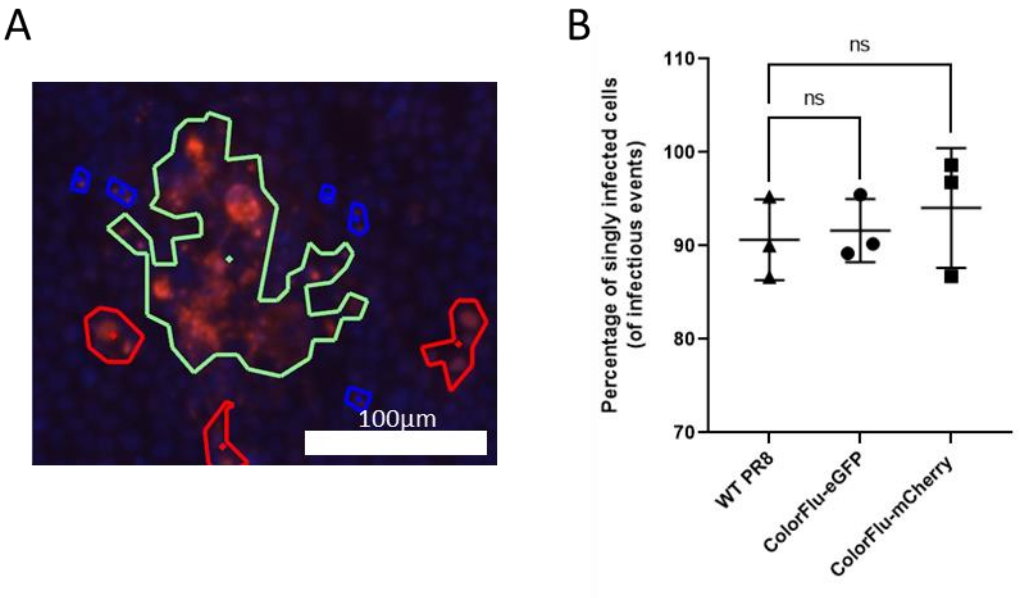

Figure 3.6: Equal proportions of SIPs to FIPs in the viral populations of WT PR8, ColorFlu eGFP and ColorFlu mCherry

Confluent MDCK monolayers were infected with virus at a range of dilutions and then overlaid with a 1% agarose overlay. At 24hpi the agarose was removed, and the cells were stained for viral NP and the nuclei stained with DAPI. (A) gating of infected foci with Celigo Imaging Cytometer. Objects circled in blue represent red fluorescence in an area smaller than a nucleus and has been ignored, objects in red represent one or two adjacent fluorescent cells which have been quantified a singly infected cell/cell pair, and objects in green represent a three or more adjacent fluorescent cells which have been quantified as plaques. Scale bar = 100µm (B) Data represent the mean percentage of the total foci quantified that were singly infected cells/cell pairs, n = 3. Error bars represent the standard deviation, ns denotes non-significant by Kruskal-Wallis test $p > 0.05$.

3.2.2 BrightFlu is an improved system for studying single infections *in vitro* and *in vivo*

The BrightFlu design and cloning was conducted by C. Pirillo, S. Al Khalidi and E. Roberts, rescue of BrightFlu was conducted by myself, S. Jasim, R. Pinto and characterisation of BrightFlu conducted by myself.

We wished to design a new ColorFlu variant reporter virus that we could use for 3D imaging of virus infection *in vivo* and which addresses a couple of disadvantages of the ColorFlu system I observed during their use. The disadvantages of ColorFlu are 2-fold. Firstly, eGFP is not an ideal fluorophore for *in vivo* imaging as the fluorophore is only 10-fold brighter than the autofluorescence of the cell in 2D cell culture [240]. Observation of the decreased signal to noise ratio of eGFP compared to mCherry can be made from fig. 3.2A and fig. 3.5A of this thesis. *In vivo* this problem is worse, as the

signal must compete with the background of green autofluorescence from collagen [241]. We therefore wanted to design a reporter system with a brighter fluorophore, such as ZsGreen. ZsGreen is a tetrameric green fluorescent protein which is significantly brighter than eGFP - estimations between 4 and 8.6-fold brighter, depending on the cell type [242]. This would make this virus easier to detect in more complex environments such as mouse lungs lobes. Secondly, due to the C-terminal fusion of the fluorophore to the NS1 protein, it has been reported that ColorFlu has a reduced functionality of NS1 [243]. It was found that the mutations in PB2 and HA that are required to rescue ColorFlu compensated for this, not through boosting NS1 function, but instead by increasing the rate of ColorFlu replication such that it can outcompete the immune system. To make viruses with increased functionality of NS1, especially for studying immune functions *in vivo*, we added a 2A autoproteolytic sequence upstream of the fluorophore which in theory separates the NS1 protein from the fluorophore – theoretically maintaining NS1 function (fig. 3.7A). Following rescue of BrightFlu virus, with the accompanying mutations in PB2 and HA described in the original ColorFlu paper [186], I found that BrightFlu formed bright green plaques 48 hpi in MDCK cells (fig. 3.7B).

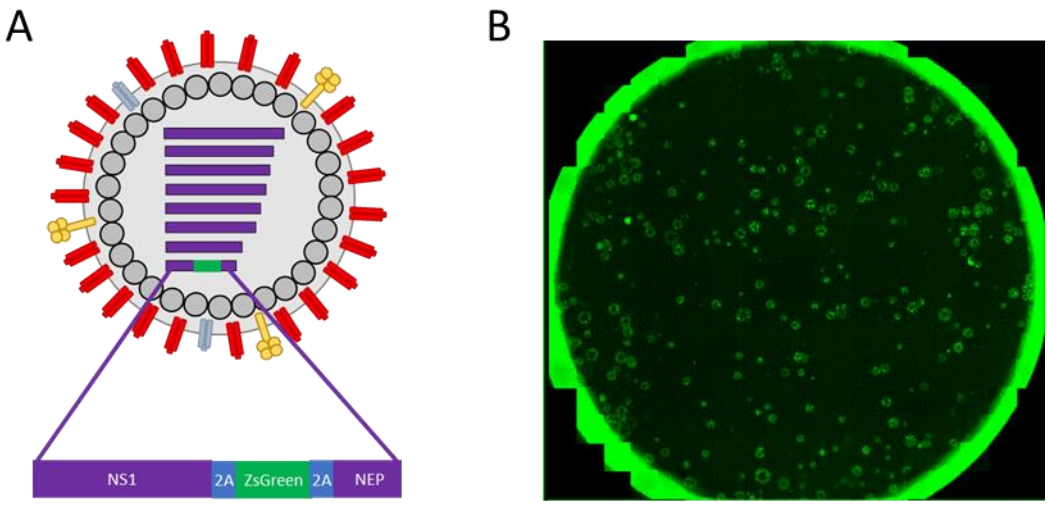

Figure 3.7: Schematic of BrightFlu.

(A) Schematic of BrightFlu designed by C. Pirillo, S. Al Khalidi and E. Roberts (B) Monolayers of MDCK cells were infected with 10-fold dilutions of Brightflu viruses. At 48 hpi, brightlu plaques were imaged using the Celigo cytometer. Image shows well image for 10^{-3} dilution.

To characterise BrightFlu, I first ensured that the virus propagated as expected under multicycle conditions, the conditions they would be subjected to when used in mouse infections. I found that Brightflu replicated efficiently in MDCK cells (fig. 3.8A). I also found that the ratio of ZsGreen to NP positive plaques was ~1 for BrightFlu, and therefore I concluded that ZsGreen is expressed in nearly all infected cells (fig. 3.8B). Correspondingly, I also found that BrightFlu has a comparable proportion of SIPs than WT PR8 (non-significant by Mann-Whitney U Test, $p>0.05$) (fig. 3.8C). Therefore, we concluded that BrightFlu grows as expected and therefore is a useful tool for measuring infection.

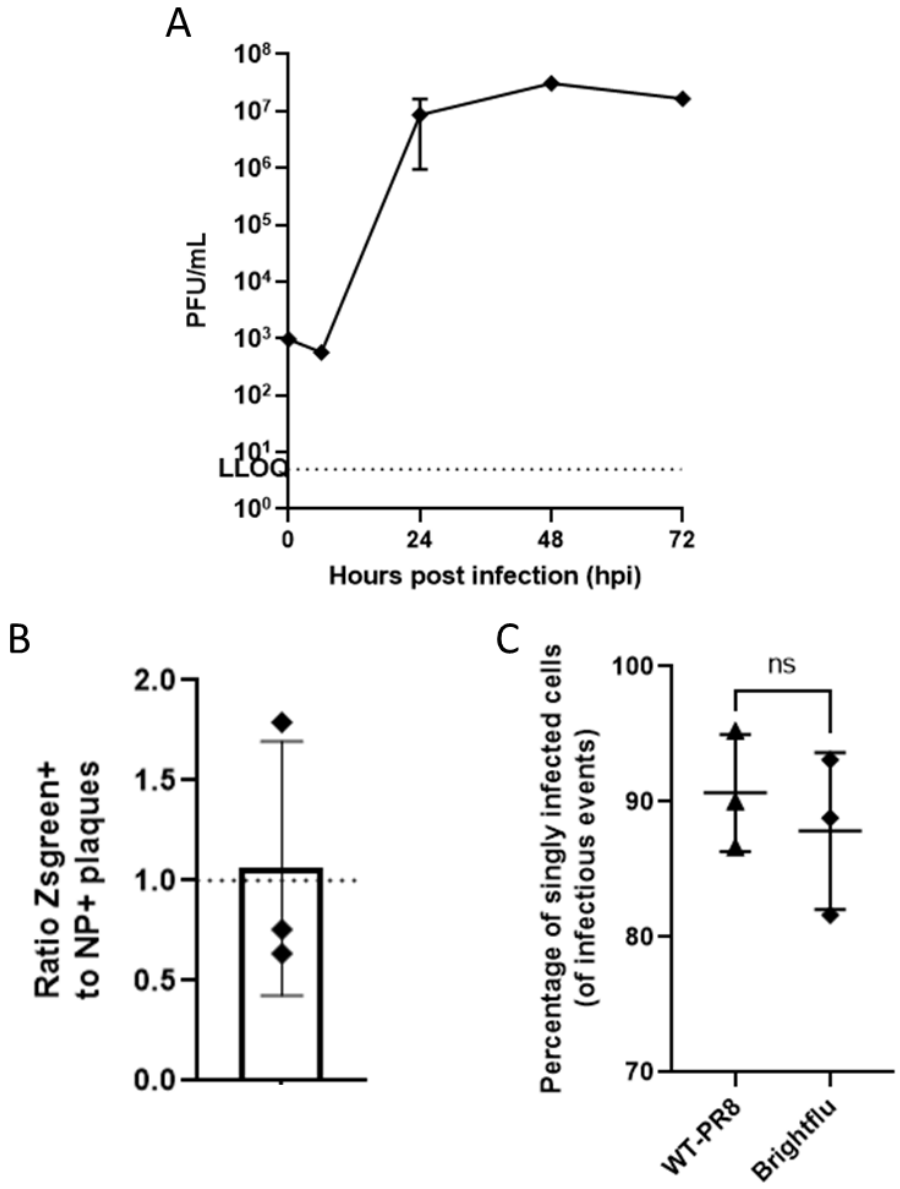

Figure 3.8: BrightFlu viruses are a useful reporter virus for studying infection.

(A) Multicycle growth kinetics of BrightFlu viruses were assessed by infecting MDCK cell monolayers at an MOI of 0.001 PFU/cell respectively and harvesting the supernatant at the time points indicated. Virus titre was assessed using plaque assay on MDCK cells. The mean and SD are shown (n=3), LLOQ=Lower limit of quantification. (B) Monolayers of MDCK cells were infected with 10-fold serial dilutions of viruses and incubated under plaque assay conditions. At 24 hpi the agarose was removed, and the cells immunostained with a IAV NP antibody and visualised in Celigo cytometer. Plaques over 2500µm^2 counted. Data shown as ratio of fluorophore positive plaques (ZsGreen$^+$) to NP positive plaques (NP$^+$), Mean and SD are shown (n = 3). Line at 1 denotes equal proportion between fluorophore and NP positive plaques. (C) Percentage of singly infected cells. Data represents the mean percentage of the total foci quantified that were singly infected cells/cell pairs, n=3, error bars represent SD. Not significant (ns) by Mann-Whitney U Test p>0.05.

3.3 Coinfection of cells with IAV occurs independently before the onset of SIE

To begin we wanted to characterise the interactions between viruses as they were applied to cells simultaneously, before the onset of superinfection exclusion (SIE). To determine the potential for coinfection of cells, I varied the ratio between eGFP and mCherry-tagged ColorFlu viruses and applied them simultaneously to MDCK cells. At 16 hpi the cells were harvested and the proportion of red, green and coinfected cells was measured using flow cytometry. I noted that it is possible that some multicycle infection would be theoretically possible during the 16 h incubation time but reasoned that it was unlikely to impact our results. This is because the cells were infected at a combined MOI of both viruses of 2 FFU/cell, and therefore most of the cells would be infected at time point 0 and, due to SIE, after 6 h the cells would be refractory to secondary infection, before we would expect the first nascent virions would emerge [244]. We envisioned two models that could describe the interaction between the viruses, first, the infection of the two viruses occur independently during simultaneous infection, and therefore coinfection occurs readily – peaking when the viruses are in equal proportion (fig. 3.9A). The second model is a mutually exclusive model whereby the replication of one virus in the cell suppresses the replication of another during simultaneous infection, and therefore coinfection is completely suppressed and only one virus of each type can be expressed in the cell (fig. 3.9B). Both models assume viruses are distributed equally at the point of adsorption to the cells, in line with the assumptions of the Poisson distribution (details about the models can be found in materials and methods).

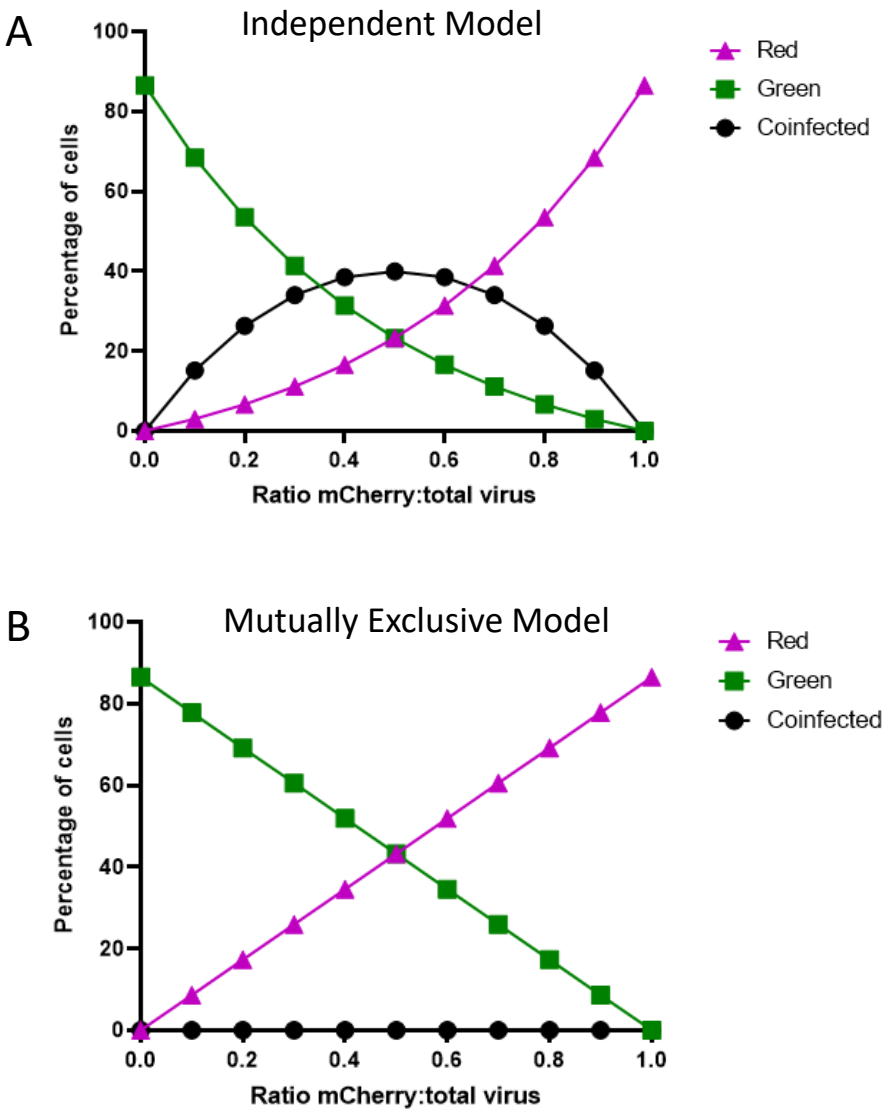

Figure 3.9: Proposed models for interactions between coinfecting viruses during simultaneous infection.

(A) An independent model and (B) mutually exclusive model for the interaction between eGFP and mCherry viruses during simultaneous coinfection.

The harvested cells were gated according to the gating strategy outlined in section 2.4.4.2 and the cells were separated by the expression of eGFP and mCherry. When both viruses were present in the well, a proportion of cells grouped into the upper right quadrant, indicating these cells were expressing both eGFP and mCherry, and therefore coinfection was possible (fig. 3.10A). Coinfection between the viruses occurred readily, peaking when the ratio of eGFP and mCherry labelled viruses was equal (MOI of 1 FFU/cell for each virus) at around 40% of the cells being coinfected, and that

the proportion of coinfection dipped when the ratio between the viruses was unbalanced (fig. 9B). When compared to the models outlined in fig. 3.9, adjusted for the experimental maximum input MOI of each virus, the data more closely matched the independent model (fig. 3.10C) than the mutually exclusive model (fig. 3.10D). This shows that when cells are infected simultaneously prior to onset of SIE, the infection events are independent of each other.

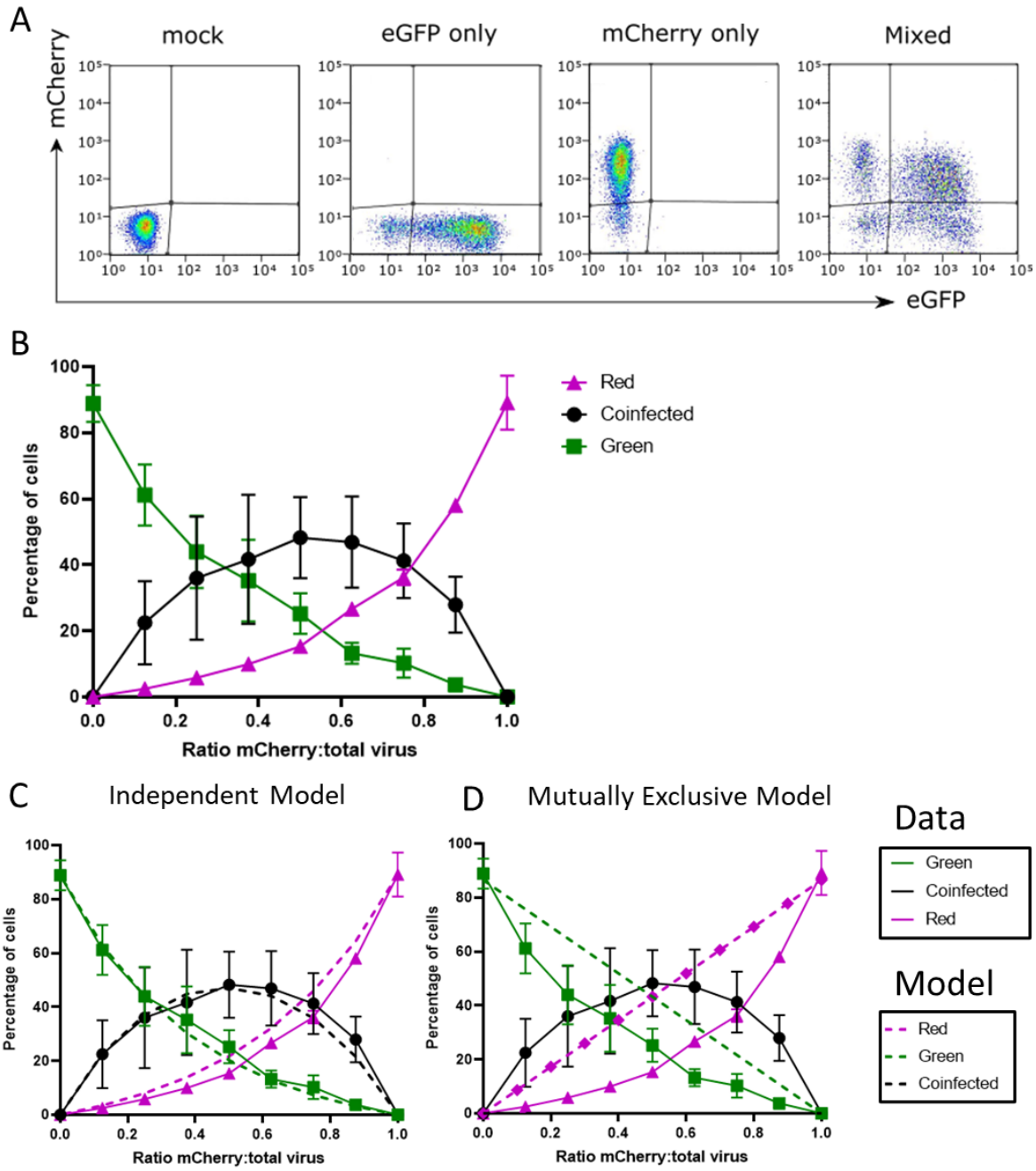

Figure 3.10: Simultaneously infecting viruses coinfect independently of each other.

(A) Flow cytometry of cells infected with reporter viruses. MDCK cells were infected with the ratios of mCherry and eGFP viruses indicated. Representative plots are shown. (B) Proportion of singly and coinfected cells measured by flow cytometry. mCherry and eGFP tagged viruses were diluted in set ratios and used to infect MDCK cell monolayers. 16 hpi the cells were harvested and measured for fluorophore expression. Data represents mean and SD, n=3. Comparison of experimental data to MOI adjusted (C) independent (D) mutually exclusive infection model. Models given by dashed lines, experimental data represented by symbols and solid lines.

3.4 Coinfection of cells with IAV is restricted 2 h post primary infection due to the onset of SIE

Next, we wanted to investigate the capacity for coinfection between viruses when they are applied to the cells at different times. The time delay between infection events allows the possibility of SIE onset, which previous studies have indicated is around 6 h post primary infection [122,245]. We wanted to investigate whether SIE onset occurs in this timeframe using the ColorFlu system and additionally describe the effect of SIE on coinfection between 0 hours and "end-point" at 6 hours. To do this, I infected monolayers of MDCK cells first with eGFP-tagged viruses and, then after various time intervals, infected the cells with mCherry-tagged virus. In these experiments, the viruses were restricted to a single cycle of replication by removing TPCK-trypsin and 10% FBS added to the media. As a caveat, I aimed to infect the cells at an MOI of 1 FFU/cell of each virus, however I note that there were slightly more mCherry positive cells than eGFP positive cells in individual infections (fig. 3.11A). When both viruses were present together, extensive coinfection is observed during simultaneous infection (0 h between primary and secondary infection) – but that this coinfected population is reduced when the time between infection events is increased to 8 h (fig. 3.11B). There is no significant change in the proportion of cells expressing mCherry for intervals between infections of 1 or 2 h. However, with increasing interval between infection events, the cells became less permissive to secondary infection and the proportion of cells expressing mCherry decreased (fig. 11C), with a significant reduction in the percentage of coinfected cells observed with an interval of 3 h ($p = 0.0074$, Kruskal–Wallis test) and at every subsequent interval ($p < 0.0001$). The percentage of coinfected cells declined to nearly zero once the interval between infections reached 7 h (fig. 11C). This data is consistent with previous studies that found robust SIE when there is an interval of 6 h between infection events [122,146]. Additionally, this data shows that up to 2 h post primary infection there is no restriction on coinfection, and thereafter, there is a progressive shift in the cells from a permissive to an exclusionary state as intervals between infections increase.

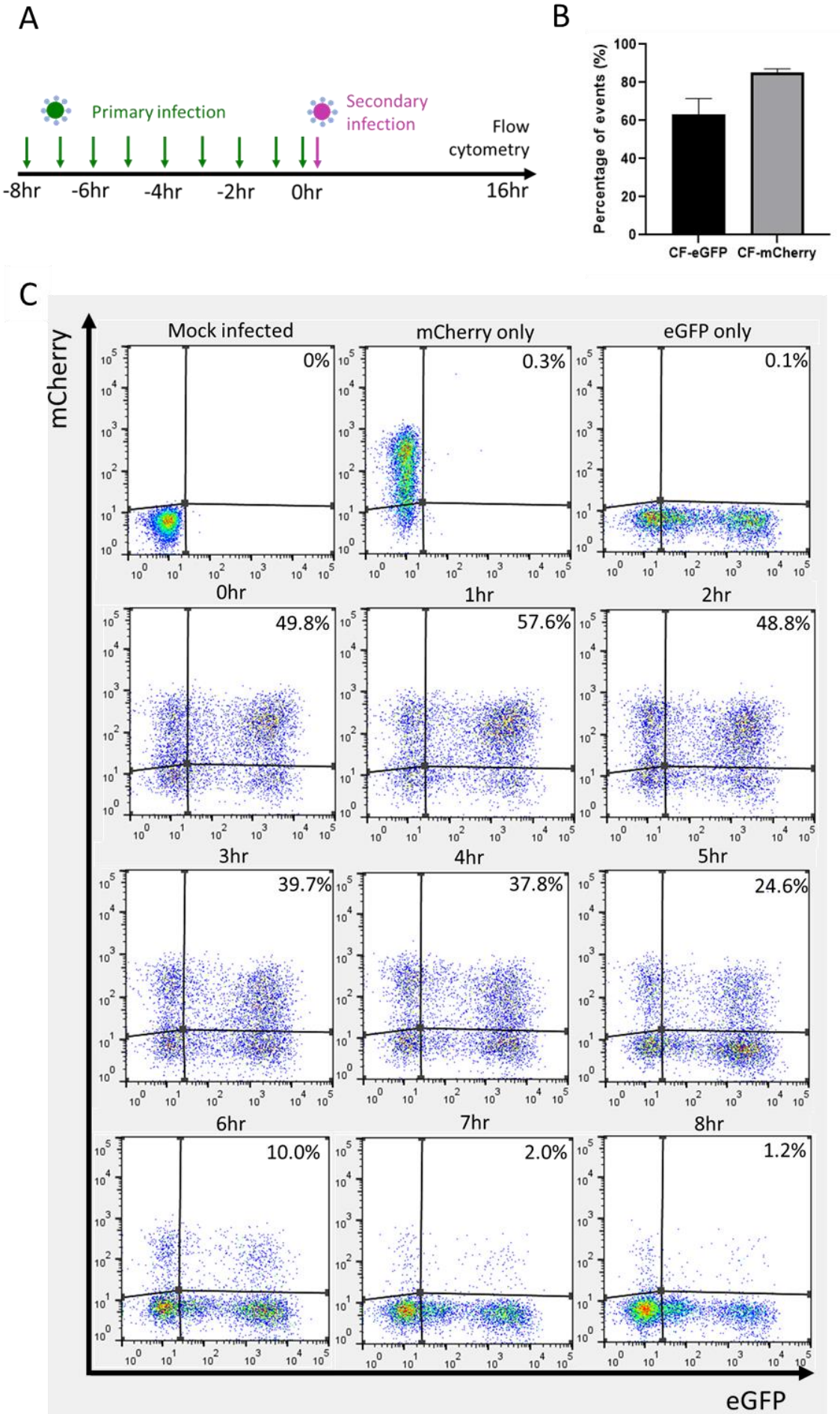
A
Primary infection
Secondary infection
Flow cytometry
-8hr
-6hr
-4hr
-2hr
0hr
16hr
B
Percentage of events (%)
100
80
60
40
20
0
CF-eGFP
CF-mCherry
C
mCherry
eGFP
Mock infected
mCherry only
eGFP only
0%
0.3%
0.1%
0hr
1hr
2hr
49.8%
57.6%
48.8%
3hr
4hr
5hr
39.7%
37.8%
24.6%
6hr
7hr
8hr
10.0%
2.0%
1.2%

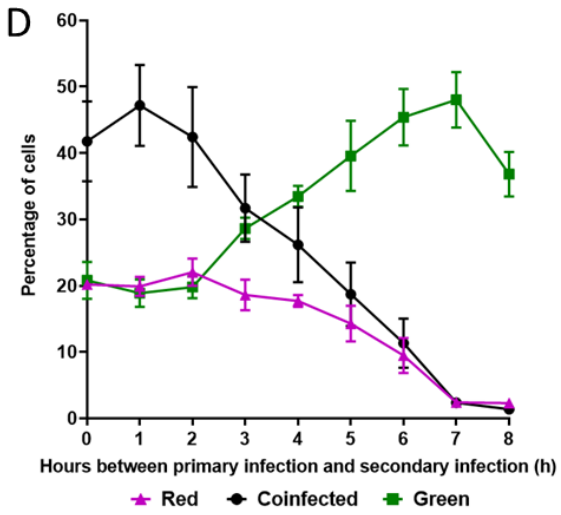

Figure 3.11: IAV begins to exclude superinfection following 2 hpi and is complete by 6 hpi

(A) Schematic of experimental set up. Cells were infected with the eGFP expressing virus at the time points indicated, at 0 hr all samples were infected with mCherry expressing virus. 0hr sample indicates simultaneously infected cells. After 16hr the cells were harvested and fluorescent protein expression assessed using flow cytometry (B) Input of CF-eGFP and CF-mCherry viruses in the experiment. Measurement of singly infected MDCK cells with mCherry or eGFP viruses and cells harvested for flow cytometry 16 hpi. Data represents mean and SD, n = 6. (C) Flow cytometry of cells infected with reporter viruses. MDCK cells were first infected with ColorFlu-eGFP, before secondary infection at the time points indicated with ColorFlu-mCherry, with both viruses at MOI 1 FFU/cell. Representative plots are shown. The percentage of cells in the coinfected gate are highlighted (D) Kinetics of onset of SIE, determined from flow cytometry analysis; means and SD are shown (n = 6). Differences in the percentage of coinfected cells, compared to simultaneous infection (time = 0 h), were tested for significance by one-way ANOVA. By 3 h, the difference was significant ($p = 0.0074$), and at every subsequent time point ($p < 0.0001$).

3.5 The kinetics of SIE by IAV are described by a plateau-exponential model

Having defined the kinetics of SIE induced by IAV, we wanted to fit models to the data to potentially provide information into the mechanism of SIE by IAV. To do this we needed to examine the effect of SIE on the fluorophore expression from the primary (eGFP) and secondary (mCherry) viruses separately. As, without the effect of SIE, the viruses infected cells independently of each other (as shown in fig. 10C), the viruses could be modelled by a Poisson distribution. Therefore, I used the proportions of cells expressing one or both fluorophores to infer the numbers of viruses per cell that had caused expression of eGFP (green forming units per cell (GFU/cell) or mCherry (red forming units per cell, RFU/cell). Details of the calculations for GFU/cell and RFU/cell can be found in section

2.5.2. In short, the amount of red cells were combined with the amount of coinfected cells (as a coinfected cell expresses both red and green fluorescent proteins). I then estimated, using a known number of cells, the approximate MOI of the viruses that would give rise to that percentage of fluorescent cells. I reasoned that with the onset of SIE the probability of the secondary virus being able to express its fluorophore would be reduced.

I observed that the number GFU (primary virus) per cell remained consistent as the time between infections was increased, up to 6 h (non-significant, $p>0.05$, one-way ANOVA). With intervals of greater than 6 h, there is a significant reduction in GFU per cell ($p = 0.0076$ and $p < 0.0001$ at 7 h and 8 h respectively, one way ANOVA), which I attributed to the cells that have been infected for the longest dying and therefore becoming detached and lost from the analysis (fig. 3.12A) [244]. This was consistent with a proportional increase in the detection of uninfected cells when there was an interval of 7 h or 8 h before secondary infection (fig. 3.12B). In contrast, although the number of RFU per cell (secondary virus) remained consistent for intervals of up to 2 h, after this point it declined rapidly, demonstrating the onset of SIE (At 3 h $p = 0.0004$, and thereafter $p <0.0001$, one way ANOVA) (fig. 3.12A).

Having isolated the effect of SIE on the mCherry-tagged (secondary infecting) virus, we proposed three models describing different mechanisms of SIE, and compared how well they fit the observed reduction in RFU/cell (fig. 3.12C). First, we considered a linear model, which would result from an inhibitory factor whose effectiveness increased at a consistent rate following infection. The best fit of this model is still a fairly poor fit to the data, especially at early and late timepoints ($R^2= 0.88$ and total sum of squares (SST) = 1.05). Next, we considered an exponential model, in which the likelihood of an infection being successful decreased from the moment of infection. Although the mechanism for SIE onset by IAV is unknown, there has been some suggestion in the literature that it involves actively replicating influenza polymerase [122]. As the products of viral transcription and replication appear to accumulate exponentially in a newly infected cell [246,247] We hypothesised that the SIE onset may also occur exponentially once a primary infection is established. However, the exponential model was another poor match to the data, especially in the middle timepoints (R^2

= 0.86 and SST=1.28). Finally, we reasoned that in the virus replication cycle, there is an initial lag for cell entry, uncoating and transport of the viral genome to the nucleus before the exponential accumulation of viral products in the cell. On that basis, we fit a model that includes a plateau to represent the lag phase before an exponential decrease in RFU/cell. This model not only provides the best fit to the data (R^2= 0.92 and SST=0.74) but considers the reality of viral replication, whereby replication must be proceeded by the entry of the virus into the cell and the transport of vRNPs to the nucleus, which is hypothesised to take around 2 h [245]. The best fit the model describes a relationship with an initial plateau phase of 2.2 h (95% confidence interval (CI) 1.8 to 2.6 h) followed by an exponential decay with a half-life of 1.7 h (95% CI 1.4 to 2.1 h). I noted that, similar to the linear model, the 7 h and 8 h samples are less well described by the model, however this could be due to the death of the infected cells at these late timepoints.

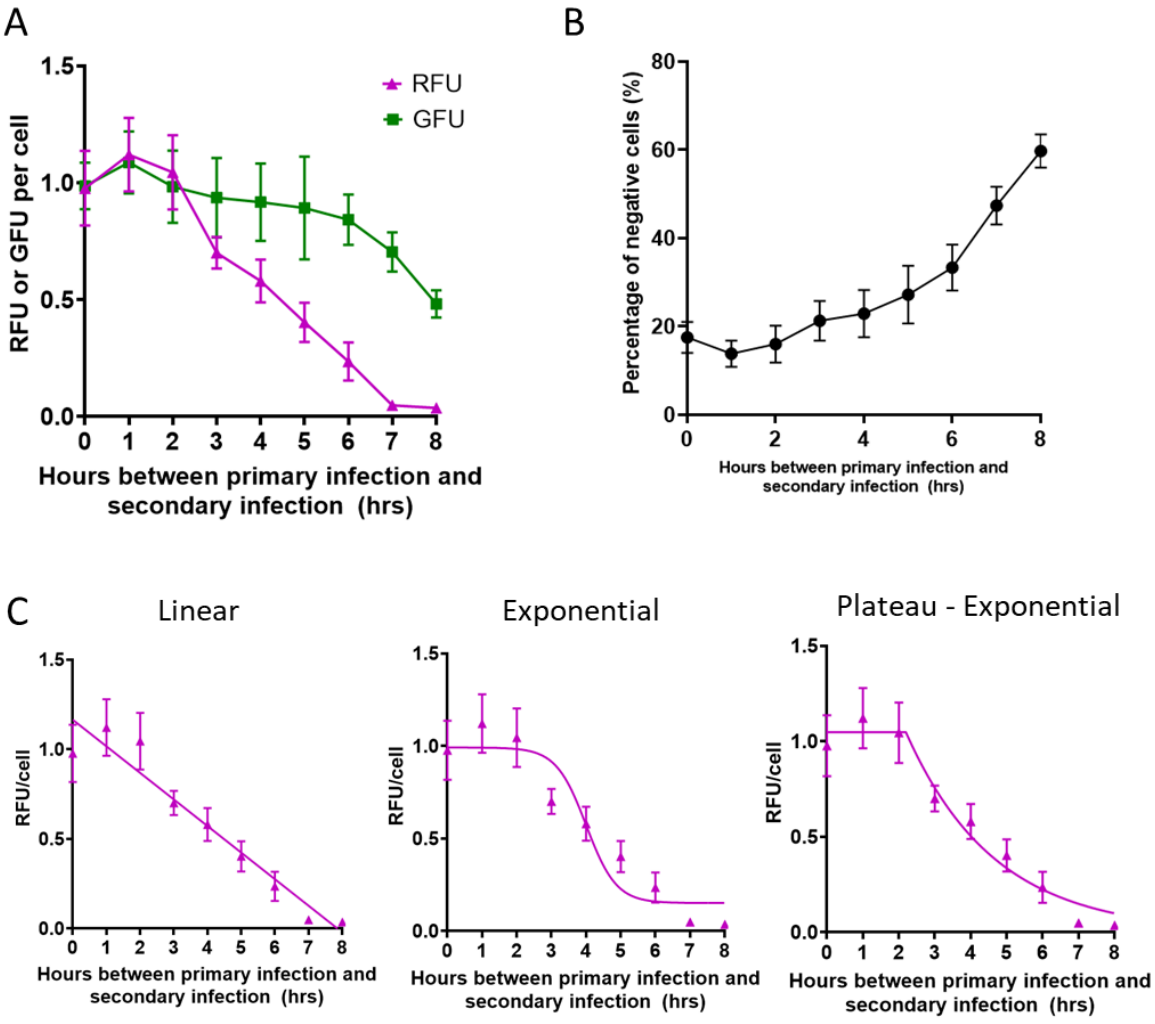

Figure 3.12: The reduction in the ability of the secondary infecting virus to infect the cells is explained by a plateau- exponential reduction model.

(A) The number of reporter viruses per cell that were able to cause expression of their fluorophore, with varying intervals between infection with primary (green) and secondary (red) viruses. Viruses were quantified as GFU and RFU per cell, calculated from the proportions of red, green, and coinfected cells. The mean and SD are shown (n = 6). (B) Proportion of negative cells at each time point of the experiments, means and SD are shown (n = 6). (C) The relationship between the expression of the secondary virus and the interval between infections, as shown in (A), modelled by linear, exponential and plateau- exponential model. R^2 for each model is 0.88, 0.86 and 0.92 respectively. For each model, the total sum of squares (SST) = 1.05, 1.28 and 0.74 respectively.

Using the plateau-exponential model, I have created a working model of what I believe is occurring in the kinetics of the onset of SIE by IAVs (fig. 3.13). At time point 0, the primary infecting virus enters cells, beginning a lag phase where no active SIE producing factor is present. This corresponds with the time it takes for the first viral genomes to enter the cells, uncoat, translocate to the nucleus

and begin replicating [245]. During this time (0-2 h post primary infection) the cells are permissive to secondary infection. From 2 h post primary infection however, viral transcription and replication begins and the active inhibitory factor accumulates within the cell exponentially, resulting in a rapid induction of an exclusionary state in the cell, explaining the progressive shift in permissivity. By 6 h post primary infection, the active inhibitory factor has accumulated to such a point and therefore secondary infection is completely blocked.

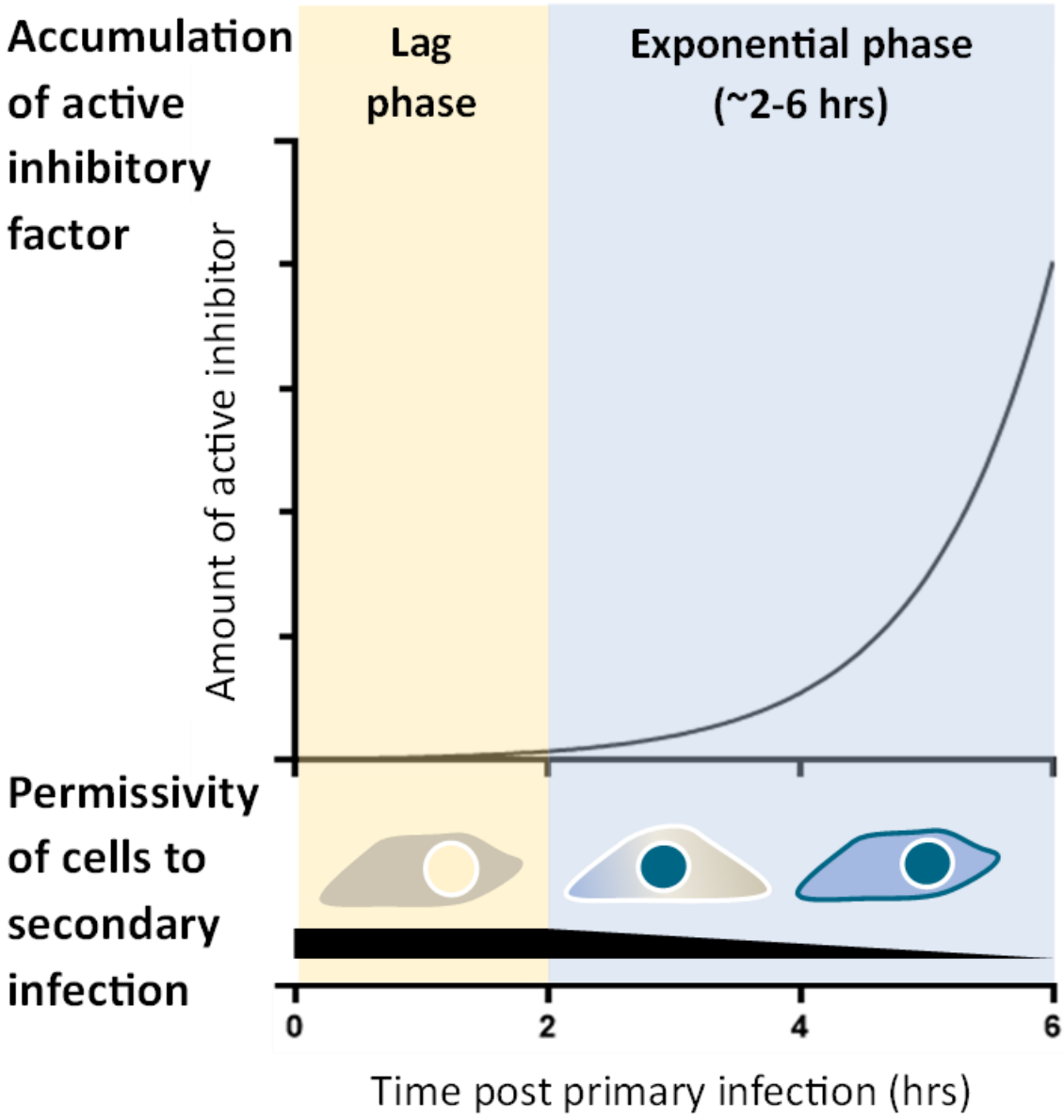

Figure 3.13: Working model of the kinetics of SIE initiated by IAV.

Graph represents the accumulation of an inhibitory factor that causes the exclusionary state in the cell following time post primary infection. Accumulation follows two phases: the lag/plateau phase (yellow section) and the exponential phase (blue section), and corresponding decrease of cells permissivity to secondary infection.

Interestingly, when the order of the infecting viruses was reversed (primary infection with ColorFlu-mCherry and secondary infection with ColorFlu eGFP), the kinetics of SIE were slightly altered (fig. 3.14B and C). The data show a lag phase out to 2 h and then an exponential decrease in the ability of the secondary infecting virus to infect the cells, as before. However, the extent of the exclusion at end point (6 h) is less stringent when mCherry is the primary infecting virus. This could be caused

by the identity of the fluorophore altering the onset of SIE by an unknown mechanism, despite no significant advantages in replication between the two viruses, but to date the reason for this discrepancy is unclear.

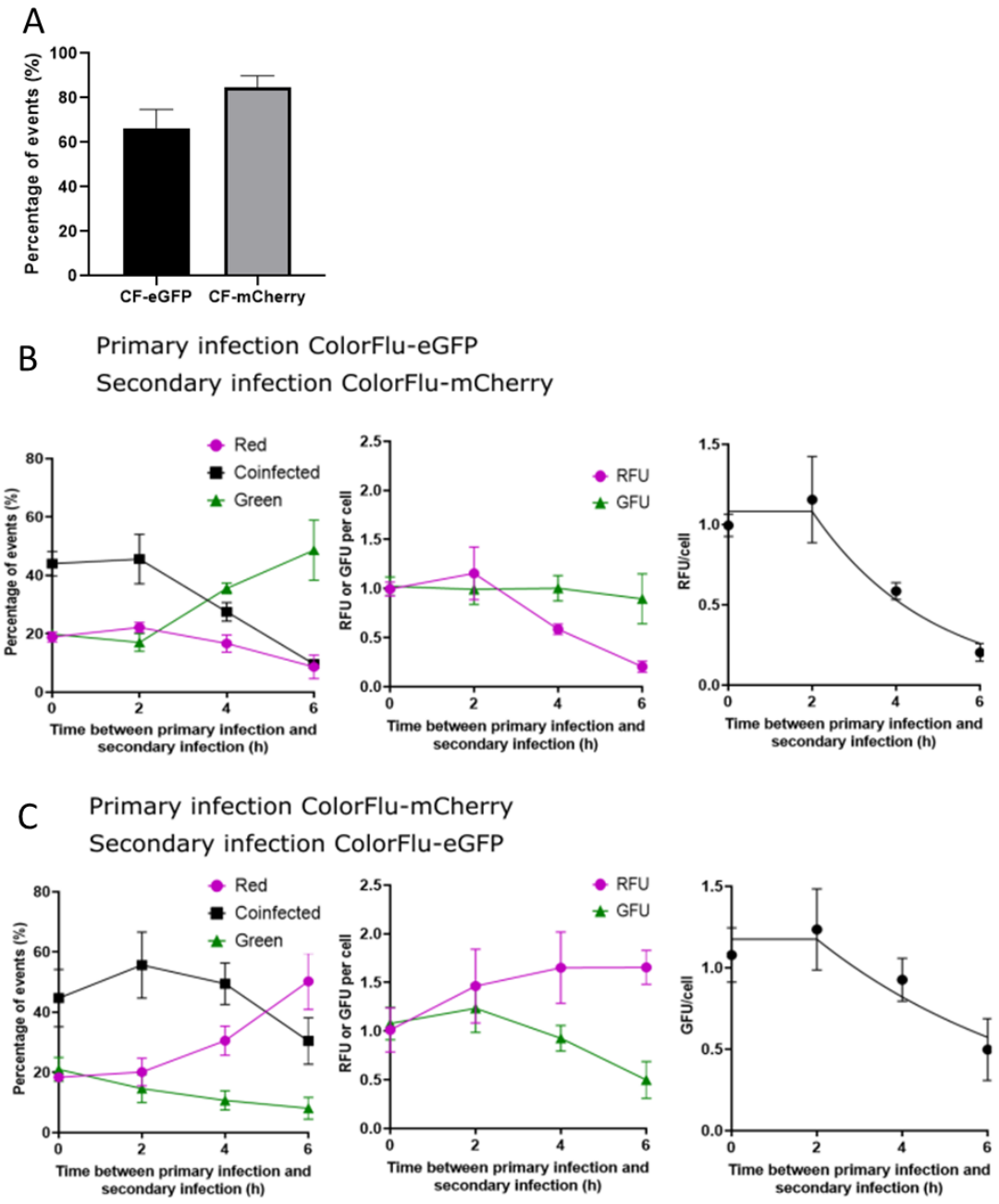

Figure 3.14: The fluorophore colours are considerations in the kinetics of SIE.

(A) Input of CF-eGFP and CF-mCherry viruses in the experiment. Measurement of singly infected MDCK cells with mCherry or eGFP viruses and cells harvested for flow cytometry 16 hpi. Data represents mean and SD, n=3 (B) ColorFlu-eGFP or (C) ColorFlu-mCherry before secondary infection at the time points indicated with the other virus, with both viruses at MOI 1 FFU/cell. The percentage of fluorescent cells was then assessed using flow cytometry. The number of red and green forming units per cell (RFU, GFU) was calculated from the percentage of red, green, and coinfected cells under the assumption that infection follows a Poisson distribution. The number of secondary viruses detected per cell were used to fit a model in which the number of secondary viruses per cell that could be detected was constant for 2 h and then decayed exponentially to zero with increasing intervals between infections. The SST for the models in (B) and (C) are 0.22 and 0.24, respectively. Data are presented as mean and SD (n = 3).

3.6 Discussion

In this chapter, I investigated the interactions during simultaneous and non-simultaneous infection between genetically related IAVs using a reporter system. Firstly, I assessed that the established reporter system ColorFlu is a suitable to assess coinfection between viruses. I showed that coinfection during simultaneous infection occurs freely, and the viruses replicate independently of each other. However, I found that as the time between primary and secondary infection is increased, SIE onset results in the cells becoming increasingly refractory to secondary infection.

Additionally, I described our development of BrightFlu reporter virus in conjunction with C. Pirillo, S. Al Khalidi and E. Roberts from the Beatson Institute, Glasgow. I show that BrightFlu stably expresses the ZsGreen fluorophore which correlates with NP expression, and the viruses replicate as expected. As ZsGreen is significantly brighter than eGFP, it is a more useful reporter system for use in complex or highly autofluorescent systems such as whole lung lobes [188]. In BrightFlu, 2A autoproteolytic sequences have been included flanking the fluorophore gene so that the viral NS1 protein is liberated from the fluorophore protein. Therefore, it is likely that the NS1 from BrightFlu would be more functional than the NS1-fluorophore fusion protein from ColorFlu which has been shown to be compromised in function [243]. However, this requires experimental proof, firstly that the protein is liberated and that it has increased functionality compared to ColorFlu virus NS1. Overall, BrightFlu has some advantages over ColorFlu but the full extent has yet to be elucidated. At the time of the experiments in this thesis, only the green fluorescing BrightFlu existed and therefore BrightFlu could not be used to investigated coinfection, so in ongoing investigations I used ColorFlu rather than BrightFlu.

I found that the ColorFlu viruses are suitable for modelling coinfection between progeny viruses, firstly as there is no growth advantage between the two viruses in either single or multicycle infection and secondly, as most infected foci express both the fluorophore and NP, fluorophore expression is a reasonable proxy measure for infection status of the cell. However, it is important to recognise that this assumption will cause the mischaracterisation of cells that are infected, but do not express the NS1-fluorophore fusion protein. Although I believe that this proportion of cells is

small, as most plaques express fluorophore and NP in multicycle infection, it is nevertheless a limitation of this approach. Furthermore, during the flow cytometry experiments, the infection status is binarised by gating cells into negative, singly infected eGFP+ or mCherry+, and coinfected groups, any information about the intensity of the eGFP and mCherry signal has been simplified. The intensity of the signal may indicate differences in the number of virus particles infecting the cell, a factor which has been suggested to effect the kinetics of SIE [122]. The allocation of thousands of cells into gate therefore may give us an idea of how SIE onset occurs in these cells overall but misses the nuances of the kinetics in each cell. To address this, it may be prudent to investigate SIE using an assay that takes into account the number of genome copies per cell such as qPCR.

I showed that IAV coinfection potential during simultaneous infection occurs freely, independent of any interference between the viruses, and peaks when the input of the two viruses is equal. I subsequently show that the capacity for coinfection is reduced during non-simultaneous infection due to the onset of SIE. By varying the time between primary and secondary infection, I found that the potential for coinfection between coinfecting viruses is initially unrestricted during a 2 h window following primary infection but then exponentially decreases with increasing times between the primary and secondary infections. This suggests that SIE may be connected to the replication of the primary infecting virus, as 2 h is approximately the amount of time it takes for a typical incoming virion to enter the cell, uncoat, translocate to the nucleus and begin replicating – after which replication of the viral genomes occurs exponentially. This finding implies that the replication or production of viral products may be involved either directly or indirectly with the onset of SIE. The mechanism for IAV induced SIE is not yet known, but there has been some suggestion that replicating influenza polymerase complexes are required for onset of SIE [122], which is consistent with a plateau-exponential model. Overall, my data suggests that SIE is driven by the production or activation of an inhibitory factor which is linked to the replication rate of the primary infecting virus, which is represented by our working model. Possible identities of the inhibitory factor or factors are explored in chapter 5.

Overall, in this chapter, I have outlined a model system for our exploration of coinfection and SIE, defined the kinetics of SIE in individual cells and begun to explore the mechanisms underlying SIE induced by IAV. In the next chapter, I will investigate the effect of SIE on the coinfection of viruses during spatial spread of the viruses within hosts.

Chapter 4: Exploring the impact of SIE on the patterning of IAV infections during localised viral spread

4.1 Introduction

4.1.1 Within-host spatial spread

Spatial spread of infections refers to the propagation of viral infections in space. Spatial structuring of infections occurs over multiple scales: intracellular, within-host and between-host (fig. 4.1). In this section I will briefly outline our current understanding of spatial structure of infections in single cells and at the between host level, before outlining our current understanding of within-host spread, which will be the focus of this chapter.

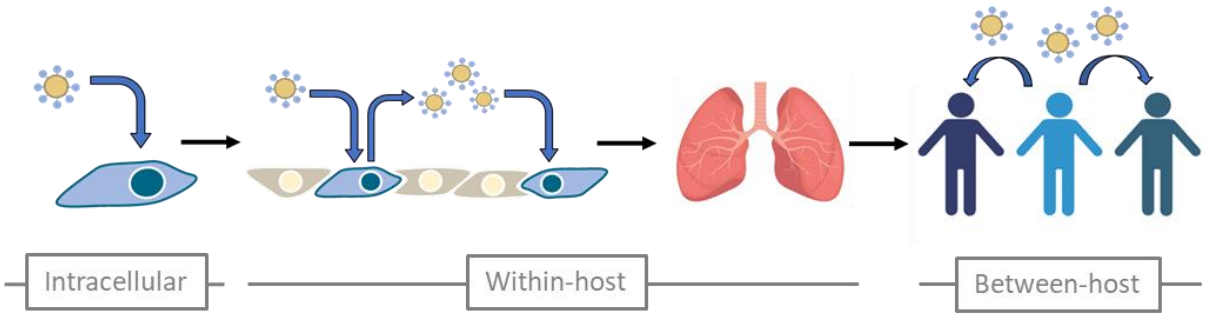

Figure 4.1: The scales of infections

Inside cells, viruses induce vast remodeling to bring components together to complete their replication cycle. An example is ensuring the genomes are in the correct compartment for replication. Most viruses replicate by creating specific replication complexes, which requires extensive remodeling of cellular membranes [248]. These replication compartments offer two advantages for the virus: firstly, allowing the gathering of cofactors into one place for efficient replication and secondly sequestering replication intermediates to avoid detection by the cellular innate immune sensors [249]. Additional remodeling of the cellular cytoskeleton is required by

many viruses, for example IAV hijacks the cellular cytoskeleton for nuclear import of the genomes for replication [250]. Egress of IAV genome segments from the cell, similarly, requires the genomes to be gathered into the correct place at the plasma membrane for budding. The proposed model for this is that the nascent genome segments associate with Rab11 positive vesicles to bring them to the plasma membrane together [251]. Therefore, spatial structuring inside cells is important to ensuring efficient replication of many viruses and studying these processes inside cells potentially allows us to identify new targets for drug discovery.

Additionally, we understand much about the spread of viruses is at the between-host level, usually through spatial epidemiology studies sequencing viruses across a large geographical area. When applied to endemic viruses, this can provide insight into seasonality and circulation at the population level [86,252]. In a pandemic setting, this approach can provide insight into the evolutionary history of the virus and identify likely candidates for the host species from which the pandemic virus emerged [253]. At a finer scale, understanding local community transmissions or transmission within dwellings or in work settings can aid understanding successful modes of transmission and risk factors for acquiring disease [254–256]. Therefore, studying between-host spatial distribution is key for predicting disease incidence and informing disease control strategies.

There is a growing understanding of how virus infections are spatially structured inside hosts. More focus in recent years has come from understanding tissue tropism for different viruses. The main determinant of tropism for enveloped viruses is the expression the viral receptor on the surface of cells [257–259]. However, recently the focus has expanded to include other determinants of host organ tropism such as the differential expression of cytokine receptors in different organs resulting in some being refractory to infection [260]. When it comes to viral spread within organs, there are experimental challenges in imaging infections in situ while retaining spatial information. One approach is to stain for viral antigen in tissue from experimentally infected animals or in biopsies from infected patients [261]. In liver biopsies from patients with viral hepatitis, for example, scientists observed clusters of HCV infected cells, which implied random seeding of infections from the blood which then expanded locally within liver tissue [262]. This approach is valuable, especially

when combined with mathematical modelling to predict how the clusters formed but misses temporal information as to the expansion of the foci. Similarly experimental *in vivo* approaches, which take snapshots of the target infected organ at various timepoints cannot provide temporal information due to the reliance on fixed tissue [186]. Approaches that allow the imaging of expanding infections over time in live animals, such as luciferase reporter viruses, have been developed but generally do not have the resolution to investigate individual foci [263,264]. Therefore, although there is evidence that within-organ spread of viruses is spatially structured, experimental challenges have meant that there are knowledge gaps in both fine spatial and temporal information as to how these foci expand and interact in live cells [265].

4.1.2 Localised spread of IAV

In this section I will review the evidence we have for the spatial structure of IAV infections in the respiratory tract. Intranasal inoculation of high doses (10^5 – 10^7 pfu per animal) of luciferase-expressing IAVs into mice show replication in the upper respiratory tract by 1 dpi, followed by dissemination of the infection to the lungs by 2 dpi [264]. When examining virus spread inside the organs, we often observe evidence of localised viral spread, with limited evidence for long-range spread, shown by the appearance of individual foci of infection. Immunostaining of viral antigen in tissue sections has shown discrete foci in the bronchi of human patients who succumbed to fatal influenza [261]. Interestingly in experimentally infected ferrets, investigators observed that different strains of influenza viruses all form foci, but in different parts of the nasal epithelium showing the effect of different target cells on spatial spread [266]. The use of fluorescently tagged IAVs has also revealed foci formation in mouse lungs by 4 dpi, which is maintained out to 5 dpi without long-range dissemination [267]. Together these studies reveal that spread of IAV in the upper and lower respiratory tract occurs locally cell-to-cell with limited long-range spread during natural infections and in experimentally infected animals.

Local viral spread with occasional long-range dissemination could be due to a number of non-mutually exclusive mechanisms [265]. Firstly, this could be an effect of mucus and the directionally of the beating cilia suppressing dispersal of nascent virions and directing the virions to a specific

area of the tissue [268]. It has been shown that mutations that reduce HA binding to sialic acid expressed on free glycoproteins in mucus promotes virulence in a mouse model, possibly through increasing the release of virions for long-range spread [269]. Alternatively, a limit to long-range dissemination may result from a limited role for extracellular viral spread, and instead implies a role for direct cell-to-cell spread. One such mechanism of direct cell-to-cell spread is tunnelling nanotubules, thin actin-containing structures can transfer viral genomes between cells [270–272]. A possible advantage of this approach for the viruses is it protects the virus from exposure to neutralising antibodies. More studies are required to determine the extent to which these mechanisms contribute to the apparent suppression of long-range dispersal.

Overall, IAV infections within the upper and lower respiratory tract are highly structured and are characterised by the appearance of discrete foci of infection, with occasional long-distance spread.

4.1.3 Localised viral spread and its consequences for IAV evolution

Localised spread of infectious foci has implications for virus coinfection, and as discussed in the main thesis introduction, coinfection has implications for the diversity of the viral population.

Firstly, localised spread increases the likelihood that cells within a focus of infection are coinfected with more than one virus particle. Infection of cells with multiple virus particles has been repeatedly shown to promote the production of DIPs [108]. As reviewed in section 1.3.2.4, when DIPs accumulate within the viral population they can destabilise the population by outcompeting FIPs. Therefore, localised spread of a virus may promote the genetic instability over multiple rounds of infection, which could potentially limit the size of the focus [104]. However, the increase in multiple infection also allows SIPs to contribute to propagation of the viral population, which could expand the size of the focus [170]. Therefore, the consequences of spatial spread may affect how many cells the virus can infect, and the genetic stability of the virus population.

Secondly, as the viruses that coinfect cells within an individual focus have been produced from a founder infection of one cell, the coinfecting viruses are most likely to be genetically alike. This promotes founder effects and therefore reduces the capacity for diversity with a single focus [273].

In this way, individual foci act as islands of low genetic diversity. On the other hand, founder effects may promote genetic diversity at the whole viral population level by allowing the expansion of rare mutants in isolated foci [274]. Recent studies of IAV using barcoded viruses in the lungs of experimentally infected animals has shown this very effect, with each lobe displaying genetically distinct populations, despite a very diverse population at the whole organism level [275]. Therefore, spatial restriction of viral spread, results in a reduction in localised diversity due to within-host bottlenecks but may promote diversity in the viral population overall.

Thirdly, although coinfection within a focus would be common, the physical distance between foci would likely limit the coinfection of cells with viruses from different foci. We presume that reassortment between different strains of influenza virus, the scenario which would lead to the generation of pandemic viruses, would necessitate interaction between viruses from different foci. This is because it is unlikely that different strains of virus would be delivered to the host simultaneously and would therefore be distributed into different foci [235,236]. Indeed, one study which observed compartmentalisation of virus lineages to separate lung lobes in a porcine model showed a reduced production of reassortant progeny compared to guinea pig or ferret models that displayed less extensive compartmentalisation, showing an impact of spatial distribution on reassortment [276]. Similarly, it has been shown that coinfection and therefore reassortment is increased if a primary infecting viruses is permitted to spread for 12 h prior to secondary infection, presumably due to the expansion of the primary virus foci [233]. Therefore, the distribution of viruses into separate foci can prevent coinfection of viruses from different foci, and therefore prevent reassortment.

Overall, spatial distribution of infections can control the potential for coinfection within and between foci of infection which can impact the evolution of the virus population. Much of the evidence we have for these processes come from sequencing studies but direct evidence for how these foci of infection expand and interact is currently lacking.

Current data suggest that IAV infections are spatially structured, and although there is some evidence for the increase of coinfection within a focus, and decreased coinfection of viruses from separate foci, direct spatio-temporal information about these interactions is limited [265].

4.1.4 Chapter Aims

In this chapter, I explored how SIE, which imposes a temporal block to coinfection in individual cells, impact coinfection over multiple rounds of infection in a spatial context. First, I modelled the foci of infection we observe in the lungs of naturally infected patients and experimentally infected animals *in vitro* using plaque assays. The plaque assays replicate the observations of localised cell-to-cell spread and limited long range dissemination we observe in IAV infections. I used MDCK cells as they are a common epithelial model for IAV infections, and the output of virus from MDCK cells is well characterised [234,277]. Using this model, I show that SIE does not restrict virus coinfection within a plaque, which indicates that coinfection between progeny occurs freely. Using the same model, I then show that SIE restricts coinfection of cells by viruses from different foci to only a small area of the cell monolayer where the foci meet. As MDCK cell monolayers lack the structure and complexity of the airway epithelium, I then collaborated with scientists from the Beatson Institute to confirm the same this observation in mouse lungs. Overall, in this chapter I show that SIE restricts interactions between IAVs during spatial spread within a host and argue that this is likely to impact viral evolution and reassortment.

4.2 BrightFlu infection forms individual foci in mouse lungs

To begin, we wanted to confirm the observations from the literature that IAV forms discrete foci of infection in the respiratory tract of infected hosts. To do this we collaborated with the lab of Dr Ed Roberts (Beatson Institute, Glasgow), and infected mice intranasally with BrightFlu viruses (100 PFU per animal) (explanation of design and characterisation of BrightFlu can be found in section 3.2.2). At 3 dpi, the whole middle lung lobe was harvested, cleared, and imaged using light sheet microscopy. Using this approach, we could observe extensive infection of the bronchi with evidence of discrete foci of infection in the lungs (fig. 4.2). Therefore, we confirmed the appearance of foci *in*

vivo experimental mouse infection which suggests localised viral spread with limited long-range dispersal.

Infection and preparation of samples performed by E. Roberts and C. Pirillo. Light sheet microcopy performed by E. Roberts, C. Loney and C. Pirillo. Images prepared by C. Bentley-Abott. These images form part of a published study which can be access here [188].

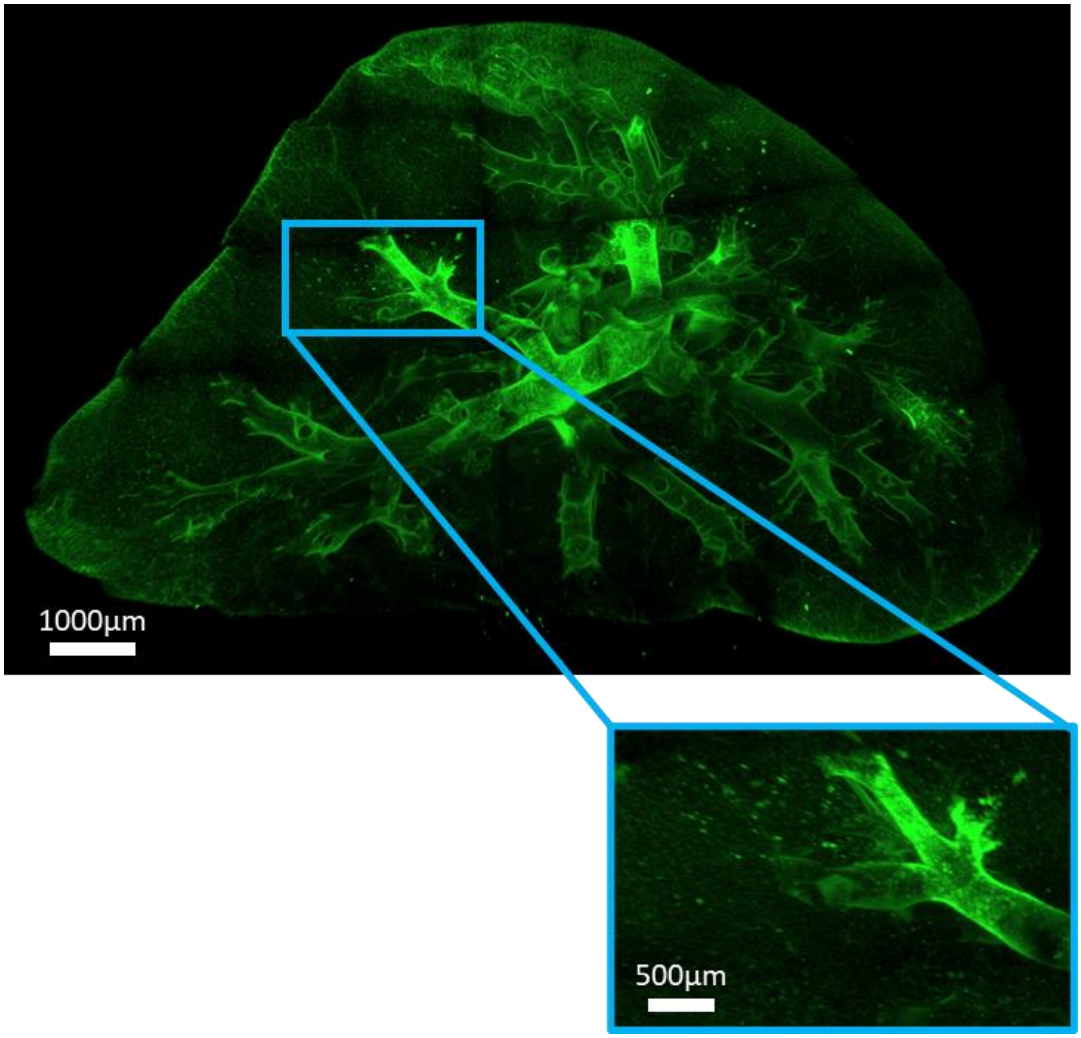

Figure 4.2: BrightFlu forms individual foci in mouse lung lobes.

Image of whole middle lung lobe from mice infected with 100 PFU of BrightFlu. At 3 dpi the lobes were removed, cleared using ethyl cinnamate and inflated using 2% agarose and imaged using light sheet microscopy. Scale bar = 1000µm. Enlarged image of region of interest also shown, scale bar = 500µm.

4.3 SIE does not prevent coinfection between viruses within a focus of infection

Having observed foci in mouse lungs, we wanted to investigate the effect of SIE on the interactions of viruses within individual foci. We anticipated that coinfection between viruses within foci would occur often due to the limitation of long-range spread. We know from studies of PR8 in MDCK cells that in our model the virions are likely to begin to be released from the cells between 4 and 8 hpi (estimation from high MOI infections, MOI 10) [244]. Therefore, as we showed that SIE onset occurs at 2 hpi, it was conceivable to us that SIE onset could occur between the viral bursts of a newly infected cell and therefore restrict coinfection between progeny viruses within a single focus of infection. To investigate this we devised an experimental set up whereby we created a population of coinfected cells through high MOI simultaneous infection. After infection, I dispersed the cells using trypsin, diluted them and overlayed them on fresh cell monolayers – effectively seeding the viruses into the same area of the monolayer to create coinfected foci. After 4 hours, I overlayed the assay with agarose to contain the viruses to localised spread (fig. 4.3).

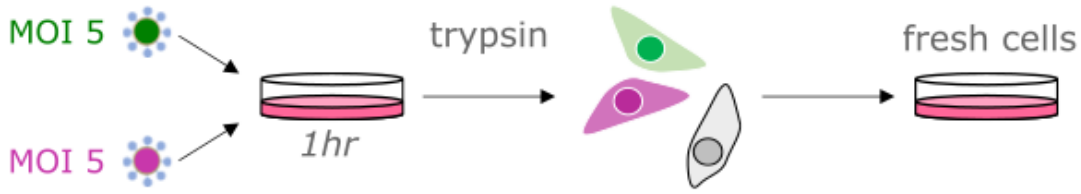

Figure 4.3: Experimental design of investigating spread from a single focus of infection.

Monolayers of MDCK cells were coinfected simultaneously with MOI 5 of each eGFP and mCherry-tagged viruses. After 1 h the coinfected cells were dispersed using trypsin, diluted and overlayed onto fresh cells and allowed to settle for 4 hours before overlay with agarose.

We proposed two models for what could happens as the viruses spread outwards from a coinfected cell (displayed as white fluorescence) (fig. 4.4). In a single round of infection with a limited number of viruses (estimates place burst size of an individual cell in a single round of infection to around 10 PFU/cell [234]) we would expect the cells around the foci to be infected with a small number of particles, possibly consisting only of particles carrying one fluorophore gene. If SIE is established in

these cells before the next round of particle release, we would expect all subsequent infection to be blocked and therefore that cell would remain the colour of the initially infecting viruses. Over multiple rounds of this process, we could envision that the whole plaque would split out into singly infected areas (fig. 4.4A). On the other hand, if SIE onset is too slow to prevent secondary infection from viruses from the next viral burst, we would expect the focus to remain coinfected as the plaque expands (fig. 4.4B).

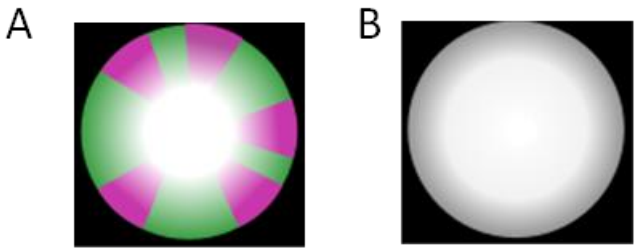

Figure 4.4: Models of the effect of SIE on spread from a single focus of infection.

(A) Rapid onset of SIE between viral bursts would result in the establishment of distinct regions of infection where one tagged virus dominates. (B) Spread of both viruses are uninhibited by SIE onset.

When I imaged the plaques, I observed that as the coinfected plaques expanded, both fluorophores were expressed across the entire plaque area (fig. 4.5). I did observe regions where one fluorophore excludes the other, this appears to be driven by rare long-range dispersal of a tagged virus landing in a separate area and establishing a separate region of infection in that area. We therefore hypothesise that this is due to a breakdown in localised spread rather than an effect of SIE between progeny viruses. The intensity of the fluorophores also varied across the plaques, which we reason may be due to the cells receiving an unequal amount of the two tagged viruses or by differential fluorophore stability, which may result in one brighter than the other. However, as both tags are expressed across the plaque, we concluded that progeny viruses of a single focus are able to coinfect freely with no restriction from SIE.

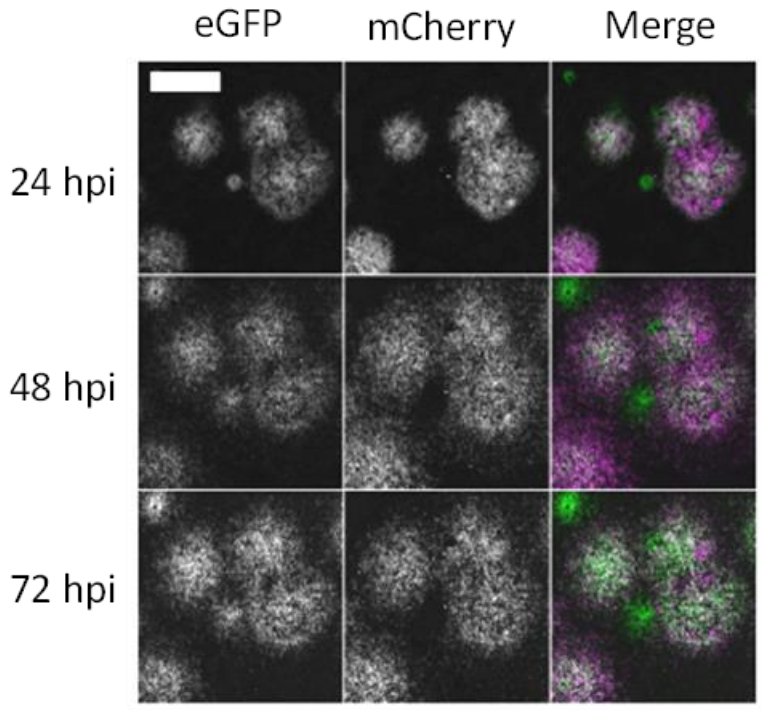

Figure 4.5: SIE does not impact the interactions between viruses as they spread from a single focus of infection.

The spread of coinfected foci of infection, showing the same region at 3 different time points. Viruses were seeded onto monolayers of MDCK cells, overlayed with agarose, and imaged every 24 h. Images were taken on Celigo fluorescence microscope and a representative field of view is shown. Scale bar = 2 mm

I did note that the white signal is concentrated at the centre of plaques compared to the edges. To quantify this observation, I applied a binary threshold to the images at each time point, which collapses the intensity information and determines whether each pixel is red, green or coinfected (white) (fig. 4.6A). I then calculated the percentage of pixels that were white compared to the percentage that were red, green or white, for each timepoint. I found that the percentage of white pixels, which responds to the plaque area that was coinfected, was significantly higher at 24 hpi compared to 48 or 72 hpi (One way ANOVA, $p<0.00001$). This effect could be due to two non-mutually exclusive phenomena. Firstly, as the plaque gets bigger, the number of cells at the leading-edge increases, and therefore theoretically, during restricted local spread, the MOI and therefore the likelihood of coinfection reduces as the plaque expands. Secondly, using live cell imagining, we have observed that cells migrate inwards towards the centre of the plaque as they die [116].

Therefore, the centre of the plaque could represent a clump of dead coinfected cells. So, although SIE does not restrict coinfection between progeny viruses, our data suggests that, through action of a second mechanism, coinfection is more likely in the centre of the plaques.

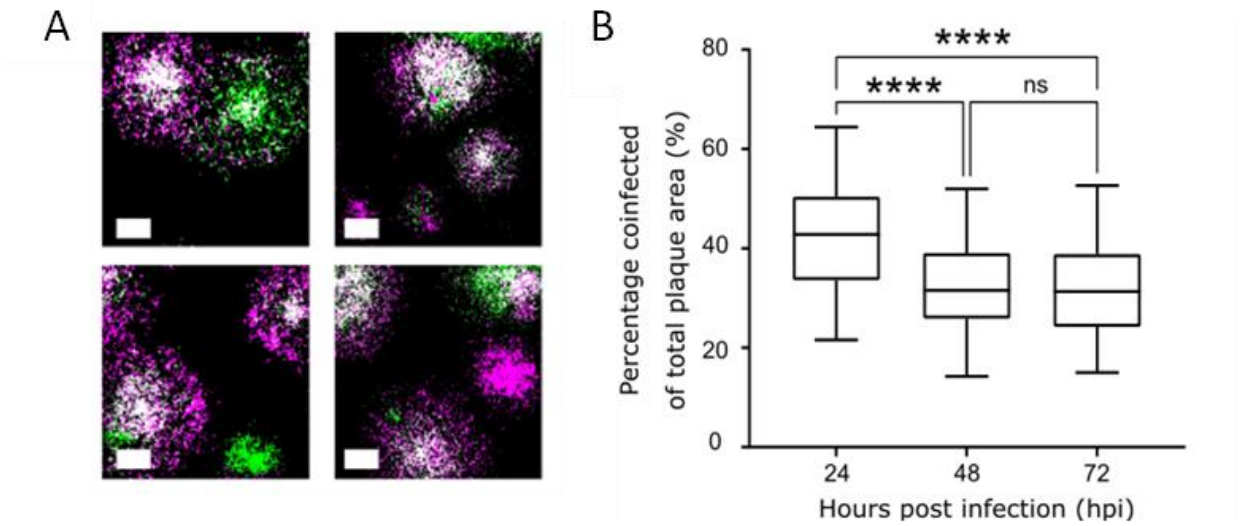

Figure 4.6: The centre of infectious foci act as hub of coinfection

(A) A binary threshold was applied to images of plaques to distinguish coinfected cells (white) from singly infected cells (magenta or green); representative images of plaques at 48 hpi are shown. Scale bars = 1 mm. (B) The percentage of total plaque area that was coinfected, calculated from binarised images at taken at each time point. Box and whisker plots show the percentages of infected areas from 71 individual fields of view at 3 time points in 1 experiment. Differences between the coinfected percentage at different time points were tested for significance by one-way ANOVA (**** $p < 0.0001$)

4.4 SIE prevents coinfection between viruses from different foci of infection

Having established that SIE does not restrict coinfection between viruses within a focus of infection, we wanted to investigate how it would impact viruses from separate foci of infection. This more accurately models the interaction required for the generation of reassortant viruses, as during initial infection of a host, different strains of the virus are unlikely to encounter the exact same cell at the same time. To model these interactions, I infected monolayers of MDCK cells at low MOI of eGFP and mCherry-tagged viruses, such that each plaque was initiated by a single virus, overlaid them with agarose and took images of the plaques every 24 h for 72 h. I observed that where a green and

red plaque grew into each other, the fluorophores remained almost completely distinct, with no evidence that the plaques were growing over each other. Instead, I observed that each plaque was blocked from expanding further by the presence of the other plaque. (fig. 4.7 and fig. 4.8).

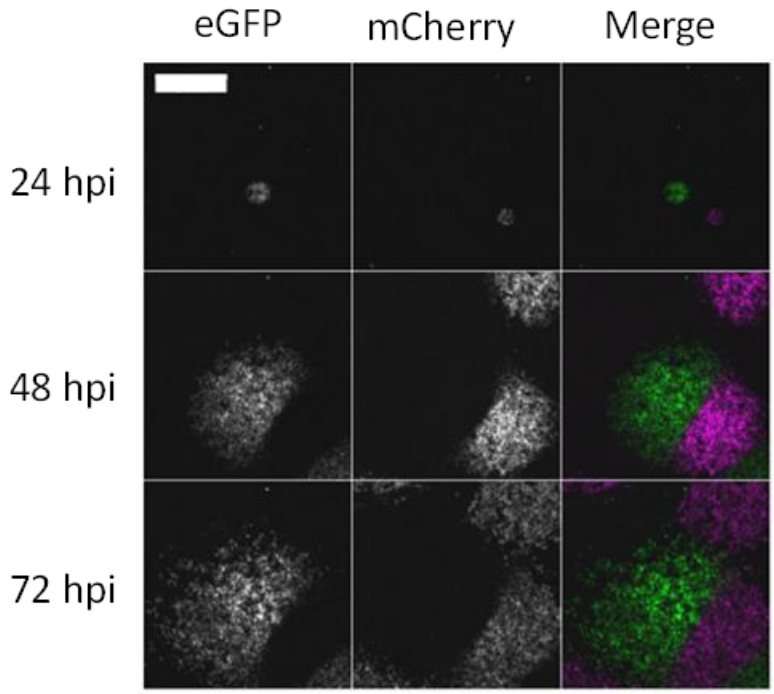

Figure 4.7: SIE restricts interactions between viruses from different foci of infection.

Representative image of plaque interaction. Monolayers of MDCK cells were infected with eGFP and mCherry tagged viruses, overlayed with agarose, and imaged every 24 h. Representative images, taken on Celigo fluorescent microscope, are shown. Scale bar = 2 mm.

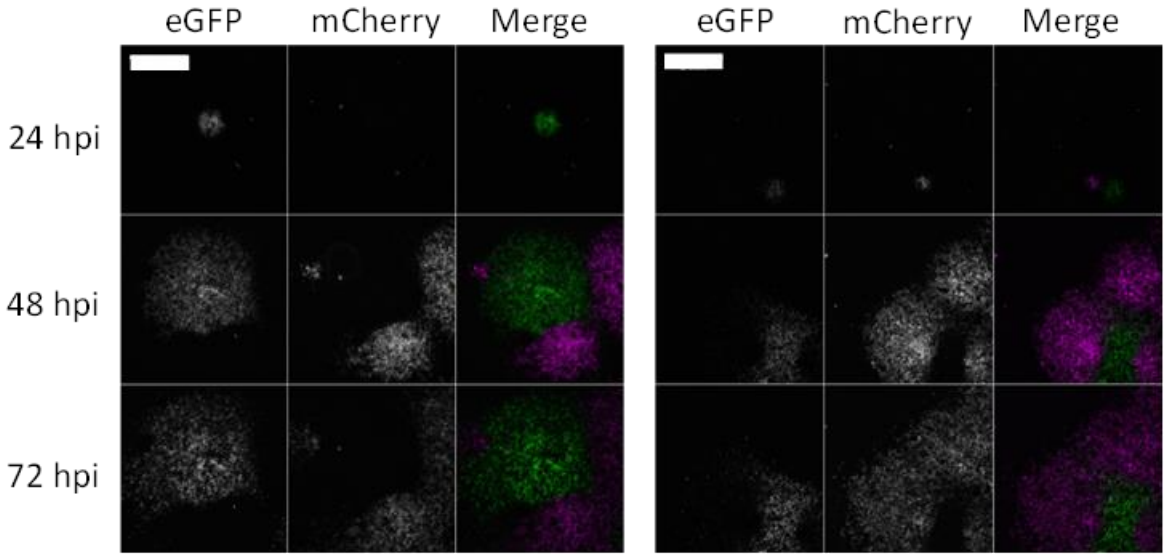

Figure 4.8: Further examples of SIE restricting interactions between viruses from different foci of infection.

Further examples of representative images of plaque interaction. Monolayers of MDCK cells were infected with eGFP and mCherry tagged viruses, overlayed with agarose, and imaged every 24 h. Representative images, taken on Celigo fluorescent microscope, are shown. Scale bar = 2 mm.

When I investigated the boundary between the two differently coloured plaques, we observed a thin region where the two fluorophores are expressed (fig. 4.9A). To investigate the size of this region, I applied a binary threshold to the images of the plaques at 72 hpi and calculated the area of coinfection as above (details of the image analysis macros used in this study can be found in materials and methods) (fig. 4.9B). I found that the coinfected area constituted around 1% of the total plaque area (fig. 4.9C). Therefore, SIE restricts coinfection between progeny of separate foci to a small region at the boundary of the two foci.

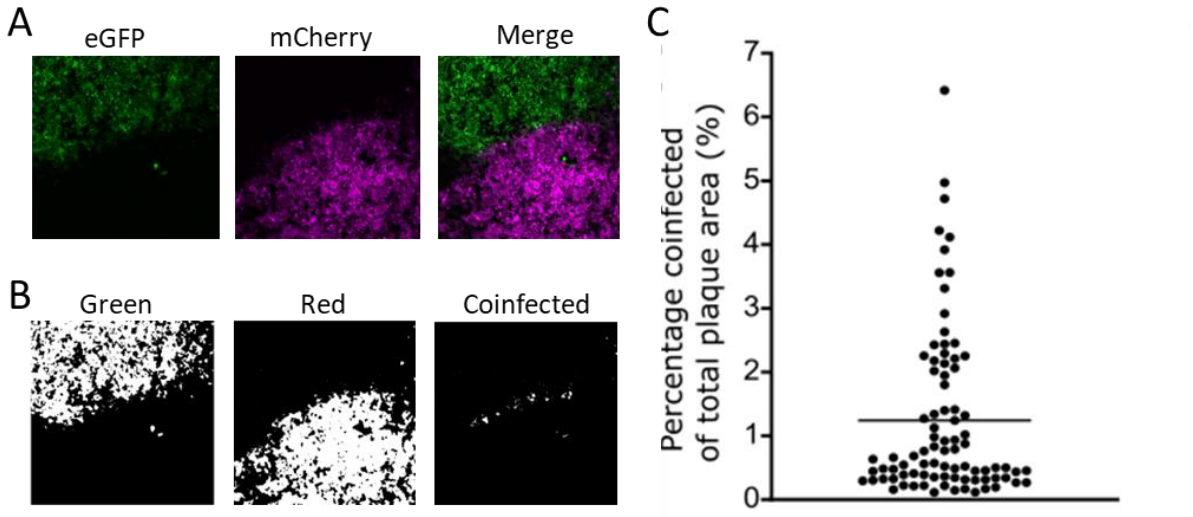

Figure 4.9: SIE restricts coinfection between different foci to a tiny region of the infection.

(A) Image of a representative interacting plaque. Monolayers of MDCK cells were infected with eGFP and mCherry tagged viruses, overlayed with agarose, and imaged in the Celigo fluorescent microscope (B) Binary threshold was applied to image shown in (A) to distinguish cells expressing the eGFP, mCherry, or both fluorophores together. (C) The percentage of coinfected areas in comparison to total plaque area was calculated from images at taken at 72 hpi. The mean and the percentage areas of 86 individual fields of view from 1 experiment are shown.

However, this finding was in 2D cell culture which lacks the complexity and structure of the airway epithelium. Therefore, it is possible that this observation is an artefact of cell culture. We therefore transferred our investigation *in vivo*, in conjunction with the lab of Dr E. Roberts (Beatson Institute, Glasgow). In order to maximise the chance of observing interactions between differently coloured foci, we simultaneously infected C57BL/6 mice intranasally with a mixture containing high dose of both ColorFlu-eGFP and ColorFlu-mCherry (500 PFU of each virus) and took lung sections at both 3- and 6-days post infection (dpi). We found that at 3 dpi the infection was mostly centred within the bronchi, but by 6 dpi the viruses had disseminated out of the airways into the alveoli and established red and green foci of infection (fig. 4.10).

Infection, preparation of samples, confocal microscopy and preparation of images was performed by E. Roberts, C. Pirillo and R. Devlin

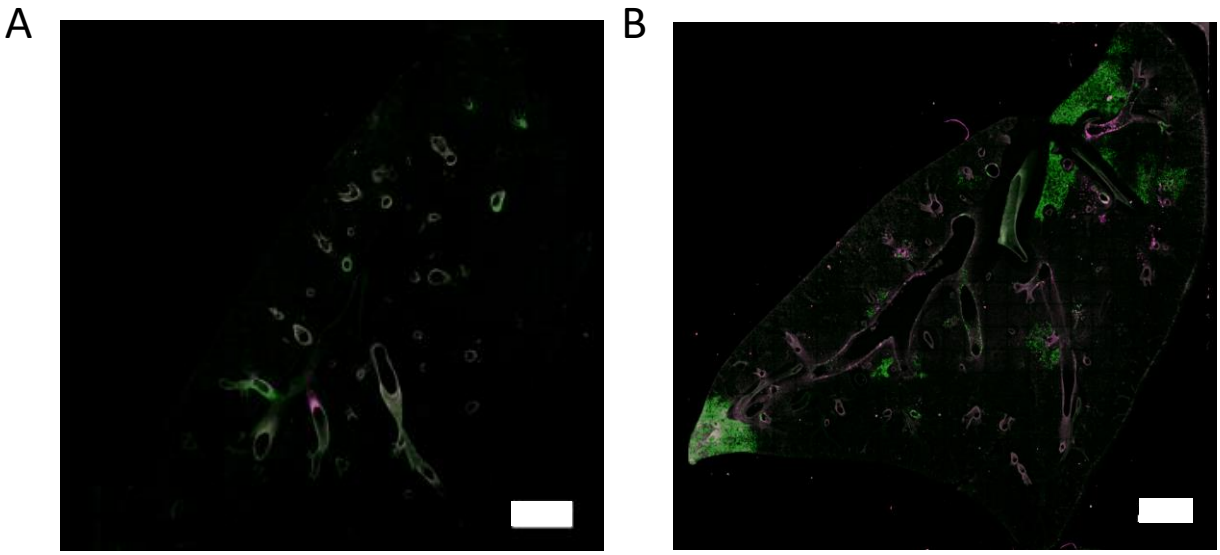

Figure 4.10: Dissemination of ColorFlu viruses occur from the mouse bronchi to into established lesions between 3 and 6 dpi.

C57BL/6 mice were intranasally inoculated with mixtures of mCherry and eGFP expressing ColorFlu viruses (500 PFU of each virus). Lung sections, taken at (A) 3 dpi and (B) 6 dpi, were imaged using a Zeiss LSM 800 with a 20× objective lens. Scale bar = 1,500 µm.

When we investigated the infected lungs at 6 dpi more closely, we found regions where adjacent green and red foci were interacting (fig. 4.10). I then applied the binary threshold we used previously to assess the amount of coinfected pixels. Like the observation with made *in vitro* with monolayers of cells, I found that only a small area between the foci where coinfection is supported (fig. 4.11 and fig. 4.12). Therefore, we concluded that SIE restricts coinfection, and therefore, reassortment between viruses from different foci *in vivo*.

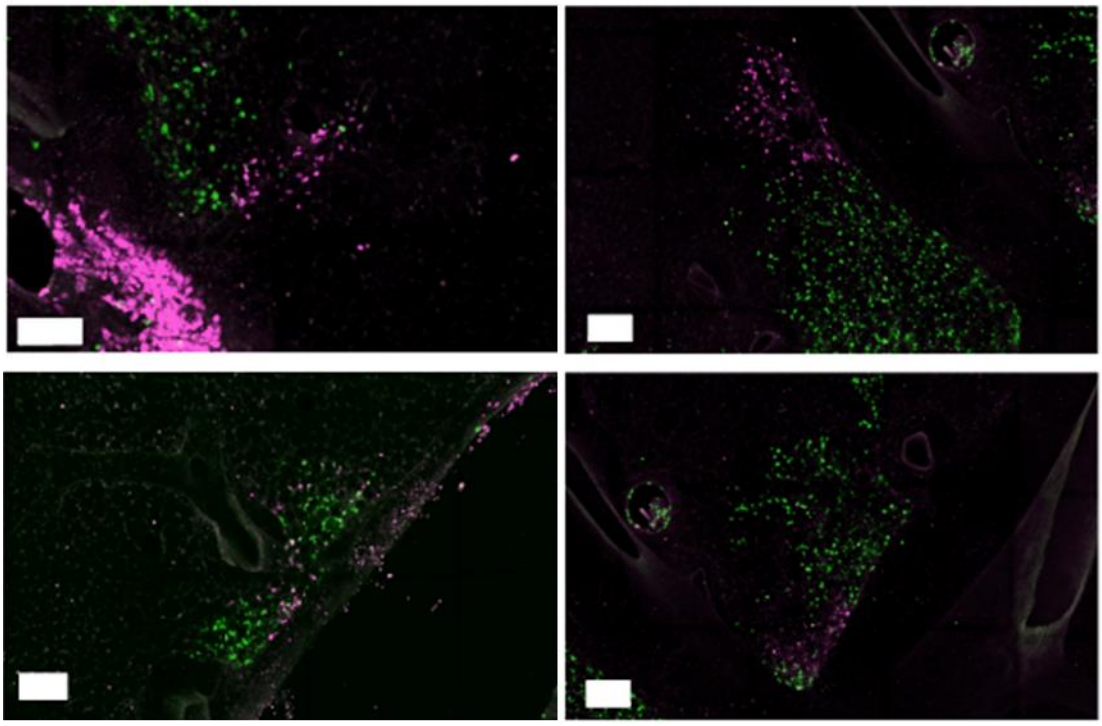

Figure 4.11: ColorFlu viruses establish separate foci of infection *in vivo.*

Additional representative enlarged images of infected foci from confocal images of mouse lung sections at 6 dpi. C57BL/6 mice were intranasally inoculated with mixtures of mCherry and eGFP expressing viruses (500 PFU of each virus). Lung sections were imaged with a Zeiss LSM 800 using a 20× objective lens. Scale bar = 100 µm.

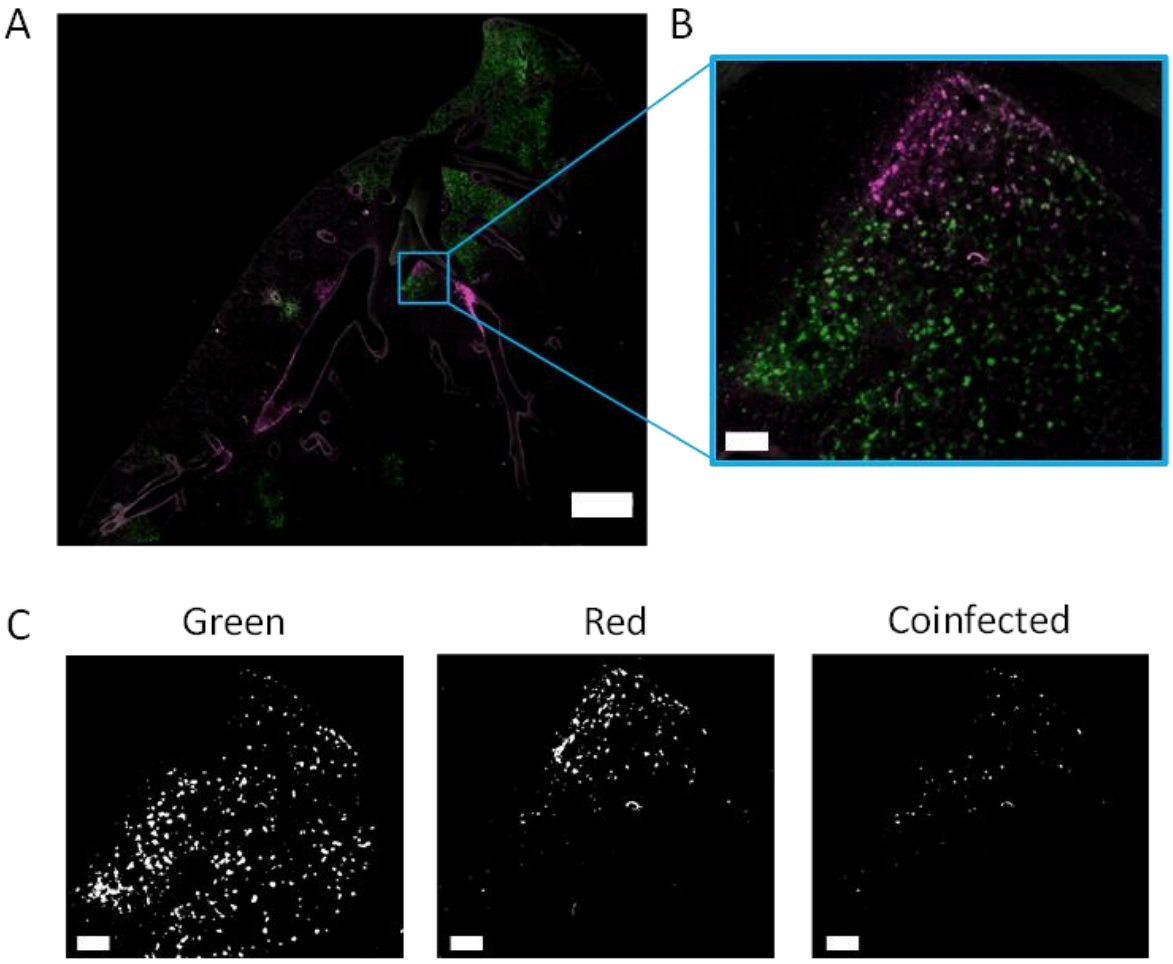

Figure 4.12: SIE restricts coinfection between foci of infection *in vivo.*

Lung sections from infected mice at 6 dpi. C57BL/6 mice were intranasally inoculated with mixtures of mCherry and eGFP expressing viruses (500 PFU of each virus). Lungs were harvested, sectioned, and imaged with an LSM 880 confocal microscope (Zeiss) using a 20× objective; scale bar = 1,500 µm. (B) Enlarged image of a lesion showing coinfection; scale bar = 100 µm. (C) Binary threshold was applied to distinguish cells expressing the eGFP, mCherry, or both fluorophores together, scale bar= 100 µm.

4.5 Discussion

The findings in this chapter reveal that SIE defines regions of infected cells where coinfection between viruses can and cannot occur, and therefore SIE and the spatial distribution of infectious foci acts as a previously unappreciated barrier to viral reassortment. In this chapter I propose two scenarios where viruses interact; one where the viruses interact within a single focus of infection, and the other modelling interactions between viruses from two different foci of infection. The former is likely to model interactions between progeny viruses, which we show is not restricted by SIE. The latter is likely to model the interactions between different strains of IAV, leading to the generation of reassortment viruses, which we show is subject to restriction by SIE.

In a simplified cell culture model, I showed that coinfection between separate foci of infection is limited to around 1% of the infected area. We corroborated this finding in mouse lungs which implies that reassortment is restricted spatially *in vivo* by SIE. However, previous observations show that reassortment occurs readily in experimental and natural infections [91,230,231,233–236]; so how can we reconcile these two observations? Importantly, we still observe a small number of coinfected cells showing that, although limited, coinfection is still possible in our model. This occurs due to the time delay in the onset of SIE for IAVs, resulting in a region of cells that are still permissive to coinfection for a short period of time. So, although our model reveals strong spatial restriction to coinfection and reassortment, given enough interacting foci there could still be a substantial number of coinfected cells. Similarly, when considering the epidemiological evidence for reassortment, the number of individual hosts infected by IAVs is extremely large [278], which may provide ample opportunity for rare interactions between viral strains. Additionally, we do not know how many cells need to be coinfected to give rise to variants that can be detected at an epidemiological scale. In a single round of infection, it has been shown that relatively low numbers of coinfected cells give rise to a high percentage of reassortment virus output [233]. Although we did not count the number of individual coinfected cells directly, we observed a substantial but small area where coinfection and therefore possibly reassortment can occur. Therefore, despite the restriction imposed by SIE, reassortment may still occur at appreciable levels.

In contrast, our data shows that viruses within a single focus of infection can coinfect freely during localised viral spread. This allows these viruses to benefit from the advantages of coinfection, most relevantly multiplicity reactivation between SIPs (reviewed in section 1.3.2.3). This is a key interaction to allow a virus population to propagate as 90% of the particles require coinfection to initiate multicycle infection [98,170,279]. As viruses within a plaque are likely progeny of the same parental virus, our observations follow the reasoning from sociovirology (reviewed in chapter 1) which argues that cooperative interactions are likely to evolve between genetically related viruses.

Coinfection has also been shown to promote the maintenance of rare virus mutants within populations [166,280]. This could work to maintain diversity and allow the virus population to continue to propagate. We did however observe that coinfection may have a time limit as viruses propagate within one focus of infection, as suggested by the concentration of coinfected cells decreasing towards the edge as the plaque expands. We suggest this is due to a spatial or cytopathic effect, which causes the cells to migrate to the centre. My data implies that coinfection within a plaque may be an unstable state, one that can only be supported for a few rounds of replication. The reason for the concentration of signal to the centre of the plaque is currently unknown but has interesting implications for viral evolution of a single virus population, if similar effects occur within infected respiratory epithelium.

Together, my data demonstrates that SIE induction leads to the development of a pattern of infections within host tissue, where some viruses can coinfect cells and where others are prevented from coinfection. Therefore, SIE and spatial dynamics offer a previously underappreciated barrier to coinfection between IAVs, and potentially other viruses which propagate locally in the host. We will investigate the applicability of this phenomenon to SARS-CoV-2 in chapter 6. In the next chapter, however, we will explore the potential mechanisms underlying SIE in individual cells for IAV.

Chapter 5: Exploring potential mechanisms of SIE induced by IAV

5.1 Introduction

5.1.1. Current knowledge of IAV SIE mechanisms

To date there has been limited investigation into the molecular mechanisms driving SIE induced by IAV, despite its clear consequences for viral reassortment. In this chapter I will review the current knowledge and present the results of our my investigations.

As reviewed in section 1.4.3, mechanisms for SIE induction occur at every stage of the viral lifecycle. The first in depth study of IAV SIE concluded that SIE was mediated by NA protein rapidly depleting the sialic acid receptors from the surface of previously infected cells, therefore blocking subsequent SIE entry [146]. The group used a pseudotyped retrovirus approach, which expressed the three proteins expressed on the virion surface, HA, NA and M2, in the absence of the other viral proteins, and carried a GFP reporter which was used to measure infection. Using these viruses, they infected cells that were transduced to express HA, NA or M2 proteins. They found that cells expressing the N1 subtype of NA potently blocked infection with the pseudotyped retroviruses, whereas expression of the H1 or H5 subtypes of HA, or of the M2 protein, did not block infection. Using commercially available NA inhibitors, oseltamivir and zanamivir, the group found they were able to recover infectivity in a dose-dependent manner in a way that correlated with increased surface availability of SA molecules. NA enzymatic activity was shown to be crucial as mutated “dead” NA did not block infection by the pseudotyped viruses. Together this provided compelling evidence that NA mediates SIE through receptor destruction, which is an approach commonly used by other viruses to establish SIE [130,147,168].

However, these conclusions were thrown into doubt in a subsequent publication by Sun and Brooke, 2018 [122]. They found that viruses that did not express NA at all were able to induce SIE, albeit to a lesser degree (at endpoint) compared to NA expressing viruses. Additionally, viruses expressing a mutated NA which has reduced surface expression had no discernible difference in the extent of

SIE, and in the researchers' hands, zanamivir had little difference on SIE. These findings imply a role for NA in SIE, but it is clearly not the only factor driving SIE induced by IAV. Sun and Brooke propose that the reason for this discrepancy could be vast over-expression of NA due to the method used to transfect the cells in the previous study.

Another study by Dou et al. 2017 found a limited role for NA in SIE induced by IAV [238]. By directly labelling secondary incoming viral genomes the researchers found that entry of the genomes was unimpaired by the establishment of SIE, and in fact they were arrested by SIE at a cytoplasmic location before entering the nucleus. There is also doubt that NA could be expressed, localised to the cell surface and active within the 2 h timeframe we have defined for onset of SIE. Recent quantitative mass-spectrometry data found that NA is not expressed to detectable levels until 5 hpi in MDCK cells [281]. Studies performed by Dr Jinqi Fu and Dr Nicole Baird found no significant depreciation in detectable SA levels following infection in the time frame for SIE, meaning there was still available receptors for secondary virus infection [282,283]. Together, this casts doubt on NA being the dominant factor in SIE during infection of cells with IAV.

Instead of NA, Sun and Brooke implicate a role for active influenza polymerase complexes in the establishment of SIE [122]. By employing a flow cytometric approach and detecting viral protein expression from the two coinfecting viruses using specific antibodies, they found that the more viral proteins the primary infecting virus expresses, the stronger the exclusion effect at 6 h post primary infection. They found that they could replicate this exclusion effect by transfecting a minireplicon (expression plasmids encoding the viral polymerase components and nucleoprotein), as well as a plasmid encoding a vRNA template for the polymerase to replicate and transcribe. This effect was independent of the identity of the vRNA template, as templates encoding the eGFP gene also induced this effect. This suggests a mechanism involving the influenza polymerase, which is consistent with our discovery in section 3.4, that the kinetics of SIE includes a 2 h lag phase which implies that primary infecting genomes must reach the nucleus and start replicating before onset. The authors did not propose a particular mechanism for this effect, but as each vRNP is proposed to bring its own polymerase complex, it is unlikely to be competition for viral polymerase

components instead perhaps competition for cellular cofactors, such as trans-complementing polymerases, or for space, either volume or cellular niche, inside the nucleus. The authors did suggest a role for the cellular anti-viral response, although they recognised that this model is challenging to explain as they found that SIE is induced in Vero cells, which lack expression of the interferon receptor (IFNAR). In view of this, they proposed that cell-intrinsic antiviral mechanisms independent of the IFNAR may be involved.

To summarise, at the present time there is no clear mechanism for the induction of IAV by SIE. Based on the evidence available, the leading hypotheses are a mechanism involving the influenza polymerase, competition between the two viruses, for space and resources, or the involvement of cellular anti-viral immunity.

5.1.2. Chapter Aims

In this chapter, I use our established ColorFlu system to test the involvement of two common suggestions for the mechanisms of SIE by IAV: competition between viruses and anti-viral immunity. Although the mechanism for IAV induction is still unclear, here I show a limited role for both competition and anti-viral immunity. I additionally uncover that the block to secondary viral infection occurs upstream of replication. Together with the finding that secondary infecting genomes do not enter the nucleus, we hypothesise that the block imposed by SIE occurs in the cytoplasm, prior to nuclear import.

5.2 IAV SIE blocks virus replication and protein expression

We, and other groups, have measured SIE by observing a block to protein expression from the secondary infecting virus [122,146]. However, we did not investigate an effect of SIE on genome replication of the secondary infecting viruses, and therefore it could be that SIE only represents a block to translation while the production of progeny viruses is unimpeded. Dou *et al.* 2017 observed that secondary infecting influenza virus genomes were prevented from entering the nucleus, which is the site of influenza virus replication [238], however, the impact on SIE on the production of nascent influenza virions has not been directly investigated. To investigate this, I employed our SIE assay established in section 3.4, and again observed a progressive block to protein expression for the secondary infecting virus as time between viral infection is increased (fig. 5.1A). However, in addition, I took the media from each time point and sampled the newly produced viruses that were present in a plaque assay (fig. 5.1B). When I counted the number of plaques expressing each fluorophore, I observed that the number of green plaques (descendants of the primary infecting virus) remained consistent as the time between primary and secondary infection is increased (ns, $p>0.05$, Kruskal-Wallis test). However, I observed a significant reduction in red plaques (descendants of the secondary infecting virus) by 6 h post primary infection ($p = 0.0382$, Kruskal-Wallis test) (fig. 5.1C). Therefore, we confirmed that SIE blocks both protein expression and production of nascent secondary infecting virus particles. We hypothesise that this means SIE blocks viral protein expression and replication of progeny genomes. This finding is consistent with the observation by Dou *et al*. 2017, that block must occur at or upstream to import of secondary virus genomes into the nucleus.

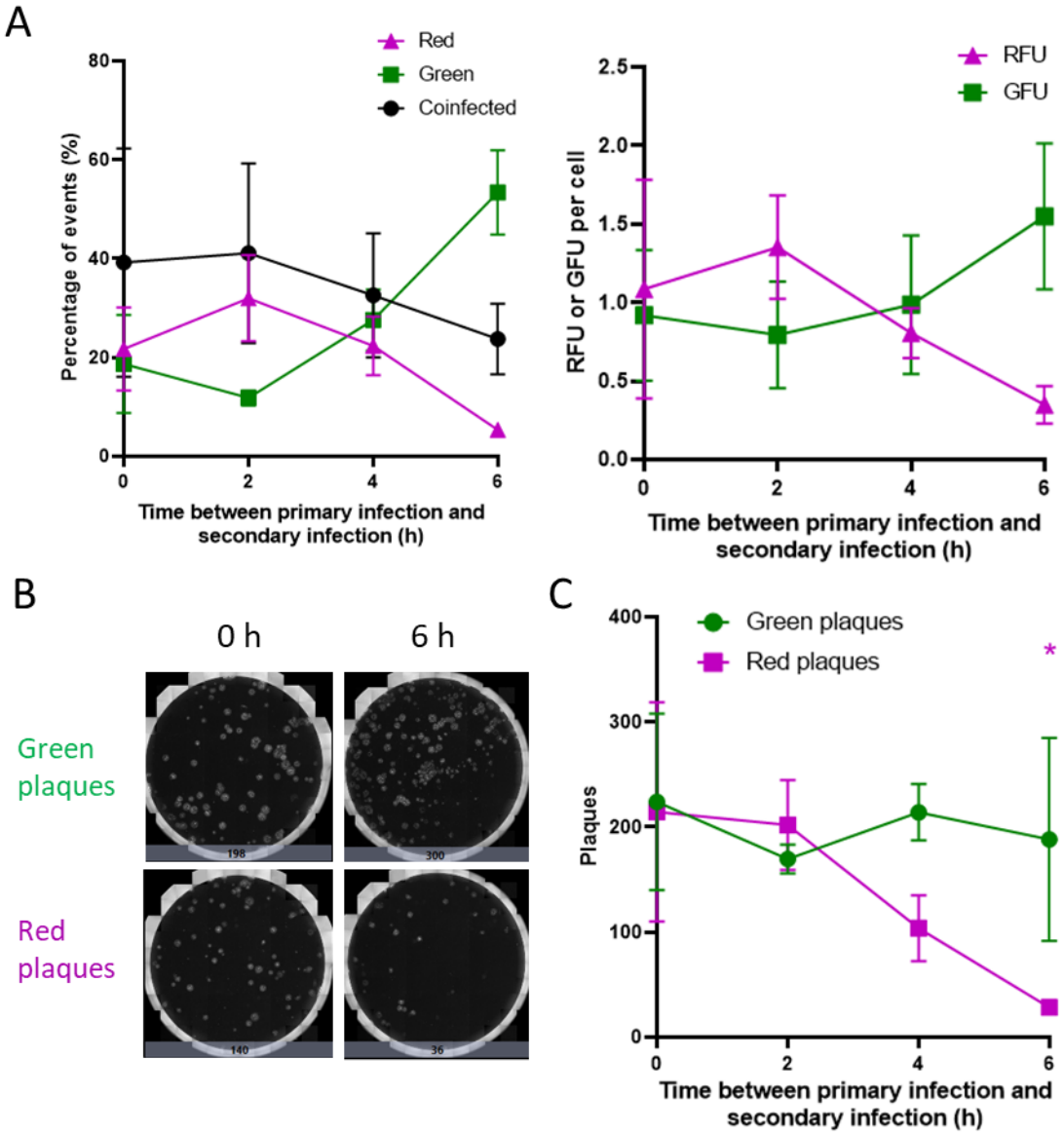

Figure 5.1: SIE represents a block to secondary virus protein expression and replication.

(A) Flow cytometry of cells infected with reporter viruses. MDCK cells were first infected with ColorFlu-eGFP, before secondary infection at the time points indicated with ColorFlu-mCherry, with both viruses at MOI 1 FFU/cell. The percentage of fluorescent cells was then assessed using flow cytometry. Differences between these values and those observed with at 0 h were determined non-significant (ns) by Kruskal–Wallis test ($p > 0.05$) means and SD are shown (n=3). The number of red and green forming units per cell (RFU, GFU) was calculated from the percentage of red, green, and coinfected cells under the assumption that infection follows a Poisson distribution. (B) Representative plaque images of viruses contained in the media of the experiment described in part (A). Media was taken 16 h post-secondary infection, diluted and applied to fresh cell monolayers. Images of the plaques were taken on the Celigo fluorescent microscope at 48hpi, and (C) the number of plaques expressing eGFP and mCherry were counted using Celigo gating tool. Differences between these intervals and those observed with at 0 h were determined by Kruskal–Wallis test (*$p < 0.05$). Data represents mean and SD, n=3.

5.3 IAV SIE is not driven by competition between the primary and secondary infecting viruses

It has been proposed that SIE could be driven by competition for space or host resources between the two coinfecting viruses [122]. We reasoned if this was the case, the secondary infecting virus would act as a competitive inhibitor of primary virus infection. Using this logic, increasing the amount of secondary virus should reduce the rate of SIE onset ((fig. 5.2a) measured in biochemistry as the Michaelis-Menten constant, Km). We hypothesised that we could use the model of the kinetics of SIE defined in section 3.4, and when altering increasing the amount of either the primary or secondary infecting viruses, measure the half-life of the decay phase of the kinetics as a proxy Km. We wanted to use half-life of the decay phase of the model to compare between experiments because the overall amount of virus in each sample was being altered and therefore the percentage of coinfected cells cannot be directly compared. Similarly, because our model is based on the Poisson distribution, the RFU/cell becomes skewed when not in the linear range of this distribution (at very high and very low amounts of virus), and therefore the end-point (at 6 h between primary and secondary infection) cannot be directly compared. We therefore use our kinetic model and half-life of the decay phase to compare between conditions.

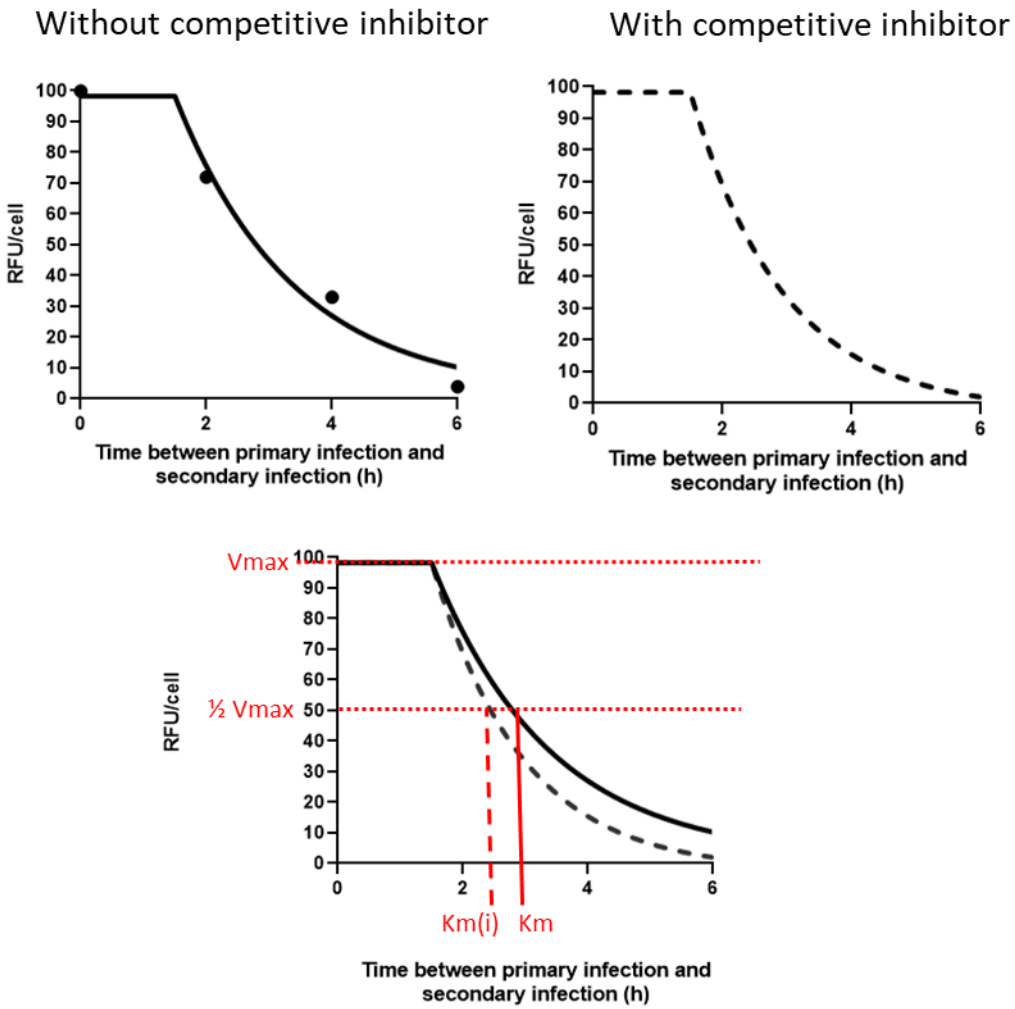

Figure 5.2a: The half-life of the decay phase of the model would be reduced in circumstances of competitive inhibition.

(A) Example data set for the reduction of RFU/cell during SIE onset without the presence of an inhibitor (solid line). (B) Example data set for the reduction of RFU/cell during SIE onset with the presence of a competitive inhibitor (dashed line). (C) Graph showing the rate (Km) is reduced with a competitive inhibitor present. Vmax = maximum RFU/cell (dashed red line), Km = rate of onset, Km(i) = Km with competitive inhibitor.

To begin, I again established the kinetics of SIE when the amounts of input viruses were equal (1 FFU/cell for each virus), using the same experimental set up as in section 3.4. I then increased the input of either the primary infecting virus (ColorFlu-eGFP) (fig. 5.2bA, upper panels) or the secondary infecting virus (ColorFlu-mCherry) (fig. 5.2bB, lower panels) by 2.5- or 5-fold the original amount. I found similar kinetics for all the conditions tested, with an initial onset of SIE at around 2 h, and a significant drop in the percentage of coinfected cells by 6 h compared to 0 h (Kruskal-Wallis

test, $p<0.05$ for 6 hpi for each condition). I did note a proportional increase in the percentage of coinfected cells in the experiments where 2.5 times or 5 times the amount of virus was used, due to there being more of either virus in the experiment (fig. 5.2bA).

When I fit plateau-exponential model we defined in Chapter 3 to the data for the different conditions, constraining the plateau to 2 h and the bottom of the decay phase to 0, I found that the model was a reasonable fit to the data (Total Sum of Squares (SST) $\leqslant 0.46$ when increasing the primary virus and $\leqslant 1.1$ when increasing the secondary virus). I then used the model to predict the half-life of the decay phase, as a proxy measure for the rate of SIE onset. I established that when the amount of input viruses was equal (1 FFU/cell for each virus), the half-life of the decay phase was 2.3 h. Unexpectedly, I found that SIE onset was significantly faster when the amount of primary infecting virus was increased to 5-times the initial amount (Kruskal-Wallis test, $p<0.05$; fig. 5.2bB), indicating the SIE kinetics are sensitive to the amount of primary infecting virus. We hypothesised that this may due to the faster replication rate observed in IAV when a higher number of particles infect the same cell [112] leading to a faster accumulation of the inhibitory factor. However, conversely, no significant change in SIE rate was observed when the amount of secondary infecting virus was increased (fig. 5.2bC). This implies that the second virus cannot outcompete the SIE mechanism driven by the first virus by sheer numbers. Therefore, this indicates that, at the range of MOIs I tested, SIE is not primarily mediated by competition between viruses. Instead, it implies that SIE is established by an SIE mediating factor, either viral or host in origin, acting either directly or indirectly to initiate an exclusionary state in the cell. At least within the range tested here, this effect cannot be outcompeted by overwhelming the cell with secondary infecting virus.

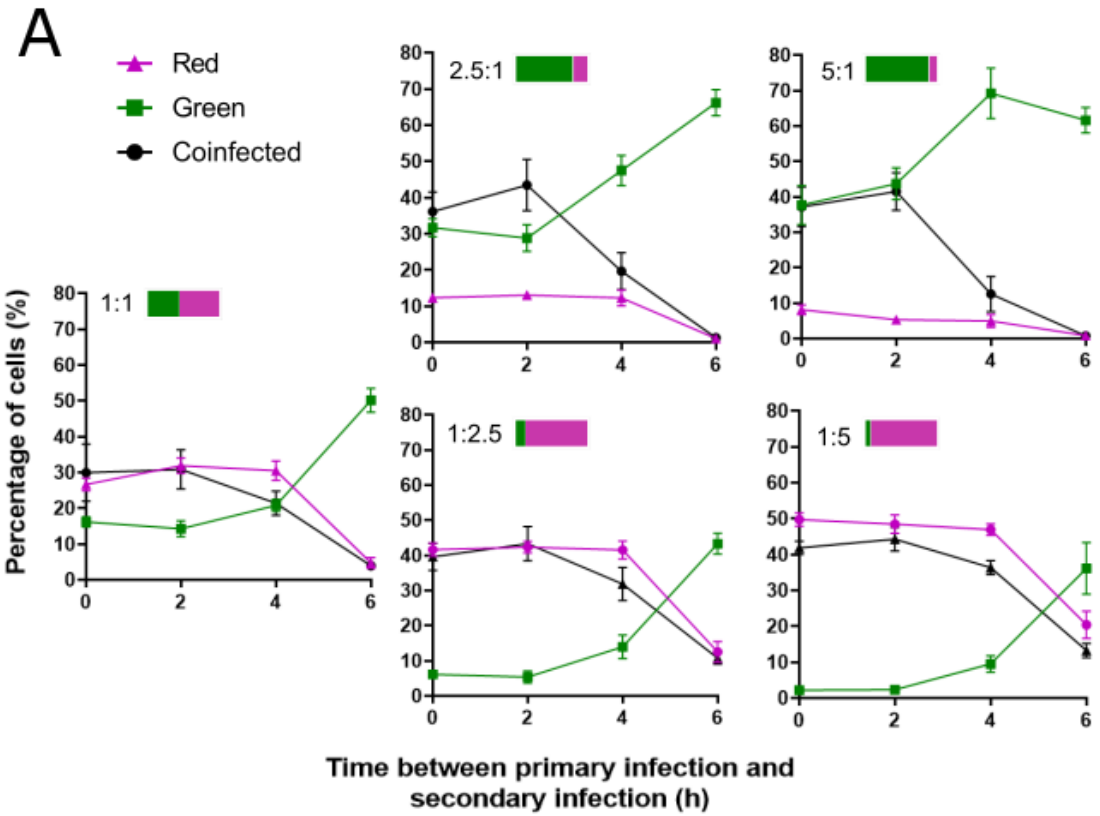
A
Red
Green
Coinfected
1:1
2.5:1
5:1
1:2.5
1:5
Percentage of cells (%)
Time between primary infection and secondary infection (h)

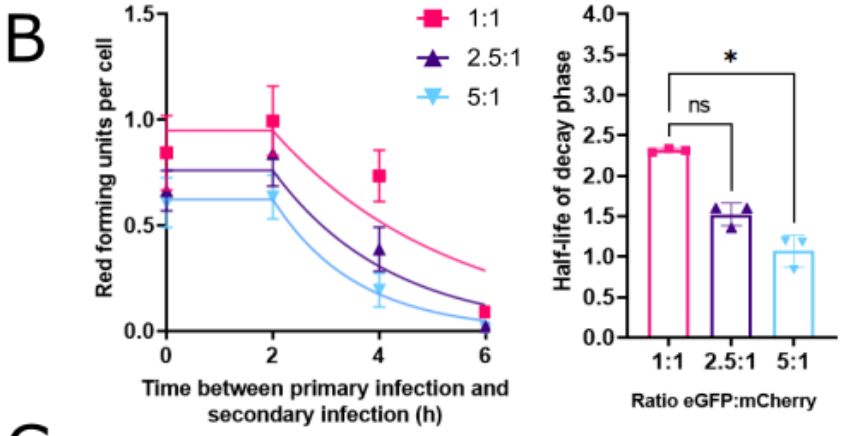
B
1:1
2.5:1
5:1
Red forming units per cell
Time between primary infection and secondary infection (h)
Half-life of decay phase
*
ns
Ratio eGFP:mCherry

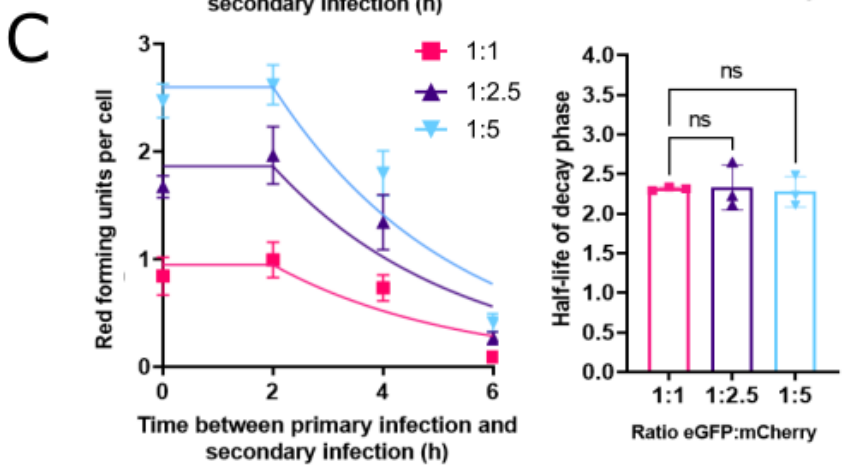
C
1:1
1:2.5
1:5
Red forming units per cell
Time between primary infection and secondary infection (h)
Half-life of decay phase
ns
ns
Ratio eGFP:mCherry

Figure 5.2b: SIE kinetics are sensitive to the amount of primary infecting virus.

(A) To assess the effects of altering the ratios of primary (ColorFlu-eGFP, green) and secondary (ColorFlu-mCherry, magenta) infecting viruses, SIE was measured as in Fig 5.1. Five different conditions are shown, with the ratios of primary and secondary viruses for each experiment indicated as bars. The initial FFU/cell for 1:1 ratio is 0.66 for ColorFlu-eGFP and 0.72 for ColorFlu-mCherry. These data were used to calculate how the expression of secondary virus (RFU per cell) changes with the interval between infections. This is shown when changing the ratios of (B) primary and (C) secondary infecting viruses. The RFU per cell was then fit to a model describing an initial constant phase of 2 h, followed by exponential decay plateauing at 0 (B, C: left-hand panels). The SST of the models fitted for 1:1, 2.5:1, and 5:1 are 0.43, 0.18, and 0.067, respectively. The SSTs for the models fitted for 1:1, 1:2.5, and 1:5 are 0.43, 1.01, and 1.10, respectively. The half-life of the decay phase, after the initial constant phase of 2 h, was then calculated (B, C: right-hand panels). Differences between these intervals and those observed with a 1:1 ratio were determined by Kruskal–Wallis test (*$p < 0.05$). For all data the mean and SD are shown (n = 3)

5.4 IAV SIE is not driven by type 1 interferon

Having established that the SIE establishing factor acts upstream of nuclear import, we wanted to investigate factors present in the cytoplasm which could block secondary infection. As reviewed in section 1.3.1.2, interferon (IFN) is the causative agent behind viral interference, and acts to create an exclusionary state in the cell [284]. As type-1 IFN responses can be induced by viral infection, these IFNs are a reasonable candidate for the exclusionary factor which drives SIE. However, there is already evidence in the literature that IFN may not be essential for SIE induced by IAV as VeroE6 cells, which lack interferon receptor, still initiate SIE [122]. We wanted to investigate the importance of IFN for IAV SIE in our own experimental system, so I first we used ruxolitinib, a small molecule drug which blocks STAT phosphorylation by Janus kinase (JAK) (fig 5.3A). When I measured the expression of Mx1, a key interferon stimulated gene (ISG), via western blot, I showed that MDCK cells produce interferon in response to WT PR8 infection (MOI 2) which leads to an upregulation of Mx1, and that this effect is blocked by addition of ruxolitinib (fig. 5.3B). Again, by measuring Mx1 expression in infected cells that had been with different concentrations of ruxolitinib, and I identified that 0.32µM ruxolitinib in the overlay medium was sufficient to block this effect (fig. 5.3C). When I included ruxolitinib into the SIE assay we had established in section 3.4, we found no significant difference in the ability of the viruses to establish SIE at 6 h compared to DMSO controls (ns, $p>0.05$, two-tailed Wilcoxon test; fig. 5.3D). This is consistent with previous observations in VeroE6 cells that type-1 interferon does not drive SIE induced by IAV.

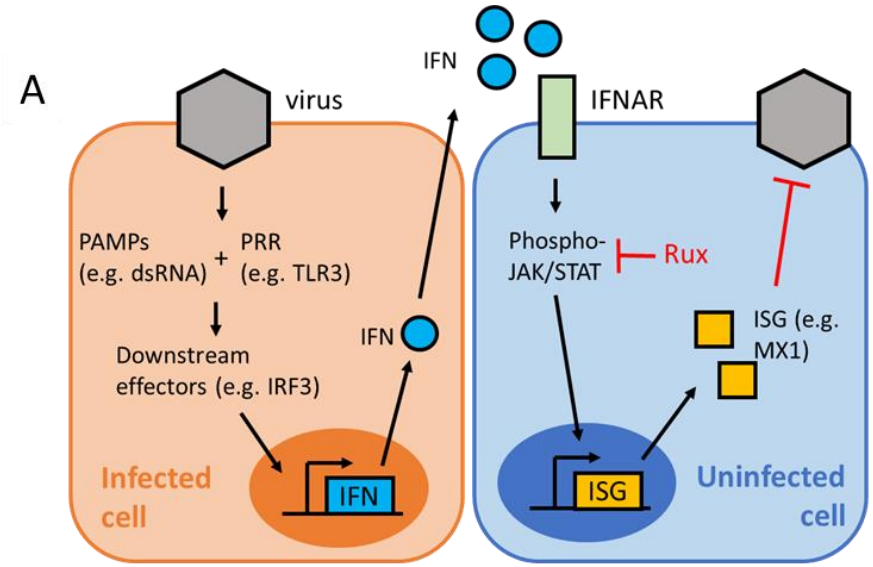
A
virus
IFN
IFNAR
PAMPs
(e.g. dsRNA)
+
PRR
(e.g. TLR3)
Phospho-
JAK/STAT
Rux
ISG (e.g.
MX1)
Downstream
effectors (e.g. IRF3)
IFN
Infected
cell
IFN
ISG
Uninfected
cell

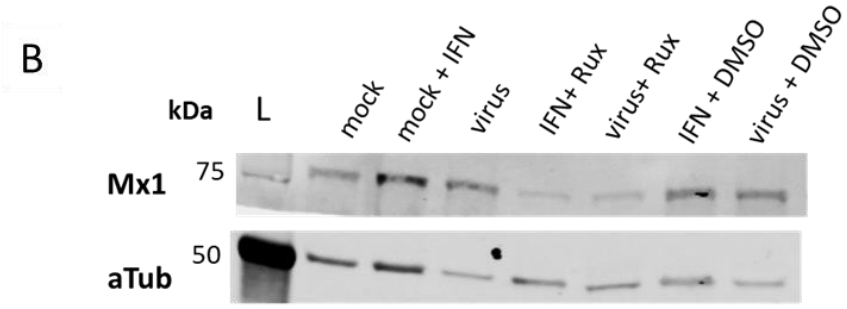
B
kDa
L
mock
mock + IFN
virus
IFN+ Rux
virus+ Rux
IFN + DMSO
virus + DMSO
Mx1
75
aTub
50

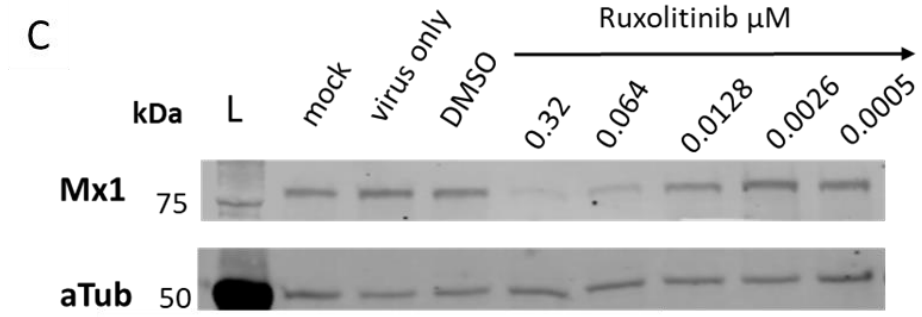
C
Ruxolitinib µM
kDa
L
mock
virus only
DMSO
0.32
0.064
0.0128
0.0026
0.0005
Mx1
75
aTub
50

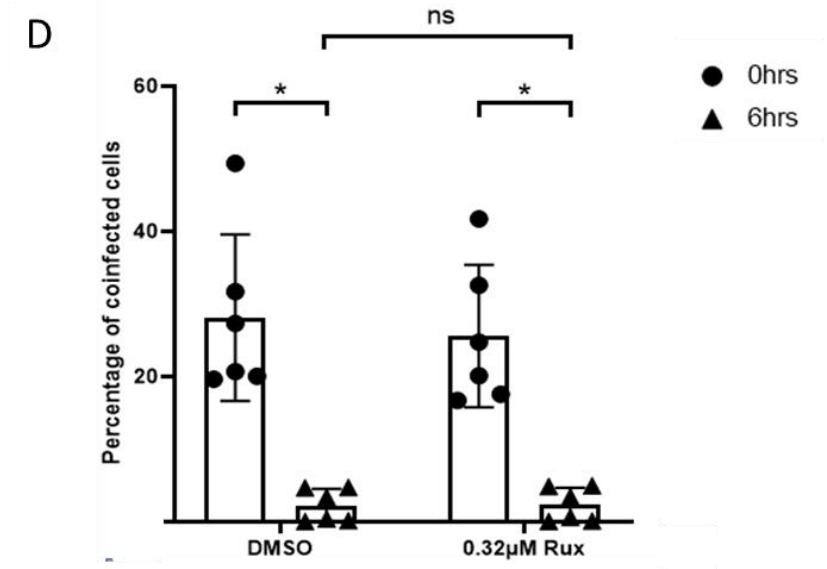
D
ns
*
*
0hrs
6hrs
Percentage of coinfected cells
60
40
20
DMSO
0.32µM Rux

Figure 5.3: Ruxolitinib drug treatment does not affect SIE at 6 h between infection events.

(A) Diagram of the action of Ruxolitinib to block the action of IFN in cells. IFN is produced in infected cells in response to viral infection. Infection produces pathogen related molecular patterns (PAMPs) which are sensed by the cell encoded pattern recognition receptors (PRRs). These activate downstream effectors which upregulate the production of IFN. IFN is then secreted and detected by another cell via IFN α/β receptor (IFNAR), this leads to the phosphorylation of STAT by JAK which activates downstream effectors, leading to the upregulation of ISGs which act to block viral infection. (B) MDCK cells induce ISG expression (MX1) in response to IFN treatment and IAV infection, which can be blocked with IFN blocking drug Ruxolitinib. Western blot of MX1 expression in MDCK with or without WT PR8 infection (MOI 2) and IFN and ruxolitinib treatment, and DMSO controls. Alpha-tubulin was used as loading control. (C) Titration of ruxolitinib blocks IFN induction from IAV infection as shown by MX1 expression. Alpha-tubulin was used as loading control. (D) Percentage of coinfected cells measured by flow cytometry with 0 h (circles) or 6 h (triangles) between primary and secondary infection, treated with 0.32 µM Ruxolitinib or with DMSO. MDCK cells were infected with ColorFlu-eGFP and ColorFlu-mCherry at an MOI of 2 FFU/cell. Data represent mean and SD from 5 independent experiments (n=5). * indicates significance by two-tailed Wilcoxon test ($p < 0.05$) and ns indicates non-significant.

We recognised that ruxolitinib blocks the IFN response downstream of IFN induction, at the point where IFN produced from an infected cell acts on adjacent cells. Therefore, to investigate the involvement of the innate immune signalling in the infected cell, we used cells that were deficient in the downstream effector protein IRF3 (fig. 5.4A). In the SIE kinetics assay I developed in section 3.4 I found no difference in the ability of these cells to induce SIE compared to control cells which still expressed IRF3 (fig. 5.4B). Although we were only able to obtain preliminary data in the timeframe of this PhD, these results indicate that IFN production in the infected cell has limited role in induction of SIE.

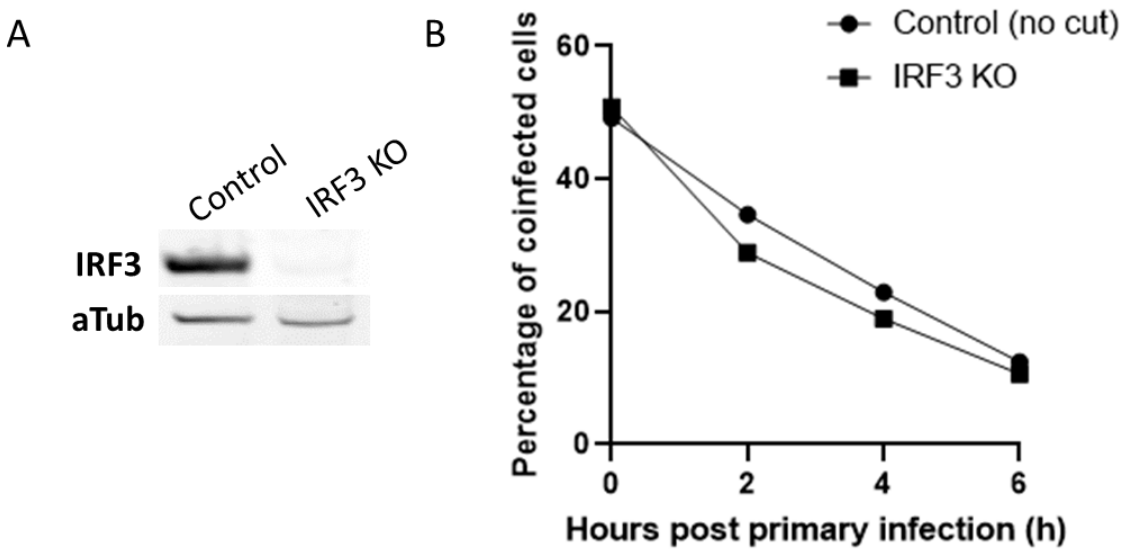

Figure 5.4: SIE kinetics are not affected by IRF3 knock out (KO).

(A) Western blot showing KO of IRF3 in A549-IRF3 KO cells with alpha tubulin as loading control. (B) Percentage of coinfected A549-IRF3 KO (squares) or control (no cut) (circles) cells measured by flow cytometry at indicted timepoints between primary and secondary infection. MDCK cells were infected with ColorFlu-eGFP and ColorFlu-mCherry at an MOI of 2 FFU/cell. Data represent n=1.

5.5 Discussion

The causative factor of SIE for IAV is not yet known. In this chapter, I present evidence suggesting that SIE acts upstream of translation and production of the secondary infecting virus particles, and is not primarily driven by competition between the coinfecting input viruses, or by the cellular type-1 interferon response.

Although I show that competition between input viruses does not drive SIE, as increasing the amount of secondary virus does not alter the kinetics of SIE, I found the kinetics of SIE are set by the amount of primary infecting virus. This is consistent with the finding that the more viral genomes introduced during primary infection, the stronger the SIE effect proposed by Sun and Brooke, 2018 [122]. How could this be affecting the rate SIE if not through direct competition between these viruses and the secondary infecting viruses? We propose that primary infection with multiple viruses increases the replication rate of the virus, which in turn increases the rate of accumulation of the active inhibitory factor driving SIE [112]. The link between rate of virus replication and onset of SIE has yet to be fully explored but there appears to be correlations for some other viruses (reviewed in section 1.4.2). An increased replication rate would most obviously increase the amount of an inhibitory factor if this factor was a viral protein, but could also affect SIE if inhibition is mediated by a host factor that is expressed in response to viral infection or which is activated through interaction with a viral protein.

It Is worth briefly noting that although my data show no decrease in the rate of SIE onset when increasing the amount of secondary virus, this was shown over a small range of MOIs (1-5). It is possible that over a larger range (MOI 50 – 100 for example), the kinetics of SIE may change. However, we do note that exponential models such as ours are very sensitive to the starting amount of virus, and therefore a 5-fold increase may amount to a substantial difference in the cell.

What could be the SIE inducing factor? As we observe a block to secondary infecting virus replication and transcription, and as there is a reported block to the import of secondary infecting virus genomes into the nucleus [238], we hypothesise that the factor acts either at the uncoating or

nuclear import steps of the virus lifecycle. This would be consistent with a factor present in the cytoplasm initiating SIE.

It has been hypothesised that the cellular innate immune response may onset SIE, which could fit with a cytoplasmic restriction factor. However, the results rule out involvement of type 1 IFN as we found no difference in the induction of SIE when using ruxolitinib, or in the absence of IRF3. This is consistent with previous findings that Vero cells can induce SIE, despite these cells not expressing IFNARs [122]. Innate immune signalling is redundant however, so we cannot at this point rule out involvement of NF-kB, type III IFN or other antiviral mechanisms. In more general terms we argue that the cellular innate immune response, although a plausible explanation for broad viral interference between different viral genera, is unlikely to explain the very specific effects of SIE in which one virus specifically excludes related viruses. Indeed, one study proposing NA as a mechanism for IAV induced SIE showed that murine leukaemia virus (MLV) and vesticular stomatis virus (VSV) can readily infect cells that have undergone SIE onset caused by IAV infection [146]. This shows the specificity of the SIE mediated block, although how closely the viruses need to be related for exclusion via SIE induced by IAV has not been resolved.

The specific mechanism of SIE for IAV is currently unknown, but I find a limited role for the IFN response or direct competition. Instead, I propose that SIE is driven by the activation or expression of an inhibitory factor, which has yet to be identified, that acts in the cytoplasm, and arrests the secondary infecting virus genomes from being replicated or transcribed. Our theoretical candidates for the inhibitory factor will be discussed in the main thesis discussion.

Chapter 6: Revealing SARS-CoV-2 SIE and exploring the dynamics of coinfection between IAV and SARS-CoV-2

6.1 Introduction

6.1.1 SARS-CoV-2 emergence and importance

In 2019, the World Health Organization (WHO) was alerted to a number of cases of fatal viral pneumonia in Wuhan, China [3,285]. This disease, which came to be known as coronavirus disease 19 (COVID-19), was subsequently shown to be caused by severe acute respiratory syndrome coronavirus 2 (SARS-CoV-2). The WHO rapidly declared the disease as a worldwide public health emergency and, as of November 2023, there is has been approaching 800 million confirmed cases, and nearly 8 million deaths [286]. SARS-CoV-2 therefore is a virus of enormous public health concern and in this chapter we will examine the role of SIE in the replication of this virus.

6.1.2 SARS-CoV-2 taxonomy, particle structure and genome

Coronaviruses (CoVs) are part of *Orthocoronaviridae* subfamily within the large and diverse *Coronaviridae* family. The subfamily is further divided into 4 genera: *alpha-, beta-, gamma* and *deltacoronavirus.* SARS-CoV-2 belongs to the *sarbecovirus* subgenus within the *betacoronavirus* genus. SARS-CoV-2 is genetically similar to the original SARS-CoV-1 (previously known as SARS-CoV) which emerged in Asia in April 2003 (80-94% sequence identity) [287]. Over the course of the pandemic, mutation of the SARS-CoV-2 genome and selection pressure resulted in waves of variants of concern (VOCs) [288].

SARS-CoV-2 has a non-segmented positive-sense ssRNA genome, consisting of 2 major open reading frames (ORFs) and additional accessory genes [287,289]. The genome of SARS-CoV-2 has typical organisation for *betacoronaviruses*, which is extremely large for RNA viruses [290,291], indeed SARS-CoV-2 has a genome of around 29.9 kb (for comparison, IAV has a genome size of approximately 13.5kb) [292–294]. In its entirety, the genome encodes 29 proteins. An up-to-date summary of our current knowledge of the structure and function of the SARS-CoV-2 proteins can be

found in Bai *et al*. 2022 [295]. The virus particle is enveloped and is roughly spherical in morphology (fig. 6.1). The virion is composed of 4 main structural proteins: nucleocapsid (N), envelope (E), spike (S) and membrane (M), which are indispensable for virus replication and pathogenesis [289].

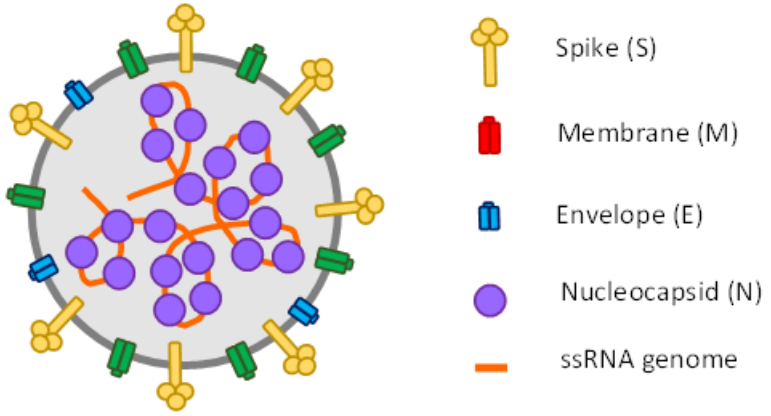

Figure 6.1: Composition of the SARS-CoV-2 virion.

The enveloped SARS-CoV-2 virus particle represented on the left. The structural proteins and genome that compose the virus particle are represented on the right. Inside the virus particle, the positive-sense ssRNA genome is sequestered with nucleocapsid protein forming a coiled tubular structure. The lipid bilayer is studded with three glycoproteins: spike (S), which is the major attachment factor for SARS-CoV-2, membrane (M) which gives the particle its shape and envelope (E) which is required for particle assembly.

6.1.3 SARS-CoV-2 replication in cells

The replication of SARS-CoV-2 in cells has been excellently reviewed by V'Kowski *et al*. 2021: [296], and generally follows the features of coronavirus replication reviewed by Fehr and Portman *et al*. 2015 [297].

In brief, the spike protein assembles into trimers and mediates cellular attachment and fusion of the viral and cellular membranes. The S protein is also the major target of the immune system and as such has been the focus of the production of SARS-CoV-2 vaccines [298]. Angiotensin-converting enzyme 2 (ACE2) was identified as the receptor bound by SARS-CoV-2 spike, as it is for SARS-CoV-1 and HCoV-NL63 spike proteins [289,299]. S protein must be cleaved by host proteases to mediate fusion, which can either happen in the endosome, or at the cell surface, mediated by transmembrane protease serine 2 (TMPRSS2) [296]. SARS-CoV-2 has acquired a polybasic cleavage

site in S protein which can be cleaved by furin protease, which allows pre-processing of spike and faster entry into cells – and possibly contributed to the expansion of host range [300,301].

When the positive sense ssRNA genome enters the cytoplasm, it can be immediately translated to produce viral protein. Some proteins are translated into polyproteins which must be proteolytically cleaved to gain function [302]. Following this the non-structural proteins assemble the viral replication and transcription complexes which appear as perinuclear double membrane vesicles (DMVs) [303]. The DMVs are the site of viral replication and transcription, and sequestering this process in this way has two main benefits for the virus: hides the dsRNA intermediates from the cellular immune system and gathers cofactors together for efficient replication. Viral replication occurs from negative sense anti-genome copies which can be used as templates to produce both genomes and the sub-genomic RNAs which are expressed to produce more viral proteins [304] (the production of sub-genomic RNAs is reviewed in Sola *et al*. 2015: [305]). Recombination, the genetic exchange between different SARS-CoV-2 genomes, is likely to happen due to strand-switching of the polymerase during replication and is therefore thought to occur within DMVs [90,306].

For egress, E, M and S proteins are inserted into the ER membrane, and then move along to the ER-Golgi intermediate compartment. During this, the viral genomes are encapsulated by N protein and combine to form the virion [307]. Canonically, the virions leave via exocytosis, but there is increasing evidence that SARS-CoV-2 utilises the lysosomal trafficking pathway [296].

6.1.4 SARS-CoV-2 replication within hosts

The focus of this thesis is within-host viral interactions, and therefore it is important to discuss the organ and cell tropism of SARS-CoV-2.

SARS-CoV-2 is mostly transmitted by respiratory droplets, therefore the primary organ tropism is the bronchioles and trachea in the respiratory tract [308–310]. However, viral antigens have also been observed in the epithelia of the small intestine and kidneys, and tissues in the pancreas, heart and brain of patients that have succumbed to fatal SARS-CoV-2 infection, suggesting that during severe illness the virus can disseminate in the host [311]. In the lungs, SARS-CoV-2 primarily infects

goblet and ciliated cells in the airway, which co-express ACE2 receptor and transmembrane protease seine 2 (TMPRSS2). Interestingly, despite extensive alveolar damage being a hallmark of COVID-19, ACE2 expression reduces in a gradient as you descend the respiratory tract, with susceptible cells only comprising 1-7% of the alveolar cell population [312–315]. Additionally, there is evidence that SARS-CoV-2 can infect basal cells despite this cell type lacking ACE2 expression and reciprocally we observe ACE2 expression in tissues that are not antigen positive [316]. Although there is evidence of interferon mediated transient ACE2 expression in some organs, the literature suggests that ACE2 is not the only determinant of cell tropism, which could possibly be explained by alternative entry ACE2-independent mechanisms [317].

There is evidence of localised viral spread within the organs of SARS-CoV-2 infected patients and experimentally infected animals. Antigen in post-mortem samples cluster to form foci in tissues of the lung, small intestine, and kidney [316]. There is evidence that clusters of antigen positive cells form early in the course of fatal SARS-CoV-2 infection, and the clustering is partially lost later in the course of disease [318–320]. Experimental infection of human *ex vivo* lung and bronchi tissues show distinct SARS-CoV-2 N-positive foci with multiple SARS-CoV-2 variants (Alpha, Beta, Delta and Omicron) [321]. Similar foci have been observed in human epithelial cell cultures [322,323]. In animal models of SARS-CoV-2 infection, injection of antibody-based probes into live experimentally-infected rhesus macaques show different distributions of infected cells within the lungs, with some animals displaying dispersed cellular infection and others containing small clusters of cells, however all the animals show clusters of infected cells around major airways [324]. This is corroborated by fixed tissue samples from ferrets which show distinct clusters of infected cells in the nasal turbinates at day 5 post infection, that is more diffused than is observed at day 3 [325]. One study utilised light sheet microscopy to visualise SARS-CoV-2 foci in nasal turbinates of ferrets at day 4 post infection [326]. Using this technique, they could not only image the foci in whole lungs but measure the actual distance between the foci in micrometers. In the lower respiratory tract, the group could not observe clear foci, but instead observed diffuse signal near the major airways, which they hypothesise to be antigen debris inhaled from the upper respiratory tract (URT), is consistent with

the observation that the URT is the preferential site of infection in ferrets, which present a mild disease phenotype [327]. Therefore, all the evidence we have of direct visualisation of infection in lungs show discrete foci formed by localised SARS-CoV-2 spread.

6.1.5 SARS-CoV-2 cellular coinfection and SIE

There is little direct evidence of SARS-CoV-2 coinfection in individual cells, and no known observation of SIE between SARS-CoV-2. In fact, to my knowledge, SIE has never been observed for any coronavirus. Instead, our evidence for cellular coinfection of coronaviruses comes indirectly from genetic observations of genome recombination between different SARS-CoV-2 variants [90]. As recombinant genomes are subject to natural selection, the question of how frequent recombination is for SARS-CoV-2 at the cellular level is up for debate. There is evidence of recombination in the genetic history of multiple coronaviruses that infect humans such as HCoV-OC43 and MERS-CoV [328,329]. There have been suggestions that historical recombination between related coronaviruses may have led to the emergence of the original SARS-CoV-1 in 2003 [330]. Similarly, there is evidence for recombination in the evolutionary history of SARS-CoV-2 [288]. The receptor binding motif (RBM) and the furin cleavage site of the spike protein may have been acquired through recombination events [331–333]. Therefore, recombination is an important part of SARS-CoV-2 evolution and possibly emergence of pandemic coronaviruses. Recombinant lineages of SARS-CoV-2 were found to be circulating in the United Kingdom in late 2020 and early 2021 [334]. Recombination was even detected within a single individual superinfected with different variants (Alpha and Epsilon) of SARS-CoV-2, with recombination detected in S, N and ORF8 coding regions of the genome [335]. While this is a limited study, it implies that if coinfection of individuals occurs, recombination and therefore cellular coinfection may be commonplace. In contrast to this, there is evidence that when the global population of viruses is considered recombination in SARS-CoV-2 is quite rare, with only 2.7% of SARS-CoV-2 genomes having recombinant ancestry [336]. Similarly, sequencing studies noted a lack of recombinant variants circulating during the pandemic [337,338]. This observation likely severely underestimates cellular coinfection for a few reasons. Firstly, identifying recombinant viruses, especially between closely-related viral variants is very difficult, as

it requires many high-quality sequences to be reported [339]. Secondly, circulation of recombinant viruses requires them to be successfully replicated and transmitted, and therefore unfit recombinant variants are likely to be lost from sequencing studies. Finally, recombination requires the genomes to not just reach the same cell, but presumably also the colocalisation of genomes to individual DMVs where genome replication occurs. Therefore, coinfection of cells is likely to be more common than recombination, and even when recombination occurs it may not produce a successful virus [97]. Therefore, although recombination is evidence for the existence of cellular coinfection, it cannot be used to accurately predict the likelihood of coinfection.

Aside from coinfection between different lineages of SARS-CoV-2, we also wished to investigate coinfection between SARS-CoV-2 and IAV, as this has been associated repeatedly with poor clinical outcomes in humans [340–343]. Several groups have attempted *in vitro* competition studies between SARS-CoV-2 and IAV, which have yielded contradictory results. In all these investigations, the authors looked at the difference in viral titre output from singly infected and coinfected cells, and not coinfection at the single cell level. In human bronchial air-liquid interface (ALI) cultures, it was shown that IAV inhibits SARS-CoV-2 replication [85]. This was driven by the strong interferon response to IAV infection severely inhibiting SARS-CoV-2, as shown by Mx1 induction and rescue of SARS-CoV-2 titres when using interferon blocking drugs. Contrastingly, in lung organoids enriched in susceptible alveolar cells, there was reciprocal enhancement of infection by the presence of the other virus [344]. This was due to IAV upregulating ACE2 expression on the cells, therefore increasing the number of cells susceptible to SARS-CoV-2 infection. This seemed to be a paracrine effect, as cells not infected by IAV also showed elevated ACE2 and implies the involvement of interferon-induced expression of ACE2 [317]. This observation has also been corroborated in A549 and human bronchial epithelial cells [345]. Therefore, paracrine interferon signalling may either enhance or reduce viral replication during coinfection of a tissue. To my knowledge, no one has investigated the interactions between the two viruses at the single cell level.

6.1.6 Chapter Aims

In this chapter, I evaluate the role of SIE in restricting coinfection between SARS-CoV-2 viruses at the level of individual cells, as this has never been investigated before and has important implications for SARS-CoV-2 recombination. To simplify my observations I focus on evaluating interactions between isogenic viruses as they are likely to have matched replication kinetics and the literature implies that isogenic viruses are likely to have the strongest SIE effect (reviewed in section 1.4.1) [126]. Using a fluorescent reporter virus system I show preliminary evidence for SIE between SARS-CoV-2 viruses, in both single cells and during localised viral spread. I then investigate the possibility of SIE between IAV and SARS-CoV-2 during the coinfection of individual cells. I found no evidence for SIE at the single cell level. Instead, I observe viral interference between the two viruses, driven by interferon. Together, the findings from this chapter reveal the effect of SIE I have modelled using IAV in previous chapters (Chapters 3 and 4) are applicable to other viruses, and demonstrates the difference between SIE and viral interference.

6.2 Reporter SARS-CoV-2 viruses are suitable for studying coinfection and SIE

Similar to our investigations with IAV in chapter 3 we wished to begin our investigation of SARS-CoV-2 SIE by studying closely related viruses. To do this we chose to use an established reporter virus system [187]. The system consists of isogenic SARS-CoV-2 viruses based on the Wuhan-Hu-1 isolate which carry a fluorescent protein (in this thesis; ZsGreen or mCherry) downstream of the *ORF7a* gene (which encodes the NS7A protein) (fig 6.2A). In theory, the fluorescent tag would be liberated from the NS7A protein by due to foot and mouth disease virus (FMDV) 2A linker. The putative start codon for the *ORF7b* gene is out of frame with the *ORF7a* and fluorophore tag gene, and therefore is assumed to be unattached from the tag fusion protein [346].

To check the expression of the reporter in AAT cells (ACE2 and TMPRSS2-overexpressing A549 human lung cells), which have been shown to be susceptible to SARS-CoV-2 infection [187], I infected the cells on coverslips with 0.5 PFU/cell of each virus and imaged at 24 hpi using a confocal microscope. I observed singly infected cells (appearing either magenta or green fluorescence), in addition to coinfected (appearing white) and uninfected cells (where only the nuclear DAPI stain can be seen); (fig. 6.2B). Therefore, these SARS-CoV-2 reporter viruses can be used to distinguish between singly, coinfected and uninfected cells in a similar way to the reporter IAVs used in section 3.2.1.

However, unlike the diffused fluorophore signal across the cell we expected, and I observed for fluorescently tagged IAV, I observed that the fluorescence appears to be punctate in infected cells, which indicates that the fluorophore is being concentrated in subcellular compartments (fig. 6.2B). We therefore hypothesise that the 2A site may not be functioning as intended – and the fluorophore may be fused to the NS7A viral protein. NS7A protein is a type-1 transmembrane protein that is predicted to have a role in immunomodulation and possibly virus assembly [347,348]. If the fluorophore is attached to NS7A protein we would hypothesise that the marker would localise to membranes, which may explain the punctate appearance of the fluorescence. The punctate nature of the fluorescence in single cells, and the reasons for it, is unlikely to affect the ability to categorise

the differential expression of the fluorophores in the cells using flow cytometry, meaning the system is still suitable for the experiments in this thesis.

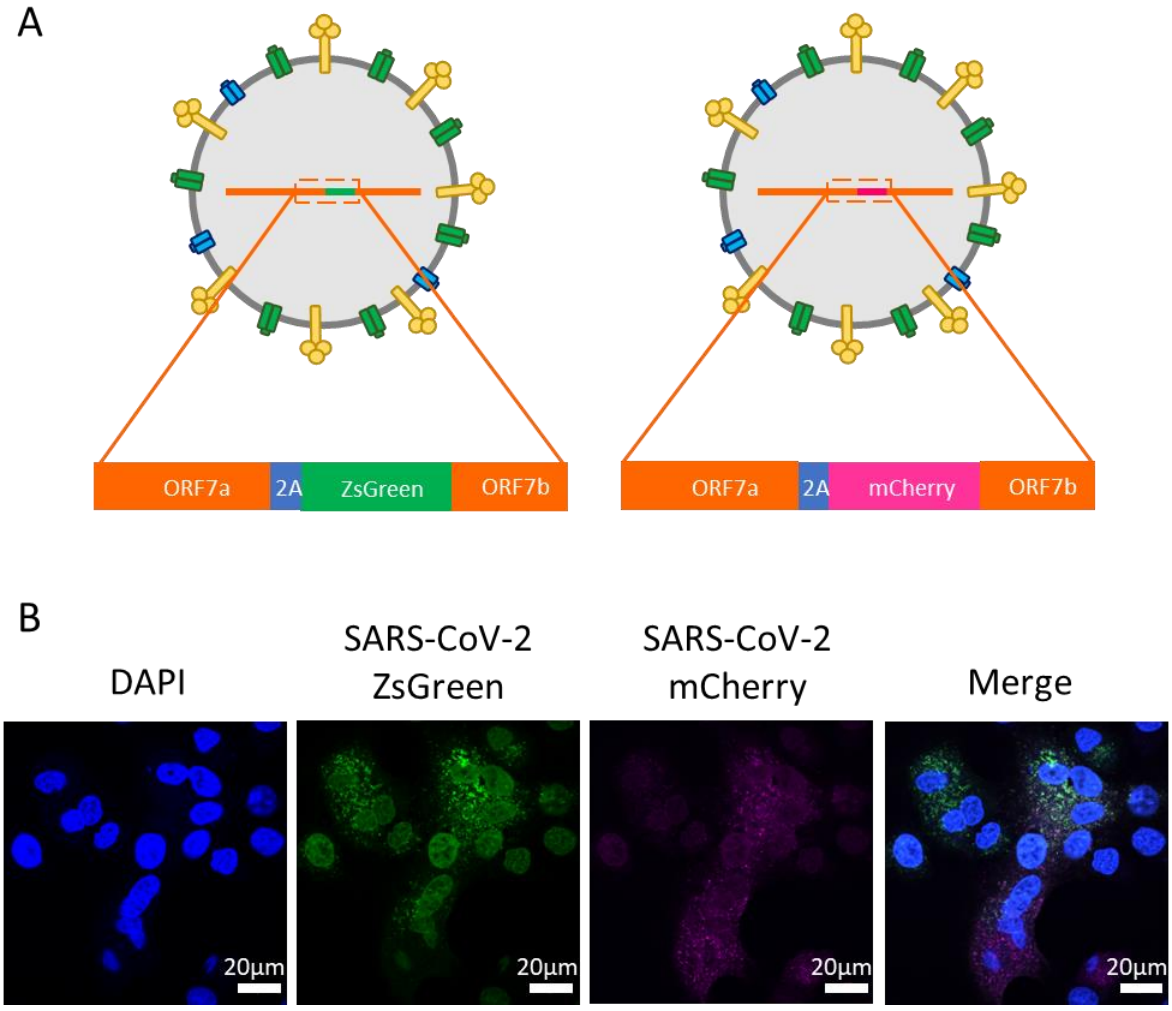

Figure 6.2: Punctate signal in cells infected with SARS-CoV-2 fluorescent reporter viruses.

(A) Schematic of ZsGreen and mCherry SARS-CoV-2 variants as designed by Rihn and colleagues. ORF7a-2A reporter cassettes shown which encodes ORF7a and b viral proteins in addition to either ZsGreen and mCherry. 2A represents a FMDV 2A cleavage site. (B) Confocal images of SARS-CoV-2 reporter virus infected cells. AAT cells were infected with 0.5 MOI each of SARS-CoV-2 ZsGreen and mCherry on glass coverslips, with nuclei stained using DAPI. Images were taken 24 hpi using 63x objective lens. Scale bar = 20µm.

6.3 SIE inhibits coinfection between SARS-CoV-2 viruses in single cells

Currently, it is not known whether SARS-CoV-2 infection causes SIE onset in cells. We set out to investigate this in AAT cells using our fluorescent reporter system. To do this, I infected monolayers of AAT cells first with one tagged virus and then, at various time intervals, subsequently infected them with the other tagged virus. I then harvested the cells at 16hpi and measured the expression

of the fluorophores using flow cytometry. I found fluorescently-tagged SARS-CoV-2 strains challenging to grow and therefore the stock of virus we used were low titre. To maximise the chance of coinfection at time point 0, rather than controlling the input MOI, I simply diluted the virus 1:1 with SARS-CoV-2 viral growth media (SARS-VGM, details listed in materials and methods) and applied it to cells, aiming to infect as many as possible. This resulted in 42% and 12% of the cells positive for the fluorophore for the SARS-CoV-2 ZsGreen and mCherry cells respectively during infection with the individual viruses (fig. 6.3A). In the flow cytometry results, I observed a population of coinfected cells present during simultaneous infection (0 hr between primary and secondary infection), which was reduced when the time to secondary infection is extended to 6 h post primary infection (fig.6.3B). Indeed, when either ZsGreen or mCherry tagged viruses were used to infect cells first (fig. 6.3C and fig.6.3D, respectively), I found a progressive reduction in the amount of coinfected cells for the time period of 0 – 6 hr between primary and secondary infection, indicating that SARS-CoV-2 infection initiates SIE in individual cells. Interestingly, I did not note a plateau or lag phase as we have described between 0-2 hrs for IAV induction of SIE (section 3.4), potentially indicating a distinct mechanism of SIE with a faster onset for SARS-CoV-2. The viral titres in this experiment was vastly unbalanced as we noted before, and only represents one experimental repeat, but this work provides preliminary evidence that SARS-CoV-2 viruses initiate SIE in cells, an observation that has never been made before.

A

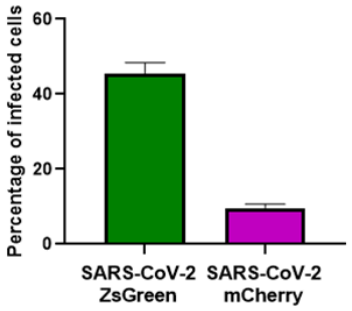

B

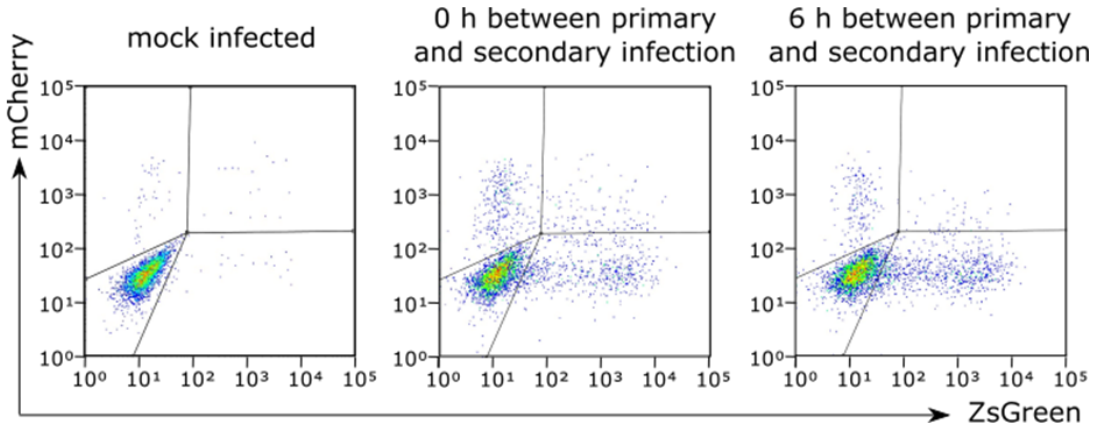

C

Primary infection: SARS-CoV-2 ZsGreen
Secondary infection: SARS-CoV-2 mCherry

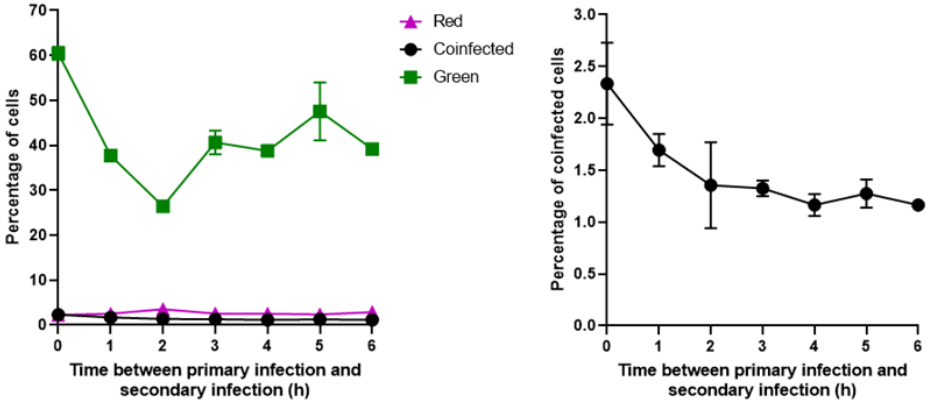

D

Primary infection: SARS-CoV-2 mCherry
Secondary infection: SARS-CoV-2 ZsGreen

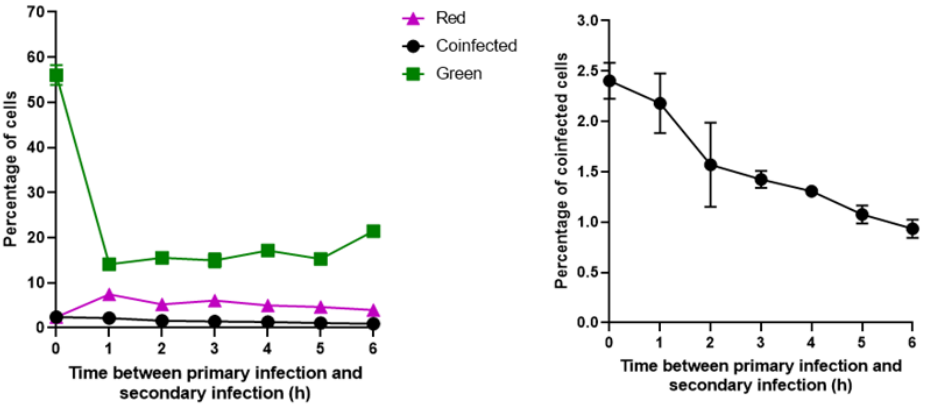

Figure 6.3: Evidence of SIE initiation by SARS-CoV-2 infection in AAT cells

(A) Percentage of positive cells during individual infection of SARS-CoV-2 ZsGreen and mCherry viruses in the experiment. Measurement of singly infected AAT cells with tagged viruses harvested for flow cytometry at 16 hpi. Data represents mean and SD of 3 technical repeats, n = 1. (B) Representative flow cytometry plots of cells infected with reporter viruses. AAT cells were first infected with SARS-CoV-2 ZsGreen, before secondary infection at the time points indicated with SARS-CoV-2 mCherry. Kinetics of onset of SIE with (C) SARS-CoV-2 ZsGreen or (D) SARS-CoV-2 mCherry before secondary infection at the time points indicated with the other virus, determined from flow cytometry analysis; means and SD of 3 technical repeats, n = 1.

6.4 SIE inhibits coinfection between SARS-CoV-2 viruses during localised viral spread

Next, we investigated if we could observe a block of coinfection due to SIE during localised spread of SARS-CoV-2 viruses – an observation I previously made for IAV (as described in section 4.4). To do this, I infected AAT monolayers with a mixture of ZsGreen and mCherry viruses and restricted the viruses to local spread by applying an 0.6% Avicel overlay. At 72 hpi I removed the Avicel, fixed the cells and imaged using the Celigo fluorescent microscope. Similar to the observations I made for IAV, I observed that where red and green plaques met, they did not extensively overlap. Instead, the presence of one plaque blocked the other from expanding (fig 6.4A and B). When a binary threshold was applied to the images, I identified only a small number of pixels that were displaying both red and green signal, and therefore coinfection was strongly inhibited (fig 6.4C). This provides further evidence that SARS-CoV-2 initiates SIE in infected cells and that SIE limits coinfection of SARS-CoV-2 during localised viral spread. This is likely to affect the evolution of SARS-CoV-2 viruses, by reducing the likelihood of recombination between viral strains.

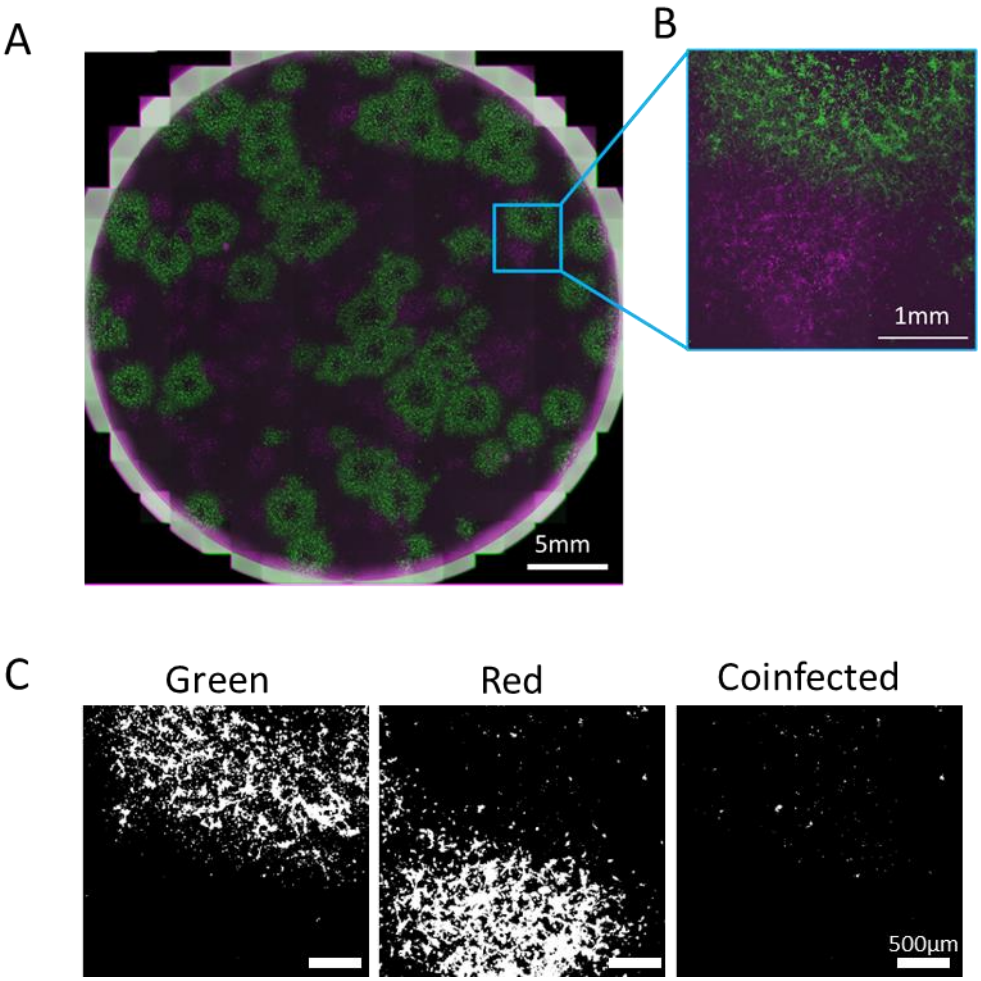

Figure 6.4: SIE spatially restricts interactions between viruses from separate SARS-CoV-2 foci of infection.

Representative images of plaque interaction. (A) Monolayers of AAT cells were infected with ZsGreen and mCherry tagged viruses, overlayed with agarose, fixed at 72 hr and imaged using Celigo fluorescent microscope. Scale bar = 5 mm. (B) Enlarged image of interacting foci; scale bar = 1 mm. (C) Binary threshold was applied to distinguish cells expressing the eGFP, mCherry, or both fluorophores together. Scale bars = 500 µm.

6.5 IAV and SARS-CoV-2 within-host interactions

We have established that SIE is active in single cells and during localised spread of both IAV and SARS-CoV-2, when the coinfected viruses are isogenic. SARS-CoV-2 and IAV both replicate in the upper and lower respiratory tract and therefore there is a possibility that they could encounter each other in coinfected patients [342]. Despite evidence that SARS-CoV-2 and IAV coinfection in patients and animal models with can exacerbate disease, to my knowledge there are no publications describing the virus interactions between SARS-CoV-2 and IAV in individual cells [340,341,349]. We

therefore wanted to investigate whether we could observe SIE between IAV and SARS-CoV-2 when they are coinfecting cells, using our fluorescent reporter virus strains.

6.5.1 Influenza virus infection induces SIE in AAT cells

To assess potential SIE between IAV and SARS-CoV-2 we needed to use a cell line that was permissive to both viruses. I chose to use AAT cells as they support the replication of both viruses, and are relevant to the biology of both viruses as they are from a human lung origin. To begin, before investigating the interactions between IAV and SARS-CoV-2, I needed to confirm SIE onset occurs AAT cells following IAV infection. To do this I used our established plaque interaction assay protocol to assess SIE during the spread of ColorFlu viruses in AAT cell monolayers. As with our observations in MDCK cells, I found that the plaques were blocked from growing into each other (fig 6.5). This indicates that SIE between IAVs is active in AAT cells, just as it is in MDCK cells.

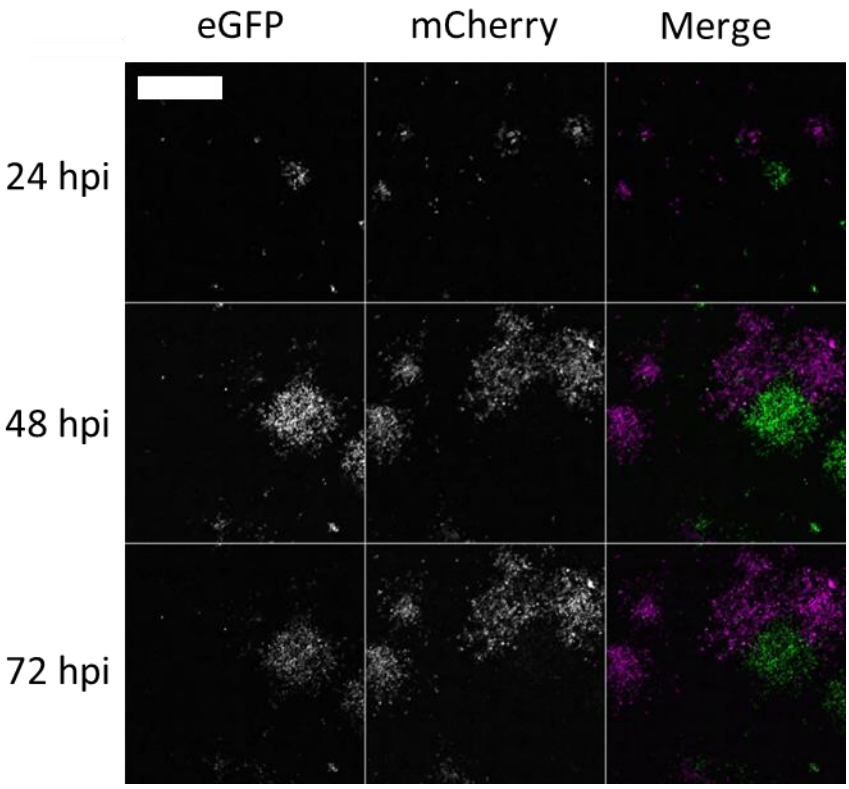

Figure 6.5: SIE restricts interactions of ColorFlu viruses in AAT cells.

Representative image of plaque interaction. Monolayers of AAT cells were infected with eGFP and mCherry tagged ColorFlu viruses, overlayed with agarose, and imaged every 24 h. Representative images, taken on Celigo fluorescent microscope, are shown. Scale bar = 2 mm.

6.5.2 SIE does not inhibit coinfection between IAV and SARS-CoV-2 in individual cells

We wanted to investigate the effect of IAV infection on SARS-CoV-2 superinfection, and conversely the effect of SARS-CoV-2 infection on IAV superinfection. I used our flow cytometry-based SIE kinetics assay to assess the extent of coinfection between the viruses during these two scenarios. I infected monolayers of AAT cells first with the green ColorFlu or SARS-CoV-2 fluorescent reporter viruses (eGFP and ZsGreen respectively) and then at various time intervals subsequently infected them with the other red-tagged virus (both IAV and SARS-CoV-2 tagged with mCherry), and then harvested the cells at 16hpi and measured the expression of the fluorophores using flow cytometry. Again, I maximised the chance of coinfection with SARS-CoV-2 by diluting the virus stock 1:1 with SARS-CoV-2 VGM (more details in materials in methods). However, as I had a high titre stock of ColorFlu, we limited these viruses to an input 2 FFU/cell which resulted in a percentage of positive cells during single infection of around 75% (fig. 6.6A). In the flow cytometry results, I observed a population of coinfected cells when there was 0 h between primary and secondary infection, however unlike during coinfections with isogenic viruses, the population was maintained even when there was 6 h between infections (fig 6.6B). Indeed, the percentage of coinfected cells remains consistent as the time between primary and secondary infection was increased in both primary infection with IAV and secondary infection with SARS-CoV-2 (fig. 6.6C) and primary infection with SARS-CoV-2 and secondary infection with IAV (fig.6.6D). Despite only being one experimental repeat, this data provides preliminary evidence that SIE initiated by both viruses, which is so effective against like viruses, does not block secondary infection with different viruses.

A

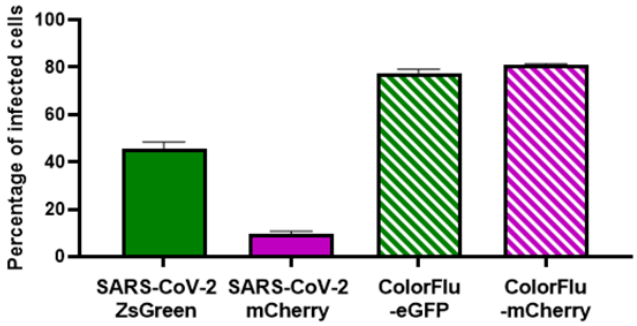

B

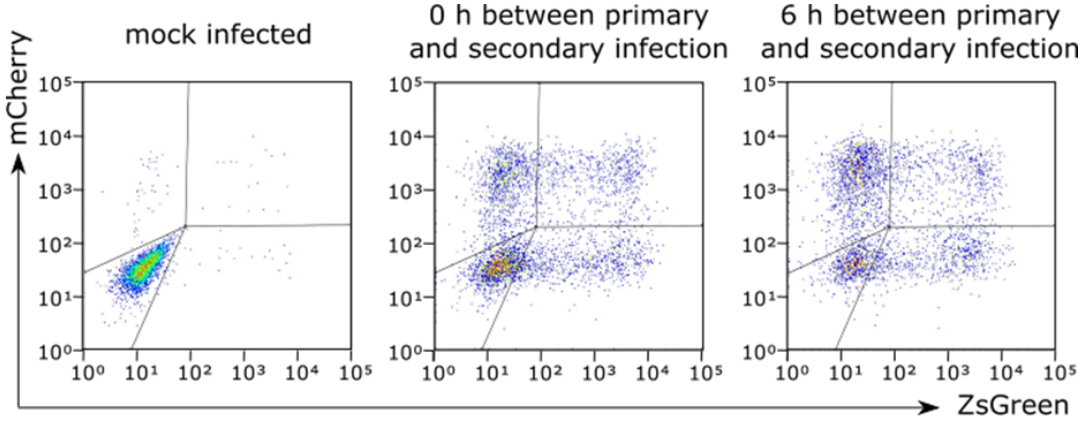

C

Primary infection: ColorFlu-eGFP
Secondary infection: SARS-CoV-2 mCherry

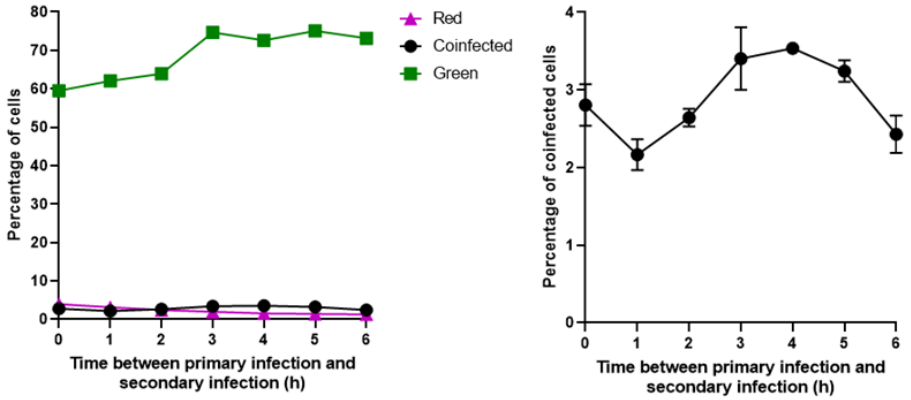

D

Primary infection: SARS-CoV-2 ZsGreen
Secondary infection: ColorFlu-mCherry

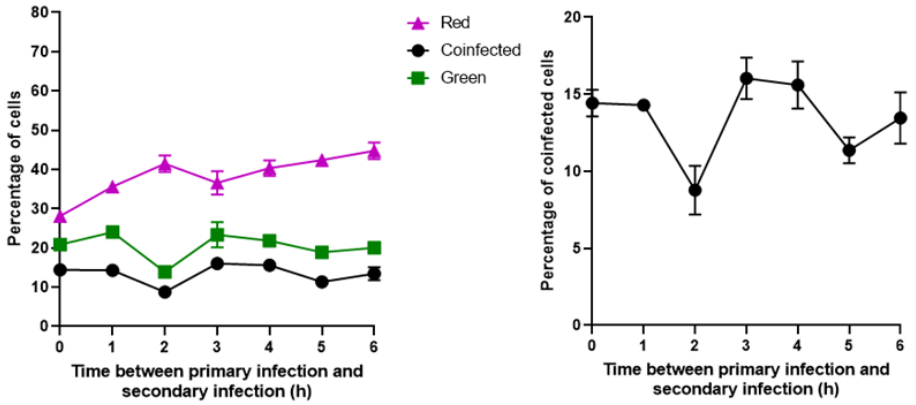

Figure 6.6: No evidence of SIE between SARS-CoV-2 and ColorFlu viruses in AAT infected cells.

(A) Percentage of positive cells during individual infection of SARS-CoV-2 and ColorFlu viruses in the experiment. Measurement of singly infected AAT cells with tagged viruses harvested for flow cytometry at 16 hpi. Data represents mean and SD of 3 technical repeats, n = 1. (B) Representative flow cytometry plots of cells infected with reporter viruses. AAT cells were first infected with ColorFlu-mCherry before secondary infection at the time points indicated with SARS-CoV-2 ZsGreen. Kinetics of onset of SIE with (C) ColorFlu-eGFP or (D) SARS-CoV-2 ZsGreen before secondary infection at the time points indicated with red tagged ColorFlu or SARS-CoV-2 as indicated. Data represents means and SD of 3 technical repeats, n = 1.

6.5.3 SIE does not inhibit coinfection between IAV and SARS-CoV-2 during localised viral spread

Finally, we wanted to examine whether we could observe SIE onset during multicycle viral spread of SARS-CoV-2 and IAV. When SARS-CoV-2 ZsGreen and ColorFlu-mCherry were simultaneously applied to AAT cells under plaque assay conditions, I found that neither viruses could propagate (fig. 6.7) whereas alone they both produce plaques in AAT cells (fig. 6.4 for SARS-CoV-2 and fig. 6.5 for IAV). We hypothesised that this could be due to the phenomenon of viral interference between the two viruses, as had been reported previously [85]. Viral interference is mediated by IFN, and therefore I blocked the IFN response using ruxolitinib. I found that we could recover multicycle infection of both viruses with 0.32µM of ruxolitinib in the overlay, showing that the block on multicycle infection of the two viruses was mediated by interferon (fig. 6.7). However, SARS-CoV-2 did not form plaques in this experiment, instead it seems that there is dispersed spread of the virus. This contrasts with ColorFlu-mCherry which form the typical plaques we observed previously in AAT cells. The reason for the difference in method of spread between the two viruses, and why SARS-CoV-2 did not form plaques is currently not known. I did however observe uniform dispersed green signal across the well, and therefore conclude that SARS-CoV-2 propagation but not infection was affected by the presence of the ColorFlu plaques. Similarly, the ColorFlu plaques seemed to grow uninhibited by the replication of SARS-CoV-2. This provides additional preliminary evidence that SIE initiated by SARS-CoV-2 or IAV does not inhibit coinfection of individual cells by the other virus.

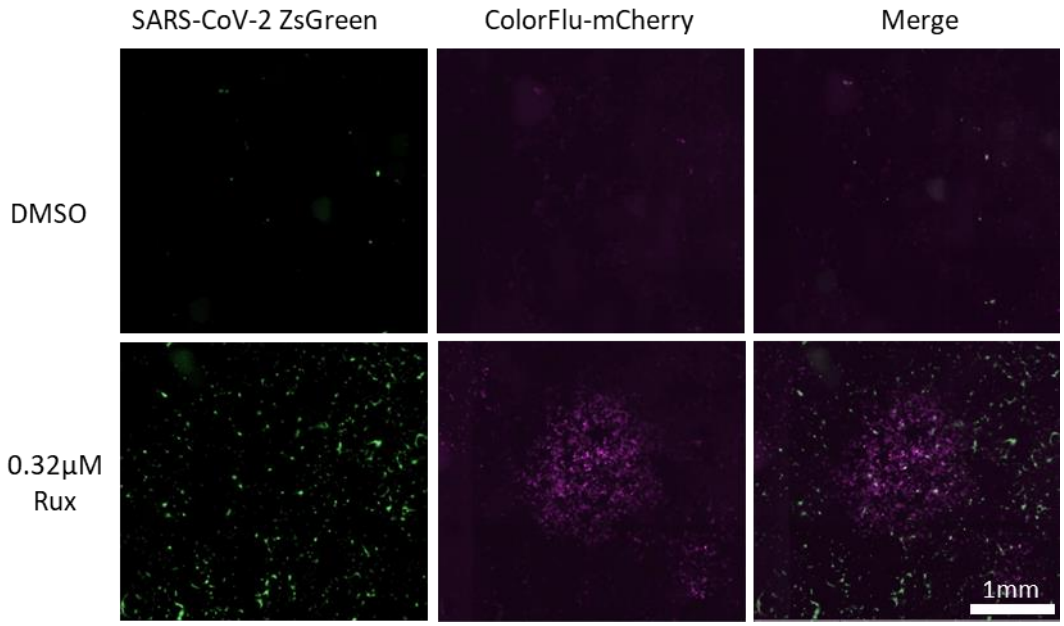

Figure 6.7: Evidence for viral interference between SARS-CoV-2 and ColorFlu viruses during multicycle infection.

Monolayers of AAT cells were infected with SARS-CoV-2 ZsGreen and ColorFlu mCherry viruses, overlayed with agarose containing 0.32µM ruxolitinib or DMSO control. The cells were fixed and imaged at 72 hpi. Representative images, taken on Celigo fluorescent microscope, are shown. Scale bar = 1 mm.

6.6 Discussion

In this chapter, we provide preliminary evidence that SARS-CoV-2 initiates SIE in single cells and during localised viral spread – the first time this has been observed for any coronavirus. Subsequently, we show that SIE does not block coinfection between IAV and SARS-CoV-2, and instead coinfection between these different viruses is primarily controlled by IFN-mediated viral interference.

The finding that SARS-CoV-2 initiates SIE has interesting implications for SARS-CoV-2 evolution, most notably the likelihood of generating recombinant progeny. Following the same rationale as IAV, we hypothesise that different strains of SARS-CoV-2 would be localised to different foci of infection, due to asynchronous introduction to hosts and that SIE would severely limit opportunities for interactions between the viruses in these foci. Therefore, my data suggests that SIE would limit recombination between different strains of SARS-CoV-2. Recombination via strand-swapping is hypothesised to occur if the genomes are present and being replicated within the same DMV [97]. Although we do not currently know the stage of the SARS-CoV-2 lifecycle that SIE inhibits coinfection of the cells, if it upstream of replication, it is likely to prevent recombination. For this reason, it would be fascinating to investigate whether SIE prevents blocks the formation of DMVs containing genomic RNA from both coinfecting viruses. Additionally, there is evidence in the literature that the strength of the exclusionary effect is at least partially determined by the genetic relatedness between the coinfected viruses [126] (reviewed in section 1.4.2). My study only identifies SIE between isogenic SARS-CoV-2 viruses; it might also be interesting to investigate the SIE phenomenon between different variants of SARS-CoV-2.

The observation we have made that coinfection occurs freely between SARS-CoV-2 and IAV in single cells, in the same time frame that the isogenic viruses are excluded, is consistent with suggestions in the literature that the exclusionary effect of SIE is strongest when the viruses are closely related to each other [126,127]. This observation also implies that SIE is mediated by different mechanisms unique to each virus as, if there was a shared mechanism, we would expect the viruses to inhibit each other. This may also suggest that SIE is a virus driven mechanism, as this implies that is not

driven by the infected state of the cell, such as the cellular stress response. It does not rule out a mechanism driven by a host protein however, as although the SARS-CoV-2 and IAV lifecycles differ quite extensively, and it is possible that the same host factors may be involved but target different stages or locations in the virus lifecycles.

My data suggest that although SIE does not block coinfection of a cell with SARS-CoV-2 and IAV, viral interference acts strongly to inhibit spread of the viruses, which likely prevents coinfection of cells in natural infections. This is consistent with some literature reporting that viral interference is active between the two viruses [85] but contradict reports which suggest an enhancement of spread during coinfection [344,345]. Interestingly, Dee and colleagues found that prior IAV infection inhibits SARS-CoV-2 infection but not the reciprocal, whereas I found that the spread of both viruses were inhibited by the presence of the other [85]. This study argues that IAV induces strong expression of ISGs which inhibits the slower growing SARS-CoV-2. There could be several reasons for this discrepancy. Firstly, different responses to IFN in the cell type used - Dee and colleagues used air-liquid interface cultures with primary human bronchial epithelial cells, whereas I was using a simplified model based on human lung fibroblast cells. Secondly, Dee and colleagues used different viral strains to our study which may induce a different balance of interferon response (BetaCoV/England/02/2020 and IAV H3N2 A/Norway/3275/2018 whereas I used SARS-CoV-2 Wuhan-1 variant and IAV PR8 H1N1). Thirdly, the use of the Avicell overlay in our experiment may affect the distribution of IFN across the cells which may differentially inhibit both viruses. The reason for the discrepancies in our studies is unclear, but they agree that viral interference is driven by IFN and can be blocked by the use of drugs that block the IFN response. These findings highlight that viral interference and SIE are separate mechanisms but may act together to restrict viral coinfection.

Overall, in this chapter I show that SIE does not just restrict coinfection between isogenic IAVs but is also a relevant mechanism for interactions between SARS-CoV-2 and perhaps other isogenic viruses. We suspect that any virus that spreads locally and initiates SIE would be subject to the kind of spatial restriction to coinfection that we have observed for IAV and for SARS-CoV-2. I additionally offer evidence that SIE initiated by IAV does not restrict SARS-CoV-2 protein expression, and vice

versa. This expands on our understanding of SIE as a mechanism that restricts like-viruses and highlights the differences between SIE and viral interference.

Chapter 7: Discussion

7.1 Summary of key findings

In section 1.5, I outlined 4 key aims of this project. In this section, I will state each aim, explain the methods used to investigate them and state the key findings.

> **Aim 1**: Characterise an isogenic IAV reporter virus system for studying coinfection and define the kinetics of SIE by IAV.

In chapter 3, I investigated whether we could use the established isogenic fluorescently tagged IAV reporter virus system ColorFlu to investigate coinfection and SIE. I found that during infection using these viruses, we could easily distinguish between cells that had been singly-infected and coinfected in both microscopy and flow cytometry experiments. By increasing the time points between primary and secondary infection with the tagged viruses, and measuring the proportion of coinfected cells by flow cytometry (referred to as an SIE kinetics assay), I showed that onset of SIE by IAV occurs 2 – 4 h following primary infection. By fitting the kinetics to various models, I showed that the data is best described by model involving a 2 h plateau followed by an exponential reduction, which is consistent with the time required for the viral genomes to enter the nucleus and start replicating.

> **Aim 2:** Explore how SIE at the level of individual cells affects the ability of viruses to coinfect during localised viral spread. Model these interactions both *in vitro* and *in vivo.*

In chapter 4, I modelled the foci of infection we observe in lung tissue during natural IAV infection *in vitro* using plaque assays using the ColorFlu viruses and observed the viral spread over time using fluorescence microscopy (referred to as a plaque interaction assay). First, I investigated the potential for coinfection between progeny viruses, by observing spread from single coinfected plaque. I observed that coinfection between viruses spreading within a plaque occurred freely, without restriction by SIE. Then I observed that viruses from separate plaques were not able to coinfect freely, instead where two plaques met SIE defined only a small region where coinfection was permitted. In collaboration with scientists from the Beatson Institute I confirmed observed the same pattern in the lungs of mice that had been infected with ColorFlu. From this, I hypothesised that SIE

restricts the potential for coinfection between progeny from different strains of viruses. I concluded that SIE divides spreading viral infections into a patchwork of distinct regions, within which coinfection can occur freely, and between which they are blocked. Importantly, these observations are not exclusive to influenza viruses, and can be generalised to any virus that initiates SIE and spreads locally within tissue to form foci of infection.

Aim 3: Investigate potential mechanisms for SIE initiated by IAV infection.

In chapter 5, I investigated which stage of the secondary virus lifecycle is blocked by SIE. By harvesting the viruses produced from cells that established SIE, I showed that the production of secondary infecting virus particles was reduced and therefore SIE likely both blocks the translation of viral protein and replication of viral genomes. Next, I investigated two common suggestions for mechanisms of SIE by IAV using flow cytometry: direct competition between the viruses for cellular resources, and the type 1 interferon response. Using SIE kinetics assays, I showed a limited role for direct competition between the viruses, as increasing the ratio of secondary to primary infecting virus did not alter the kinetics of SIE. I found no evidence that type 1 interferon mediated SIE, as use of 157uxolitinib and knock out of IRF3 had no effect on SIE. I did show that increasing the ratio of primary to secondary infecting virus resulted in faster SIE onset, which I interpreted to mean that faster virus lifecycle results in a faster onset of SIE.

Aim 4: Use an isogenic SARS-CoV-2 fluorescent reporter virus system to investigate SIE by coronaviruses and explore the dynamics of coinfection between IAV and SARS-CoV-2.

In chapter 6, I presented the first preliminary evidence for SIE between coronaviruses, using SARS-CoV-2 reporter viruses in SIE kinetic assays. I then also showed that SIE limits coinfection between SARS-CoV-2 viruses originating from different plaques using plaque interaction assays. I then used these assays to investigate the potential for SIE between IAV and SARS-CoV-2. I found no evidence for SIE at the single cell level as percentage of coinfected cells remained consistent as the time between primary and secondary infection was increased. In the plaque interaction assays, I again found that IAV and SARS-CoV-2 coinfects cells freely, but that for both viruses, plaque growth was

strongly inhibited in the presence of the other virus. This was due to type 1 interferon signalling, as addition of ruxolitinib alleviated the block to IAV plaque formation, and therefore I concluded that the limitation in plaque growth was due to viral interference mechanisms between SARS-CoV-2 and IAV.

These findings have consequences for our understanding of viral infections, and how pandemic viruses are generated and controlled. In the next sections, we will discuss the relevance of these findings to our understanding of aspects of fundamental virology, the emergence and adaptation of respiratory viruses, and the control of viral disease.

7.2 Fundamental virology

In this section I will discuss how my findings expand our understanding of fundamental aspects of virology.

7.2.1 Spatial spread of infections

In chapter 1.3, I introduced the framework of sociovirology, which seeks to understand how social traits between viruses evolved. One of the core tenants of sociovirology is that cooperative traits are likely to evolve between very closely related viruses (e.g. progeny viruses of the same parental virus genome) due to kin selection [67,73]. However, SIE is a competitive trait, and occurs specifically between isogenic or closely related viruses which is initially hard to reconcile with the predictions of sociovirology. Based on the findings of this thesis, I now consider that the spatial nature of spreading viral infections may provide an answer to this discrepancy.

In chapter 4 of this thesis, I examined how viruses interact as they spread locally within tissues using a plaque assay model. I found that viruses spreading with a single focus of infection were able to coinfect freely without a block by SIE. To assess this, I observed viruses spreading from a coinfected cell, but it would also apply to progeny viruses spreading outwards from a cell infected with a single parental virus. This suggests that progeny viruses, which are closely related to each other, readily coinfect together allowing for beneficial virus-virus interactions to take place such as multiplicity reactivation. Localised viral spread allows progeny viruses to cooperate before SIE onset, in line with kin selection theory.

Sociovirology also predicts that in cases where there is likely to be high MOI infections between unrelated viruses, competitive traits are likely to offer a selective advantage to the individual. The cells at the site of interaction between two different foci of infection would be a place where a high MOI infection between unrelated viruses could occur. When I modelled these interaction sites *in vitro* in chapter 4, I found that SIE restricts coinfection to only a small area of cells at the boundary where the two plaques meet. We found that this phenomenon also occurs in the lungs of mice coinfected with viruses, which shows this likely also occurs in natural infections. As coinfection is restricted by SIE, all the intracellular resources required for replication are reserved to replicate the primary infecting virus. This is a therefore a competitive interaction and follows the predictions of sociovirology.

Therefore, the localised spread of infections together with the delayed onset of SIE allows progeny viruses to coinfect freely, and prevents coinfection between unrelated viruses. In other words, SIE may be a way to control the resources to benefit "self", while excluding "other." This suggests fascinating parallels across the wider context of biology, in which territory establishment and defence is common observation, from wolves [350], to trees [351], to bacteria [352]. Our data extend these observations of macro-scale ecology to the within-host microenvironment.

7.2.2 Replication of progeny genomes

For a virus to evolve a trait, that trait must be beneficial to the viral genome that is performing the trait. It is not enough that the trait is beneficial at the whole population level. In section 1.4.4, I described some of the potential selective advantages of encoding an SIE mechanism which may have led to its evolution, such as preventing competition and generation of defective viral genomes (DVGs).

In that section I also mentioned that SIE may be a "spandrel", a trait that occurs as a byproduct of the evolution of another effect which does not offer a fitness advantage on its own [353]. One compelling explanation that follows this line of thinking has been proposed by Perdoncini Carvalho *et al*. 2022 [164]. The authors use turnip crinkle virus (TCV), a positive-sense single-stranded RNA plant virus to demonstrate their point, but explain that their framework may be applied to viruses

with other genome types. They present the Bottleneck, Isolate, Amplify, Select (BIAS) hypothesis, which asserts that viruses evolved strategies to limit the number of replicating genome in each infected cell. Encoding these strategies offer two potential competitive advantages for the virus: firstly, it prevents coinfecting virus genomes from replicating and secondly it prevents genome replication from recently synthesised daughter genomes. If we consider that SIE as a trait is neutral from an evolutionary perspective, perhaps it evolved because viruses may be under strong selection pressure not to replicate from progeny genomes. This is because replicating from progeny rapidly leads to the accumulation of mutations, leading rapidly to population crash as the nascent viruses can no longer replicate. Perdoncini Carvalho *et al*. use an example positive (+)sense ssRNA virus that has an error rate of one for every 10^{-4} nucleotides, and a genome of around 5000 nucleotides to demonstrate how quickly these mutations can accumulate [164]. I will use IAV as an example as it is more relevant for the data in this thesis, and SARS-CoV-2 has an unusually low mutation rate among RNA viruses due to error-correcting mechanisms [354]. IAV has a reported mutation rate of $2x10^{-4}$ – $2.7x10^{-6}$ substitutions per nucleotide per strand copied, depending on the strain and the method used to calculate mutation rate [355]. For this example, I will use an average of $1.4x10^{-5}$ substitutions per nucleotide per strand copied. IAV has a genome length of approximately 13,500 nucleotides [192]. To produce a negative-sense progeny genome of IAV, first it is copied from a positive-sense RNA intermediate which is copied from the negative-sense parent genome [356]. Therefore the FluPol replicates 27,000 nucleotides per replication cycle. With a mutation rate of $1.4x10^{-5}$ substitutions per nucleotide per strand, we would therefore expect one nucleotide change for every five replication cycles. The proportion of mutations that are lethal to IAV has been estimated to be around 32% [357]. According to this estimate, a lethal mutation is likely to be generated every 15 replication cycles. In other words, if replication from progeny genomes is permitted to occur three times in every cell, the virus would only be able to spread to five consecutive cells before every genome copy is defective. One way to prevent this is to ensure replication only occurs from one parental virus genome, and not from progeny genomes. To do this, Perdoncini Carvalho and colleagues argue, the viruses enforce an intracellular bottleneck by

expressing bottleneck enforcing proteins (BNEPs). They propose incoming genomes resemble daughter genomes to such an extent that they are recognised by BNEPs and therefore blocked from replicating. In this way SIE may be a side effect of a mechanism evolved to block replication from progeny genomes.

This hypothesis has interesting implications for the mode of IAV genome replication. Single-stranded RNA viruses are thought to replicate in two distinct ways as reviewed by Sanjuán and Domingo-Calap, 2016 [358]. The first is “stamping machine” replication, where nascent genomes are produced from the original infecting template genome. The second is “semi-conservative” replication, where nascent genomes are used as templates for further replication. The presence of BNEPs would imply that viruses replicate predominantly by stamping machine replication. For IAV, this is supported by evidence from modelling studies, that positive-sense anti-genomes molecules accumulate linearly within the first 6 h of infection [355,359,360]. However the kinetics of SIE onset I observed in chapter 3 would imply that the BNEPs would not be active until 2 h post infection. This implies that influenza viruses could initially replicate via a semi-conservative mechanism, but progressively shift to a stamping-machine mechanism after SIE onset at 2 hpi, becoming dominated by stamping-machine replication after about 6h.

To further support this hypothesis, I found in chapter 5 that SIE of IAV reduces the production of nascent particles from the secondary infecting virus, implying that secondary virus genome replication is blocked by SIE. Based on this, and on microscopy observations that secondary infecting IAV genomes are blocked from entering the nucleus [238], I hypothesised in chapter 5 that the undiscovered excluding factor acts in the cytoplasm to block in nuclear import of secondary viral genomes, and potentially daughter genomes.

Our strongest candidate for an excluding factor is the viral protein matrix protein (M1). M1 controls the movement of vRNPs across the nuclear membrane, and has been shown to bind to nascent vRNPs in the nucleus, coordinating their export to the cytoplasm and conversely, during entry of a virus into new host cells, M1 dissociation from vRNPs allows them to enter the nucleus [224,225].

Whittaker *et al.* 1996 investigated the role of M1 in preventing reimport of nascent vRNPs into the nucleus using heterokaryon cells carrying nuclei from infected and uninfected cells [361]. The infected nuclei were infected with an IAV carrying a mutant M1 which can associate with vRNPs in the nucleus and mediate their export to the cytoplasm, but association with vRNPs in the cytoplasm is temperature sensitive. At 39°C, when M1 cannot associate with vRNPs, they were able to enter the non-infected cell nuclei as shown by nucleoprotein (NP) staining. At 33°C, when M1 does associate with vRNPs, they found that the nascent vRNPs cannot enter the uninfected nuclei. This shows that M1 binding to vRNPs in the cytoplasm prevents their import to the nucleus. The authors suggest several possible mechanisms for this, M1 may cover import signals present on the vRNPs and thus prevent their association with proteins for nuclear import, alternatively, M1 may mediate the anchoring of vRNPs to the cytoskeleton which would retain it in the cytoplasm or finally M1 may coordinate the multimerisation of the vRNPs which could make the complex too large to enter the nucleus. In this way, M1 seems to be acting as a BNEP, as defined by Perdoncini Carvalho and colleagues [164], for IAV. But does M1 also act as an excluding factor? Some circumstantial evidence is the report that M1 is expressed to detectable levels by approximately 4-5 hours post infection using stable isotype labelling and quantitative mass spectrometry [281,362]. I did not have time to directly address this hypothesis in my thesis, but, if true, it would not only solve the mechanism of SIE by IAV but have interesting implications on the dynamics of influenza genome replication.

7.4.3 Within-host viral population diversity

Another aspect of fundamental biology that our findings highlight is the complexity of the viral interactions within hosts and how they shape viral evolution. Typically, the diversity of IAV in patients are collapsed into consensus sequences, which represent the most frequent nucleotide at each site. However, the high mutation rate of IAV lead to the generation of genetically diverse populations within hosts [357]. It has been posited that spatial structure of infections may be important in shaping within-host viral diversity (reviewed by Xue *et al*. 2018 and Gallagher *et al.* 2018 [265,363]. This is supported by recent studies which monitored the within-host diversity of experimentally infected animals using a library of IAVs containing unique genetic barcodes

[275,276]. The researchers found the maintenance of a rich population at the level of the whole respiratory tract but was strongly compartmentalised into different areas of respiratory tract. For example, diversity reduced as the infection descended from the upper to lower respiratory tract and different populations of barcoded viruses seemed to dominate individual lung lobes. The researchers concluded that this compartmentalisation was due to the existence of multiple bottlenecks within the respiratory tract that restricts population diversity through founder effects. Complementary to this is my findings in chapters 4 and 6 where I modelled the foci of infection observed in natural infections of IAV and SARS-CoV-2 respectively. I show that for both viruses that SIE segregates viral populations into separate islands of infection. By limiting mixing between emerging virus populations in the respiratory tract, we hypothesise that this can lead to the generation of genetically separate low diversity areas of infection, which cumulatively generates a rich population at the tissue level. Together these studies and our data demonstrate the power of spatial structure of infections on shaping viral population diversity at the level of the tissue and the respiratory tract. To fully understand the within-host evolution of viruses then, we must consider the spatial structure of infection and the effect on viral interactions at every scale: between hosts, within hosts and within individual cells.

7.3 Emergence and adaptation of pandemic respiratory viruses

In chapters 4 and 6, I found that SIE restricts coinfection of cells with IAV and SARS-CoV-2 viruses respectively from different infectious foci. This is likely to restrict the ability of viruses from different strains undergoing genetic exchange by reassortment or recombination. This means that my data suggests SIE is an underappreciated barrier to generation of novel pandemic viruses and the sudden acquisition of genes leading to increased virulence in humans, which we will discuss in the next sections. Therefore, the findings from this thesis are relevant to epidemiologists and other scientists that are responsible for identifying the emergence and incidence of respiratory viral disease. Potentially studying SIE could allow us to more accurately determine the circumstances that are likely to lead to the generation of dangerous viral variants.

7.3.1 Emergence of novel viral strains

Genetic exchange is a major mechanism leading to the emergence of pandemic respiratory viruses. IAV and SARS-CoV-2 both circulate in natural animal reservoirs and occasionally spill over into humans (zoonosis) [364]. The risk of zoonosis is driven by many factors. Some of these factors are determined (at least in part) by the genetic make-up of the virus including, but not limited to, the prevalence of the infection in animal hosts, the amount of virus shed from the animal hosts and the stability of virus in the environment (reviewed by Plowright *et al*. 2017 [365]). Genetic exchange therefore is dangerous because it allows viruses to potentially obtain genes increasing the risk of zoonotic spillover [366]. Zoonotic viruses that have not previously circulated in humans are particularly dangerous as there is no preexisting immunity in humans, which can lead to rapid transmission and high mortality. Genetic exchange has been implicated directly in the zoonotic emergence of SARS-CoV-2 into humans. Li et al. 2020 and Zhu et al. 2020 both propose that the entire receptor binding motif (RBM) of the spike protein was acquired through recombination events with human, bat and pangolin viruses [331,333]. Recombination with between viruses from pangolins has since been disputed [367], but recombination between viruses remains the most likely hypothesis for the emergence of SARS-CoV-2 [90,368]. For IAV, all of the pandemic strains since at least 1918-19 “Spanish” influenza have occurred from zoonotic spillover events. It is not clear whether the pandemic 1918 H1N1 virus emerged into humans directly from an avian origin, transmitted following reassortment in an intermediate host [369,370]. However, all subsequent pandemic influenza strains were generated by reassortment between viruses of different strains [91]. The most recent influenza pandemic the 2009 H1N1 “Swine” influenza was caused by reassortment between four virus strains of avian, human and swine in origin [371].

7.3.2 Adaptation of circulating viral strains

Aside from zoonosis, genetic exchange between circulating strains can lead to sudden changes in virus phenotype, and subsequently changes to disease.

The most dangerous of this is a sudden increase in disease virulence. Reassortment can lead to increased virulence of H5N1 AIV in mammals. One study investigated the effect of reassortment

between avian H5N1 and human H3N2 viruses cocirculating in 2006-2007 [372]. By generating all the 254 theoretical combinations of the segments by reverse genetics the group found that only 70 were non-viable *in vitro*. They then selected 75 viable viruses to test for pathogenicity *in vivo*, and found 22 were more virulent in mice than the parental H5N1 virus, which was associated with acquisition of the PB2 segment from the human H3N2 virus. The recombinant viruses in this study were generated in vitro, but a study of experimental infection with avian H5N1 and human H3N2 viruses in ferrets showed that reassortant viruses are generated at high frequency – although none of these viruses transmitted between animals [373]. Similar studies have demonstrated increased pathogenicity is a potential outcome of reassortment between co-circulating human seasonal and pandemic viruses [374,375]. This shows that reassortment can alter disease severity of circulating strains, as well as mediating the emergence of animal viruses into humans.

Similarly, there is evidence that recombination was occurring between strains of SARS-CoV-2 during the COVID-19 pandemic, after it emerged into humans, typified by the generation of an omicron-derived variant of concern XBB, which arose during the late part of 2022 [376]. Recombinant hotspot analysis has revealed breakpoints around the spike (S) gene, implying that SARS-CoV-2 viruses can effectively to swap S genes via recombination [377]. This is of note, as it could allow the acquisition of S proteins that are not recognised by host immunity leading to a strong evolutionary advantage for this virus. As the majority of neutralising antibodies target the S protein following natural infection and vaccination [378], swapping S genes efficiently may allow SARS-CoV-2 to generate and then spread in an otherwise immune population.

7.4 Controlling respiratory viral disease.

Understanding SIE may help us understand how pandemic viruses emerge and adapt, but how can understanding SIE help us develop strategies to control infection?

Most obviously, if the exclusionary state of SIE is induced through the action of a simple protein, there may be a way to infuse or otherwise cause this protein to be expressed in patients and trigger the exclusionary state in the cells to protect a patient against subsequent infection. We are quite far away from SIE being a realistic druggable target, not least because we first need to discover the

mechanisms driving SIE. However, SIE may be key to unlocking optimal design for live attenuated influenza virus vaccines (LAIVs). Quadrivalent LAIVs (QLAIVs) consists of four live strains of influenza viruses, namely 2 IAVs (pdmH1N1 and H3N2) with 2 IBVs (Yamagata and Victoria lineages) which get delivered to the nasal tract of the vaccinee via a nasal spray. Unlike in natural respiratory infections, this delivery method ensures that all the strains are simultaneously delivered to the same area of respiratory mucosa [379]. Despite this, it has been well documented that some strains confer better immune protection than others [380]. H1N1 strains in the years since the 2009 pandemic have conferred particularly poor immunogenicity, with the AstraZeneca (AZ) LAIV (branded Fluenz in the UK and EU, and FluMist in the USA) losing its recommendation in the USA from the Advisory Committee on Immunization Practices in 2016 for this very reason (although this recommendation was later reinstated for the 2018-19 season) [381]. There has been no definitive explanation for this phenomenon, but one study demonstrated that H1N1 strains replicate poorly in combination with other strains in ferrets, which resulted in lower protection in a vaccination-challenge model [382]. The authors note this effect was most pronounced when the viruses were used in tetravalent or quadrivalent formulations compared to monovalent formulations. They hypothesised that this effect may be due to strain interference within the nasal tract, with SIE possibly playing a role. We could envision a scenario where faster onset of SIE with infection from fitter strains, could lead to exclusion and poor replication of less fit strains – resulting in poor immunogenicity. We would need direct evidence of SIE between the AZ LAIV strains to test this theory but, if proven true, SIE could contribute to poor vaccine effectiveness. If this is the case, then with a better understanding of the mechanism of SIE perhaps “release” of the block caused by SIE could be engineered into the vaccine to prevent poor response to components of the QLAIV. Even if this is not possible, determining the degree of competition may allow us to better formulate a vaccine by, for example, increasing the dose of a less fit virus compared to the others. Alternatively, it might allow us to design better vaccine administration strategy, for example by removing a less fit virus from the formulation – or indeed the most competitive virus – and delivering it separately to the patient at a later date.

Indeed, these findings and strategies may be relevant for other multivalent live virus vaccines such as the RotaTeq (rotavirus) vaccine [383].

7.5 Conclusion

Overall, this thesis set out to determine the kinetics of SIE for IAV and SARS-CoV-2, and to observe the effect of SIE on the spatial patterning of respiratory viral infections within hosts. By focussing on interactions occurring within hosts, a usually neglected area of virological research, I was able to uncover that SIE defines where coinfection between viruses can happen, overall, likely shapes viral population dynamics and the landscape of viral evolution. From this I infer that SIE is a previously underappreciated barrier to the emergence and adaptation of pandemic viruses. With the fundamental biological knowledge acquired in this thesis, and with further study, we could potentially develop methods to predict and control emergence of pandemic respiratory viruses.

References

1. (ONS) O for NS. Deaths from respiratory disease from 2015 to 2020 and influenza and pneumonia in 2020. 2021 [cited 12 Jan 2024]. Available: https://www.ons.gov.uk/aboutus/transparencyandgovernance/freedomofinformationfoi/deathsfromrespiratorydiseasefrom2015to2020andinfluenzaandpneumoniain2020

2. WHO. Fact Sheet: Influenza (Seasonal). [cited 12 Jan 2024]. Available: https://www.who.int/news-room/fact-sheets/detail/influenza-(seasonal)#:~:text=Seasonal influenza (the flu) is,way to prevent the disease.

3. WHO. Interactive Timeline: WHO's COVID-19 response. [cited 29 Nov 2023]. Available: https://www.who.int/emergencies/diseases/novel-coronavirus-2019/interactive-timeline#!

4. WHO. Fact Sheets: Coronavirus disease (COVID-19). 2023 [cited 12 Jan 2024]. Available: https://www.who.int/news-room/fact-sheets/detail/coronavirus-disease-(covid-19)

5. Hatchett RJ, Mecher CE, Lipsitch M. Public health interventions and epidemic intensity during the 1918 influenza pandemic. Proceedings of the National Academy of Sciences. 2007;104: 7582–7587. doi:10.1073/pnas.0610941104

6. Ferguson NM, Cummings DAT, Fraser C, Cajka JC, Cooley PC, Burke DS. Strategies for mitigating an influenza pandemic. Nature. 2006;442: 448–452. doi:10.1038/nature04795

7. Leung NHL. Transmissibility and transmission of respiratory viruses. Nat Rev Microbiol. 2021;19: 528–545. doi:10.1038/s41579-021-00535-6

8. Mégarbane B, Bourasset F, Scherrmann J-M. Is Lockdown Effective in Limiting SARS-CoV-2 Epidemic Progression?-a Cross-Country Comparative Evaluation Using Epidemiokinetic Tools. J Gen Intern Med. 2021;36: 746–752. doi:10.1007/s11606-020-06345-5

9. Glogowsky U, Hansen E, Schächtele S. How effective are social distancing policies? Evidence on the fight against COVID-19. PLoS One. 2021;16: e0257363. doi:10.1371/journal.pone.0257363

10. Benke C, Autenrieth LK, Asselmann E, Pané-Farré CA. Lockdown, quarantine measures, and social distancing: Associations with depression, anxiety and distress at the beginning of the COVID-19 pandemic among adults from Germany. Psychiatry Res. 2020;293: 113462. doi:https://doi.org/10.1016/j.psychres.2020.113462

11. Wang CC, Prather KA, Sznitman J, Jimenez JL, Lakdawala SS, Tufekci Z, et al. Airborne transmission of respiratory viruses. Science. 2021;373. doi:10.1126/science.abd9149

12. Markel H, Lipman HB, Navarro JA, Sloan A, Michalsen JR, Stern AM, et al. Nonpharmaceutical Interventions Implemented by US Cities During the 1918-1919 Influenza Pandemic. JAMA. 2007;298: 644–654. doi:10.1001/jama.298.6.644

13. Zhao H, Jatana S, Bartoszko J, Loeb M. Nonpharmaceutical interventions to prevent viral respiratory infection in community settings: an umbrella review. ERJ Open Res. 2022;8. doi:10.1183/23120541.00650-2021

14. Paget J, Caini S, Del Riccio M, van Waarden W, Meijer A. Has influenza B/Yamagata become extinct and what implications might this have for quadrivalent influenza vaccines? Euro Surveill. 2022;27. doi:10.2807/1560-7917.ES.2022.27.39.2200753

15. Tompa DR, Immanuel A, Srikanth S, Kadhirvel S. Trends and strategies to combat viral infections: A review on FDA approved antiviral drugs. Int J Biol Macromol. 2021;172: 524–541. doi:10.1016/j.ijbiomac.2021.01.076

16. Okoli GN, Otete HE, Beck CR, Nguyen-Van-Tam JS. Use of neuraminidase inhibitors for rapid containment of influenza: a systematic review and meta-analysis of individual and household transmission studies. PLoS One. 2014;9: e113633. doi:10.1371/journal.pone.0113633

17. CDC. Influenza. For Clinicians: Antiviral Medication. 2023 [cited 13 Jan 2024]. Available: https://www.cdc.gov/flu/professionals/antivirals/summary-clinicians.htm#:~:text=Three drugs are chemically related,)%2C inhaled zanamivir (trade name

18. Hayden FG, Asher J, Cowling BJ, Hurt AC, Ikematsu H, Kuhlbusch K, et al. Reducing Influenza Virus Transmission: The Potential Value of Antiviral Treatment. Clin Infect Dis. 2022;74: 532–540. doi:10.1093/cid/ciab625

19. Carrat F, Vergu E, Ferguson NM, Lemaitre M, Cauchemez S, Leach S, et al. Time lines of infection and disease in human influenza: a review of volunteer challenge studies. Am J Epidemiol. 2008;167: 775–785. doi:10.1093/aje/kwm375

20. Roberts KL, Shelton H, Stilwell P, Barclay WS. Transmission of a 2009 H1N1 Pandemic Influenza Virus Occurs before Fever Is Detected, in the Ferret Model. PLoS One. 2012;7: e43303. Available: https://doi.org/10.1371/journal.pone.0043303

21. Hussain M, Galvin HD, Haw TY, Nutsford AN, Husain M. Drug resistance in influenza A virus: the epidemiology and management. Infect Drug Resist. 2017;10: 121–134. doi:10.2147/IDR.S105473

22. Sanderson T, Hisner R, Donovan-Banfield I, Hartman H, Løchen A, Peacock TP, et al. A molnupiravir-associated mutational signature in global SARS-CoV-2 genomes. Nature. 2023;623: 594–600. doi:10.1038/s41586-023-06649-6

23. Chakraborty C, Bhattacharya M, Dhama K. SARS-CoV-2 Vaccines, Vaccine Development Technologies, and Significant Efforts in Vaccine Development during the Pandemic: The Lessons Learned Might Help to Fight against the Next Pandemic. Vaccines (Basel). 2023;11: 1–19. doi:10.3390/vaccines11030682

24. Tregoning JS, Flight KE, Higham SL, Wang Z, Pierce BF. Progress of the COVID-19 vaccine effort: viruses, vaccines and variants versus efficacy, effectiveness and escape. Nat Rev Immunol. 2021;21: 626–636. doi:10.1038/s41577-021-00592-1

25. Gouma S, Anderson EM, Hensley SE. Challenges of Making Effective Influenza Vaccines. Annu Rev Virol. 2020;7: 495–512. doi:10.1146/annurev-virology-010320-044746

26. Krammer F, Palese P. Influenza virus hemagglutinin stalk-based antibodies and vaccines. Curr Opin Virol. 2013;3: 521–530. doi:https://doi.org/10.1016/j.coviro.2013.07.007

27. Hu L, Lao G, Liu R, Feng J, Long F, Peng T. The race toward a universal influenza vaccine: Front runners and the future directions. Antiviral Res. 2023;210: 105505. doi:https://doi.org/10.1016/j.antiviral.2022.105505

28. Belongia EA, Simpson MD, King JP, Sundaram ME, Kelley NS, Osterholm MT, et al. Variable influenza vaccine effectiveness by subtype: a systematic review and meta-analysis of test-negative design studies. Lancet Infect Dis. 2016;16: 942–951. doi:10.1016/S1473-3099(16)00129-8

29. Wu NC, Zost SJ, Thompson AJ, Oyen D, Nycholat CM, McBride R, et al. A structural explanation for the low effectiveness of the seasonal influenza H3N2 vaccine. PLoS Pathog. 2017;13: 1–17. doi:10.1371/journal.ppat.1006682

30. PHE. Health matters: delivering the flu immunisation programme during the COVID-19 pandemic. 2020 [cited 13 Jan 2024]. Available: https://www.gov.uk/government/publications/health-matters-flu-immunisation-programme-and-covid-19/health-matters-delivering-the-flu-immunisation-programme-during-the-covid-19-pandemic

31. Martinez ME. The calendar of epidemics: Seasonal cycles of infectious diseases. PLoS Pathog. 2018;14: e1007327. Available: https://doi.org/10.1371/journal.ppat.1007327

32. Lam TT, Tang JW, Lai FY, Zaraket H, Dbaibo G, Bialasiewicz S, et al. Comparative global epidemiology of influenza, respiratory syncytial and parainfluenza viruses, 2010-2015. J Infect. 2019;79: 373–382. doi:10.1016/j.jinf.2019.07.008

33. Moriyama M, Hugentobler WJ, Iwasaki A. Seasonality of Respiratory Viral Infections. Annu Rev Virol. 2020;7: 83–101. doi:10.1146/annurev-virology-012420-022445

34. Wiemken TL, Khan F, Puzniak L, Yang W, Simmering J, Polgreen P, et al. Seasonal trends in COVID-19 cases, hospitalizations, and mortality in the United States and Europe. Sci Rep. 2023;13: 3886. doi:10.1038/s41598-023-31057-1

35. Audi A, AlIbrahim M, Kaddoura M, Hijazi G, Yassine HM, Zaraket H. Seasonality of Respiratory Viral Infections: Will COVID-19 Follow Suit? Front Public Health. 2020;8: 567184. doi:10.3389/fpubh.2020.567184

36. Choi Y-W, Tuel A, Eltahir EAB. On the Environmental Determinants of COVID-19 Seasonality. Geohealth. 2021;5: e2021GH000413. doi:10.1029/2021GH000413

37. Bardhan M, Ray I, Roy S, Bhatt P, Patel S, Asri S, et al. Emerging zoonotic diseases and COVID-19 pandemic: global Perspective and Indian Scenario. Ann Med Surg (Lond). 2023;85: 3997–4004. doi:10.1097/MS9.0000000000001057

38. Johnson NPAS, Mueller J. Updating the accounts: global mortality of the 1918-1920 “Spanish” influenza pandemic. Bull Hist Med. 2002;76: 105–115. doi:10.1353/bhm.2002.0022

39. Du Y, Wang C, Zhang Y. Viral Coinfections. Viruses. 2022;14. doi:10.3390/v14122645

40. Kumar N, Sharma S, Barua S, Tripathi BN, Rouse BT. Virological and Immunological Outcomes of Coinfections. Clin Microbiol Rev. 2018;31. doi:10.1128/CMR.00111-17

41. Echenique IA, Chan PA, Chapin KC, Andrea SB, Fava JL, Mermel LA. Clinical characteristics and outcomes in hospitalized patients with respiratory viral co-infection during the 2009 H1N1 influenza pandemic. PLoS One. 2013;8: e60845. doi:10.1371/journal.pone.0060845

42. Marcone DN, Ellis A, Videla C, Ekstrom J, Ricarte C, Carballal G, et al. Viral etiology of acute respiratory infections in hospitalized and outpatient children in Buenos Aires, Argentina. Pediatr Infect Dis J. 2013;32: e105-10. doi:10.1097/INF.0b013e31827cd06f

43. Schnepf N, Resche-Rigon M, Chaillon A, Scemla A, Gras G, Semoun O, et al. High burden of non-influenza viruses in influenza-like illness in the early weeks of H1N1v epidemic in France. PLoS One. 2011;6: e23514. doi:10.1371/journal.pone.0023514

44. Zhang D, He Z, Xu L, Zhu X, Wu J, Wen W, et al. Epidemiology characteristics of respiratory viruses found in children and adults with respiratory tract infections in southern China. Int J Infect Dis. 2014;25: 159–164. doi:10.1016/j.ijid.2014.02.019

45. Martin ET, Kuypers J, Wald A, Englund JA. Multiple versus single virus respiratory infections: viral load and clinical disease severity in hospitalized children. Influenza Other Respir Viruses. 2012;6: 71–77. doi:10.1111/j.1750-2659.2011.00265.x

46. Kim D, Quinn J, Pinsky B, Shah NH, Brown I. Rates of Co-infection Between SARS-CoV-2 and Other Respiratory Pathogens. JAMA. 2020;323: 2085–2086. doi:10.1001/jama.2020.6266

47. Mandelia Y, Procop GW, Richter SS, Worley S, Liu W, Esper F. Dynamics and predisposition of respiratory viral co-infections in children and adults. Clin Microbiol Infect. 2021;27: 631.e1-631.e6. doi:10.1016/j.cmi.2020.05.042

48. Goka EA, Vallely PJ, Mutton KJ, Klapper PE. Single, dual and multiple respiratory virus infections and risk of hospitalization and mortality. Epidemiol Infect. 2015;143: 37–47. doi:10.1017/S0950268814000302

49. Peacey M, Hall RJ, Sonnberg S, Ducatez M, Paine S, Nicol M, et al. Pandemic (H1N1) 2009 and seasonal influenza A (H1N1) co-infection, New Zealand, 2009. Emerg Infect Dis. 2010;16: 1618–1620. doi:10.3201/eid1610.100116

50. Falchi A, Arena C, Andreoletti L, Jacques J, Leveque N, Blanchon T, et al. Dual infections by influenza A/H3N2 and B viruses and by influenza A/H3N2 and A/H1N1 viruses during winter 2007, Corsica Island, France. Journal of Clinical Virology. 2008;41: 148–151. doi:https://doi.org/10.1016/j.jcv.2007.11.003

51. Odun-Ayo F, Odaibo G, Olaleye D. Influenza virus A (H1 and H3) and B co-circulation among patient presenting with acute respiratory tract infection in Ibadan, Nigeria. Afr Health Sci. 2018;18: 1134–1143. doi:10.4314/ahs.v18i4.34

52. Myers CA, Kasper MR, Yasuda CY, Savuth C, Spiro DJ, Halpin R, et al. Dual infection of novel influenza viruses A/H1N1 and A/H3N2 in a cluster of Cambodian patients. Am J Trop Med Hyg. 2011;85: 961–963. doi:10.4269/ajtmh.2011.11-0098

53. Kendal AP, Lee DT, Parish HS, Raines D, Noble GR, Dowdle WR. Laboratory-based surveillance of influenza virus in the United States during the winter of 1977--1978.

II. Isolation of a mixture of A/Victoria- and A/USSR-like viruses from a single person during an epidemic in Wyoming, USA, January 1978. Am J Epidemiol. 1979;110: 462–468. doi:10.1093/oxfordjournals.aje.a112827

54. Liu W, Li Z-D, Tang F, Wei M-T, Tong Y-G, Zhang L, et al. Mixed Infections of Pandemic H1N1 and Seasonal H3N2 Viruses in 1 Outbreak. Clinical Infectious Diseases. 2010;50: 1359–1365. doi:10.1086/652143

55. Palacios G, Hornig M, Cisterna D, Savji N, Bussetti AV, Kapoor V, et al. Streptococcus pneumoniae coinfection is correlated with the severity of H1N1 pandemic influenza. PLoS One. 2009;4: e8540. doi:10.1371/journal.pone.0008540

56. Markov P V., Ghafari M, Beer M, Lythgoe K, Simmonds P, Stilianakis NI, et al. The evolution of SARS-CoV-2. Nat Rev Microbiol. 2023;21: 361–379. doi:10.1038/s41579-023-00878-2

57. Bal A, Simon B, Destras G, Chalvignac R, Semanas Q, Oblette A, et al. Detection and prevalence of SARS-CoV-2 co-infections during the Omicron variant circulation in France. Nat Commun. 2022;13: 6316. doi:10.1038/s41467-022-33910-9

58. Bolze A, Basler T, White S, Dei Rossi A, Wyman D, Dai H, et al. Evidence for SARS-CoV-2 Delta and Omicron co-infections and recombination. Med. 2022;3: 848-859.e4. doi:10.1016/j.medj.2022.10.002

59. Rockett RJ, Draper J, Gall M, Sim EM, Arnott A, Agius JE, et al. Co-infection with SARS-CoV-2 Omicron and Delta variants revealed by genomic surveillance. Nat Commun. 2022;13: 2745. doi:10.1038/s41467-022-30518-x

60. Sanz I, Perez D, Rojo S, Domínguez-Gil M, de Lejarazu RO, Eiros JM. Coinfections of influenza and other respiratory viruses are associated to children. Anales de Pediatría (English Edition). 2022;96: 334–341. doi:https://doi.org/10.1016/j.anpede.2021.03.002

61. Peñas-Utrilla D, Pérez-Lago L, Molero-Salinas A, Estévez A, Sanz A, Herranz M, et al. Systematic genomic analysis of SARS-CoV-2 co-infections throughout the pandemic and segregation of the strains involved. Genome Med. 2023;15: 1–16. doi:10.1186/s13073-023-01198-z

62. Musuuza JS, Watson L, Parmasad V, Putman-Buehler N, Christensen L, Safdar N. Prevalence and outcomes of co-infection and superinfection with SARS-CoV-2 and other pathogens: A systematic review and metaanalysis. PLoS One. 2021;16: 1–23. doi:10.1371/journal.pone.0251170

63. Swets MC, Russell CD, Harrison EM, Docherty AB, Lone N, Girvan M, et al. SARS-CoV-2 co-infection with influenza viruses, respiratory syncytial virus, or adenoviruses. The Lancet. 2022;399: 1463–1464. doi:10.1016/S0140-6736(22)00383-X

64. Le Glass E, Hoang VT, Boschi C, Ninove L, Zandotti C, Boutin A, et al. Incidence and Outcome of Coinfections with SARS-CoV-2 and Rhinovirus. Viruses. 2021. doi:10.3390/v13122528

65. Chesson P, Kuang JJ. The interaction between predation and competition. Nature. 2008;456: 235–238. doi:10.1038/nature07248

66. La Scola B, Desnues C, Pagnier I, Robert C, Barrassi L, Fournous G, et al. The virophage as a unique parasite of the giant mimivirus. Nature. 2008;455: 100–104. doi:10.1038/nature07218

67. Díaz-Muñoz SL, Sanjuán R, West S. Sociovirology: Conflict, Cooperation, and Communication among Viruses. Cell Host Microbe. 2017;22: 437–441. doi:10.1016/j.chom.2017.09.012

68. Birch J, Okasha S. Kin Selection and Its Critics. Bioscience. 2015;65: 22–32. doi:10.1093/biosci/biu196

69. Belcher LJ, Dewar AE, Hao C, Ghoul M, West SA. Signatures of kin selection in a natural population of the bacteria Bacillus subtilis. Evol Lett. 2023;7: 315–330. doi:10.1093/evlett/qrad029

70. Buckling A, Brockhurst MA. Kin selection and the evolution of virulence. Heredity (Edinb). 2008;100: 484–488. doi:10.1038/sj.hdy.6801093

71. Domingo-Calap P, Segredo-Otero E, Durán-Moreno M, Sanjuán R. Social evolution of innate immunity evasion in a virus. Nat Microbiol. 2019;4: 1006–1013. doi:10.1038/s41564-019-0379-8

72. Leeks A, West S. Altruism in a virus. Nat Microbiol. 2019;4: 910–911. doi:10.1038/s41564-019-0463-0

73. Leeks A, Bono LM, Ampolini EA, Souza LS, Höfler T, Mattson CL, et al. Open questions in the social lives of viruses. J Evol Biol. 2023;36: 1551–1567. doi:10.1111/jeb.14203

74. Gallego del Sol F, Quiles-Puchalt N, Brady A, Penadés JR, Marina A. Insights into the mechanism of action of the arbitrium communication system in SPbeta phages. Nat Commun. 2022;13: 3627. doi:10.1038/s41467-022-31144-3

75. West SA, Griffin AS, Gardner A, Diggle SP. Social evolution theory for microorganisms. Nat Rev Microbiol. 2006;4: 597–607. doi:10.1038/nrmicro1461

76. Cheng X, Uchida T, Xia Y, Umarova R, Liu C-J, Chen P-J, et al. Diminished hepatic IFN response following HCV clearance triggers HBV reactivation in coinfection. J Clin Invest. 2020;130: 3205–3220. doi:10.1172/JCI135616

77. Whitaker-Dowling P, Youngner JS. Vaccinia rescue of VSV from interferon-induced resistance: reversal of translation block and inhibition of protein kinase activity. Virology. 1983;131: 128–136. doi:10.1016/0042-6822(83)90539-1

78. Goto H, Ihira H, Morishita K, Tsuchiya M, Ohta K, Yumine N, et al. Enhanced growth of influenza A virus by coinfection with human parainfluenza virus type 2. Med Microbiol Immunol. 2016;205: 209–218. doi:10.1007/s00430-015-0441-y

79. Makoti P, Fielding BC. HIV and Human Coronavirus Coinfections: A Historical Perspective. Viruses. 2020;12. doi:10.3390/v12090937

80. Basoulis D, Mastrogianni E, Voutsinas PM, Psichogiou M. HIV and COVID-19 Co-Infection: Epidemiology, Clinical Characteristics, and Treatment. Viruses. 2023;15: 1–21. doi:10.3390/v15020577

81. González Álvarez DA, López Cortés LF, Cordero E. Impact of HIV on the severity of influenza. Expert Rev Respir Med. 2016;10: 463–472. doi:10.1586/17476348.2016.1157474

82. Stoeger T, Adler H. “Novel” Triggers of Herpesvirus Reactivation and Their Potential Health Relevance. Front Microbiol. 2018;9: 3207. doi:10.3389/fmicb.2018.03207

83. Dianzani F. Viral interference and interferon. Ricerca in clinica e in laboratorio. 1975;5: 196–213. doi:10.1007/BF02908284

84. Piret J, Boivin G. Viral Interference between Respiratory Viruses. Emerg Infect Dis. 2022;28: 273–281. doi:10.3201/eid2802.211727

85. Dee K, Schultz V, Haney J, Bissett LA, Magill C, Murcia PR. Influenza A and Respiratory Syncytial Virus Trigger a Cellular Response That Blocks Severe Acute Respiratory Syndrome Virus 2 Infection in the Respiratory Tract. Journal of Infectious Diseases. 2023;227: 1396–1406. doi:10.1093/infdis/jiac494

86. Nickbakhsh S, Mair C, Matthews L, Reeve R, Johnson PCD, Thorburn F, et al. Virus-virus interactions impact the population dynamics of influenza and the common cold. Proc Natl Acad Sci U S A. 2019;116: 27142–27150. doi:10.1073/pnas.1911083116

87. Wansley EK, Grayson JM, Parks GD. Apoptosis induction and interferon signaling but not IFN-beta promoter induction by an SV5 P/V mutant are rescued by coinfection with wild-type SV5. Virology. 2003;316: 41–54. doi:10.1016/s0042-6822(03)00584-1

88. Hao X, Li Y, Chen H, Chen B, Liu R, Wu Y, et al. Canine Circovirus Suppresses the Type I Interferon Response and Protein Expression but Promotes CPV-2 Replication. Int J Mol Sci. 2022;23. doi:10.3390/ijms23126382

89. Haney J, Vijayakrishnan S, Streetley J, Dee K, Goldfarb DM, Clarke M, et al. Coinfection by influenza A virus and respiratory syncytial virus produces hybrid virus particles. Nat Microbiol. 2022;7: 1879–1890. doi:10.1038/s41564-022-01242-5

90. Focosi D, Maggi F. Recombination in Coronaviruses, with a Focus on SARS-CoV-2. Viruses. 2022;14. doi:10.3390/v14061239

91. Steel J, Lowen AC. Influenza A virus reassortment. Curr Top Microbiol Immunol. 2014;385: 377–401. doi:10.1007/82_2014_395

92. Gerber M, Isel C, Moules V, Marquet R. Selective packaging of the influenza A genome and consequences for genetic reassortment. Trends Microbiol. 2014;22: 446–455. doi:10.1016/j.tim.2014.04.001

93. Baker SF, Nogales A, Finch C, Tuffy KM, Domm W, Perez DR, et al. Influenza A and B virus intertypic reassortment through compatible viral packaging signals. J Virol. 2014;88: 10778–10791. doi:10.1128/JVI.01440-14

94. Essere B, Yver M, Gavazzi C, Terrier O, Isel C, Fournier E, et al. Critical role of segment-specific packaging signals in genetic reassortment of influenza A viruses. Proc Natl Acad Sci U S A. 2013;110: E3840-8. doi:10.1073/pnas.1308649110

95. White MC, Lowen AC. Implications of segment mismatch for influenza A virus evolution. J Gen Virol. 2018;99: 3–16. doi:10.1099/jgv.0.000989

96. Worobey M, Holmes EC. Evolutionary aspects of recombination in RNA viruses. J Gen Virol. 1999;80 (Pt 10: 2535–2543. doi:10.1099/0022-1317-80-10-2535

97. Wells HL, Bonavita CM, Navarrete-Macias I, Vilchez B, Rasmussen AL, Anthony SJ. The coronavirus recombination pathway. Cell Host Microbe. 2023;31: 874–889. doi:10.1016/j.chom.2023.05.003

98. Brooke CB, Ince WL, Wrammert J, Ahmed R, Wilson PC, Bennink JR, et al. Most Influenza A Virions Fail To Express at Least One Essential Viral Protein. J Virol. 2013;87: 3155–3162. doi:10.1128/jvi.02284-12

99. Farrell A, Brooke C, Koelle K, Ke R. Coinfection of semi-infectious particles can contribute substantially to influenza infection dynamics. bioRxiv. 2019; 1–27. doi:10.1101/547349

100. Diefenbacher M, Sun J, Brooke CB. The parts are greater than the whole: the role of semi-infectious particles in influenza A virus biology. Curr Opin Virol. 2018;33: 42–46. doi:10.1016/j.coviro.2018.07.002

101. Fenner F. GENETICS OF ANIMAL VIRUSES. Encyclopedia of Virology. 1999. pp. 606–613. doi:10.1006/rwvi.1999.0111

102. VON MAGNUS P. Incomplete forms of influenza virus. Adv Virus Res. 1954;2: 59–79. doi:10.1016/s0065-3527(08)60529-1

103. Zhou T, Gilliam NJ, Li S, Spaudau S, Osborn RM, Anderson CS, et al. Generation and functional analysis of defective viral genomes during SARS-CoV-2 infection. bioRxiv : the preprint server for biology. United States; 2022. doi:10.1101/2022.09.22.509123

104. Vignuzzi M, López CB. Defective viral genomes are key drivers of the virus–host interaction. Nat Microbiol. 2019;4: 1075–1087. doi:10.1038/s41564-019-0465-y

105. Huang AS, Baltimore D. Defective Viral Particles and Viral Disease Processes. Nature. 1970;226: 325–327. doi:10.1038/226325a0

106. Ziegler CM, Botten JW. Defective Interfering Particles of Negative-Strand RNA Viruses. Trends Microbiol. 2020; 0–11. doi:10.1016/j.tim.2020.02.006

107. Genoyer E, López CB. The Impact of Defective Viruses on Infection and Immunity. Annu Rev Virol. 2019;6: 547–566. doi:10.1146/annurev-virology-092818-015652

108. Rezelj V V., Levi LI, Vignuzzi M. The defective component of viral populations. Curr Opin Virol. 2018;33: 74–80. doi:10.1016/j.coviro.2018.07.014

109. Brooke CB. Population Diversity and Collective Infection. 2017;91: 1–13.

110. Wang C, Forst C V, Chou T-W, Geber A, Wang M, Hamou W, et al. Cell-to-Cell Variation in Defective Virus Expression and Effects on Host Responses during Influenza Virus Infection. mBio. 2020;11. doi:10.1128/mBio.02880-19

111. Saira K, Lin X, DePasse J V, Halpin R, Twaddle A, Stockwell T, et al. Sequence analysis of in vivo defective interfering-like RNA of influenza A H1N1 pandemic virus. J Virol. 2013;87: 8064–8074. doi:10.1128/JVI.00240-13

112. Phipps KL, Ganti K, Jacobs NT, Lee C-Y, Carnaccini S, White MC, et al. Collective interactions augment influenza A virus replication in a host-dependent manner. Nat Microbiol. 2020;5: 1158–1169. doi:10.1038/s41564-020-0749-2

113. Ellenberg P, Edreira M, Scolaro L. Resistance to superinfection of Vero cells persistently infected with Junin virus. Arch Virol. 2004;149: 507–522. doi:10.1007/s00705-003-0227-1

114. Schaller T, Appel N, Koutsoudakis G, Kallis S, Lohmann V, Pietschmann T, et al. Analysis of Hepatitis C Virus Superinfection Exclusion by Using Novel Fluorochrome Gene-Tagged Viral Genomes. J Virol. 2007;81: 4591–4603. doi:10.1128/jvi.02144-06

115. Ludlow M, McQuaid S, Cosby SL, Cattaneo R, Rima BK, Duprex WP. Measles virus superinfection immunity and receptor redistribution in persistently infected NT2 cells. Journal of General Virology. 2005;86: 2291–2303. doi:10.1099/vir.0.81052-0

116. Sims A, Tornaletti LB, Jasim S, Pirillo C, Devlin R, Hirst JC, et al. Superinfection exclusion creates spatially distinct influenza virus populations. PLoS Biol. 2023;21: 1–19. doi:10.1371/journal.pbio.3001941

117. LENNETTE EH, KOPROWSKI H. Interference between viruses in tissue culture. J Exp Med. 1946;83: 195–219. doi:10.1084/jem.83.3.195

118. ISAACS A, BURKE DC. VIRAL INTERFERENCE AND INTERFERON. Br Med Bull. 1959;15: 185–188. doi:10.1093/oxfordjournals.bmb.a069760

119. Blattner RJ. Interferon, an antiviral substance. J Pediatr. 1966;68: 488–491. doi:https://doi.org/10.1016/S0022-3476(66)80257-3

120. Drori Y, Jacob-Hirsch J, Pando R, Glatman-Freedman A, Friedman N, Mendelson E, et al. Influenza a virus inhibits RSV infection via a two-wave expression of IFIT proteins. Viruses. 2020;12: 1–14. doi:10.3390/v12101171

121. Desmyter J, Melnick JL, Rawls WE. Defectiveness of Interferon Production and of Rubella Virus Interference in a Line of African Green Monkey Kidney Cells (Vero). J Virol. 1968;2: 955–961. doi:10.1128/jvi.2.10.955-961.1968

122. Sun J, Brooke CB. Influenza A Virus Superinfection Potential Is Regulated by Viral Genomic Heterogeneity. mBio. 2018;9: 1–13. doi:10.1128/mBio.01761-18

123. Geib T, Sauder C, Venturelli S, Hässler C, Staeheli P, Schwemmle M. Selective Virus Resistance Conferred by Expression of Borna Disease Virus Nucleocapsid Components. J Virol. 2003;77: 4283–4290. doi:10.1128/jvi.77.7.4283-4290.2003

124. Boussier J, Levi L, Weger-Lucarelli J, Poirier EZ, Vignuzzi M, Albert ML. Chikungunya virus superinfection exclusion is mediated by a block in viral replication and does not rely on non-structural protein 2. PLoS One. 2020;15. doi:10.1371/journal.pone.0241592

125. Laliberte JP, Moss B. A Novel Mode of Poxvirus Superinfection Exclusion That Prevents Fusion of the Lipid Bilayers of Viral and Cellular Membranes. J Virol. 2014;88: 9751–9768. doi:10.1128/jvi.00816-14

126. Zou G, Zhang B, Lim P-Y, Yuan Z, Bernard KA, Shi P-Y. Exclusion of West Nile Virus Superinfection through RNA Replication. J Virol. 2009;83: 11765–11776. doi:10.1128/jvi.01205-09

127. Whitaker-Dowling P, Youngner JS, Widnell CC, Wilcox DK. Superinfection exclusion by vesicular stomatitis virus. Virology. 1983;131: 137–143. doi:10.1016/0042-6822(83)90540-8

128. Benson RE, Sanfridson A, Ottinger JS, Doyle C, Cullen BP. Downregulation of ceil-surface CD4 expression by simian immunodeficiency virus nef prevents viralsuper infection. Journal of Experimental Medicine. 1993;177: 1561–1566. doi:10.1084/jem.177.6.1561

129. Johnson RM, Spear PG. Herpes simplex virus glycoprotein D mediates interference with herpes simplex virus infection. J Virol. 1989;63: 819–827. doi:10.1128/jvi.63.2.819-827.1989

130. Horga M-A, Gusella GL, Greengard O, Poltoratskaia N, Porotto M, Moscona A. Mechanism of Interference Mediated by Human Parainfluenza Virus Type 3 Infection. J Virol. 2000;74: 11792–11799. doi:10.1128/jvi.74.24.11792-11799.2000

131. Singh IR, Suomalainen M, Varadarajan S, Garoff H, Helenius A. Multiple mechanisms for the inhibition of entry and uncoating of superinfecting Semliki Forest virus. Virology. 1997;231: 59–71. doi:10.1006/viro.1997.8492

132. Lee Y-M, Tscherne DM, Yun S-I, Frolov I, Rice CM. Dual Mechanisms of Pestiviral Superinfection Exclusion at Entry and RNA Replication. J Virol. 2005;79: 3231–3242. doi:10.1128/jvi.79.6.3231-3242.2005

133. Christen L, Seto J, Niles EG. Superinfection exclusion of vaccinia virus in virus-infected cell cultures. Virology. 1990;174: 35–42. doi:10.1016/0042-6822(90)90051-r

134. Martin BE, Harris JD, Sun J, Koelle K, Brooke CB. Cellular co-infection can modulate the efficiency of influenza A virus production and shape the interferon response. PLoS Pathog. 2020;16. doi:10.1371/journal.ppat.1008974

135. Claus C, Tzeng WP, Liebert UG, Frey TK. Rubella virus-induced superinfection exclusion studied in cells with persisting replicons. Journal of General Virology. 2007;88: 2769–2773. doi:10.1099/vir.0.83092-0

136. Julve JM, Gandía A, Fernández-del-Carmen A, Sarrion-Perdigones A, Castelijns B, Granell A, et al. A coat-independent superinfection exclusion rapidly imposed in Nicotiana benthamiana cells by tobacco mosaic virus is not prevented by depletion of the movement protein. Plant Mol Biol. 2013;81: 553–564. doi:10.1007/s11103-013-0028-1

137. Zhang XF, Zhang S, Guo Q, Sun R, Wei T, Qu F. A new mechanistic model for viral cross protection and superinfection exclusion. Front Plant Sci. 2018;9: 1–9. doi:10.3389/fpls.2018.00040

138. McAllister WT, Barrett CL. Superinfection exclusion by bacteriophage T7. J Virol. 1977;24: 709–711. doi:10.1128/jvi.24.2.709-711.1977

139. Ellenberg P, Linero FN, Scolaro LA. Superinfection exclusion in BHK-21 cells persistently infected with Junín virus. J Gen Virol. 2007;88: 2730–2739. doi:10.1099/vir.0.83041-0

140. Gaudin R, Kirchhausen T. Superinfection exclusion is absent during acute Junin virus infection of Vero and A549 cells. Sci Rep. 2015;5: 15990. doi:10.1038/srep15990

141. Nethe M, Berkhout B, van der Kuyl AC. Retroviral superinfection resistance. Retrovirology. 2005;2: 52. doi:10.1186/1742-4690-2-52

142. Willey RL, Maldarelli F, Martin MA, Strebel K. Human immunodeficiency virus type 1 Vpu protein regulates the formation of intracellular gp160-CD4 complexes. J Virol. 1992;66: 226–234. doi:10.1128/jvi.66.1.226-234.1992

143. Herchenröder O, Moosmayer D, Bock M, Pietschmann T, Rethwilm A, Bieniasz PD, et al. Specific Binding of Recombinant Foamy Virus Envelope Protein to Host Cells Correlates with Susceptibility to Infection. Virology. 1999;255: 228–236. doi:10.1006/VIRO.1998.9570

144. Schneider-Schaulies J, Schnorr JJ, Brinckmann U, Dunster LM, Baczko K, Liebert UG, et al. Receptor usage and differential downregulation of CD46 by measles virus wild-type and vaccine strains. Proc Natl Acad Sci U S A. 1995;92: 3943–3947. doi:10.1073/pnas.92.9.3943

145. Biryukov J, Meyers C. Superinfection Exclusion between Two High-Risk Human Papillomavirus Types during a Coinfection. J Virol. 2018;92. doi:10.1128/jvi.01993-17

146. Huang I-C, Li W, Sui J, Marasco W, Choe H, Farzan M. Influenza A Virus Neuraminidase Limits Viral Superinfection. J Virol. 2008;82: 4834–4843. doi:10.1128/jvi.00079-08

147. Morrison TG, McGinnes LW. Avian cells expressing the Newcastle disease virus hemagglutinin-neuraminidase protein are resistant to Newcastle disease virus infection. Virology. 1989;171: 10–17. doi:10.1016/0042-6822(89)90505-9

148. Doceul V, Hollinshead M, Van Der Linden L, Smith GL. Repulsion of superinfecting virions: A mechanism for rapid virus spread. Science (1979). 2010;327: 873–876. doi:10.1126/science.1183173

149. Simon KO, Cardamone JJJ, Whitaker-Dowling PA, Youngner JS, Widnell CC. Cellular mechanisms in the superinfection exclusion of vesicular stomatitis virus. Virology. 1990;177: 375–379. doi:10.1016/0042-6822(90)90494-c

150. Turner PC, Moyer RW. The vaccinia virus fusion inhibitor proteins SPI-3 (K2) and HA (A56) expressed by infected cells reduce the entry of superinfecting virus. Virology. 2008;380: 226–233. doi:10.1016/j.virol.2008.07.020

151. Criddle A, Thornburg T, Kochetkova I, DePartee M, Taylor MP. gD-Independent Superinfection Exclusion of Alphaherpesviruses. J Virol. 2016;90: 4049–4058. doi:10.1128/JVI.00089-16

152. Cwick JP, Owen JE, Kochetkova I, Hain KS, Horssen N Van, Taylor MP. Superinfection Exclusion of Alphaherpesviruses Interferes with Virion Trafficking. Microbiol Spectr. 2022;10. doi:10.1128/spectrum.00684-22

153. Tscherne DM, Evans MJ, von Hahn T, Jones CT, Stamataki Z, McKeating JA, et al. Superinfection exclusion in cells infected with hepatitis C virus. J Virol. 2007;81: 3693–3703. doi:10.1128/JVI.01748-06

154. Karpf AR, Lenches E, Strauss EG, Strauss JH, Brown DT. Superinfection exclusion of alphaviruses in three mosquito cell lines persistently infected with Sindbis virus. J Virol. 1997;71: 7119–7123. doi:10.1128/JVI.71.9.7119-7123.1997

155. Adams RH, Brown DT. BHK cells expressing Sindbis virus-induced homologous interference allow the translation of nonstructural genes of superinfecting virus. J Virol. 1985;54: 351–357. doi:10.1128/JVI.54.2.351-357.1985

156. McAuley JL, Gilbertson BP, Trifkovic S, Brown LE, McKimm-Breschkin JL. Influenza virus neuraminidase structure and functions. Front Microbiol. 2019;10. doi:10.3389/fmicb.2019.00039

157. Stokes G V. High-voltage electron microscope study of the release of vaccinia virus from whole cells. J Virol. 1976;18: 636–643. doi:10.1128/JVI.18.2.636-643.1976

158. Cureton DK, Massol RH, Saffarian S, Kirchhausen TL, Whelan SPJ. Vesicular Stomatitis Virus Enters Cells through Vesicles Incompletely Coated with Clathrin That Depend upon Actin for Internalization. PLoS Pathog. 2009;5. doi:10.1371/journal.ppat.1000394

159. Bhargava AK, Rothlauf PW, Krummenacher C. Herpes simplex virus glycoprotein D relocates nectin-1 from intercellular contacts. Virology. 2016;499: 267–277. doi:10.1016/j.virol.2016.09.019

160. Stegmann T. Membrane fusion mechanisms: The influenza hemagglutinin paradigm and its implications for intracellular fusion. Traffic. 2000;1: 598–604. doi:10.1034/j.1600-0854.2000.010803.x

161. Singh I, Helenius A. Role of ribosomes in Semliki Forest virus nucleocapsid uncoating. J Virol. 1992;66: 7049–7058. doi:10.1128/jvi.66.12.7049-7058.1992

162. Komar AA, Hatzoglou M. Cellular IRES-mediated translation: the war of ITAFs in pathophysiological states. Cell Cycle. 2011;10: 229–240. doi:10.4161/cc.10.2.14472

163. Goila-Gaur R, Demirov DG, Orenstein JM, Ono A, Freed EO. Defects in human immunodeficiency virus budding and endosomal sorting induced by TSG101 overexpression. J Virol. 2003;77: 6507–6519. doi:10.1128/jvi.77.11.6507-6519.2003

164. Perdoncini Carvalho C, Ren R, Han J, Qu F. Natural Selection, Intracellular Bottlenecks of Virus Populations, and Viral Superinfection Exclusion. Annu Rev Virol. 2022;9: 121–137. doi:10.1146/annurev-virology-100520-114758

165. Donahue DA, Bastarache SM, Sloan RD, Wainberg MA. Latent HIV-1 can be reactivated by cellular superinfection in a Tat-dependent manner, which can lead to the emergence of multidrug-resistant recombinant viruses. J Virol. 2013;87: 9620–9632. doi:10.1128/JVI.01165-13

166. Hunter M, Fusco D. Superinfection exclusion: A viral strategy with short-term benefits and long-term drawbacks. PLoS Comput Biol. 2022;18: e1010125. Available: https://doi.org/10.1371/journal.pcbi.1010125

167. Delima GK, Ganti K, Holmes KE, Shartouny JR, Lowen AC. Influenza A virus coinfection dynamics are shaped by distinct virus-virus interactions within and between cells. PLoS Pathog. 2023;19. doi:10.1371/journal.ppat.1010978

168. Wildum S, Schindler M, Münch J, Kirchhoff F. Contribution of Vpu, Env, and Nef to CD4 Down-Modulation and Resistance of Human Immunodeficiency Virus Type 1-Infected T Cells to Superinfection. J Virol. 2006;80: 8047–8059. doi:10.1128/jvi.00252-06

169. Sigal D, Reid JNS, Wahl LM. Effects of Transmission Bottlenecks on the Diversity of Influenza A Virus. Genetics. 2018/09/04. 2018;210: 1075–1088. doi:10.1534/genetics.118.301510

170. Brooke CB. Biological activities of “noninfectious” influenza A virus particles. Future Virol. 2014;9: 41–51. doi:10.2217/fvl.13.118

171. Wodarz D, Levy DN, Komarova NL. Multiple infection of cells changes the dynamics of basic viral evolutionary processes. Evolution Letters. John Wiley and Sons Inc; 2019. pp. 104–115. doi:10.1002/evl3.95

172. Leeks A, Segredo-Otero EA, Sanjuán R, West SA. Beneficial coinfection can promote within-host viral diversity. Virus Evol. 2018;4. doi:10.1093/ve/vey028

173. Fitzsimmons WJ, Woods RJ, McCrone JT, Woodman A, Arnold JJ, Yennawar M, et al. A speed–fidelity trade-off determines the mutation rate and virulence of an RNA virus. PLoS Biol. 2018;16: e2006459. Available: https://doi.org/10.1371/journal.pbio.2006459

174. Berngruber TW, Weissing FJ, Gandon S. Inhibition of Superinfection and the Evolution of Viral Latency. J Virol. 2010;84: 10200–10208. doi:10.1128/jvi.00865-10

175. Zhang XF, Sun R, Guo Q, Zhang S, Meulia T, Halfmann R, et al. A self-perpetuating repressive state of a viral replication protein blocks superinfection by the same virus. PLoS Pathog. 2017;13: 1–24. doi:10.1371/journal.ppat.1006253

176. Julve JM, Gandía A, Fernández-del-Carmen A, Sarrion-Perdigones A, Castelijns B, Granell A, et al. A coat-independent superinfection exclusion rapidly imposed in Nicotiana benthamiana cells by tobacco mosaic virus is not prevented by depletion of the movement protein. Plant Mol Biol. 2013;81: 553–564. doi:10.1007/s11103-013-0028-1

177. Ziebell H, Carr JP. Cross-Protection. 2010. pp. 211–264. doi:10.1016/s0065-3527(10)76006-1

178. Bergua M, Zwart MP, El-Mohtar C, Shilts T, Elena SF, Folimonova SY. A Viral Protein Mediates Superinfection Exclusion at the Whole-Organism Level but Is Not Required for Exclusion at the Cellular Level. J Virol. 2014;88: 11327–11338. doi:10.1128/jvi.01612-14

179. Laureti M, Paradkar PN, Fazakerley JK, Rodriguez-Andres J. Superinfection exclusion in mosquitoes and its potential as an arbovirus control strategy. Viruses. 2020;12: 1–17. doi:10.3390/v12111259

180. Adelman ZN, Blair CD, Carlson JO, Beaty BJ, Olson KE. Sindbis virus-induced silencing of dengue viruses in mosquitoes. Insect Mol Biol. 2001;10: 265–273. doi:10.1046/j.1365-2583.2001.00267.x

181. Muturi EJ, Bara J. Sindbis virus interferes with dengue 4 virus replication and its potential transmission by Aedes albopictus. Parasit Vectors. 2015;8: 1–10. doi:10.1186/s13071-015-0667-y

182. Billecocq A, Vazeille-Falcoz M, Rodhain F, Bouloy M. Pathogen-specific resistance to Rift Valley fever virus infection is induced in mosquito cells by expression of the recombinant nucleoprotein but not NSs non-structural protein sequences. Journal of General Virology. 2000;81: 2161–2166. doi:10.1099/0022-1317-81-9-2161

183. Olson KE, Higgs S, Gaines PJ, Powers AM, Davis BS, Kamrud KI, et al. Genetically engineered resistance to dengue-2 virus transmission in mosquitoes. Science (1979). 1996;272: 884–886. doi:10.1126/science.272.5263.884

184. Kohl A, Billecocq A, Préhaud C, Yadani FZ, Bouloy M. Transient gene expression in mammalian and mosquito cells using a recombinant Semliki Forest virus expressing T7 RNA polymerase. Appl Microbiol Biotechnol. 1999;53: 51–56. doi:10.1007/s002530051613

185. De Wit E, Spronken MIJ, Bestebroer TM, Rimmelzwaan GF, Osterhaus ADME, Fouchier RAM. Efficient generation and growth of influenza virus A/PR/8/34 from eight cDNA fragments. Virus Research. Elsevier; 2004. pp. 155–161. doi:10.1016/j.virusres.2004.02.028

186. Fukuyama S, Katsura H, Zhao D, Ozawa M, Ando T, Shoemaker JE, et al. Multi-spectral fluorescent reporter influenza viruses (Color-flu) as powerful tools for in vivo studies. Nat Commun. 2015;6. doi:10.1038/ncomms7600

187. Rihn SJ, Merits A, Bakshi S, Turnbull ML, Wickenhagen A, Alexander AJT, et al. A plasmid DNA-launched SARS-CoV-2 reverse genetics system and coronavirus toolkit for COVID-19 research. PLoS Biol. 2021;19: 1–22. doi:10.1371/journal.pbio.3001091

188. Pirillo C, Al Khalidi S, Sims A, Devlin R, Zhao H, Pinto R, et al. Cotransfer of antigen and contextual information harmonizes peripheral and lymph node conventional dendritic cell activation. Sci Immunol. 2023;8. doi:10.1126/sciimmunol.adg8249

189. Schindelin J, Arganda-Carreras I, Frise E, Kaynig V, Longair M, Pietzsch T, et al. Fiji: An open-source platform for biological-image analysis. Nat Methods. 2012;9: 676–682. doi:10.1038/nmeth.2019

190. Figliozzi RW, Chen F, Chi A, Hsia SCV. Using the inverse Poisson distribution to calculate multiplicity of infection and viral replication by a high-throughput fluorescent imaging system. Virol Sin. 2016;31: 180–183. doi:10.1007/s12250-015-3662-8

191. Paules C, Subbarao K. Influenza. Lancet. 2017;390: 697–708. doi:10.1016/S0140-6736(17)30129-0

192. Hutchinson EC, Yamauchi Y. Understanding Influenza. In: Yamauchi Y, editor. Influenza Virus: Methods and Protocols. New York, NY: Springer New York; 2018. pp. 1–21. doi:10.1007/978-1-4939-8678-1_1

193. White SK, Ma W, McDaniel CJ, Gray GC, Lednicky JA. Serologic evidence of exposure to influenza D virus among persons with occupational contact with cattle. Journal of Clinical Virology. 2016;81: 31–33. doi:10.1016/j.jcv.2016.05.017

194. Arbeitskreis Blut, Untergruppe «Bewertung Blutassoziierter Krankheitserreger» A, Krankheitserreger» U «Bewertung B. Influenza Virus. Transfus Med Hemother. 2009;36: 32–39. doi:10.1159/000197314

195. Bouvier NM, Palese P. The biology of influenza viruses. Vaccine. 2008;26 Suppl 4: D49-53. Available: http://www.ncbi.nlm.nih.gov/pubmed/19230160

196. Dadonaite B, Vijayakrishnan S, Fodor E, Bhella D, Hutchinson EC. Filamentous influenza viruses. Journal of General Virology. 2016;97: 1755–1764. doi:10.1099/jgv.0.000535

197. Lamb RA, Krug RM. Orthomyxoviridae: The viruses and their replication. Lippincott-Raven Press; 1996. Available: https://www.scholars.northwestern.edu/en/publications/orthomyxoviridae-the-viruses-and-their-replication

198. Wise HM, Foeglein A, Sun J, Dalton RM, Patel S, Howard W, et al. A complicated message: Identification of a novel PB1-related protein translated from influenza A virus segment 2 mRNA. J Virol. 2009;83: 8021–31. doi:10.1128/JVI.00826-09

199. Jagger BW, Wise HM, Kash JC, Walters KA, Wills NM, Xiao YL, et al. An overlapping protein-coding region in influenza A virus segment 3 modulates the host response. Science (1979). 2012;337: 199–204. doi:10.1126/science.1222213

200. Wise HM, Hutchinson EC, Jagger BW, Stuart AD, Kang ZH, Robb N, et al. Identification of a novel splice variant form of the influenza A virus M2 ion channel with an antigenically distinct ectodomain. PLoS Pathog. 2012;8: e1002998. doi:10.1371/journal.ppat.1002998

201. Forbes NE, Ping J, Dankar SK, Jia J-J, Selman M, Keleta L, et al. Multifunctional Adaptive NS1 Mutations Are Selected upon Human Influenza Virus Evolution in the Mouse. Pekosz A, editor. PLoS One. 2012;7: e31839. doi:10.1371/journal.pone.0031839

202. Zhang L, Wang J, Muñoz-Moreno R, Kim M, Sakthivel R, Mo W, et al. Influenza Virus NS1 Protein-RNA Interactome Reveals Intron Targeting. Sandri-Goldin RM, editor. J Virol. 2018;92. doi:10.1128/JVI.01634-18

203. Hale BG, Randall RE, Ortin J, Jackson D. The multifunctional NS1 protein of influenza A viruses. Journal of General Virology. 2008;89: 2359–2376. doi:10.1099/vir.0.2008/004606-0

204. Hutchinson EC, Charles PD, Hester SS, Thomas B, Trudgian D, Martínez-Alonso M, et al. Conserved and host-specific features of influenza virion architecture. Nat Commun. 2014;5: 4816. doi:10.1038/ncomms5816

205. Breen M, Nogales A, Baker SF, Martínez-Sobrido L. Replication-Competent Influenza A Viruses Expressing Reporter Genes. Viruses. 2016;8. doi:10.3390/v8070179

206. Samji T. Influenza A: understanding the viral life cycle. Yale J Biol Med. 2009;82: 153–159.

207. Deng T, Vreede FT, Brownlee GG. Different de novo initiation strategies are used by influenza virus RNA polymerase on its cRNA and viral RNA promoters during viral RNA replication. J Virol. 2006;80: 2337–48. doi:10.1128/JVI.80.5.2337-2348.2006

208. Plotch SJ, Bouloy M, Krug RM. Transfer of 5'-terminal cap of globin mRNA to influenza viral complementary RNA during transcription in vitro. Proc Natl Acad Sci U S A. 1979;76: 1618–22. Available: http://www.ncbi.nlm.nih.gov/pubmed/287003

209. Zhao C, Pu J. Influence of Host Sialic Acid Receptors Structure on the Host Specificity of Influenza Viruses. Viruses. 2022;14. doi:10.3390/v14102141

210. Daniels RS, Douglas AR, Skehel JJ, Wiley DC, Naeve CW, Webster RG, et al. Antigenic analyses of influenza virus haemagglutinins with different receptor-binding specificities. Virology. 1984;138: 174–177. doi:10.1016/0042-6822(84)90158-2

211. Connor RJ, Kawaoka Y, Webster RG, Paulson JC. Receptor Specificity in Human, Avian, and Equine H2 and H3 Influenza Virus Isolates. Virology. 1994;205: 17–23. doi:10.1006/VIRO.1994.1615

212. Weis W, Brown JH, Cusack S, Paulson JC, Skehel JJ, Wiley DC. Structure of the influenza virus haemagglutinin complexed with its receptor, sialic acid. Nature. 1988;333: 426–431. doi:10.1038/333426a0

213. Burckhardt CJ, Greber UF. Virus Movements on the Plasma Membrane Support Infection and Transmission between Cells. Manchester M, editor. PLoS Pathog. 2009;5: e1000621. doi:10.1371/journal.ppat.1000621

214. Yamauchi Y, Helenius A. Virus entry at a glance. J Cell Sci. 2013;126: 1289–95. doi:10.1242/jcs.119685

215. Lakadamyali M, Rust MJ, Zhuang X. Endocytosis of influenza viruses. Microbes Infect. 2004;6: 929–936. doi:10.1016/j.micinf.2004.05.002

216. Jolly CL, Sattentau QJ. Attachment Factors. Springer, New York, NY; 2006. pp. 1–23. doi:10.1007/978-1-4614-7651-1_1

217. de Vries E, Tscherne DM, Wienholts MJ, Cobos-Jiménez V, Scholte F, García-Sastre A, et al. Dissection of the Influenza A Virus Endocytic Routes Reveals Macropinocytosis as an Alternative Entry Pathway. Pekosz A, editor. PLoS Pathog. 2011;7: e1001329. doi:10.1371/journal.ppat.1001329

218. Cossart P, Helenius A. Endocytosis of viruses and bacteria. Cold Spring Harb Perspect Biol. 2014;6. doi:10.1101/cshperspect.a016972

219. Huotari J, Helenius A. Endosome maturation. EMBO J. 2011;30: 3481–500. doi:10.1038/emboj.2011.286

220. Cross K, Langley W, Russell R, Skehel J, Steinhauer D. Composition and Functions of the Influenza Fusion Peptide. Protein Pept Lett. 2009;16: 766–778. doi:10.2174/092986609788681715

221. Carrique L, Fan H, Walker AP, Keown JR, Sharps J, Staller E, et al. Host ANP32A mediates the assembly of the influenza virus replicase. Nature. 2020;587: 638–643. doi:10.1038/s41586-020-2927-z

222. Liang R, Swanson JMJ, Madsen JJ, Hong M, DeGrado WF, Voth GA. Acid activation mechanism of the influenza A M2 proton channel. Proc Natl Acad Sci U S A. 2016;113: E6955–E6964. doi:10.1073/pnas.1615471113

223. Neumann G, Castrucci MR, Kawaoka Y. Nuclear import and export of influenza virus nucleoprotein. J Virol. 1997;71: 9690–9700. doi:10.1128/jvi.71.12.9690-9700.1997

224. Bui M, Wills EG, Helenius A, Whittaker GR. Role of the influenza virus M1 protein in nuclear export of viral ribonucleoproteins. J Virol. 2000;74: 1781–1786. doi:10.1128/jvi.74.4.1781-1786.2000

225. Martin K, Helenius A. Nuclear transport of influenza virus ribonucleoproteins: the viral matrix protein (M1) promotes export and inhibits import. Cell. 1991;67: 117–130. doi:10.1016/0092-8674(91)90576-k

226. Jeong B-S, Dyer RB. Proton Transport Mechanism of M2 Proton Channel Studied by Laser-Induced pH Jump. J Am Chem Soc. 2017;139: 6621–6628. doi:10.1021/jacs.7b00617

227. Banerjee I, Yamauchi Y, Helenius A, Horvath P. High-Content Analysis of Sequential Events during the Early Phase of Influenza A Virus Infection. Digard P, editor. PLoS One. 2013;8: e68450. doi:10.1371/journal.pone.0068450

228. Banerjee I, Miyake Y, Nobs SP, Schneider C, Horvath P, Kopf M, et al. Influenza A virus uses the aggresome processing machinery for host cell entry. Science. 2014;346: 473–7. doi:10.1126/science.1257037

229. Postnikova Y, Treshchalina A, Boravleva E, Gambaryan A, Ishmukhametov A, Matrosovich M, et al. Diversity and reassortment rate of influenza a viruses in wild ducks and gulls. Viruses. 2021;13: 1–14. doi:10.3390/v13061010

230. Hill NJ, Hussein ITM, Davis KR, Ma EJ, Spivey TJ, Ramey AM, et al. Reassortment of Influenza A Viruses in Wild Birds in Alaska before H5 Clade 2.3.4.4 Outbreaks. Emerg Infect Dis. 2017;23: 654–657. doi:10.3201/eid2304.161668

231. Cui Y, Li Y, Li M, Zhao L, Wang D, Tian J, et al. Evolution and extensive reassortment of H5 influenza viruses isolated from wild birds in China over the past decade. Emerg Microbes Infect. 2020;9: 1793–1803. doi:10.1080/22221751.2020.1797542

232. Hoye BJ, Donato CM, Lisovski S, Deng Y-M, Warner S, Hurt AC, et al. Reassortment and Persistence of Influenza A Viruses from Diverse Geographic Origins within Australian Wild Birds: Evidence from a Small, Isolated Population of Ruddy Turnstones. J Virol. 2021;95. doi:10.1128/jvi.02193-20

233. Marshall N, Priyamvada L, Ende Z, Steel J, Lowen AC. Influenza Virus Reassortment Occurs with High Frequency in the Absence of Segment Mismatch. PLoS Pathog. 2013;9. doi:10.1371/journal.ppat.1003421

234. Jacobs NT, Onuoha NO, Antia A, Steel J, Antia R, Lowen AC. Incomplete influenza A virus genomes occur frequently but are readily complemented during localized viral spread. Nat Commun. 2019;10. doi:10.1038/s41467-019-11428-x

235. Tao H, Li L, White MC, Steel J, Lowen AC. Influenza A Virus Coinfection through Transmission Can Support High Levels of Reassortment. J Virol. 2015;89: 8453–8461. doi:10.1128/jvi.01162-15

236. Tao H, Steel J, Lowen AC. Intrahost Dynamics of Influenza Virus Reassortment. J Virol. 2014;88: 7485–7492. doi:10.1128/jvi.00715-14

237. Fonville JM, Marshall N, Tao H, Steel J, Lowen AC. Influenza Virus Reassortment Is Enhanced by Semi-infectious Particles but Can Be Suppressed by Defective Interfering Particles. PLoS Pathog. 2015;11. doi:10.1371/journal.ppat.1005204

238. Dou D, Hernández-Neuta I, Wang H, Östbye H, Qian X, Thiele S, et al. Analysis of IAV Replication and Co-infection Dynamics by a Versatile RNA Viral Genome Labeling Method. Cell Rep. 2017;20: 251–263. doi:10.1016/j.celrep.2017.06.021

239. Bodewes R, Nieuwkoop NJ, Verburgh RJ, Fouchier RAM, Osterhaus ADME, Rimmelzwaan GF. Use of influenza A viruses expressing reporter genes to assess the frequency of double infections in vitro. Journal of General Virology. 2012;93: 1645–1648. doi:10.1099/vir.0.042671-0

240. Chen Y, Müller JD, Ruan Q, Gratton E. Molecular brightness characterization of EGFP in vivo by fluorescence fluctuation spectroscopy. Biophys J. 2002;82: 133–144. doi:10.1016/S0006-3495(02)75380-0

241. Croce AC, Bottiroli G. Autofluorescence spectroscopy and imaging: a tool for biomedical research and diagnosis. Eur J Histochem. 2014;58: 2461. doi:10.4081/ejh.2014.2461

242. Nakamura Y, Ishii J, Kondo A. Bright fluorescence monitoring system utilizing zoanthus sp. green fluorescent protein (ZsGreen) for human g-protein-coupled receptor signaling in microbial yeast cells. PLoS One. 2013;8: 1–18. doi:10.1371/journal.pone.0082237

243. Katsura H, Fukuyama S, Watanabe S, Ozawa M, Neumann G, Kawaoka Y. Amino acid changes in PB2 and HA affect the growth of a recombinant influenza virus expressing a fluorescent reporter protein. Sci Rep. 2016;6. doi:10.1038/srep19933

244. Frensing T, Kupke SY, Bachmann M, Fritzsche S, Gallo-Ramirez LE, Reichl U. Influenza virus intracellular replication dynamics, release kinetics, and particle morphology during propagation in MDCK cells. Appl Microbiol Biotechnol. 2016;100: 7181–7192. doi:10.1007/s00253-016-7542-4

245. Dou D, Revol R, Östbye H, Wang H, Daniels R. Influenza A virus cell entry, replication, virion assembly and movement. Frontiers in Immunology. Frontiers Media S.A.; 2018. doi:10.3389/fimmu.2018.01581

246. Vester D, Lagoda A, Hoffmann D, Seitz C, Heldt S, Bettenbrock K, et al. Real-time RT-qPCR assay for the analysis of human influenza A virus transcription and replication dynamics. J Virol Methods. 2010;168: 63–71. doi:10.1016/j.jviromet.2010.04.017

247. Hatada E, Hasegawa M, Mukaigawa J, Shimizu K, Fukuda R. Control of influenza virus gene expression: Quantitative analysis of each viral RNA species in infected cells. J Biochem. 1989;105: 537–546. doi:10.1093/oxfordjournals.jbchem.a122702

248. Miller S, Krijnse-locker J. Modification of intracellular membrane structures for virus replication. 2008;6. doi:10.1038/nrmicro1890

249. Reid CR, Airo AM, Hobman TC. The Virus-Host Interplay: Biogenesis of +RNA Replication Complexes. Viruses. 2015;7: 4385–4413. doi:10.3390/v7082825

250. Simpson C, Yamauchi Y. Microtubules in Influenza Virus Entry and Egress. 2020; 1–20.

251. Amorim MJ, Bruce EA, Read EKC, Mahen R, Stuart AD, Digard P. A Rab11- and Microtubule-Dependent Mechanism for Cytoplasmic Transport of Influenza A Virus Viral RNA †. 2011;85: 4143–4156. doi:10.1128/JVI.02606-10

252. Viboud C, Bjørnstad ON, Smith DL, Simonsen L, Miller MA, Grenfell BT. Synchrony, waves, and spatial hierarchies in the spread of influenza. Science (1979). 2006;312: 447–451. doi:10.1126/science.1125237

253. Pekar JE, Lytras S, Ghafari M, Magee AF, Parker E, Havens JL, et al. The recency and geographical origins of the bat viruses ancestral to SARS-CoV and SARS-CoV-2. bioRxiv : the preprint server for biology. United States; 2023. doi:10.1101/2023.07.12.548617

254. Stoddard ST, Forshey BM, Morrison AC, Paz-soldan VA, Vazquez- GM. House-to-house human movement drives dengue virus transmission. 2013;110: 994–999. doi:10.1073/pnas.1213349110

255. Le Sage V, Lowen AC, Lakdawala SS. Block the Spread: Barriers to Transmission of Influenza Viruses. Annu Rev Virol. 2023;10: 347–370. doi:10.1146/annurev-virology-111821-115447

256. Mashanov GI, Mashanova A. The role of spatial structure in the infection spread models: population density map of England example. medRxiv. 2020; 2020.04.24.20077289. Available: http://medrxiv.org/content/early/2020/04/29/2020.04.24.20077289.abstract

257. Morizono K, Chen ISY. Receptors and tropisms of envelope viruses. Curr Opin Virol. 2011;1: 13–18. doi:10.1016/j.coviro.2011.05.001

258. Matrosovich MN, Matrosovich TY, Gray T, Roberts NA, Klenk H. Human and avian influenza viruses target different cell types in cultures of human airway epithelium. 2004;1. doi:10.1073/pnas.0308001101

259. Balsitis SJ, Coloma J, Castro G, Alava A, Flores D, Mckerrow JH, et al. Tropism of Dengue Virus in Mice and Humans Defined by Viral Nonstructural Protein 3-Specific Immunostaining. 2009;80: 416–424.

260. McFadden G, Mohamed MR, Rahman MM, Bartee E. Cytokine determinants of viral tropism. Nat Rev Immunol. 2009;9: 645–655. doi:10.1038/nri2623

261. Guarner J, Shieh WJ, Dawson J, Subbarao K, Shaw M, Ferebee T, et al. Immunohistochemical and in situ hybridization studies of influenza A virus infection in human lungs. Am J Clin Pathol. 2000;114: 227–233. doi:10.1309/HV74-N24T-2K2C-3E8Q

262. Graw F, Balagopal A, Kandathil AJ, Ray SC, Thomas DL, Ribeiro RM, et al. Inferring Viral Dynamics in Chronically HCV Infected Patients from the Spatial Distribution of Infected Hepatocytes. PLoS Comput Biol. 2014;10. doi:10.1371/journal.pcbi.1003934

263. Tran V, Moser LA, Poole DS, Mehle A. Highly sensitive real-time in vivo imaging of an influenza reporter virus reveals dynamics of replication and spread. J Virol. 2013;87: 13321–13329. doi:10.1128/JVI.02381-13

264. Pan W, Dong Z, Li F, Meng W, Feng L, Niu X, et al. Visualizing influenza virus infection in living mice. Nat Commun. 2013;4: 2369. doi:10.1038/ncomms3369

265. Gallagher ME, Brooke CB, Ke R, Koelle K. Causes and consequences of spatial within-host viral spread. Viruses. 2018;10: 1–23. doi:10.3390/v10110627

266. Brand JMA Van Den, Stittelaar KJ, Amerongen G Van, Reperant L, De L, Osterhaus ADME, et al. Comparison of Temporal and Spatial Dynamics of Seasonal H3N2 , Pandemic H1N1 and Highly Pathogenic Avian Influenza H5N1 Virus Infections in Ferrets. 2012;7. doi:10.1371/journal.pone.0042343

267. Manicassamy B, Manicassamy S, Belicha-villanueva A, Pisanelli G, Pulendran B. Analysis of in vivo dynamics of in fl uenza virus infection in mice using a GFP reporter virus. 2010;107: 11531–11536. doi:10.1073/pnas.0914994107

268. Ehre C, Worthington EN, Liesman RM, Grubb BR, Barbier D, Neal WKO, et al. Overexpressing mouse model demonstrates the protective role of Muc5ac in the lungs. 2012;109. doi:10.1073/pnas.1206552109

269. Job ER, Bottazzi B, Short KR, Deng Y-M, Mantovani A, Brooks AG, et al. A Single Amino Acid Substitution in the Hemagglutinin of H3N2 Subtype Influenza A Viruses Is Associated with Resistance to the Long Pentraxin PTX3 and Enhanced Virulence in Mice. The Journal of Immunology. 2014;192: 271–281. doi:10.4049/jimmunol.1301814

270. Kumar A, Kim JH, Ranjan P, Metcalfe MG, Cao W, Mishina M, et al. Influenza virus exploits tunneling nanotubes for cell-to-cell spread. Sci Rep. 2017;7: 40360. doi:10.1038/srep40360

271. Ganti K, Han J, Manicassamy B, Lowen AC. Rab11a mediates cell-cell spread and reassortment of influenza A virus genomes via tunneling nanotubes. PLoS Pathog. 2021;17: e1009321. doi:10.1371/journal.ppat.1009321

272. Roberts KL, Manicassamy B, Lamb RA. Influenza A virus uses intercellular connections to spread to neighboring cells. J Virol. 2015;89: 1537–1549. doi:10.1128/JVI.03306-14

273. Excoffier L, Hofer T, Foll M. Detecting loci under selection in a hierarchically structured population. Heredity (Edinb). 2009;103: 285–298. doi:10.1038/hdy.2009.74

274. Excoffier L, Foll M, Petit RJ. Genetic consequences of range expansions. Annu Rev Ecol Evol Syst. 2009;40: 481–501. doi:10.1146/annurev.ecolsys.39.110707.173414

275. Amato KA, Haddock LA, Braun KM, Meliopoulos V, Livingston B, Honce R, et al. Influenza A virus undergoes compartmentalized replication in vivo dominated by stochastic bottlenecks. Nat Commun. 2022;13. doi:10.1038/s41467-022-31147-0

276. Ganti K, Bagga A, Carnaccini S, Ferreri LM, Geiger G, Joaquin Caceres C, et al. Influenza A virus reassortment in mammals gives rise to genetically distinct within-host subpopulations. Nat Commun. 2022;13: 6846. doi:10.1038/s41467-022-34611-z

277. Loveday E, Humberto S, Mallory T, Connie C. Single-Cell Infection of Influenza A Virus Using Drop-Based Microfluidics. Microbiol Spectr. 2022;10: e00993-22. doi:10.1128/spectrum.00993-22

278. Webster RG, Bean WJ, Gorman OT, Chambers TM, Kawaoka Y. Evolution and ecology of influenza A viruses. Microbiol Rev. 1992;56: 152–179. doi:10.1128/mr.56.1.152-179.1992

279. Farrell A, Phan T, Brooke CB, Koelle K, Ke R. Semi-infectious particles contribute substantially to influenza virus within-host dynamics when infection is dominated by spatial structure. Virus Evol. 2023;9. doi:10.1093/ve/vead020

280. Wodarz D, Levy DN, Komarova NL. Multiple infection of cells changes the dynamics of basic viral evolutionary processes. Evol Lett. 2019;3: 104–115. doi:10.1002/evl3.95

281. Küchler J, Püttker S, Lahmann P, Genzel Y, Kupke S, Benndorf D, et al. Absolute quantification of viral proteins during single-round replication of MDCK suspension cells. J Proteomics. 2022;259: 104544. doi:https://doi.org/10.1016/j.jprot.2022.104544

282. Fu J. A tool of “barcoded viruses” to study influenza virus transmission dynamics. University of Cambridge. 2019. doi:https://doi.org/10.17863/CAM.41911

283. Baird N. Influenza virus reassortment in the absence of segment mismatch. Emory University. 2015. Available: https://etd.library.emory.edu/concern/etds/qj72p784r?locale=zh

284. BEALE AJ. Viral interference and interferon. Annu Rev Med. 1963;14: 133–140. doi:10.1146/annurev.me.14.020163.001025

285. Du Toit A. Outbreak of a novel coronavirus. Nature Reviews Microbiology. England; 2020. p. 123. doi:10.1038/s41579-020-0332-0

286. WHO. WHO COVID-19 Dashboard. Available: https://covid19.who.int/

287. Zhou P, Yang X-L, Wang X-G, Hu B, Zhang L, Zhang W, et al. A pneumonia outbreak associated with a new coronavirus of probable bat origin. Nature. 2020;579: 270–273. doi:10.1038/s41586-020-2012-7

288. Peacock TP, Penrice-Randal R, Hiscox JA, Barclay WS. SARS-CoV- 2 one year on: Evidence for ongoing viral adaptation. Journal of General Virology. 2021;102. doi:10.1099/jgv.0.001584

289. Synowiec A, Szczepański A, Barreto-Duran E, Lie LK, Pyrc K. Severe Acute Respiratory Syndrome Coronavirus 2 (SARS-CoV-2): a Systemic Infection. Clin Microbiol Rev. 2021;34. doi:10.1128/CMR.00133-20

290. Masters PS. The molecular biology of coronaviruses. Adv Virus Res. 2006;66: 193–292. doi:10.1016/S0065-3527(06)66005-3

291. Rota PA, Oberste MS, Monroe SS, Nix WA, Campagnoli R, Icenogle JP, et al. Characterization of a novel coronavirus associated with severe acute respiratory syndrome. Science. 2003;300: 1394–1399. doi:10.1126/science.1085952

292. Khailany RA, Safdar M, Ozaslan M. Genomic characterization of a novel SARS-CoV-2. Gene Rep. 2020;19: 100682. doi:10.1016/j.genrep.2020.100682

293. Naqvi AAT, Fatima K, Mohammad T, Fatima U, Singh IK, Singh A, et al. Insights into SARS-CoV-2 genome, structure, evolution, pathogenesis and therapies: Structural genomics approach. Biochim Biophys Acta Mol Basis Dis. 2020;1866: 165878. doi:10.1016/j.bbadis.2020.165878

294. Lee N, Le Sage V, Nanni A V, Snyder DJ, Cooper VS, Lakdawala SS. Genome-wide analysis of influenza viral RNA and nucleoprotein association. Nucleic Acids Res. 2017;45: 8968–8977. doi:10.1093/nar/gkx584

295. Bai C, Zhong Q, Gao GF. Overview of SARS-CoV-2 genome-encoded proteins. Sci China Life Sci. 2022;65: 280–294. doi:10.1007/s11427-021-1964-4

296. V'kovski P, Kratzel A, Steiner S, Stalder H, Thiel V. Coronavirus biology and replication: implications for SARS-CoV-2. Nat Rev Microbiol. 2021;19: 155–170. doi:10.1038/s41579-020-00468-6

297. Fehr AR, Perlman S. Coronaviruses: an overview of their replication and pathogenesis. Methods Mol Biol. 2015;1282: 1–23. doi:10.1007/978-1-4939-2438-7_1

298. Padda IS, Parmur M. COVID (SARS-CoV-2) Vaccine. In: StatPearls [Internet] [Internet]. 2023 [cited 12 Dec 2023]. Available: https://www.ncbi.nlm.nih.gov/books/NBK567793/

299. Li W, Moore MJ, Vasilieva N, Sui J, Wong SK, Berne MA, et al. Angiotensin-converting enzyme 2 is a functional receptor for the SARS coronavirus. Nature. 2003;426: 450–454. doi:10.1038/nature02145

300. Shang J, Wan Y, Luo C, Ye G, Geng Q, Auerbach A, et al. Cell entry mechanisms of SARS-CoV-2. Proc Natl Acad Sci U S A. 2020;117: 11727–11734. doi:10.1073/pnas.2003138117

301. Hoffmann M, Kleine-Weber H, Pöhlmann S. A Multibasic Cleavage Site in the Spike Protein of SARS-CoV-2 Is Essential for Infection of Human Lung Cells. Mol Cell. 2020;78: 779-784.e5. doi:10.1016/j.molcel.2020.04.022

302. Ziebuhr J, Snijder EJ, Gorbalenya AE. Virus-encoded proteinases and proteolytic processing in the Nidovirales. J Gen Virol. 2000;81: 853–879. doi:10.1099/0022-1317-81-4-853

303. V'kovski P, Gerber M, Kelly J, Pfaender S, Ebert N, Braga Lagache S, et al. Determination of host proteins composing the microenvironment of coronavirus replicase complexes by proximity-labeling. Elife. 2019;8. doi:10.7554/eLife.42037

304. Sawicki SG, Sawicki DL. Coronaviruses use discontinuous extension for synthesis of subgenome-length negative strands. Adv Exp Med Biol. 1995;380: 499–506. doi:10.1007/978-1-4615-1899-0_79

305. Sola I, Almazán F, Zúñiga S, Enjuanes L. Continuous and Discontinuous RNA Synthesis in Coronaviruses. Annu Rev Virol. 2015;2: 265–288. doi:10.1146/annurev-virology-100114-055218

306. Wang H, Cui X, Cai X, An T. Recombination in Positive-Strand RNA Viruses. Front Microbiol. 2022;13: 1–12. doi:10.3389/fmicb.2022.870759

307. Eymieux S, Uzbekov R, Rouillé Y, Blanchard E, Hourioux C, Dubuisson J, et al. Secretory Vesicles Are the Principal Means of SARS-CoV-2 Egress. Cells. 2021;10. doi:10.3390/cells10082047

308. Hu B, Guo H, Zhou P, Shi Z-L. Characteristics of SARS-CoV-2 and COVID-19. Nat Rev Microbiol. 2021;19: 141–154. doi:10.1038/s41579-020-00459-7

309. Rendeiro AF, Ravichandran H, Bram Y, Chandar V, Kim J, Meydan C, et al. The spatial landscape of lung pathology during COVID-19 progression. Nature. 2021;593: 564–569. doi:10.1038/s41586-021-03475-6

310. Zawilska JB, Lagodzinski A, Berezinska M. Covid-19: From the Structure and Replication Cycle of Sars-Cov-2 To Its Disease Symptoms and Treatment. Journal of Physiology and Pharmacology. 2021;72: 479–501. doi:10.26402/jpp.2021.4.01

311. Wong DWL, Klinkhammer BM, Djudjaj S, Villwock S, Timm MC, Buhl EM, et al. Multisystemic Cellular Tropism of SARS-CoV-2 in Autopsies of COVID-19 Patients. Cells. 2021;10. doi:10.3390/cells10081900

312. Hou YJ, Okuda K, Edwards CE, Martinez DR, Asakura T, Dinnon KH, et al. SARS-CoV-2 Reverse Genetics Reveals a Variable Infection Gradient in the Respiratory Tract. Cell. 2020;182: 429-446.e14. doi:10.1016/j.cell.2020.05.042

313. Lukassen S, Chua RL, Trefzer T, Kahn NC, Schneider MA, Muley T, et al. SARS-CoV-2 receptor ACE2 and TMPRSS2 are primarily expressed in bronchial transient secretory cells. EMBO J. 2020;39: e105114. doi:10.15252/embj.20105114

314. Ortiz ME, Thurman A, Pezzulo AA, Leidinger MR, Klesney-Tait JA, Karp PH, et al. Heterogeneous expression of the SARS-Coronavirus-2 receptor ACE2 in the human respiratory tract. EBioMedicine. 2020;60: 102976. doi:10.1016/j.ebiom.2020.102976

315. Nagpal P, Narayanasamy S, Vidholia A, Guo J, Shin KM, Lee CH, et al. Imaging of COVID-19 pneumonia: Patterns, pathogenesis, and advances. Br J Radiol. 2020;93: 20200538. doi:10.1259/bjr.20200538

316. Liu J, Li Y, Liu Q, Yao Q, Wang X, Zhang H, et al. SARS-CoV-2 cell tropism and multiorgan infection. Cell Discov. 2021;7: 2–5. doi:10.1038/s41421-021-00249-2

317. Ziegler CGK, Allon SJ, Nyquist SK, Mbano IM, Miao VN, Tzouanas CN, et al. SARS-CoV-2 Receptor ACE2 Is an Interferon-Stimulated Gene in Human Airway Epithelial Cells and Is Detected in Specific Cell Subsets across Tissues. Cell. 2020;181: 1016-1035.e19. doi:10.1016/j.cell.2020.04.035

318. Schurink B, Roos E, Radonic T, Barbe E, Bouman CSC, de Boer HH, et al. Viral presence and immunopathology in patients with lethal COVID-19: a prospective autopsy cohort study. Lancet Microbe. 2020;1: e290–e299. doi:https://doi.org/10.1016/S2666-5247(20)30144-0

319. Szabolcs M, Sauter JL, Frosina D, Geronimo JA, Hernandez E, Selbs E, et al. Identification of immunohistochemical reagents for in situ protein expression analysis of coronavirus-associated changes in human tissues. Applied Immunohistochemistry and Molecular Morphology. 2021;29: 5–12. doi:10.1097/PAI.0000000000000878

320. Schaefer IM, Padera RF, Solomon IH, Kanjilal S, Hammer MM, Hornick JL, et al. In situ detection of SARS-CoV-2 in lungs and airways of patients with COVID-19. Modern Pathology. 2020;33: 2104–2114. doi:10.1038/s41379-020-0595-z

321. Hui KPY, Ho JCW, Cheung M chun, Ng K chun, Ching RHH, Lai K ling, et al. SARS-CoV-2 Omicron variant replication in human bronchus and lung ex vivo. Nature. 2022;603: 715–720. doi:10.1038/s41586-022-04479-6

322. Morrison CB, Edwards CE, Shaffer KM, Araba KC, Wykoff JA, Williams DR, et al. SARS-CoV-2 infection of airway cells causes intense viral and cell shedding, two spreading mechanisms affected by IL-13. Proc Natl Acad Sci U S A. 2022;119: e2119680119. doi:10.1073/pnas.2119680119

323. Gamage AM, Tan K Sen, Chan WOY, Zhang Z, Lew R, Liu J, et al. Human Nasal Epithelial Cells Sustain Persistent SARS-CoV-2. mBio. 2022;13.

324. Madden PJ, Arif MS, Becker ME, McRaven MD, Carias AM, Lorenzo-Redondo R, et al. Development of an In Vivo Probe to Track SARS-CoV-2 Infection in Rhesus Macaques. Front Immunol. 2021;12: 1–14. doi:10.3389/fimmu.2021.810047

325. Au GG, Marsh GA, McAuley AJ, Lowther S, Trinidad L, Edwards S, et al. Characterisation and natural progression of SARS-CoV-2 infection in ferrets. Sci Rep. 2022;12: 1–14. doi:10.1038/s41598-022-08431-6

326. Zaeck LM, Scheibner D, Sehl J, Müller M, Hoffmann D, Beer M, et al. Light sheet microscopy-assisted 3d analysis of sars-cov-2 infection in the respiratory tract of the ferret model. Viruses. 2021;13: 1–17. doi:10.3390/v13030529

327. Fan C, Wu Y, Rui X, Yang Y, Ling C, Liu S, et al. Animal models for COVID-19: advances, gaps and perspectives. Signal Transduct Target Ther. 2022;7: 220. doi:10.1038/s41392-022-01087-8

328. Zhang Z, Shen L, Gu X. Evolutionary Dynamics of MERS-CoV: Potential Recombination, Positive Selection and Transmission. Sci Rep. 2016;6: 25049. doi:10.1038/srep25049

329. Lau SKP, Lee P, Tsang AKL, Yip CCY, Tse H, Lee RA, et al. Molecular epidemiology of human coronavirus OC43 reveals evolution of different genotypes over time and recent emergence of a novel genotype due to natural recombination. J Virol. 2011;85: 11325–11337. doi:10.1128/JVI.05512-11

330. Zhang XW, Yap YL, Danchin A. Testing the hypothesis of a recombinant origin of the SARS-associated coronavirus. Arch Virol. 2005;150: 1–20. doi:10.1007/s00705-004-0413-9

331. Li X, Giorgi EE, Marichannegowda MH, Foley B, Xiao C, Kong X-P, et al. Emergence of SARS-CoV-2 through recombination and strong purifying selection. Sci Adv. 2020;6. doi:10.1126/sciadv.abb9153

332. Zhou H, Chen X, Hu T, Li J, Song H, Liu Y, et al. A Novel Bat Coronavirus Closely Related to SARS-CoV-2 Contains Natural Insertions at the S1/S2 Cleavage Site of the Spike Protein. Curr Biol. 2020;30: 2196-2203.e3. doi:10.1016/j.cub.2020.05.023

333. Zhu Z, Meng K, Meng G. Genomic recombination events may reveal the evolution of coronavirus and the origin of SARS-CoV-2. Sci Rep. 2020;10: 21617. doi:10.1038/s41598-020-78703-6

334. Jackson B, Boni MF, Bull MJ, Colleran A, Colquhoun RM, Darby AC, et al. Generation and transmission of interlineage recombinants in the SARS-CoV-2 pandemic. Cell. 2021;184: 5179-5188.e8. doi:10.1016/j.cell.2021.08.014

335. Wertheim JO, Wang JC, Leelawong M, Martin DP, Havens JL, Chowdhury MA, et al. Detection of SARS-CoV-2 intra-host recombination during superinfection with Alpha and Epsilon variants in New York City. Nat Commun. 2022;13: 3645. doi:10.1038/s41467-022-31247-x

336. Turakhia Y, Thornlow B, Hinrichs A, McBroome J, Ayala N, Ye C, et al. Pandemic-scale phylogenomics reveals the SARS-CoV-2 recombination landscape. Nature. 2022;609: 994–997. doi:10.1038/s41586-022-05189-9

337. Richard D, Owen CJ, Dorp L van, Balloux F. No detectable signal for ongoing genetic recombination in SARS-CoV-2. bioRxiv. 2020; 2020.12.15.422866. Available: https://www.biorxiv.org/content/10.1101/2020.12.15.422866v1

338. VanInsberghe D, Neish AS, Lowen AC, Koelle K. Recombinant SARS-CoV-2 genomes are currently circulating at low levels. bioRxiv : the preprint server for biology. United States; 2021. doi:10.1101/2020.08.05.238386

339. Gutierrez B, Castelán Sánchez HG, Candido D da S, Jackson B, Fleishon S, Houzet R, et al. Emergence and widespread circulation of a recombinant SARS-CoV-2 lineage in North America. Cell Host Microbe. 2022;30: 1112-1123.e3. doi:10.1016/j.chom.2022.06.010

340. Kim E-H, Nguyen T-Q, Casel MAB, Rollon R, Kim S-M, Kim Y-I, et al. Coinfection with SARS-CoV-2 and Influenza A Virus Increases Disease Severity and Impairs Neutralizing Antibody and CD4(+) T Cell Responses. J Virol. 2022;96: e0187321. doi:10.1128/jvi.01873-21

341. Swets MC, Russell CD, Harrison EM, Docherty AB, Lone N, Girvan M, et al. SARS-CoV-2 co-infection with influenza viruses, respiratory syncytial virus, or adenoviruses. Lancet (London, England). England; 2022. pp. 1463–1464. doi:10.1016/S0140-6736(22)00383-X

342. Maltezou HC, Papanikolopoulou A, Vassiliu S, Theodoridou K, Nikolopoulou G, Sipsas N V. COVID-19 and Respiratory Virus Co-Infections: A Systematic Review of the Literature. Viruses. 2023;15. doi:10.3390/v15040865

343. Soo RJJ, Chiew CJ, Ma S, Pung R, Lee V. Decreased Influenza Incidence under COVID-19 Control Measures, Singapore. Emerg Infect Dis. 2020;26: 1933–1935. doi:10.3201/eid2608.201229

344. Kim MJ, Kim S, Kim H, Gil D, Han H-J, Thimmulappa RK, et al. Reciprocal enhancement of SARS-CoV-2 and influenza virus replication in human pluripotent stem cell-derived lung organoids(1). Emerg Microbes Infect. 2023;12: 2211685. doi:10.1080/22221751.2023.2211685

345. Bai L, Zhao Y, Dong J, Liang S, Guo M, Liu X, et al. Coinfection with influenza A virus enhances SARS-CoV-2 infectivity. Cell Res. 2021;31: 395–403. doi:10.1038/s41422-021-00473-1

346. Schaecher SR, Mackenzie JM, Pekosz A. The ORF7b protein of severe acute respiratory syndrome coronavirus (SARS-CoV) is expressed in virus-infected cells and incorporated into SARS-CoV particles. J Virol. 2007;81: 718–731. doi:10.1128/JVI.01691-06

347. Nelson CA, Pekosz A, Lee CA, Diamond MS, Fremont DH. Structure and intracellular targeting of the SARS-coronavirus orf7a accessory protein. Structure. 2005;13: 75–85. doi:10.1016/j.str.2004.10.010

348. Zhou Z, Huang C, Zhou Z, Huang Z, Su L, Kang S, et al. Structural insight reveals SARS-CoV-2 ORF7a as an immunomodulating factor for human CD14+ monocytes. iScience. 2021;24: 102187. doi:10.1016/j.isci.2021.102187

349. Achdout H, Vitner EB, Politi B, Melamed S, Yahalom-Ronen Y, Tamir H, et al. Increased lethality in influenza and SARS-CoV-2 coinfection is prevented by influenza immunity but not SARS-CoV-2 immunity. Nat Commun. 2021;12: 1–10. doi:10.1038/s41467-021-26113-1

350. Schlägel UE, Merrill EH, Lewis MA. Territory surveillance and prey management: Wolves keep track of space and time. Ecol Evol. 2017;7: 8388–8405. doi:10.1002/ece3.3176

351. Schenk HJ, Callaway RM, Mahall BE. Spatial Root Segregation: Are Plants Territorial? In: Fitter AH, Raffaelli DBT-A in ER, editors. Academic Press; 1999. pp. 145–180. doi:https://doi.org/10.1016/S0065-2504(08)60032-X

352. Mavridou DAI, Gonzalez D, Kim W, West SA, Foster KR. Bacteria Use Collective Behavior to Generate Diverse Combat Strategies. Current Biology. 2018;28: 345-355.e4. doi:10.1016/j.cub.2017.12.030

353. Gould SJ, Lewontin RC. The spandrels of San Marco and the Panglossian paradigm: A critique of the adaptationist programme. Shaping Entrepreneurship Research: Made, as Well as Found. 2020;598: 204–221.

354. Kawasaki Y, Abe H, Yasuda J. Comparison of genome replication fidelity between SARS-CoV-2 and influenza A virus in cell culture. Sci Rep. 2023;13: 1–9. doi:10.1038/s41598-023-40463-4

355. Pauly MD, Procario MC, Lauring AS. A novel twelve class fluctuation test reveals higher than expected mutation rates for influenza A viruses. Elife. 2017;6: 1–18. doi:10.7554/eLife.26437

356. Samji T. Influenza A: understanding the viral life cycle. Yale J Biol Med. 2009;82: 153–9. Available: http://www.ncbi.nlm.nih.gov/pubmed/20027280

357. Visher E, Whitefield SE, McCrone JT, Fitzsimmons W, Lauring AS. The Mutational Robustness of Influenza A Virus. PLoS Pathog. 2016;12: e1005856. doi:10.1371/journal.ppat.1005856

358. Sanjuán R, Domingo-Calap P. Mechanisms of viral mutation. Cell Mol Life Sci. 2016;73: 4433–4448. doi:10.1007/s00018-016-2299-6

359. Barrett T, Wolstenholme AJ, Mahy BWJ. Transcription and replication of influenza virus RNA. Virology. 1979;98: 211–225. doi:10.1016/0042-6822(79)90539-7

360. Vreede FT, Ng AK-L, Shaw P-C, Fodor E. Stabilization of influenza virus replication intermediates is dependent on the RNA-binding but not the homo-oligomerization activity of the viral nucleoprotein. J Virol. 2011;85: 12073–12078. doi:10.1128/JVI.00695-11

361. Whittaker G, Bui M, Helenius A. Nuclear trafficking of influenza virus ribonuleoproteins in heterokaryons. J Virol. 1996;70: 2743–2756. doi:10.1128/jvi.70.5.2743-2756.1996

362. Kummer S, Flöttmann M, Schwanhäusser B, Sieben C, Veit M, Selbach M, et al. Alteration of Protein Levels during Influenza Virus H1N1 Infection in Host Cells: A Proteomic Survey of Host and Virus Reveals Differential Dynamics. PLoS One. 2014;9: e94257. Available: https://doi.org/10.1371/journal.pone.0094257

363. Xue KS, Moncla LH, Bedford T, Bloom JD. Within-Host Evolution of Human Influenza Virus. Trends Microbiol. 2018;26: 781–793. doi:https://doi.org/10.1016/j.tim.2018.02.007

364. Ellwanger JH, Chies JAB. Zoonotic spillover: Understanding basic aspects for better prevention. Genet Mol Biol. 2021;44: e20200355. doi:10.1590/1678-4685-GMB-2020-0355

365. Plowright RK, Parrish CR, McCallum H, Hudson PJ, Ko AI, Graham AL, et al. Pathways to zoonotic spillover. Nat Rev Microbiol. 2017;15: 502–510. doi:10.1038/nrmicro.2017.45

366. Pike BL, Saylors KE, Fair JN, Lebreton M, Tamoufe U, Djoko CF, et al. The origin and prevention of pandemics. Clin Infect Dis. 2010;50: 1636–1640. doi:10.1086/652860

367. Hassanin A, Rambaud O, Klein D. Genomic Bootstrap Barcodes and Their Application to Study the Evolution of Sarbecoviruses. Viruses. 2022;14. doi:10.3390/v14020440

368. Kozlakidis Z. Evidence for Recombination as an Evolutionary Mechanism in Coronaviruses: Is SARS-CoV-2 an Exception? Front Public Health. 2022;10: 1–4. doi:10.3389/fpubh.2022.859900

369. Worobey M, Han GZ, Rambaut A. Genesis and pathogenesis of the 1918 pandemic H1N1 influenza a virus. Proc Natl Acad Sci U S A. 2014;111: 8107–8112. doi:10.1073/pnas.1324197111

370. Greenbaum BD, Levine AJ, Bhanot G, Rabadan R. Patterns of evolution and host gene mimicry in influenza and other RNA viruses. PLoS Pathog. 2008;4: e1000079. doi:10.1371/journal.ppat.1000079

371. Garten RJ, Davis CT, Russell CA, Shu B, Lindstrom S, Balish A, et al. Antigenic and genetic characteristics of swine-origin 2009 A(H1N1) influenza viruses circulating in humans. Science. 2009;325: 197–201. doi:10.1126/science.1176225

372. Li C, Hatta M, Nidom CA, Muramoto Y, Watanabe S, Neumann G, et al. Reassortment between avian H5N1 and human H3N2 influenza viruses creates hybrid viruses with substantial virulence. Proc Natl Acad Sci U S A. 2010;107: 4687–4692. doi:10.1073/pnas.0912807107

373. Jackson S, Van Hoeven N, Chen L-M, Maines TR, Cox NJ, Katz JM, et al. Reassortment between avian H5N1 and human H3N2 influenza viruses in ferrets: a public health risk assessment. J Virol. 2009;83: 8131–8140. doi:10.1128/JVI.00534-09

374. Hsieh E-F, Lin S-J, Mok C-K, Chen G-W, Huang C-H, Wang Y-C, et al. Altered Pathogenicity for Seasonal Influenza Virus by Single Reassortment of the RNP Genes Derived From the 2009 Pandemic Influenza Virus. J Infect Dis. 2011;204: 864–872. doi:10.1093/infdis/jir435

375. Song M-S, Pascua PNQ, Lee JH, Baek YH, Park KJ, Kwon H, et al. Virulence and genetic compatibility of polymerase reassortant viruses derived from the pandemic (H1N1) 2009 influenza virus and circulating influenza A viruses. J Virol. 2011;85: 6275–6286. doi:10.1128/JVI.02125-10

376. Tamura T, Ito J, Uriu K, Zahradnik J, Kida I, Anraku Y, et al. Virological characteristics of the SARS-CoV-2 XBB variant derived from recombination of two Omicron subvariants. Nat Commun. 2023;14: 2800. doi:10.1038/s41467-023-38435-3

377. Lytras S, Hughes J, Martin D, Swanepoel P, de Klerk A, Lourens R, et al. Exploring the Natural Origins of SARS-CoV-2 in the Light of Recombination. Genome Biol Evol. 2022;14. doi:10.1093/gbe/evac018

378. Chen X, Chen Z, Azman AS, Sun R, Lu W, Zheng N, et al. Neutralizing Antibodies Against Severe Acute Respiratory Syndrome Coronavirus 2 (SARS-CoV-2) Variants Induced by Natural Infection or Vaccination: A Systematic Review and Pooled Analysis. Clin Infect Dis. 2022;74: 734–742. doi:10.1093/cid/ciab646

379. MedImmune, FDA. Package Insert - FluMist Quadrivalent. 2023 [cited 4 Jan 2024]. Available: http://vaers.hhs.gov.

380. Caspard H, Mallory RM, Yu J, Ambrose CS. Live-Attenuated Influenza Vaccine Effectiveness in Children From 2009 to 2015-2016: A Systematic Review and Meta-Analysis. Open Forum Infect Dis. 2017;4: 1–9. doi:10.1093/OFID/OFX111

381. Scutti S. CDC panel again advises against FluMist. CNN. Available: https://edition.cnn.com/2017/06/21/health/flu-shot-flumist-cdc-recommendations/index.html

382. Dibben O, Crowe J, Cooper S, Hill L, Schewe KE, Bright H. Defining the root cause of reduced H1N1 live attenuated influenza vaccine effectiveness: low viral fitness leads to inter-strain competition. NPJ Vaccines. 2021;6. doi:10.1038/s41541-021-00300-z

383. Merck. RotaTeq. 2006 [cited 30 Jan 2024]. Available: https://www.merck.com/product/usa/pi_circulars/r/rotateq/rotateq_pi.pdf